Title
SURFACE CHEMISTRY OF PALLADIUM

Author
Gentle, T.M.

Publication Date
1984-05-01

Lawrence Berkeley Laboratory
UNIVERSITY OF CALIFORNIA

Materials & Molecular Research Division

SURFACE CHEMISTRY OF PALLADIUM

T.M. Gentle
(Ph.D. Thesis)

May 1984

Prepared for the U.S. Department of Energy under Contract DE-AC03-76SF00098

DISCLAIMER

LBL 17798

SURFACE CHEMISTRY OF PALLADIUM

Thomas Matthew Gentle

(Ph.D. Thesis)

Lawrence Berkeley Laboratory

and

Department of Chemistry

University of California

Berkeley, California 94720

This work was supported by the Director, Office of Energy Research, Office of Basic Energy Science, Chemical Sciences Division of the U.S. Department of Energy under Contract No. DE-AC03-76SF00098.

SURFACE CHEMISTRY OF PALLADIUM

Thomas Matthew Gentle

ABSTRACT

The surface chemistry of several classes of catalytically important molecules on palladium single crystals was pursued in this thesis research. The influence of surface structure and composition on reactions involving formation and scission of carbon–carbon and carbon–hydrogen bonds was investigated. These studies were performed under ultrahigh-vacuum (UHV) conditions on single crystals; some reactions, however, were studied at higher pressures on polycrystalline films.

Reactions of acetylene on Pd(111), Pd(100), and Pd(110) were studied using thermal desorption spectroscopy, chemical displacement reactions, and isotopic labeling techniques. Palladium single crystals were found to catalyze several reactions of acetylene, including trimerization to benzene, hydrogenation to ethylene, and hydrosilation with trimethylsilane. Several atoms such as Si, P, S, and Cl were found to have a profound influence on the catalytic activity of these surfaces.

Single-crystal surfaces of palladium were found to catalyze the dehydrogenation of organosilanes. For example, silacyclohexane chemisorbed on Pd(110) underwent dehydrogenation upon thermal desorption to form silabenzene.

Chemisorption studies of thiophene, 3-methylthiophene, and 2,5-dimethylthiophene were performed on clean and sulfided palladium single crystals. Desulfurization products were observed in the thermal desorption spectra of these molecules.

Mechanisms of carbon-hydrogen bond scission were investigated for a variety of methylsubstituted benzenes. The use of selectively labeled molecules revealed some degree of regiospecificity in C-H bond scission.

Several reactions of unsaturated hydrocarbons were also investigated at higher pressures (10^{-2} torr) on polycrystalline palladium films. A remarkable correspondence between these studies and UHV studies was observed.

To Earl - my Research Director and friend.

ACKNOWLEDGEMENT

I am deeply indebted to Professor Earl L. Muetterties for his guidance during the course of this thesis. Earl was and always will be inspirational to me in both my scientific and nonscientific endeavors. His keen interest in his students and their research made my time here at Berkeley one of the most memorable and rewarding periods of my life.

There are many individuals in MMRD whose assistance and friendship I found invaluable. Their friendship is something I will cherish for a long time. Weyland Wong, Michael Kujala, and Keith Franck are truly experts at design, fabrication, and maintenance of UHV equipment. Along with providing me with an operational vacuum chamber, they taught me a great deal. Glenn Baum offered his valuable expertise in leak detection many times. Jim Severns and Hank Brendel provided much needed assistance in design, construction, and maintenance of the electronics necessary for this research. At times when I needed materials and equipment in a hurry, Sandy Stewart and Cathy Sterling never ceased to amaze me at the speed with which they expedited the necessary purchasing paperwork. There are most certainly many others at LBL who should be thanked. Their omission is due to my absent-mindedness, not lack of gratitude.

Many current and former members of the Muetterties group are to be acknowledged. At times during this past year, life was not very easy

or pleasant; however, three members of Earl's group, Rick Wilmer, Ken Lewis, and Tom Rucker, provided a source of strength during these difficult times for which I am eternally grateful.

I would also like to thank Professor Gabor Somorjai and members of his research group for advice and assistance.

Several people were involved in the preparation of this manuscript and should also be thanked. Rich Albert and Diana Morris brought about a minor miracle in the completion of this task. Dave Nieman and Tom Rucker are to be acknowledged for their superhuman efforts in preparation of the figures for this thesis.

Several friends at Dow Corning are to be thanked. Along with much appreciated financial support, Dow Corning provided me with an opportunity to have valuable discussions on many visits back to Midland. Among these people who often gave fresh insights into my research at Berkeley are John Speier, John Ryan, Ken Sharp, Donald Weyenburg, Forest Stark, and Don Liles.

My family has provided a constant and seemingly unlimited source of support and encouragement during my studies in California. They are very important to me, and I would like to thank my parents, Thomas and Rita, my brothers, Dan and Mark and his family, and my sisters, Anne and Mary Lee and her family.

This work was supported by the Director, Office of Energy Research, Office of Basic Energy Sciences, Chemical Sciences Division of the U.S. Department of Energy under Contract No. DE-AC03-76SF00098.

TABLE OF CONTENTS

I. INTRODUCTION

"Catalysis is extremely common in chemistry. Its nature is not well understood."[1] The above quotation is taken from the Encyclopedia Americana concerning the subject of catalysis. Unraveling the mysteries of heterogeneous catalysis is an important goal of modern surface science.

The activity of transition metal catalysts can be influenced by a number of variables. Among these variables are catalyst structure and composition.[2] To understand the often complex chemistry that occurs on these catalysts, it is necessary to develop a fundamental understanding of this chemistry on a molecular level. Ultrahigh-vacuum studies of the surface chemistry of catalytically important molecules such as unsaturated hydrocarbons and organosilanes is the subject of this thesis. These studies were initiated in the hope of gaining further insights into the nature of the catalytic process.

Palladium is known to be an important catalyst for a variety of reactions.[3] For example, supported palladium catalysts are known to be extremely selective[4] for hydrogenation. The hydrogenation of acetylene to ethylene is found to proceed with nearly 100 percent selectivity; that is, no ethane formation is observed. Other transition metals are found to be less selective and follow the trend Pd > Rh > Pt > Ru > Ir > Os. Osmium is found to have a selectivity of 50 percent.

Palladium has a face-centered cubic lattice structure. The three low Miller-index surfaces are the (111), (100), and (110). The (111)

surface is close-packed with threefold symmetry. Surface metal atoms have a coordination number of nine. Fourfold symmetry is exhibited by the (100) surface. A coordination number of eight is observed for the metal atoms of this surface. A trough-like structure characterizes the (110) surface. The uppermost atoms have a coordination number of seven, and the trough atoms have a coordination number of eleven. These three surfaces are shown in Figure I-1.

Composition has been found to have a profound influence on both the activity[6] and selectivity of heterogeneous transition metal catalysts. Elements such as silicon, phosphorous, sulfur, and chlorine, or compounds containing these elements, have been of particular interest. Often these elements are found to be both beneficial "promotors" and detrimental "poisons" for catalysts. Several reviews have been published on the subject.[7] A complete review of the subject is outside the scope of this thesis, and the reader is referred to these works.

The adatoms[8] silicon, phosphous, sulfur, and chlorine have a wide-ranging impact on a variety of processes important to technology. One example that has influenced today's society is the poisoning of catalytic converters on automobiles. It is hoped that chemisorption studies of catalytically important molecules, such as unsaturated hydrocarbons, on adatom-covered transition metal surfaces will give insights into how these elements poison or promote a given reaction.

Figure I-1. The three low Miller-index surfaces for a face-centered cubic metal are shown. The (111) surface is the close pack surface; the (100) is more open and displays fourfold symmetry; and the (110) or the super-stepped is the most open of all three.

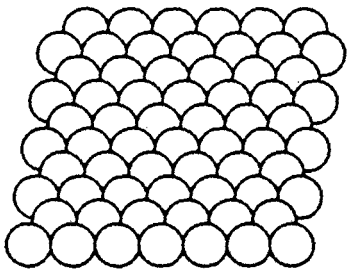

fcc (111)

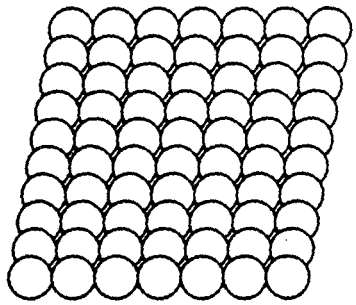

fcc (100)

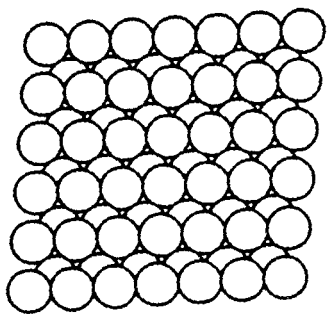

fcc (110)

XBL 802-8036

The conceptual approach of this thesis has been to merge the techniques of ultrahigh-vacuum surface physics with those of coordination chemistry. The advent of ultrahigh-vacuum technology in the past twenty years has made it possible to prepare and maintain clean transition metal surfaces for relatively long periods of time. If a vacuum chamber is operating at a base pressure of 1×10^{-9} torr, it will take 1000 seconds[9] for a monolayer of a gas to adsorb on the surface. Ultrahigh-vacuum technology also makes it possible to perform surface characterization with a variety of electron spectroscopies. Auger electron spectroscopy (AES) allows one to determine surface composition. Using low-energy electron diffraction (LEED), the structural information concerning both clean and adsorbate-covered surfaces can be obtained.[10]

Mass spectrometry allows one to determine the composition of the gas phase of a vacuum chamber. Thermal desorption spectrometry utilizes mass spectrometry to obtain useful information about the nature of the chemisorbed molecules on transition metal surfaces. In some instances where molecules desorb intact from transition metal surfaces, the activation energy of desorption and the order of the desorption process can be easily obtained. A thermal desorption experiment is performed by adsorbing a given molecule on a metal surface, which is followed by rapid heating (usually at a linear rate), while monitoring the gas phase with a mass spectrometer.

A thermal desorption spectrum is a plot with the temperature of the metal surface on the ordinate and the intensity of mass spectral

signal of the various species desorbing from the surface on the abcissa (see Figure I-2). The chemisorption of a molecule on a transition metal surface may be completely reversible (quantitative desorption). The thermal desorption spectrum derived from this process is given in Case I of Figure I-2. The position or temperature of the maximum in the plot allows one to determine the activation energy of adsorption and its change in position as a function of coverage of the order of desorption.

Many molecules exhibit more complex thermal desorption spectra. Two other possible scenarios are shown in Case II and Case III of Figure I-2. In Case II an absorbate, ABC, exhibits both reversible and irreversible chemisorption when absorbed on the metal surface, M, to form a new surface state, M-ABC. Upon heating this surface state, molecular desorption (reversible chemisorption) is observed as characterized by the thermal desorption maximum of ABC. The irreversible chemisorbed ABC is characterized by the thermal desorption maxima of A and B and the surface state M-C obtained after the experiment. In Case III, complete irreversible chemisorption is described. After forming the surface state, M-ABC, no molecular desorption is observed, but rather desorption of the two species A and B and formation of surface state M-C are observed. The above cases serve as illustration of a few of the many possible pathways thermal desorption experiments can take. Other pathways occur and will be discussed in the course of this thesis.

Figure I-2. Three possible scenarios for the course of thermal desorption of a molecule from a transition metal surface are shown. In Case A, reversible chemisorption or quantitative desorption is described. Both reversible and irreversible chemisorption are described in Case B. Irreversible chemisorption is described in Case C.

THERMAL DESORPTION SPECTROSCOPY

CASE I

$$M + A_{(g)} \rightarrow M\text{-}A \xrightarrow{\Delta} M + A_{(g)}$$

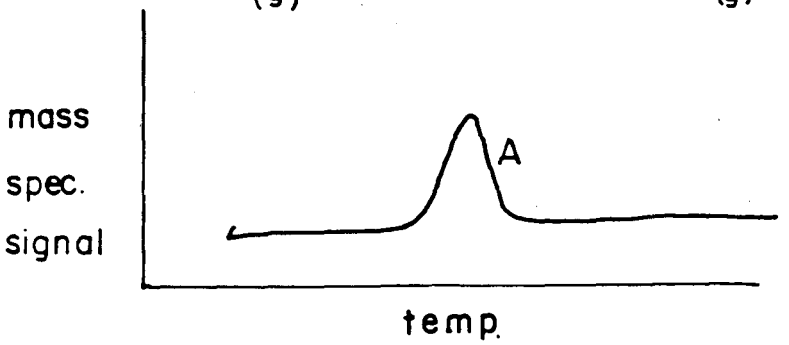

CASE II

$$M + ABC_{(g)} \rightarrow M\text{-}ABC \xrightarrow{\Delta} M\text{-}C + ABC_{(g)} + A_{(g)} + B_{(g)}$$

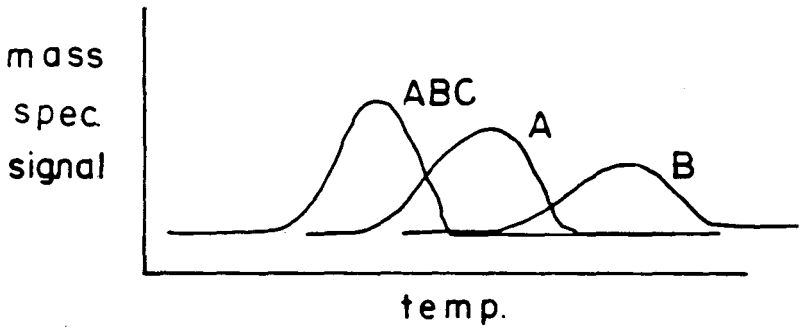

CASE III

$$M + ABC_{(g)} \rightarrow M\text{-}ABC \xrightarrow{\Delta} M\text{-}C + A_{(g)} + B_{(g)}$$

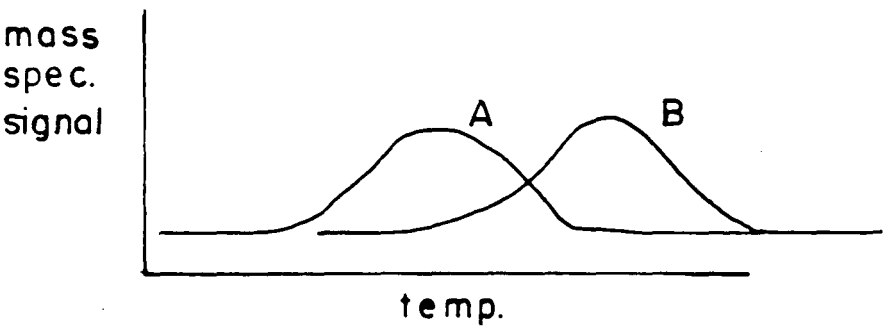

XBL 8110-11867

Applications of techniques of coordination chemistry to the problems of surface chemistry have been the hallmark of the Muetterties group.[12] Chemical displacement reactions have been applied to surface states formed by chemisorption of a variety of molecules on transition metal surfaces. These reactions are formally analogous to those found in chemistry of transition metal complexes where one ligand may be displaced by another ligand in the complex.[13] Often mechanistic insights can be gained through the use of displacement reactions. A chemical displacement is performed by first adsorbing the molecule of interest on a transition metal surface. While monitoring the gas phase with a mass spectrometer, a displacing agent, typically trimethylphosphine, is introduced into the vacuum chamber. If displacement is to take place, it occurs as the displacing agent is introduced into the system. In Figure I-3, three possible pathways for chemical displacement reactions are shown. In Case I, the situation where a molecule A is quantitatively displaced from the surface state M-A by the displacing agent, B, is described. Partial displacement of A is described in Case II. After forming surface state M-A, B does not completely displace A, and a surface state M-A-B is observed after the experiment.

In some instances no displacement of A is affected by the displacing agent, B. Case III describes this situation. Introduction of B results in the formation of the surface state M-A-B. The above cases illustrate examples of chemical displacement reactions and again are not meant to be an exhaustive list.

Figure I-3. The possible pathways for chemical displacement reactions are described. In Case I complete displacement occurs; in Case II partial displacement occurs; and in Case III no displacement occurs.

CHEMICAL DISPLACEMENT REACTIONS

CASE I

$$\underline{M} + A_{(g)} \longrightarrow \underline{M-A} \xrightarrow{B} \underline{M-B} + A_{(g)}$$

CASE II

$$\underline{M} + A_{(g)} \longrightarrow \underline{M-A} \xrightarrow{B} \underline{M-B-A} + A_{(g)}$$

CASE III

$$\underline{M} + A_{(g)} \longrightarrow \underline{M-A} \xrightarrow{B} \underline{M-B-A}$$

The interaction of acetylene with transition metal surfaces has been the subject of a number of surface-science investigations, in particular on Ni and Pt.[14] Much effort has been devoted to determining the nature of the chemisorbed species. A wide variety of techniques have been used in these studies. Recently studies of acetylene on palladium have emerged, and among the techniques used have been thermal desorption spectroscopy (TDS),[15,16,17] ultraviolet photoemission spectroscopy (UPS),[16,17] x-ray photoemission spectroscopy (XPS),[16] high resolution electron energy loss spectroscopy (HREELS),[18] and chemical displacement reactions.[15] Palladium exhibits unique chemistry under ultrahigh-vacuum conditions compared to its cognegers nickel and platinum. Although the oligomerization of acetylene is well known for transition metal complexes,[19] it is rare for heterogeneous transition metal catalysts. However, palladium under ultrahigh-vacuum conditions acts as a catalyst for both the cyclotrimerization of acetylene to benzene and the hydrogenation to ethylene. Neither nickel or platinum exhibit the ability to trimerize acetylene.[20] In Chapter III, catalytic reactions of acetylene on palladium single-crystal surfaces, such as hydrogenation, hydrosilation, and trimerization, will be discussed. The influence of surface crystallography and composition on these reactions, as well as the chemisorption of hydrogen, ethylene, and benzene, will also be discussed.

The chemistry of benzene and toluene has been investigated on nickel and platinum single-crystal surfaces by Dr. C. M. Friend[21]

and Dr. M-C. Tsai,[22] respectively. In this thesis (Chapter IV), these studies have been extended to the three low Miller-index surfaces of palladium, (111), (100), and (110). Mechanistic features of the carbon-hydrogen bond scission occurring in these molecules have been investigated through the use of selectively labeled compounds. A logical extension of these studies is to the chemisorption of other methylsubstituted benzenes on palladium surfaces. The molecules investigated were the three isomers of dimethylbenzene; ortho-, meta-, and paraxylene; and 1,3,5-trimethylbenzene.

The synthesis of compounds containing silicon-carbon multiple bonds has been of a great deal of interest to both the experimental[23] and theoretical[24] community. In Chapter V, the chemistry of organosilanes on palladium single-crystal surfaces will be discussed. Palladium single-crystal surfaces have provided novel routes to these highly reactive unsaturated organosilicon compounds.

Surface chemistry of thiophene and methylsubstituted thiophenes is the subject of Chapter VI. Chemisorption studies of thiophene have both scientific and technology importance. Thiophene is a suitable model to probe the influence of a heteroatom, sulfur, on the carbon-hydrogen bond-breaking process occurring in aromatic molecules when chemisorbed on transition metal surfaces. The use of selectively labeled thiophene to investigate carbon-hydrogen bond scission will also be discussed. An interesting feature of the chemistry of chemisorbed thiophene and its methylsubstituted derivatives is the observation of hydrocarbon formation under ultrahigh-vacuum

conditions. A variety of transition metal catalysts are useful for hydrodesulfurization of petroleum feedstocks.[25] These catalysts will become more important as the quality of the world's supply of petroleum decreases. Palladium single-crystal surfaces provide a unique opportunity to study the influence of surface crystallography (structure) and composition on desulfurization reactions in the well-defined environment of ultrahigh vacuum.

Palladium single-crystal surfaces have been effective catalysts for a variety of catalytic reactions.[26] In Chapter VIII, reactions such as hydrogenation of alkynes, cyclotrimerization reactions, and dehydrogenation of cyclic olefins will be discussed. The influence of pressure on chemistry of unsaturated hydrocarbons will also be discussed.

REFERENCES

1. Enclocypedia Americana, Vol. 6, Americana Corp., New York, 1965, p. 43.

2. G. A. Somorjai, Chemistry in Two Dimensions: Surfaces, Cornell University Press, Ithaca, New York, 1981, p. 381.

3. (a) J. E. Germain, Catalytic Conversion of Hydrocarbons, Academic Press, New York, 1969; (b) H. Pines, The Chemistry of Catalytic Hydrocarbon Conversions, Academic Press, New York, 1981.

4. The selectivity of a catalyst is its ability to influence or direct one specific reaction occurring on the catalyst.

5. P. N. Rylander, Catalytic Hydrogenation over Platinum Metals, Academic Press, New York, 1967.

6. The activity of a catalyst is related to the increase in the rate of reaction(s) occurring on the surface affected by the presence of the catalyst.

7. (a) C. H. Bartholowmew, P. T. Agrawal, and J. R. Katzer, Advances in Catalysis, D. D. Eley, H. Pines, and P. B. Weisz, eds., Academic Press, New York, 1982, p. 135; (b) B. Imelik et al., Metal-Support and Metal-Additive Effects in Catalysis, Elsevier Scientific Publishing Co., New York, 1982; (c) E. B. Maxted, Advances in Catalysis, Vol. 3, 1951, p. 129; (d) M. Shelef, K. Otto, and N. C. Otto, Advances in Catalysis, Vol. 27, 1978, p. 311.

8. An adatom is defined as an element chemisorbed on a transition metal surface. In this thesis the four adatoms studied were silicon, phosphorus, sulfur, and chlorine.

9. D. F. Klemperer, Chemisorption and Reactions on Metallic Films, J. R. Anderson, Ed., Academic Press, New York, 1971, pp. 40-117.

10. G. A. Somorjai, Chemistry in Two Dimensions: Surfaces, Cornell University Press, New York, 1981, pp. 126-283.

11. P. A. Redhead, Vacuum 1962, 12, 203.

12. (a) E. L. Muetterties, Angew. Chem. Int. Ed. Engl. 1978, 17, 645; (b) C. M. Friend, R. M. Gavin, E. L. Muetterties, and M. C. Tsai, J. Am. Chem. Soc. 1980, 102, 1717; (c) E. L. Muetterties, Pure and Applied Chem. 1981, 52, 2061; (d) C. M. Friend, J. Stein, and E. L. Muetterties, J. Am. Chem. Soc. 1981, 103, 773.

13. R. G. Wilkins, The Study of Kinetics and Mechanisms of Transition Metal Complexes, Allyn and Bacon Inc., Boston, 1974, p. 181.

14. (a) T. E. Fischer, S. R. Kelemen, and H. P. Bonzel, Surf. Sci. 1977, 64, 151-175; (b) J. E. Demuth, Surf. Sci. 1979, 84, 315-328; (c) J. E. Demuth, Surf. Sci. 1979, 80, 367-387; (d) J. E. Demuth, Chem. Phys. Lett. 1977, 45, 12-17; (e) T. E. Fischer and S. R. Kelemen, Surf. Sci. 1978, 74, 47-53; (f) W. J. Lo, Y. W. Chung, L. L. Kesmodel, P. C. Stair, and G. A. Somorjai, Solid State Commun. 1977, 22, 335-337; (g) A. E. Morgan and G. A. Somorjai, J. Chem. Phys. 1969, 51, 3309-3320; (h) L. L. Kesmodel, P. C. Stair, R. C. Baetzold, and G. A. Somorjai, Phys. Rev. Lett. 1976, 36, 1316-1319; (i) P.C. Stair and G. A. Somorjai, J. Chem. Phys. 1977, 66, 2036-2044; (j) L. L. Kesmodel, R. C. Baetzold, and G. A. Somorjai, Surf. Sci. 1977, 66, 299-320; (k) L. L. Kesmodel, L. H. Dubois, and G. A. Somorjai, Chem. Phys. Lett. 1978, 56, 267-271;

(l) L. L. Kesmodel, L. H. Dubois, and G. A. Somorjai, J. Chem. Phys. 1979, 70, 2180-2188; (m) H. Ibach, H. Hopster, and B. Sexton, Appl. Phys. 1977, 14, 21-24; (n) H. Ibach, H. Hopster, and B. Sexton, Appl. Surf. Sci. 1977, 1, 1-24; (o) H. Ibach and S. Lehwald, J. Vac. Sci. Technol. 1978, 15, 407-415; (p) A. M. Baro and H. Ibach, J. Chem. Phys. 1981, 74, 4194-4199; (q) T. E. Felter and W. H. Weinberg, Surf. Sci. 1981, 103, 265-287; (r) M. H. Howard, S. F. A. Kettle, J. A. Oxton, D. B. Powell, N. Sheppard, and P. Skinner, J. Chem. Soc. Faraday Trans. 2 1981, 77, 397-404; (s) E. L. Muetterties, M.-C. Tsai, and S. R. Kelemen, Proc. Nat. Acad. Sci. USA 1981, 78, 6571.

15. T. M. Gentle and E. L. Muetterties, J. Phys. Chem. 1983, 87, 2469.
16. W. T. Tysoe, G. L. Nyberg, and R. M. Labert, Surf. Sci. 1983, 135, 128.
17. W. Sesselman, B. Woratschek, G. Ertl, and J. Kuppers, Surf. Sci. 1983, 130, 245.
18. J. A. Gates and L. L. Kesmodel, Surf. Sci. 1983, 124, 68.
19. G. W. Parshall, Homogeneous Catalysis, John Wiley and Sons, New York, 1980, p. 147.
20. D. B. Klarup, personal communication.
21. C. M. Friend, Surface Studies of Nickel, Ph.D. Thesis, University of California Berkeley, August 1981.
22. M.-C. Tsai, Hydrocarbon Surface Chemistry of Platinum and Nickel, Ph.D. Thesis, University of California Berkeley, August 1982.

23. (a) L. E. Gusel'nikov, N. S. Nametkin, and V. M. Vdouin, Acc. Chem. Res. 1975, 8, 18; (b) L. E. Gusel'nikov and N. S. Nametkin, Chem. Rev. 1979, 79, 529; (c) B. Coleman and M. Jones, Rev. Chem. Intermed. 1981, 4, 297.

24. H. F. Schaefer III, Acc. Chem. Res. 1982, 9, 283.

25. T. Ohtsuka, Catal. Rev. Sci. Eng. 1977, 16(2), 291.

26. T. M. Gentle, V. H. Grassian, D. B. Klarup, and E. L. Muetterties, J. Am. Chem. Soc. 1983, 105, 6766.

II. EXPERIMENTAL

In this section, the vacuum chamber and general procedures for experiments will be discussed. All experiments were performed in a stainless steel ultrahigh-vacuum chamber (Varian). A base pressure of $<1 \times 10^{-10}$ torr was routinely obtained by using five 40-liter/sec triode ion pumps (Varian). The pumping station was also equipped with a titanium sublimation pump and liquid-nitrogen-cooled sorption pumps for evacuation of the system from atmosphere. An auxiliary diffusion pump was also attached to the work chamber. During argon ion bombardment, the work chamber was isolated from the pumping station and pumped using the diffusion pump.

The work chamber is a standard Varian chamber (Model 981-2765) equipped with a four-grid LEED optics, which was also used as the retarding-field analyzer for AES experiments. A glancing-incidence electron gun was used for increased surface sensitivity in the AES experiments. A multiplexed quadrupole mass spectrometer was positioned to be in line of sight of the single-crystal sample. A shield, which was a 3-in. diameter tantalum disc with a 3/8-in. diameter hole in the center, was placed in front of the mass spectrometer probe. A glancing-incidence ion-bombardment gun was used for crystal cleaning.

Single-crystal samples of palladium were spark cut from feedstocks obtained from Lawrence Livermore Laboratory for the (100) and (110) surfaces, and from Metal Crystals Ltd., Cambridge, England, for the (111) surface. All crystals were oriented to within ±0.5 degree of

the desired crystallographic plane using Laue x-ray back-reflection diffraction. The crystals were typically 3/8-in. diameter discs approximately 1/10 in. thick. After they were oriented, the crystals were polished using the following procedure: (a) The crystals were first rough polished on four grades of emery papers (0 through 0000). (2) The crystals were polished using 1-μm diamond paste (Buelher) on a felt-covered polishing wheel. (3) In the last step, 1/4-μm diamond paste on a felt-covered wheel was used to obtain the final polish. The above procedure produced a sample with a smooth, scratch-free mirror surface. Subsequent to use in the vacuum chamber, another Laue x-ray back-reflection photograph was taken to ensure that the desired orientation was maintained and, more importantly, that the surface was not disordered during the polishing process.

The crystals were mounted on a modified Varian manipulator, which allowed the sample to be heated to temperatures >1000°C by electron bombardment on the back side of the crystal and cooled to temperatures <-130°C with liquid nitrogen. Linear heating rates were obtained in the temperature range of <-130°C to 500°C. At temperatures >500°C, the heating rate was no longer linear; however, this was not of great concern because very little chemistry was observed to occur above this temperature. A heating rate of 25°C/sec was commonly used.

The crystals were spot welded to tantalum plates (.005-in. thickness) to facilitate their mounting on the manipulator. The exposed surfaces of tantalum were minimized to reduce the possibility

of unwanted desorption from supports during thermal desorption experiments. The temperature of the crystal was measured with a chromel-alumel thermocouple directly spot welded to the crystal. The voltage output from the thermocouple was amplified to facilitate storage in the memory of the programmable peak selector used to control the mass spectrometer during thermal desorption and chemical displacement experiments. A circuit diagram of the amplifier is shown in Figure II-1.

The major impurities in the palladium single crystals were sulfur, phosphorus, and carbon. Sulfur and carbon were removed by oxygen treatments of 1×10^{-5} torr at 400-500°C. Annealing to ~800-900°C removed any oxygen remaining on the surface after these treatments. Phosphorus and silicon were removed by argon-ion bombardment (800 eV, 1×10^{-5} torr). Crystals were heated to 400-500°C during bombardment to increase the rate of segregation of the impurities to the surface. Small amounts of carbon were found to diffuse into the bulk upon heating to 600°C. After these treatments the surfaces were found to be clean by AES. Before experiments were performed, the LEED pattern was monitored to ensure that the surface was still well-ordered and of the desired crystallographic orientation. Chlorine impurities were found to be thermally desorbed from all palladium surfaces by annealing to >800°C.

Gases were introduced into the work chamber through two variable-leak valves (Varian Model 951-5106), which were positioned on either side of the mass spectrometer probe. Attached to the outlets of the

valves were lengths of 1/8-in. diameter stainless steel tubing, which allowed a directional flow of gases to the crystal surface. The distance from the end of the tube to the crystal surface was approximately 3/4 in. This type of dosing device increases the pressure of the gas in front of the crystal by an order of magnitude during the dosing process. This allows one to maintain relatively low base pressure ($<1 \times 10^{-9}$ torr) during dosing, which was important when low-temperature adsorption was used in thermal desorption experiments. Exposures from these dosers were calibrated using thermal desorption spectroscopy.

The surface coverage of the various adatoms studied was determined using AES. The surface coverage of an adatom, θ_a, was calculated from the Auger spectrum using equation 1,[1]

$$\theta_a = \left\{ I(a)/S(a)/[I(a)/S(o) + I(Pd)/S(Pd)] \right\}, \qquad (1)$$

where I(a) is the intensity of the adatom AES signal, S(a) is the AES sensitivity factor of the adatom, I(Pd) is the intensity of 330-eV AES signal of palladium, and S(Pd) is the sensitivity of the 330-eV signal of palladium. The adatom-covered surfaces were prepared by adsorption of gases containing the desired adatom, typically hydrides, and were annealed to remove hydrogen. Siline (SiH_4), phosphine (PH_3), and hydrogen sulfide (H_2S) were used to deposit silicon, phosphorous, and sulfur, respectively, by adsorption at temperatures below -120°C. After adsorption, the crystal was heated to 500°C. Thiophene was also

used to deposit sulfur on the surface. After adsorption of thiophene, heating the crystal resulted in diffusion of the residual carbon into the bulk at temperatures >600°C.[2] Chlorine gas (Cl_2) was used to prepare chlorine-covered surfaces.

The composition of the gas phase during thermal desorption experiments was monitored using a quadrupole mass spectrometer (UTI Model 100C). Interfacing the mass spectrometer with a UTI programmable peak selector (PPS) allowed as many as nine masses to be monitored during the thermal desorption experiment. It was found that the optimal signal-to-noise ratio was achieved when only four or five masses were monitored. The temperature of the crystal during the thermal desorption experiment was stored in the memory of the PPS to aid in analysis of the spectra. The signal from the thermocouple was amplified by factor of 25 using the amplifier described in Figure II-1.

The following procedure was used for thermal desorption experiments using low temperature adsorption. After the crystal was cleaned or the desired adatom-covered surface was prepared, the crystal was cooled to the temperature of adsorption, typically to <-120°C. After cooling, the crystal was heated rapidly to 500°C to desorb gases adsorbed from the ambient, usually hydrogen and carbon monoxide. When the crystal returned to the desired adsorption temperature, the molecule of interest was adsorbed using the directional doser described previously. The crystal was placed in front of the shielded mass spectrometer probe, and after the base pressure of the chamber returned to the preexposure condition, the crystal was heated rapidly

Figure II-1. Circuit diagram of isolated thermocouple amplifier. This device was designed and built by the MMRD Electronics Shop staff.

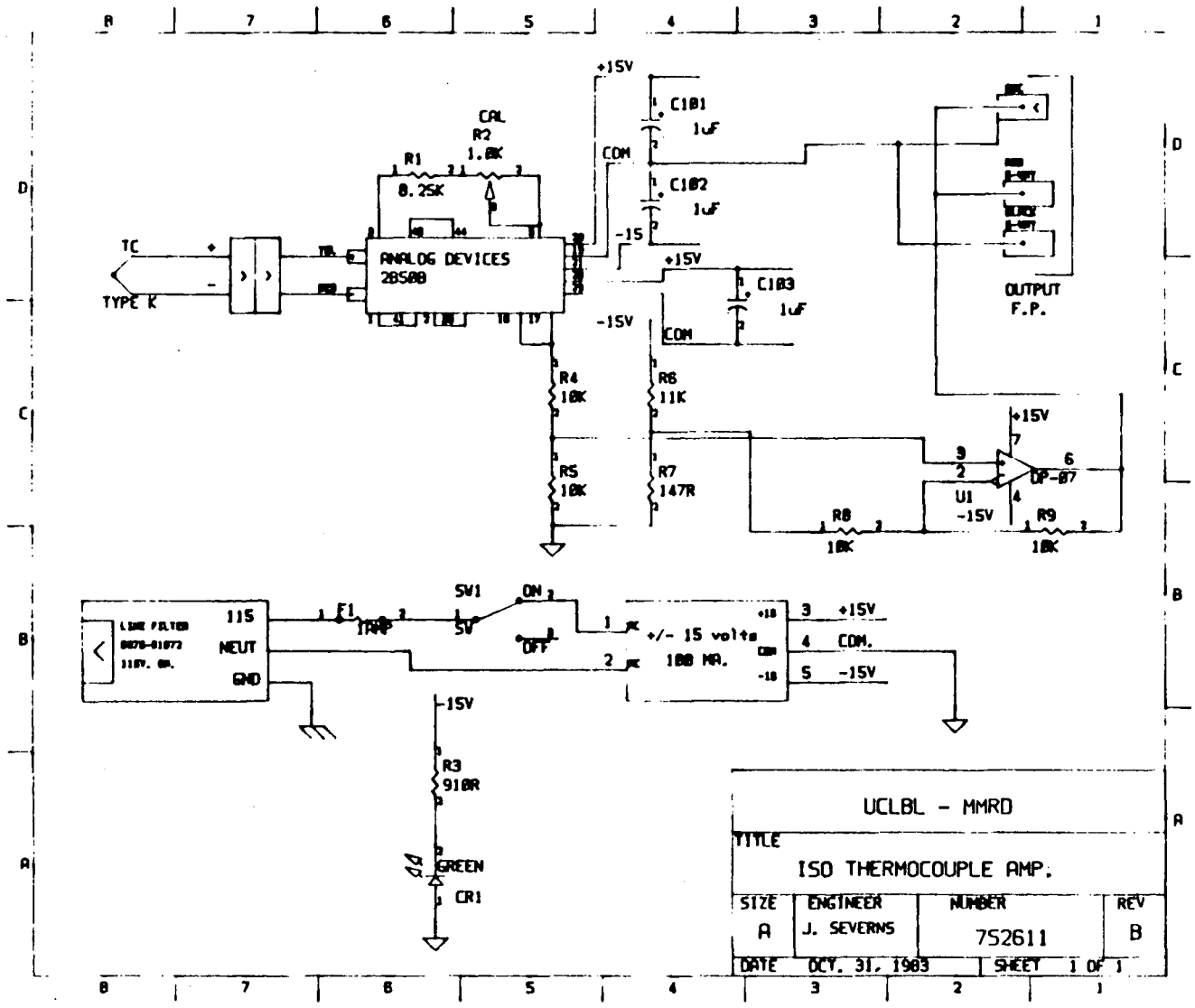
+15V
CAL
R2
1.8K
R1
8.25K
C101
1uF
COM
C102
1uF
-15
+15V
C103
1uF
-15V
COM
TC
+
-
TYPE K
ANALOG DEVICES
2B50B
OUTPUT
F.P.
R4
10K
R5
10K
R6
11K
R7
147R
+15V
U1
OP-07
-15V
R8
10K
R9
10K
115
NEUT
GND
F1
1AMP
SV1
ON
OFF
SV
+/- 15 volts
100 MA.
+15V
COM.
-15V
-15V
R3
910R
GREEN
CR1
UCLBL - MMRD
TITLE
ISO THERMOCOUPLE AMP.
SIZE
A
ENGINEER
J. SEVERNS
NUMBER
752611
REV
B
DATE
OCT. 31, 1983
SHEET 1 OF 1

XBL 845-2067

(usually at a rate of 25°C/sec) while the gas phase was monitored with the mass spectrometer-PPS system.

The experimental protocol for chemical displacement reactions was as follows: (1) The crystal was dosed with the adsorbate to be studied. (2) The crystal was rotated to a position halfway between the mass spectrometer probe and the other doser. (3) The displacing agent, typically trimethylphosphine, was introduced in the vacuum chamber while the gas phase was monitored using the mass spectrometer-PPS system.

All hydrocarbon reagents were research grade. Sources of these reagents are listed in Table II-1. In Table II-2 the sources of organosilane reagents are listed. The purity of all reagents was monitored using mass spectrometry; no impurities were detected.

In the following chapter, specific experimental details will be discussed when appropriate.

Table II-1. Sources of Hydrocarbon Reagents

Compound	Source
Acetylene	Matheson
Ethylene	Matheson
Benzene	Mallinkrodt, Inc.
Toluene	Mallinkrodt, Inc.
d^3toluene	Merck and Co.
d^{10}orthoxylene	Aldrich Chemical Co.
d^{10}paraxylene	Aldrich Chemical Co.
Metaxylene	Fisher Scientific Co.
d^6orthoxylene	Prepared by R. Lum
d^6metaxylene	Prepared by R. Lum
d^6orthoxylene	Aldrich Chemical Co.
Thiophene	Aldrich Chemical Co.
3-methylthiophene	Aldrich Chemical Co.
2,5-dimethylthiophene	Aldrich Chemical Co.
2,5-dideuterothiophene	Prepared by R. Lum
Cyclohexene	Wiley Organics
1-methylcyclohexene	Wiley Organics
3-methylcyclohexene	Wiley Organics
4-methylcyclohexene	Wiley Organics
Methylenecyclohexane	Wiley Organics
1,3,5-trimethylbenzene	Aldrich Chemical Co.

Table II-2. Sources of Organosilane Reagents

Compound	Source
Trimethylsilane	Petrach Systems, Inc.
Tetramethylsilane	Aldrich Chemical Co.
Silacyclohexane	Prepared by Dr. M. Elsheikh
Silacyclobutane	Supplied by Prof. T. Barton
Hexamethyldisilane	PCR Research Chemicals
Hexamethyldisiloxane	PCR Research Chemicals
Hexamethyldisilazane	PCR Research Chemicals
Chlorodimethylsilane	PCR Research Chemicals

REFERENCES

1. S. Mroczowski and D. Luhtman, Surf. Sci. 1983, 131, 159.

2. W. T. Tysoe, Ph.D. Thesis, Cambridge, England, 1982.

III. THE INFLUENCE OF ADATOMS ON THE CHEMISTRY OF ACETYLENE, ETHYLENE, AND BENZENE OCCURRING ON PALLADIUM SINGLE-CRYSTAL SURFACES

Studies of the chemistry of unsaturated hydrocarbons on transition metal surfaces have both scientific and technological importance. Acetylene, C_2H_2, is the simplest unsaturated hydrocarbon and provides a useful model to probe the chemistry of this class of compounds. Nickel, palladium, and platinum are known to be good catalysts for reactions of unsaturated hydrocarbons.[1] Acetylene chemisorbed on nickel and platinum has been the subject of a number of surface-science studies.[2] On nickel, acetylene chemisorption was largely irreversible. Spectroscopic studies identified the formation of methylidyne, CH, on Ni(111). Formation of ethylidyne, $\equiv CCH_3$, has been established on Pt(111). Recently, studies of chemisorbed acetylene on palladium have been reported.[3] In contrast to nickel and platinum, palladium exhibited both hydrogenation and trimerization. Palladium affords a unique opportunity to investigate catalytic reactions of acetylene that usually occur at pressures many orders of magnitude higher, under ultrahigh-vacuum conditions. In this chapter, the chemisorption of acetylene was investigated as a function of surface crystallography and composition. The effect of composition was investigated by the adsorption of the following adatoms: silicon, phosphorous, sulfur, and chlorine. Hydrogen, ethylene, and benzene were formed in the thermal desorption of chemisorbed acetylene. The chemisorption of these three molecules was also investigated on both clean and adatom-covered single-crystal surfaces.

The adatoms studied--silicon, phosphorus, sulfur, and chlorine--are known to have a marked influence on the behavior of transition metal catalysts. The presence of these adatoms has been known to be poisons for some reactions of hydrocarbons and promotors for others. Similar behavior has been observed in the ultrahigh-vacuum studies in this chapter.

RESULTS

A. Pd(111)--X--C_2H_2, where x = Si, P, S, or Cl

On clean Pd(111), chemisorbed acetylene (4.0 L) was found to undergo (a) decomposition to H_2 and surface carbon, (b) hydrogenation of acetylene to ethylene, (c) cyclotrimerization of acetylene to benzene, and (d) reversible chemisorption. A hydrogen thermal desorption maximum at 180°C was seen, with a broad plateau-like tail from 215°C to 400°C (see Figure III-1); ethylene desorbed at maximum rate at 35°C, and benzene maxima were observed at -25°C and 220°C. The presence of silicon did not substantially alter the chemistry of acetylene. At a silicon coverage of 0.25 monolayer, a decrease in the hydrogen thermal desorption maximum was observed (see Figure III-2). Phosphided Pd(111) results in an increase in the yield of benzene along with complex changes in the thermal desorption spectrum of benzene from acetylene. At a phosphorous coverage, θ_p = 0.33, four benzene maxima were observed, at -70°C, 25°C, 125°C, and 195°C, as shown in Figure III-3.

Figure III-1. Chemisorbed acetylene, T_{ads} = -150°C, was found to undergo a variety of reactions when thermally desorbed from clean Pd(111). In this figure, the following reactions or processes are evident: hydrogenation to ethylene, cyclotrimerization to benzene, decomposition to carbon and hydrogen, and reversible or molecular desorption. An exposure of 4.0 L was used in this experiment.

Figure III-2. Silicon was found to have only a slight influence on the chemistry of a chemisorbed acetylene on Pd(111). Shown in this figure is the thermal desorption spectrum of C_2H_2, exposure = 4.0 L, from a surface with a silicon coverage of 0.25 monolayer. The only change observed was a decrease in the hydrogen desorbing from the surface.

Figure III-3. At a phosphorus coverage of 0.33 monolayer on Pd(111), the thermal desorption spectrum of chemisorbed acetylene, 4.0 L, is shown. A complex benzene thermal desorption spectrum is observed with multiple maxima. Compare the benzene trace in this figure with the benzene trace in Figure III-1.

Figure III-4. The amount of both ethylene and hydrogen desorbing from the surface was found to decrease on sulfur-covered Pd(111), θ_S = 0.19. Benzene increased, with three maxima, at -25°C, 160°C, and 205°C, as shown in this thermal desorption spectrum.

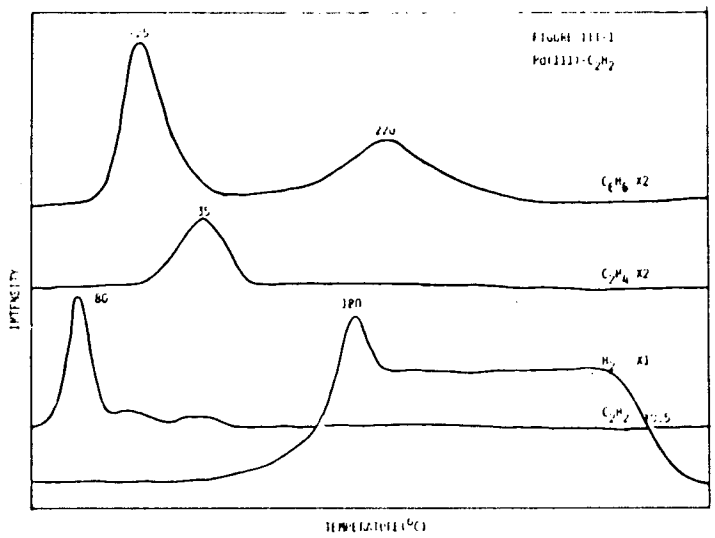
Figure III-1
Pd(111)-C_2H_2
C_6H_6 X2
C_2H_4 X2
H_2 X1
INTENSITY
TEMPERATURE (°C)

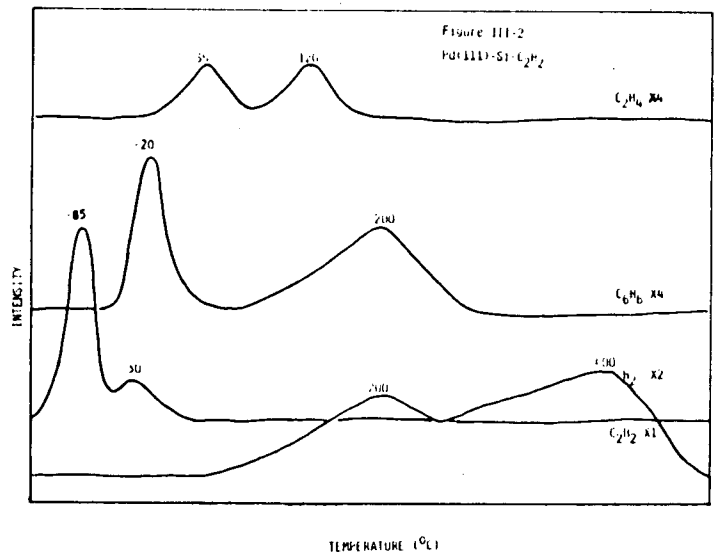
Figure III-2
Pd(111)-Si-C_2H_2
C_2H_4 X4
C_6H_6 X4
H_2 X2
C_2H_2 X1
INTENSITY
TEMPERATURE (°C)

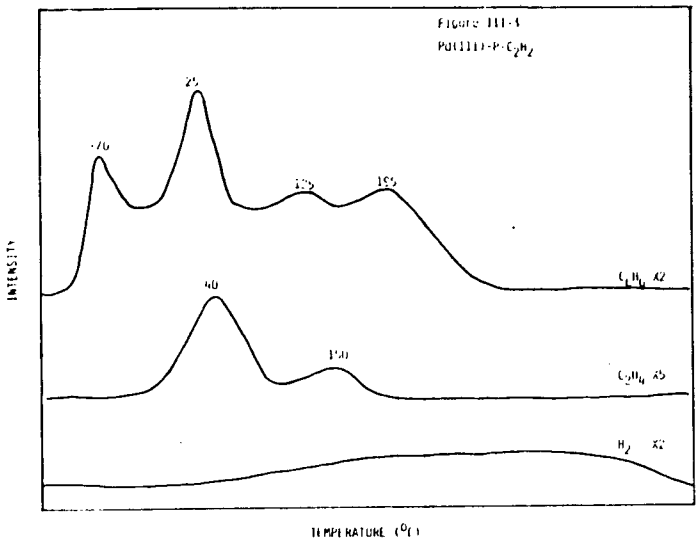
Figure III-4
Pd(111)-P-C_2H_2
C_6H_6 X2
C_2H_4 X5
H_2 X2
INTENSITY
TEMPERATURE (°C)

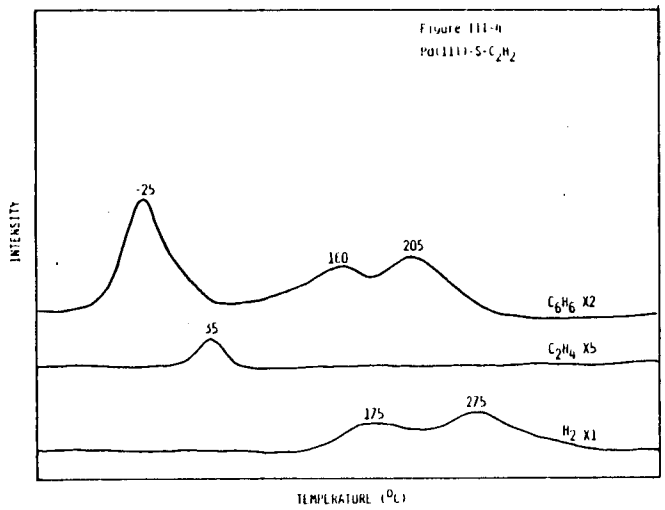
Figure III-6
Pd(111)-S-C_2H_2
C_6H_6 X2
C_2H_4 X5
H_2 X1
INTENSITY
TEMPERATURE (°C)

XBL 846-2202

Ethylene desorption maxima were observed at 40°C and 150°C. Sulfur was also found to influence the chemistry of chemisorption of acetylene on Pd(111). At a sulfur coverage of 0.20 monolayer, a decrease in the yield of ethylene, T_{max} = 35°C, and an increase in the yield of a benzene were observed (see Figure III-4). Three benzene thermal desorption maxima were observed, at -25°C, 160°C, and 205°C. At higher sulfur coverages, θ_S = 0.37, an increase in the yield of benzene was observed along with a shift to lower desorption temperatures. Benzene predominantly desorbs at a low temperature maximum at -15°C (see Figure III-5). Two weaker benzene maxima were observed, at 85°C and 155°C. The yield of ethylene was also found to decrease. At a sulfur coverage of 0.42 monolayer, two benzene maxima were observed, at -20°C and 90°C. The -20°C maximum was a factor of three more intense than the 90°C maximum. No ethylene desorption was observed (see Figure III-6). On chlorine-covered Pd(111), θ_{Cl} = 0.09, the fraction of benzene formed from the trimerization of acetylene desorbing at higher temperatures was found to increase (see Figure III-7). Three benzene maxima were observed, at 0°C, 145°C, and 225°C. At chlorine coverage of 0.23 monolayer, no low temperature benzene was observed. Benzene desorption was observed in the high temperature maxima at 120°C and 270°C. An ethylene thermal desorption maximum at 45°C was also observed (see Figure III-8).

Figure III-5. Desorption of benzene shifted to lower temperatures with increased sulfur coverage, $\theta_S = 0.37$. A further decrease in the desorption of ethylene and hydrogen is observed.

Figure III-6. Trimerization of acetylene to benzene is the only reaction observed on Pd(111) with a sulfur coverage of 0.42 monolayer. Molecular desorption, $T_{max} = -90^{\circ}C$, was also observed but is not shown.

Figure III-7. Chlorine was found to favor the desorption of reactively formed benzene at higher temperatures. The thermal desorption spectrum of chemisorbed acetylene from chlorine-covered Pd(111), $\theta_{Cl} = 0.14$, is shown. Comparing the benzene trace in this figure with the trace in Figure III-1, the shift to the higher desorption temperature is apparent.

Figure III-8. Increasing the chlorine coverage to 0.23 monolayer on Pd(111) results in a benzene desorption only at high temperature. Two benzene maxima were observed, at 120°C and 220°C, as compared to the two maxima at -25°C and 220°C on the clean surface.

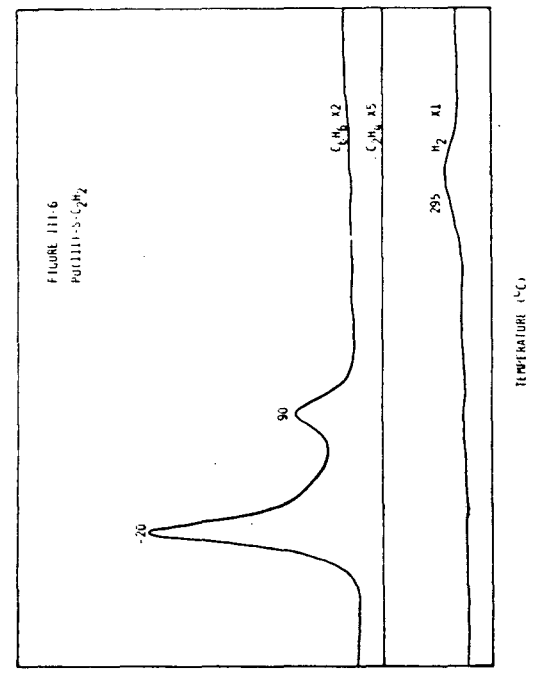
FIGURE III-6
Pd(111)-S-C_2H_2
C_6H_6 X2
C_2H_4 X5
H_2 X1
-20
90
295
INTENSITY
TEMPERATURE (°C)

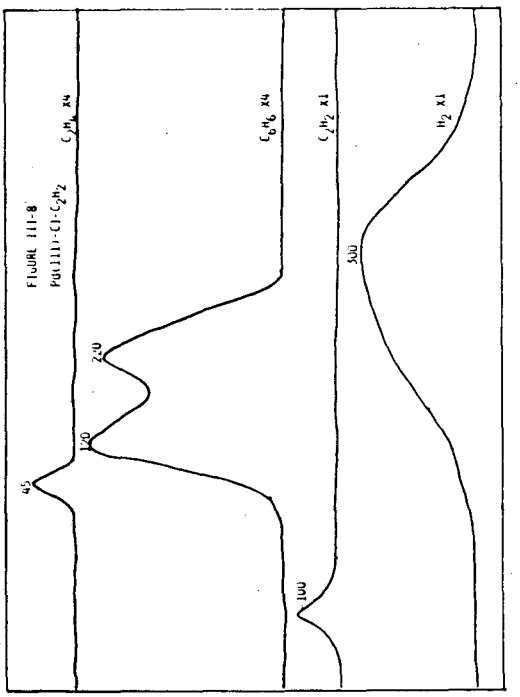
FIGURE III-8
Pd(111)-Cl-C_2H_2
C_2H_4 X4
C_6H_6 X4
C_2H_2 X1
H_2 X1
45
120
240
100
300
INTENSITY
TEMPERATURE (°C)

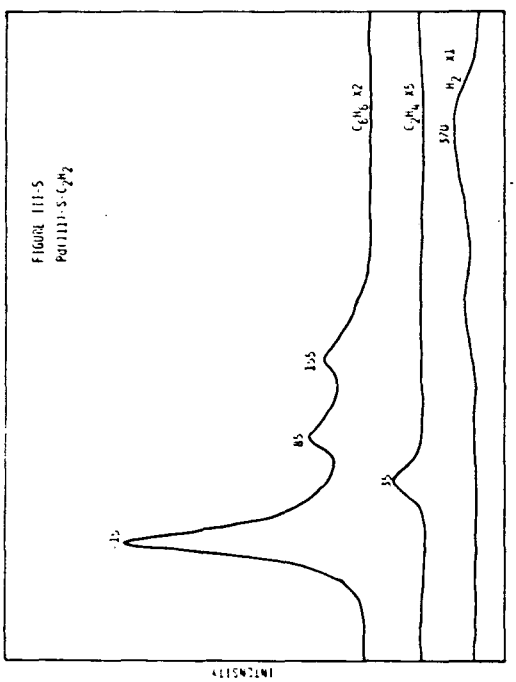
FIGURE III-5
Pd(111)-S-C_2H_2
C_6H_6 X2
C_2H_4 X5
H_2 X1
-12
85
155
35
370
INTENSITY
TEMPERATURE (°C)

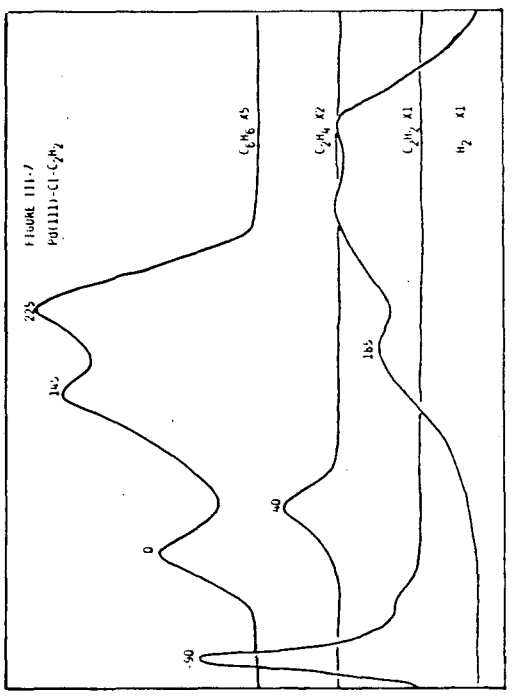
FIGURE III-7
Pd(111)-Cl-C_2H_2
C_6H_6 X5
C_2H_4 X2
C_2H_2 X1
H_2 X1
-50
0
145
225
40
185
INTENSITY
TEMPERATURE (°C)

XBL 846-2201

B. Pd(111) - x - H_2 - C_2H_2, where x = Si, P, S, or Cl

The hydrogenation of acetylene to ethylene was investigated on clean Pd(111) and on silicon-, phosphorus-, sulfur-, and chlorine-covered Pd(111). This reaction was performed by sequential adsorption of H_2 (3.0 L) followed by C_2H_2 (4.0 L) on the desired surface. On clean Pd(111), the subsequent thermal desorption spectrum exhibited an increased yield of ethylene, as compared to the thermal desorption of C_2H_2 from Pd(111). No benzene formation was observed (see Figure III-9). On silicon-covered Pd(111), θ_S = 0.24, a small increase in the yield of ethylene was observed, as compared to the clean surface. A weak benzene maximum was observed at 250°C (see Figure III-10). Phosphorus-covered Pd(111), θ_P = 0.24, produced nearly the same yield of ethylene as did the clean surface (see Figure III-11). No benzene formation was detected. The presence of sulfur on Pd(111) inhibited the hydrogenation of acetylene to ethylene. At a sulfur coverage of 0.40 monolayer, the yield of ethylene decreased by a factor of six as compared to the clean surface. Substantial amounts of benzene were found to desorb, with maxima at -15°C, 50°C, and 135°C (see Figure III-12). On chlorine-covered Pd(111), θ_{Cl} = 0.26, the yield of ethylene also decreased when compared to the clean surface, with T_{max} = 35°C. The yield of ethylene decreased by a factor of ~5. Two weak benzene maxima were observed, at 75°C and 200°C, as shown in Figure III-13.

Figure III-9. Sequential adsorption of hydrogen and acetylene, at -150°C, on clean Pd(111) resulted in an increased yield of ethylene as displayed in this figure. Another interesting facet of this reaction was the complete suppression of the trimerization reaction.

Figure III-10. The presence of silicon, $\theta_{Si} = 0.24$, on Pd(111) resulted in a slight increase in ethylene in the thermal desorption of coadsorbed hydrogen and acetylene. A small amount of benzene was observed to desorb from this surface.

Figure III-11. Phosphiding Pd(111), $\theta_P = 0.24$, did not substantially alter the thermal desorption spectrum obtained from the sequential adsorption of hydrogen and acetylene. Inhibition of the trimerization reaction is evident by the lack of benzene desorption, as shown in this spectrum.

Figure III-12. The hydrogenation of acetylene on Pd(111) was poisoned by the presence of sulfur. At a sulfur coverage of 0.40 monolayer, a dramatic decrease in the yield of ethylene and the amount of hydrogen desorption is shown. In contrast to the phosphorus-covered surface, significant quantities of benzene desorbed from this surface.

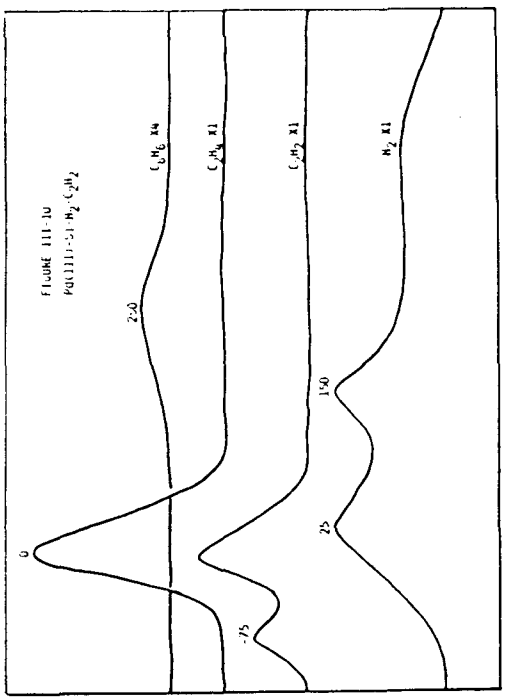
FIGURE III-10
Pd(111)-S-H2-C2H2
C6H6 X4
C2H4 X1
C2H2 X1
H2 X1
200
0
-75
150
25
INTENSITY
TEMPERATURE (°C)

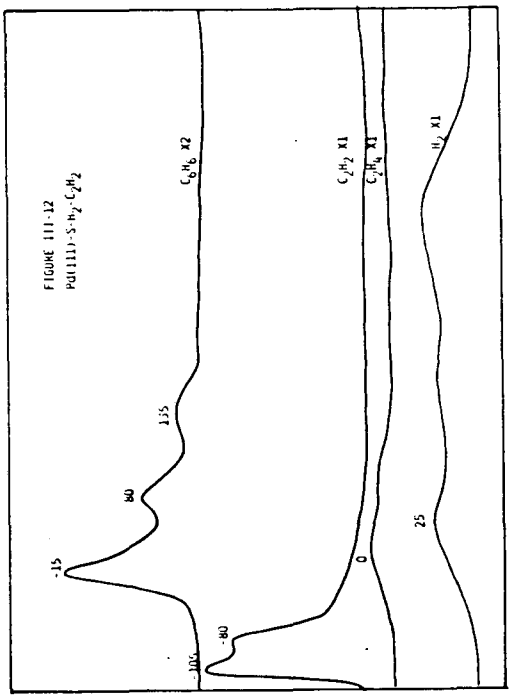
FIGURE III-12
Pd(111)-S-H2-C2H2
C6H6 X2
C2H2 X1
C2H4 X1
H2 X1
-15
90
135
-80
-105
0
25
INTENSITY
TEMPERATURE (°C)

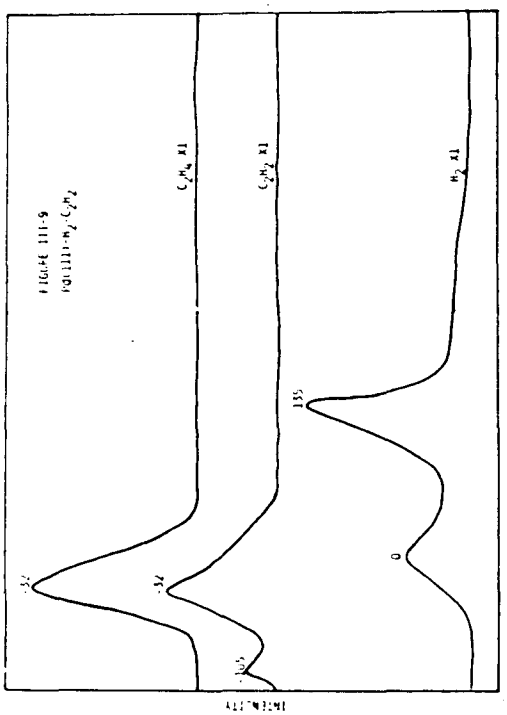
FIGURE III-9
Pd(111)-H2-C2H2
C2H4 X1
C2H2 X1
H2 X1
-34
-34
135
0
INTENSITY
TEMPERATURE (°C)

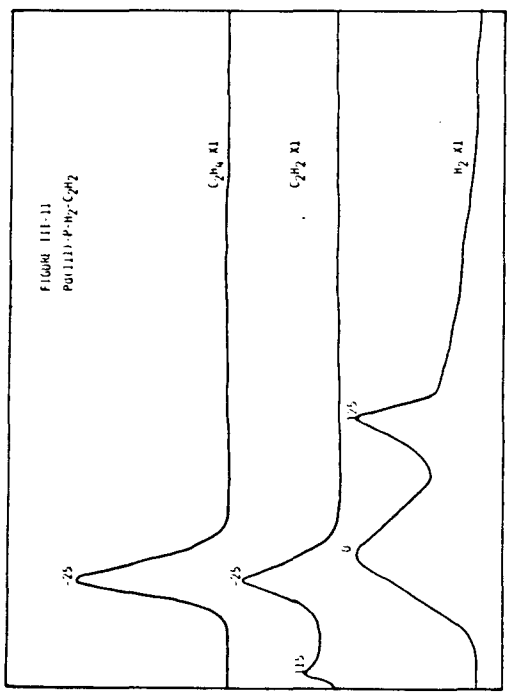
FIGURE III-11
Pd(111)-P-H2-C2H2
C2H4 X1
C2H2 X1
H2 X1
-25
-25
135
0
INTENSITY
TEMPERATURE (°C)

XBL 846-2200

Figure III-13. Chlorine also suppressed the hydrogenation of acetylene on Pd(111). At a chlorine coverage of 0.26 monolayer, a marked decrease in the amount of ethylene desorbing from the surface is observed.

Figure III-14. The sequential adsorption of deuterium and acetylene on Pd(111) leads to the formation of $C_2D_2H_2$ (30 amu). The intensities shown for 28 amu and 29 amu are due in large part to fragmentation of $C_2H_2D_2$. The yield of $C_2H_2D_2$ is found to be >90 percent.

Figure III-15. Siliciding Pd(111), $\theta_{Si} = 0.22$, did not alter the distribution of the ethylenes, $C_2D_xH_{4-x}$, obtained from the reaction of deuterium with acetylene. $C_2D_2H_2$ is the predominant species.

Figure III-16. Phosphiding Pd(111), $\theta_P = 0.24$, did not change the distribution of ethylenes, $C_2D_2H_2$ the major product, in the thermal desorption spectrum of chemisorbed deuterium and acetylene.

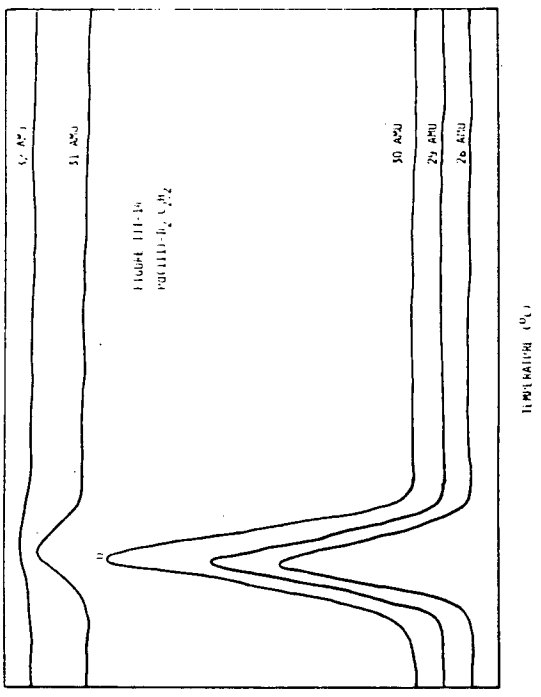
INTENSITY
TEMPERATURE (°C)
30 AMU
29 AMU
28 AMU

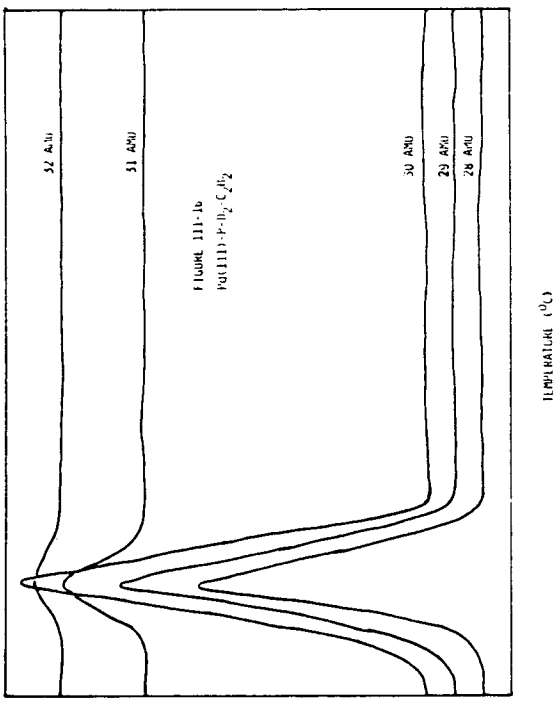
INTENSITY
TEMPERATURE (°C)
32 AMU
31 AMU
30 AMU
29 AMU
28 AMU

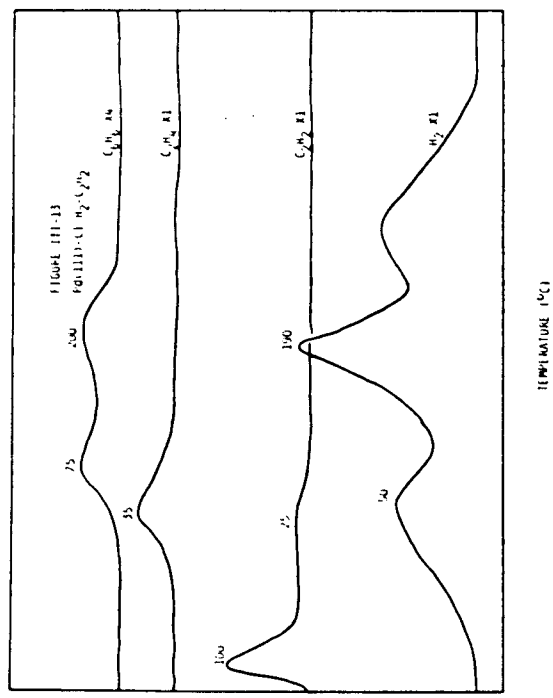
INTENSITY
TEMPERATURE (°C)
25
200
25
150
25
150

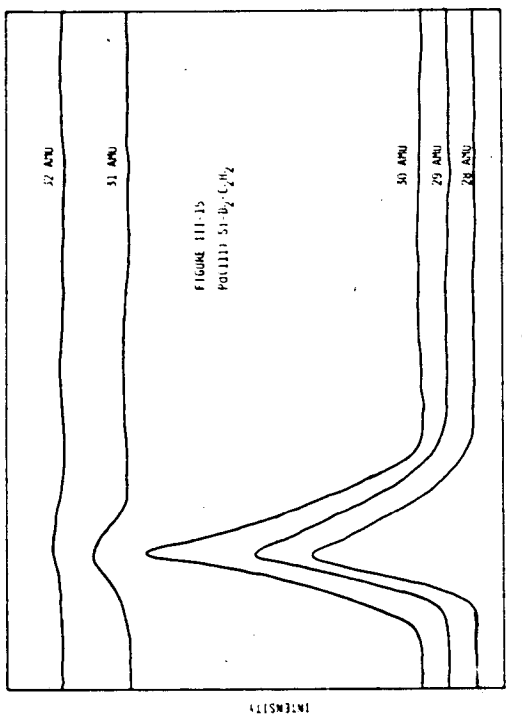
INTENSITY
TEMPERATURE (°C)
32 AMU
31 AMU
30 AMU
29 AMU
28 AMU

XBL 846-2199

Figure III-17. Although the presence of sulfur, $\theta_S = 0.41$, inhibited the hydrogenation of acetylene on Pd(111), the predominant ethylene formed in the reaction of D_2 with C_2H_2 was still $C_2D_2H_2$.

Figure III-18. Chlorine also inhibited the hydrogenation of acetylene on Pd(111), $\theta_{Cl} = 0.24$. The $C_2D_2H_2$ is the predominant species formed in the reaction of D_2 with C_2H_2.

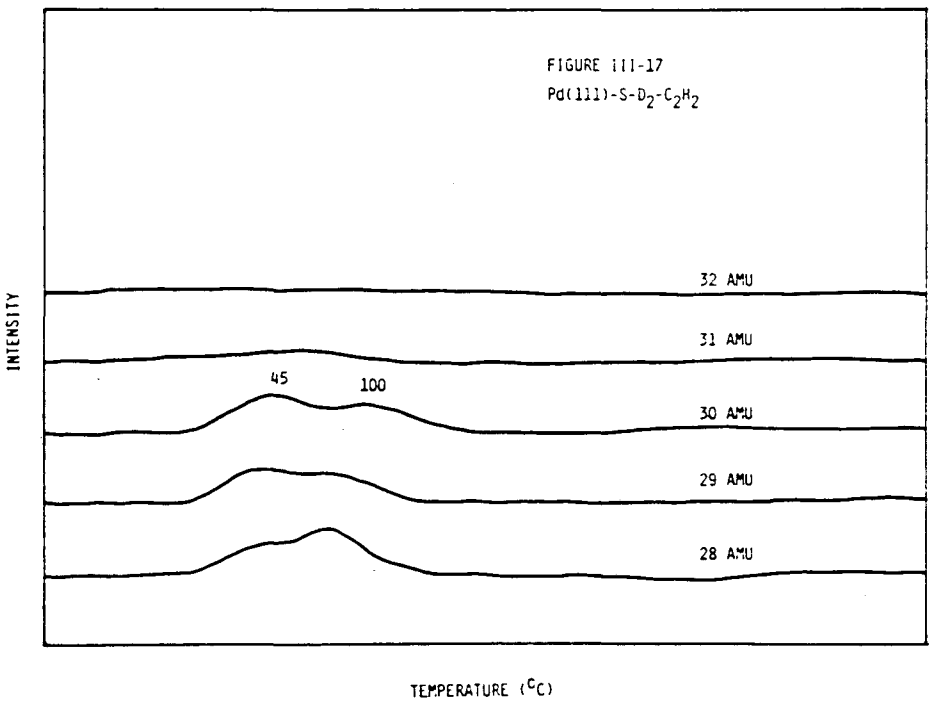
FIGURE III-17
Pd(111)-S-D_2-C_2H_2
32 AMU
31 AMU
45
100
30 AMU
29 AMU
28 AMU
INTENSITY
TEMPERATURE (°C)

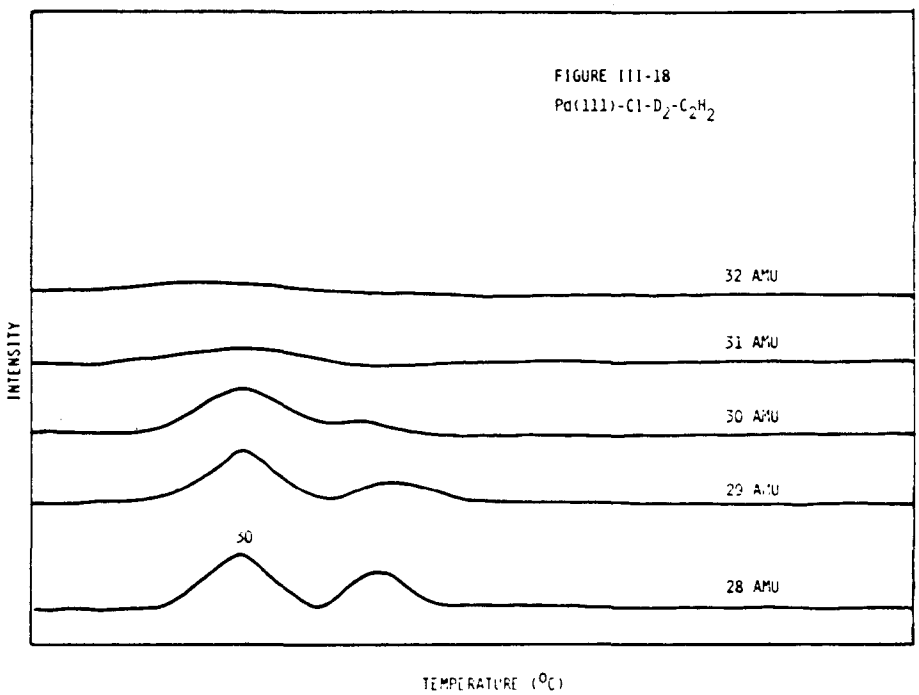
FIGURE III-18
Pd(111)-Cl-D_2-C_2H_2
32 AMU
31 AMU
30 AMU
29 AMU
50
28 AMU
INTENSITY
TEMPERATURE (°C)

XBL 846-2173

C. Pd(111) - X - D_2 - C_2H_2, where x = Si, P, S, or Cl

The hydrogenation of acetylene was investigated using deuterium on clean and silicon-, phosphorus-, sulfur-, and chlorine-covered Pd(111). As with the hydrogenation experiments, the reactions were performed by sequential adsorption of D_2 followed by acetylene. On the clean Pd(111), the predominent ethylene formed contained two deuteriums, $C_2D_2H_2$, giving a yield greater than 90 percent. On all of the other adatom-covered surfaces, $C_2H_2D_2$ was also found to be the major product (see Figures III-14 through III-18).

D. Pd(111) - X - C_2H_2 - $(CH_3)_3SiH$, where x = Si, P, S, or Cl

The hydrosilation of acetylene with trimethylsilane was investigated on both clean and adatom-covered surfaces. The reaction was performed by sequential adsorption of C_2H_2 followed by trimethylsilane. Along with the hydrosilation product (vinyltrimethylsilane), benzene and ethylene were also observed in the thermal desorption spectrum on clean Pd(111). An H_2 thermal desorption maximum with a broad plateau-like tail was observed at 175°C. Benzene desorbed with three maxima, at 25°C, 130°C, and 200°C. Both ethylene and vinyltrimethylsilane desorbed in a single maximum, at 50°C and 25°C, respectively (see Figure III-19). On silicon-covered Pd(111), Θ_{Si} = 0.20, the yield of vinyltrimethylsilane at T_{max} = 70°C increased by a factor of 2.5 (see Figure III-20). Benzene (T_{max} = -20°C and 200°C) and ethylene (T_{max} = 50°C) were also observed. Phosphided Pd(111), Θ_P = 0.21, increased the yield of vinyltrimethylsilane by a factor of 5.5. A vinyltrimethylsilane thermal maximum was

Figure III-19. The hydrosilation of acetylene, C_2H_2, with trimethylsilane, $(CH_3)_3SiH$, is affected on Pd(111) by sequential adsorption of C_2H_2 followed by $(CH_3)_3SiH$. Along with the hydrosilation product, vinyltrimethylsilane, both ethylene and benzene formation were observed in the thermal desorption experiment.

Figure III-20. Siliciding Pd(111), $\theta_{Si} = 0.20$, increased the yield of vinyltrimethylsilane in the thermal desorption of the surface state formed by sequential adsorption of acetylene and trimethylsilane. The formation of both ethylene and benzene was observed, as it was on the clean surface (see Figure III-19).

Figure III-21. A fivefold increase in the yield of vinyltrimethylsilane on a phosphided Pd(111) surface is illustrated. An increase in the yield of both ethylene and benzene was also observed at this phosphorus coverage, $\theta_P = 0.21$.

Figure III-22. The hydrosilation of acetylene with trimethylsilane was not markedly influenced by the presence of sulfur, $\theta_S = 0.21$. The desorption of benzene increased, while a decrease was observed for ethylene.

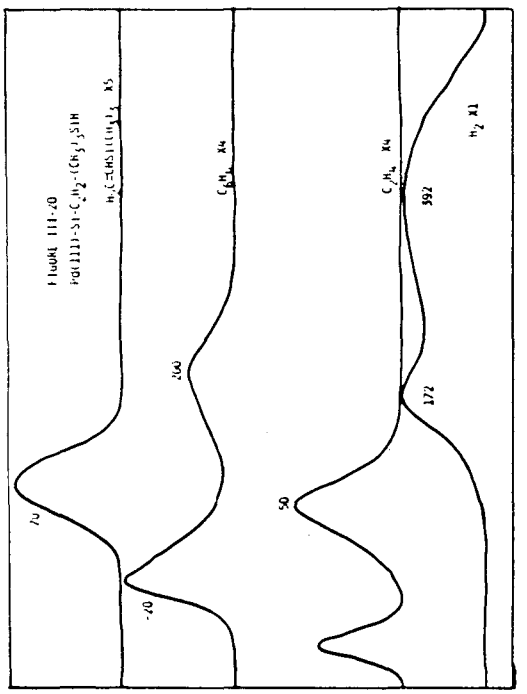
FIGURE III-20
INTENSITY
TEMPERATURE (°C)
-70
-20
50
200
172
392

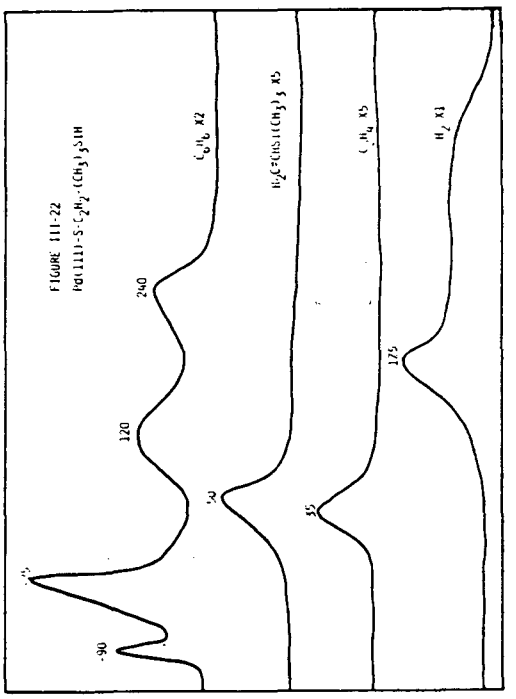
FIGURE III-22
INTENSITY
TEMPERATURE (°C)
-90
30
120
240
175

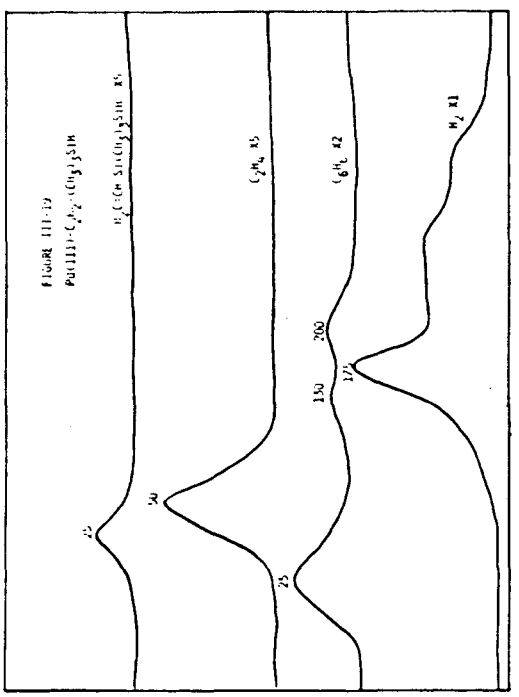
INTENSITY
TEMPERATURE (°C)
25
30
25
130
200
175

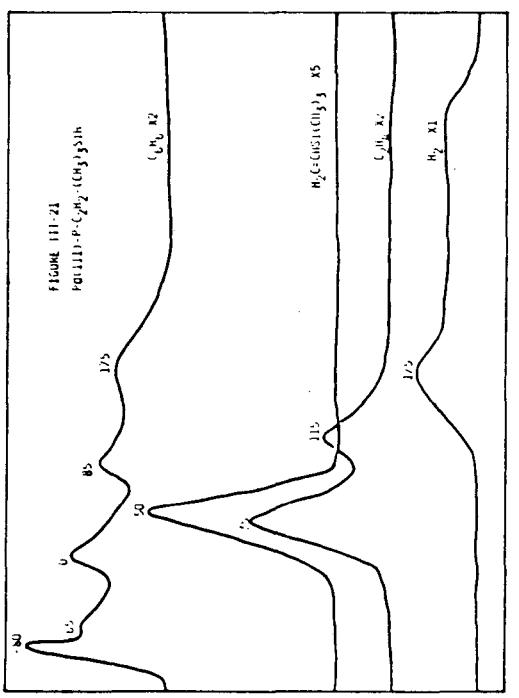
FIGURE III-21
INTENSITY
TEMPERATURE (°C)
-30
0
85
50
175
115
175

XBL 846-2198

Figure III-23. At a chlorine coverage of 0.25 monolayer, the yield of vinyltrimethylsilane from the thermal desorption of C_2H_2 and $(CH_3)_3SiH$ from Pd(111) was not significantly changed. Benzene was found to desorb at high temperatures.

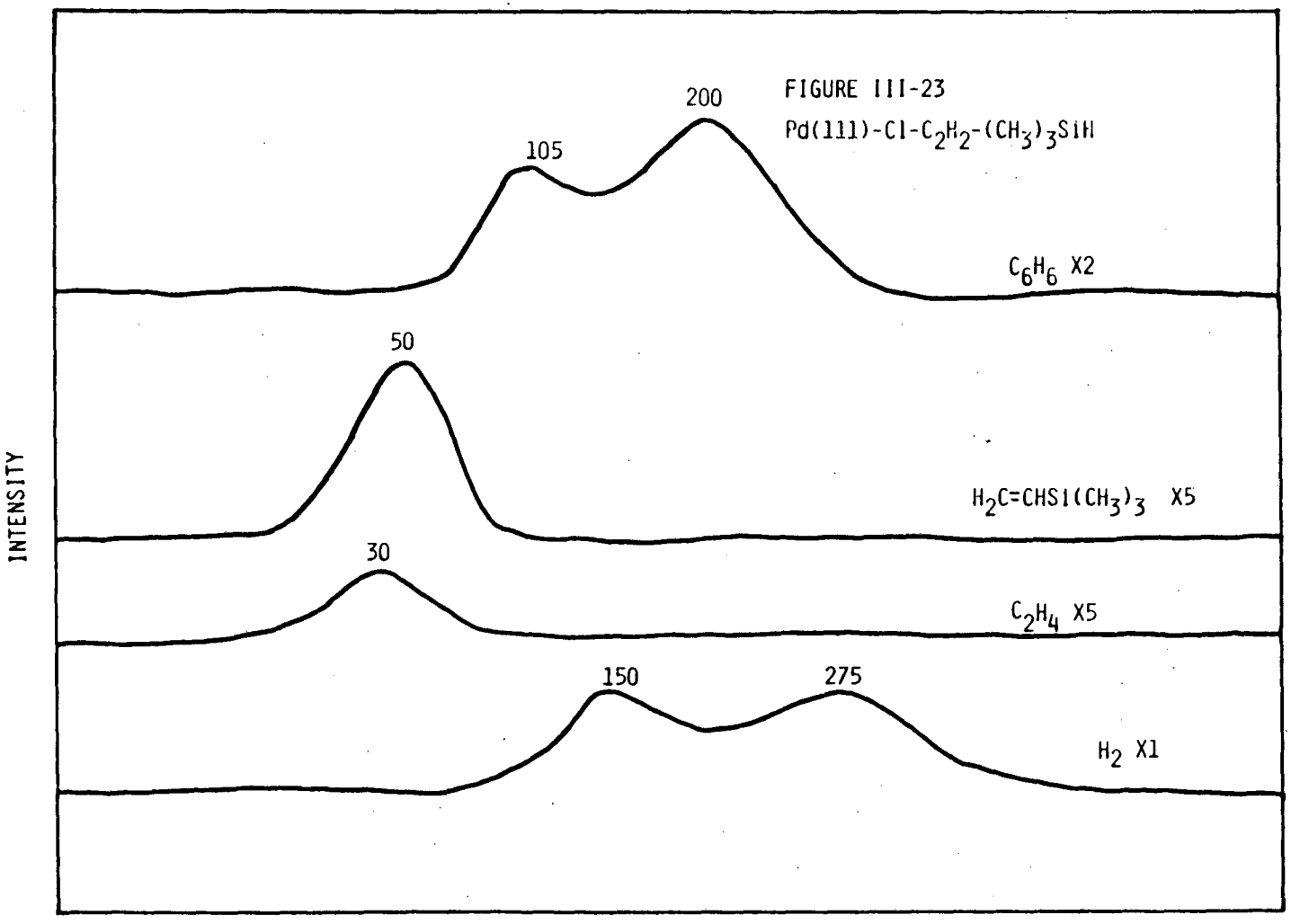
FIGURE III-23
Pd(111)-Cl-C_2H_2-$(CH_3)_3SiH$
200
105
C_6H_6 X2
50
$H_2C=CHSi(CH_3)_3$ X5
30
C_2H_4 X5
150
275
H_2 X1
INTENSITY
TEMPERATURE (^oC)

XBL 846-2169

Figure III-24. The thermal desorption of benzene from Pd(111) is shown at three exposures--1.0 L, 2.0 L, and 3.0 L--in Figures III-24A, III-24B, and III-24C, respectively. With increasing exposure and surface coverage, the fraction of benzene desorbing molecularly increased.

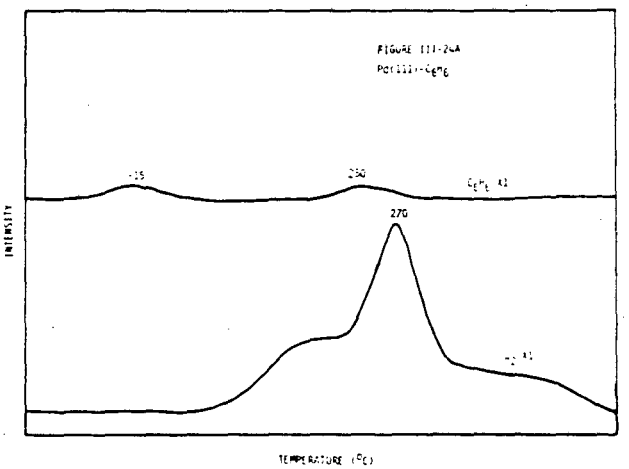
INTENSITY
270
TEMPERATURE (°C)

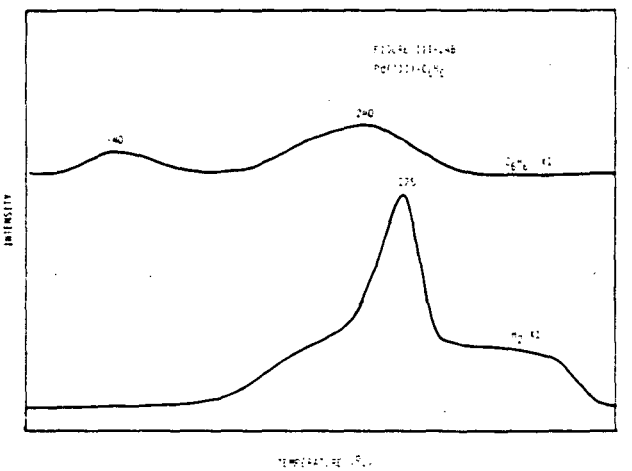
INTENSITY
240
235

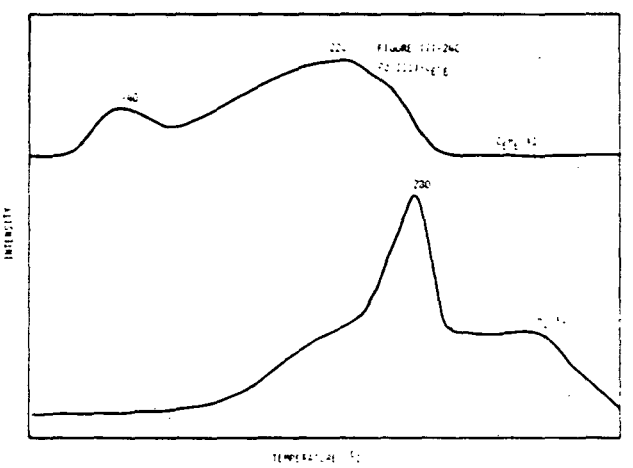
INTENSITY
230

XBL 846-2178

Figure III-25. The thermal desorption of benzene at an exposure of 1.0 L is shown at two silicon coverages, 0.18 monolayer (Figure III-25A) and 0.24 monolayer (Figure III-25B). The fraction of reversible chemisorption increased with silicon coverage (compare Figure III-25A with Figure III-25B).

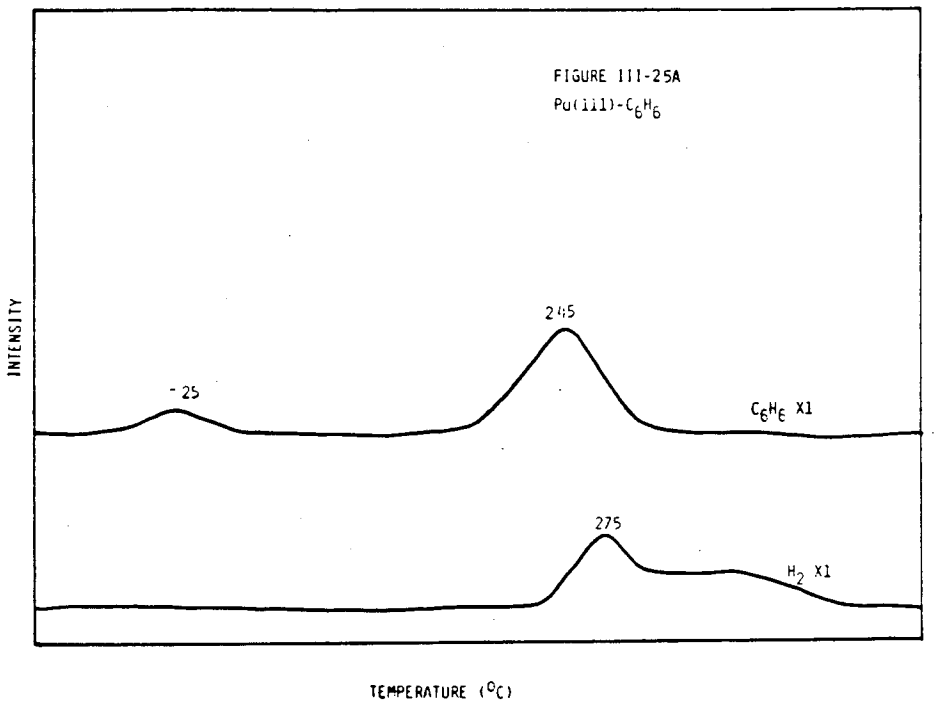
FIGURE III-25A
Pd(111)-C6H6
INTENSITY
245
-25
C6H6 X1
275
H2 X1
TEMPERATURE (°C)

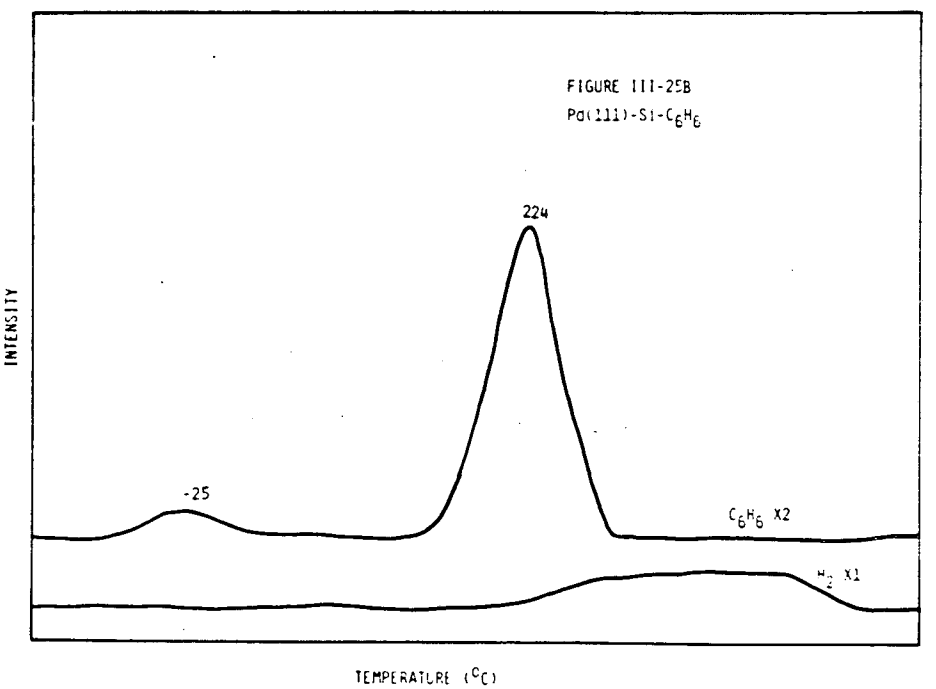
FIGURE III-25B
Pd(111)-Si-C6H6
INTENSITY
224
-25
C6H6 X2
H2 X1
TEMPERATURE (°C)

XBL 846-2172

observed at 50°C. Both ethylene and benzene were also observed. A complex thermal desorption spectrum for benzene was observed, with maxima at -80°C, -65°C, 0°C, 85°C, and 175°C. Ethylene exhibited two maxima, at 35°C and 115°C (see Figure III-21). Sulphided Pd(111), θ_S = 0.21, increased the yield of vinyltrimethylsilane only slightly. An increase of a factor of 1.6 was observed. A complex benzene thermal desorption spectrum was also observed, with maxima at -90°C, -25°C, 120°C, and 240°C (see Figure III-22). A single ethylene maximum was observed at 50°C. On a chlorine-covered Pd(111) surface, θ_{Cl} = 0.25, vinyltrimethylsilane exhibited a thermal desorption maximum at 50°C, with an intensity increased by a factor of 1.4 as compared to the clean surface. Two benzene maxima were observed, at 105°C and 200°C, and an ethylene maximum was observed at 30°C (see Figure III-23).

E. Pd(111) - X - C_6H_6, where X = Si, P, S, or Cl

The chemisorption of benzene on both clean and adatom-covered surfaces was investigated. On clean Pd(111) at low exposures (1.0 L), largely irreversible chemisorption was observed. An H_2 thermal desorption maximum was observed at 270°C, with a low temperature shoulder at 175°C and a broad high temperature tail. Two weak benzene thermal desorption maxima were observed, at -15°C and 250°C. At an exposure of 2.0 L, an increase in the amount of reversibly bound benzene was observed, with maxima at -40°C and 240°C. An H_2 maximum was observed at 275°C. At high exposures, 3.0 L, the reversible fraction continued to increase, with two maxima, at -40°C and 220°C. A hydrogen thermal desorption maximum was observed at 280°C (see

Figures III-24A through III-24C). At low benzene exposures, 1.0 L, the presence of adatoms was found to increase the fraction of reversibly bound benzene. On silicon-covered Pd(111), θ_{Si} = 0.18, two benzene maxima were observed, at -25°C and 245°C, and a hydrogen maximum was observed at 275°C (see Figure III-25A). Increasing the silicon coverage to 0.26 monolayer resulted in a marked increase in the high temperature maximum, T_{max} = 225°C, and a corresponding decrease in the amount of hydrogen desorption (see Figure III-25B). On phosphorus-covered Pd(111), θ_P = 0.39, two benzene maxima were observed, at -30°C and 225°C, and a hydrogen maximum was observed at 275°C (see Figure III-26A). Increasing the benzene exposure at this phosphorus coverage resulted in an increase in the fraction of reversibly bound benzene, characterized by maxima of 185°C and 155°C for exposures of 2.0 L and 3.0 L, respectively (see Figures III-26B and III-26C). Benzene desorbed in a broad plateau-like maximum from sulfur-covered Pd(111), θ_S = 0.35. The plateau extended from 45°C to 240°C (see Figure III-27). At a chlorine coverage of 0.07 monolayer, two benzene maxima were observed, at -25°C and 260°C, along with an H_2 maximum at 275°C (see Figure III-28A). The high temperature C_6H_6 maximum increased with increase in chlorine coverage, while the H_2 maximum decreased. At chlorine coverages of 0.16 and 0.24 monolayer, the high temperature C_6H_6 maximum was also observed at 260°C (see Figures III-28A and III-28B).

Figure III-26. Thermal desorption of benzene from phosphorus-covered Pd(111), θ_P = 0.39, at various exposures. Increasing the benzene exposure from 1.0 L (Figure III-26A) to 2.0 L (Figure III-26B), and finally to 3.0 L (Figure III-26C) results in an increase in the fraction of molecular desorption of benzene. Comparing clean (Figure III-24A) and phosphorus-covered Pd(111) (Figure III-26A) at the same benzene exposure, 1.0 L, more molecular desorption is observed on the phosphorus-covered surface.

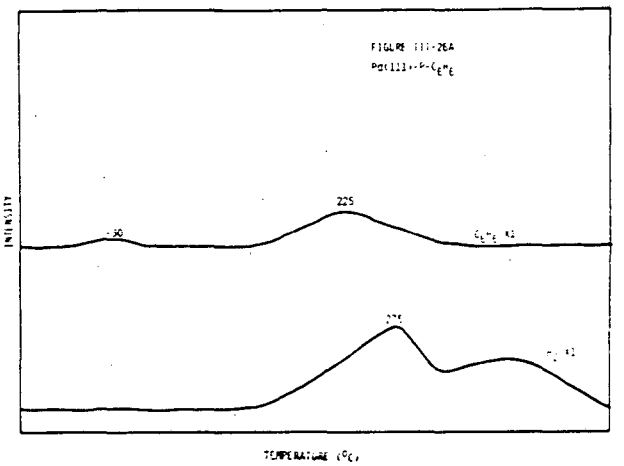
INTENSITY
225
TEMPERATURE (°C)

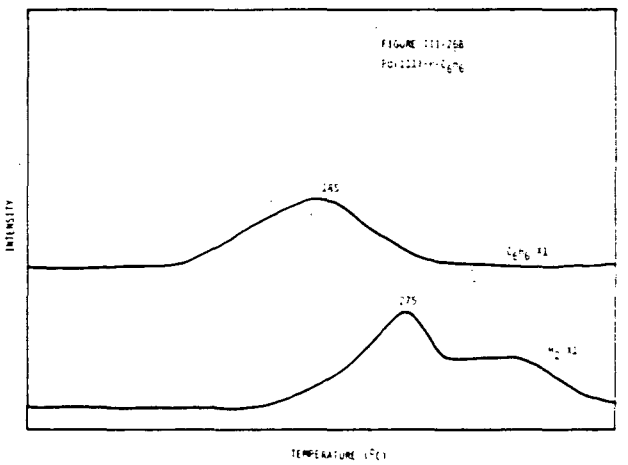
INTENSITY
245
275
TEMPERATURE (°C)

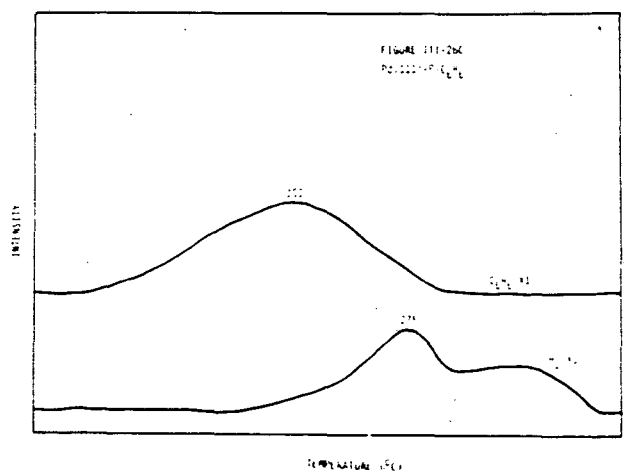
INTENSITY
TEMPERATURE (°C)

Figure III-27. On sulfur-covered Pd(111), θ_S = 0.35, benzene desorbs in a broad plateau-like maximum. At this benzene exposure, 1.0 L, a marked increase in the fraction of benzene desorbing intact is observed when compared to clean Pd(111). Compare this spectrum with Figure III-24A.

Figure III-28. The presence of chlorine results in an increase in the fraction of benzene reversibly chemisorbed. The thermal desorption spectrum of benzene from Pd(111) at three chlorine coverages is illustrated. In Figure III-28A the spectrum at a coverage of 0.07 monolayer is shown; in Figure III-28B 0.16 monolayer is shown, and in Figure III-28C 0.24 monolayer is shown. In contrast to phosphorus, increased chlorine coverage does not shift the high temperature benzene maximum to lower temperatures.

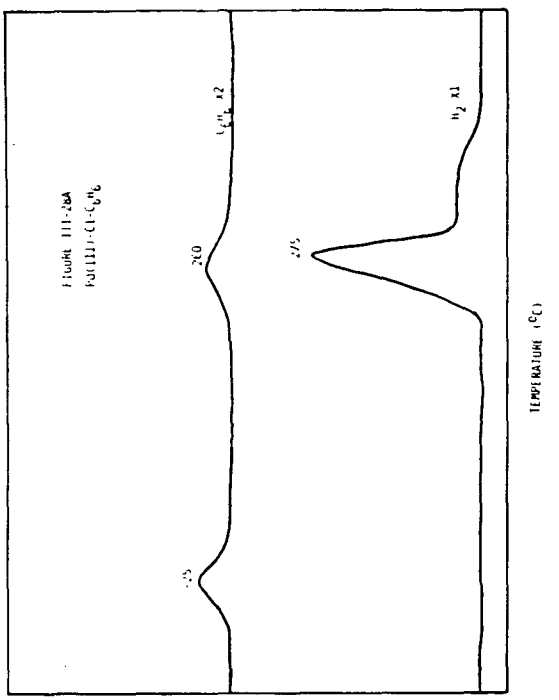
FIGURE III-26A
Pd(111)-Cl-C_6H_6
C_6H_6 X2
H_2 X1
240
275
INTENSITY
TEMPERATURE (°C)

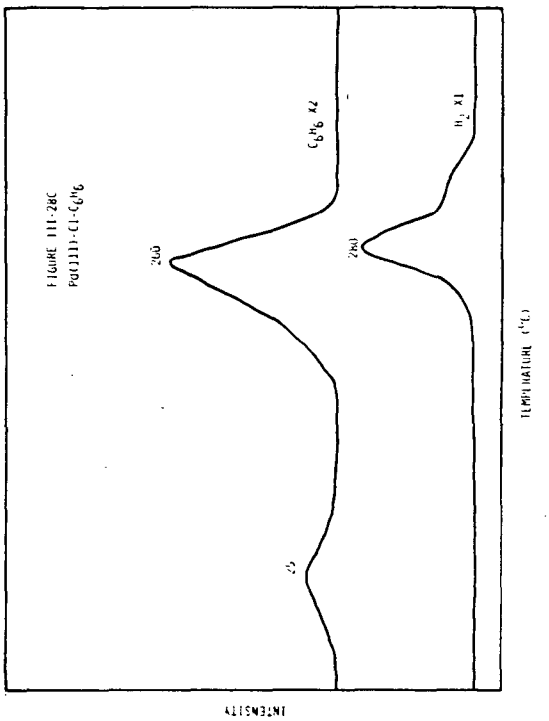
FIGURE III-26C
Pd(111)-Cl-C_6H_6
C_6H_6 X2
H_2 X1
260
280
INTENSITY
TEMPERATURE (°C)

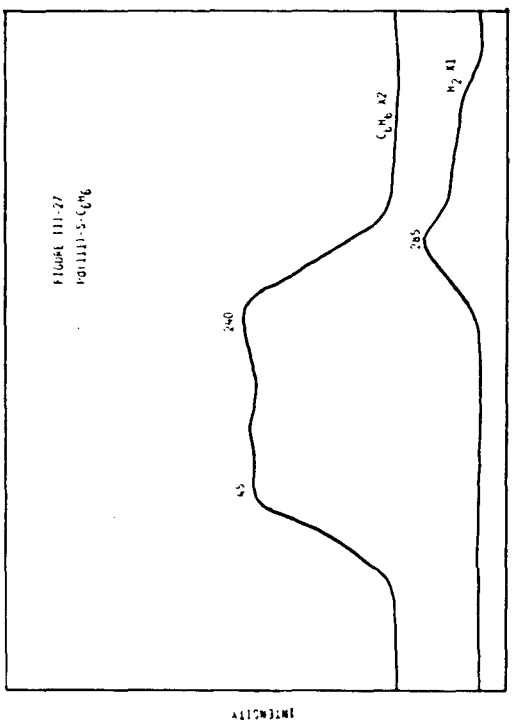
FIGURE III-27
Pd(111)-S-C_6H_6
C_6H_6 X2
H_2 X1
240
265
INTENSITY
TEMPERATURE (°C)

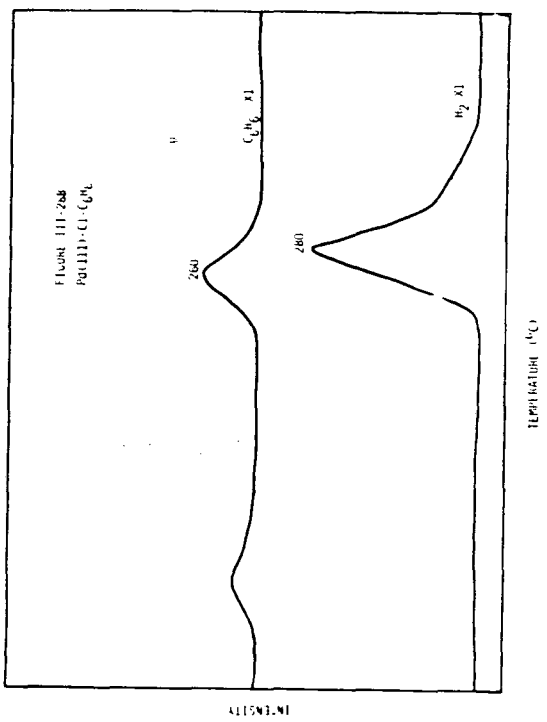
FIGURE III-26B
Pd(111)-Cl-C_6H_6
C_6H_6 X1
H_2 X1
260
280
INTENSITY
TEMPERATURE (°C)

XBL 846-2197

Figure III-29. At an exposure of 1.0 L, ethylene, both reversible and irreversible, is observed in the thermal desorption spectrum from Pd(111).

Figure III-30. The presence of silicon, $\theta_S = 0.15$, increased the fraction of benzene desorbing reversibly. In this thermal desorption experiment, 1.0 L of ethylene was adsorbed on the silicon-covered surface.

Figure III-31. Phosphorus increased the fraction of reversibly chemisorbed ethylene. In Figure III-31A the thermal desorption of ethylene, 1.0 L exposure, from a Pd(111) surface with 0.28 monolayer is shown. Nearly quantitative desorption is observed. At a higher phosphorus coverage, $\theta_P = 0.44$, quantitative desorption is observed, as illustrated in Figure III-31B.

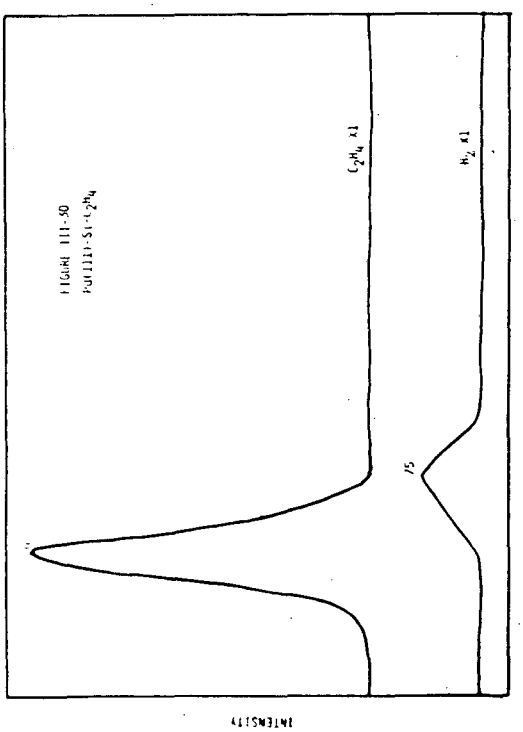
FIGURE III-30
Pd(111)-Si-C_2H_4
C_2H_4 x1
H_2 x1
25
75
INTENSITY
TEMPERATURE (°C)

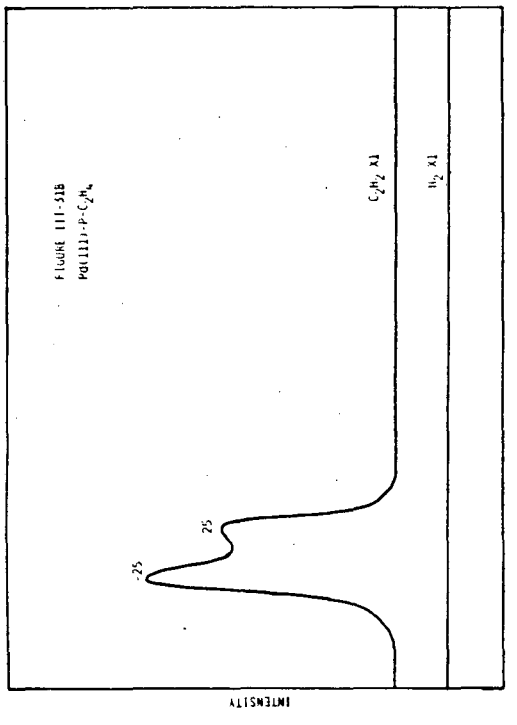
FIGURE III-31B
Pd(111)-P-C_2H_4
C_2H_4 x1
H_2 x1
-25
25
INTENSITY
TEMPERATURE (°C)

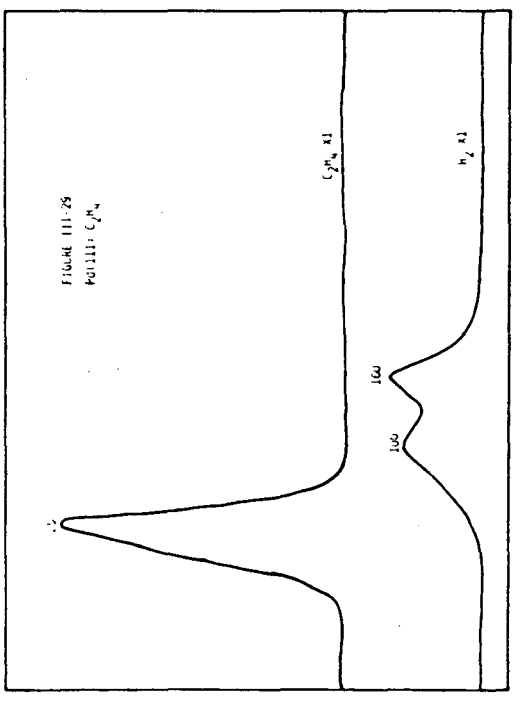
FIGURE III-29
Pd(111)-C_2H_4
C_2H_4 x1
H_2 x1
-25
100
127
INTENSITY
TEMPERATURE (°C)

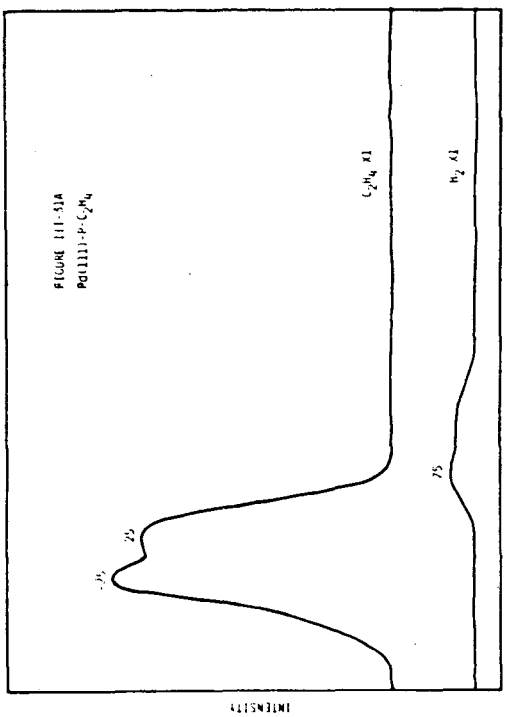
FIGURE III-31A
Pd(111)-P-C_2H_4
C_2H_4 x1
H_2 x1
-25
25
75
INTENSITY
TEMPERATURE (°C)

XBL 846-2196

F. Pd(111) - X - C_2H_4, where X = Si, P, S, or Cl

The influence of Si, P, S, and Cl on the chemisorption of ethylene on Pd(111) was investigated. All four adatoms increased the fraction of reversible desorption. On clean Pd(111) at an exposure of 1.0 L, an ethylene maximum was observed at 25°C, and two hydrogen maxima were observed, at 100°C and 160°C (see Figure III-29). On silicon-covered Pd(111), θ_{Si} = 0.15, the ethylene maximum was observed at 20°C, and a single hydrogen maximum was observed at 75°C (see Figure III-30). At a phosphorus coverage of 0.28 monolayer, two ethylene maxima were observed, at -25°C and 25°C. A weak hydrogen maximum was observed at 75°C (see Figure III-31A). Increasing the phosphorus coverage to 0.44 monolayer resulted in completely reversible ethylene chemisorption, with two maxima observed, at -25°C and 25°C (see Figure III-31B). At a sulfur coverage of 0.35 monolayer, ethylene also desorbed quantitatively, with maxima at -40°C and 0°C (see Figure III-32). Ethylene chemisorption was also largely reversible on chlorine-coverage Pd(111), θ_{Cl} = 0.18. An ethylene maximum was observed at 25°C, with two weak hydrogen maxima at 100°C and 160°C (see Figure III-33).

G. Pd(111) - X - H_2, where X = Si, P, S, or Cl

The sticking coefficient of hydrogen was determined on clean and adatom-covered Pd(111) using thermal desorption spectroscopy. At low hydrogen exposures the sticking coefficient on Pd(111) was found to be unity. The area under the curve of the hydrogen thermal desorption spectrum at low exposures (0.1 L) is proportional to the number of

Figure III-32. Quantitative desorption of ethylene from a sulfur-covered Pd(111) surface, θ_S = 0.35. In this experiment, the ethylene exposure was 1.0 L.

Figure III-33. Both reversible and irreversible chemisorption of ethylene on chlorine-covered Pd(111) are illustrated in the thermal desorption spectrum. In this experiment, the chlorine coverage was 0.18 monolayer, and the ethylene exposure was 1.0 L.

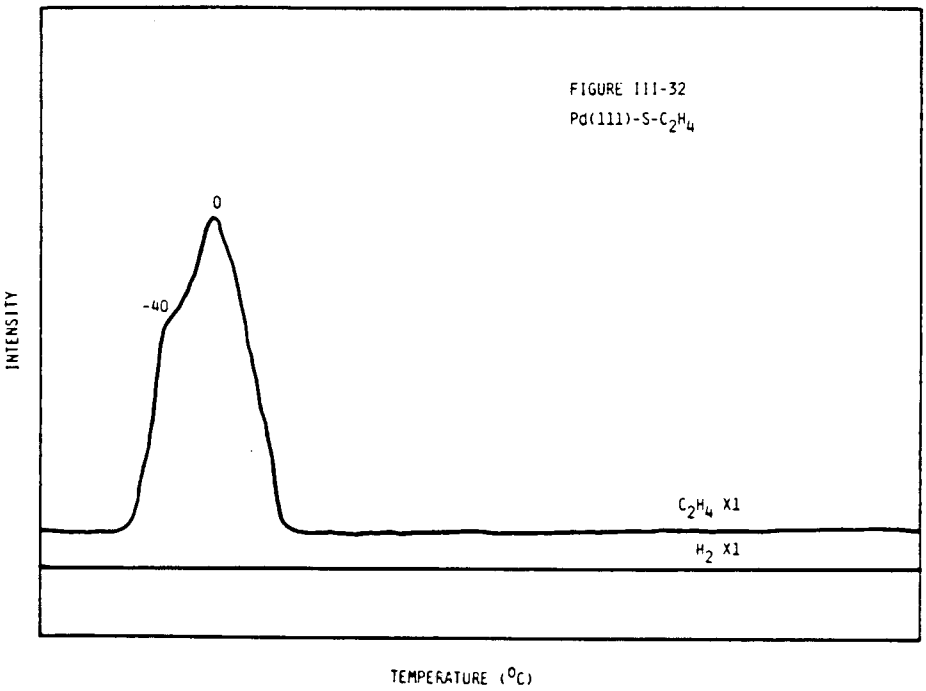
FIGURE III-32
Pd(111)-S-C_2H_4
0
-40
INTENSITY
C_2H_4 X1
H_2 X1
TEMPERATURE (°C)

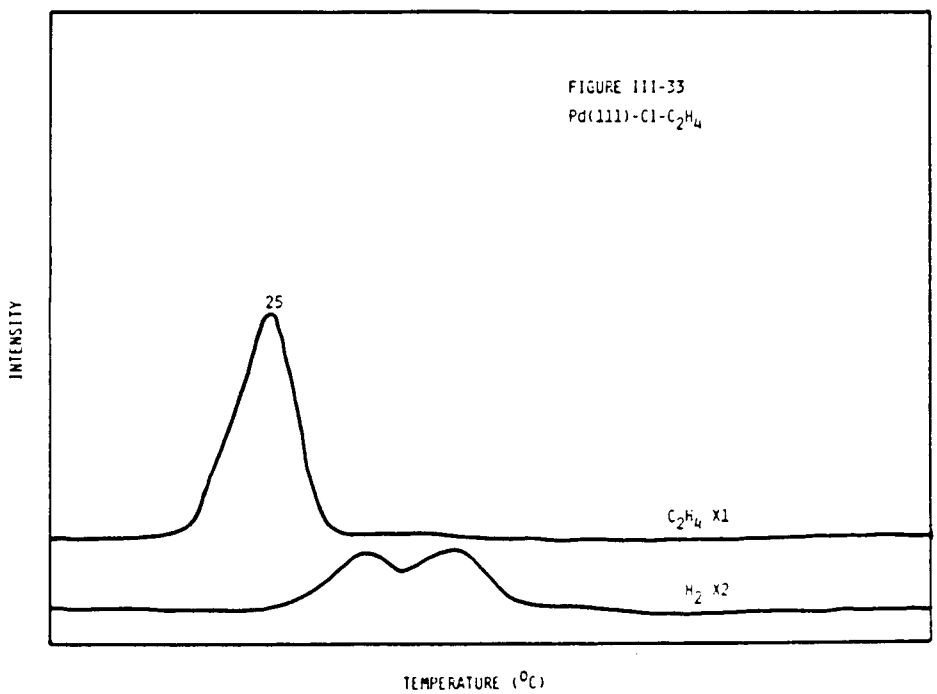
FIGURE III-33
Pd(111)-Cl-C_2H_4
25
INTENSITY
C_2H_4 X1
H_2 X2
TEMPERATURE (°C)

XBL 846-2171

Figure III-34. The relative sticking coefficient of hydrogen on clean, silicon-, phosphorus-, sulfur-, and chlorine-covered Pd(111). Increasing the electronegativity of the adatoms resulted in a greater decrease in the sticking coefficient. The sticking coefficient of hydrogen, at a given adatom coverage, followed this order: Si > P > S > Cl.

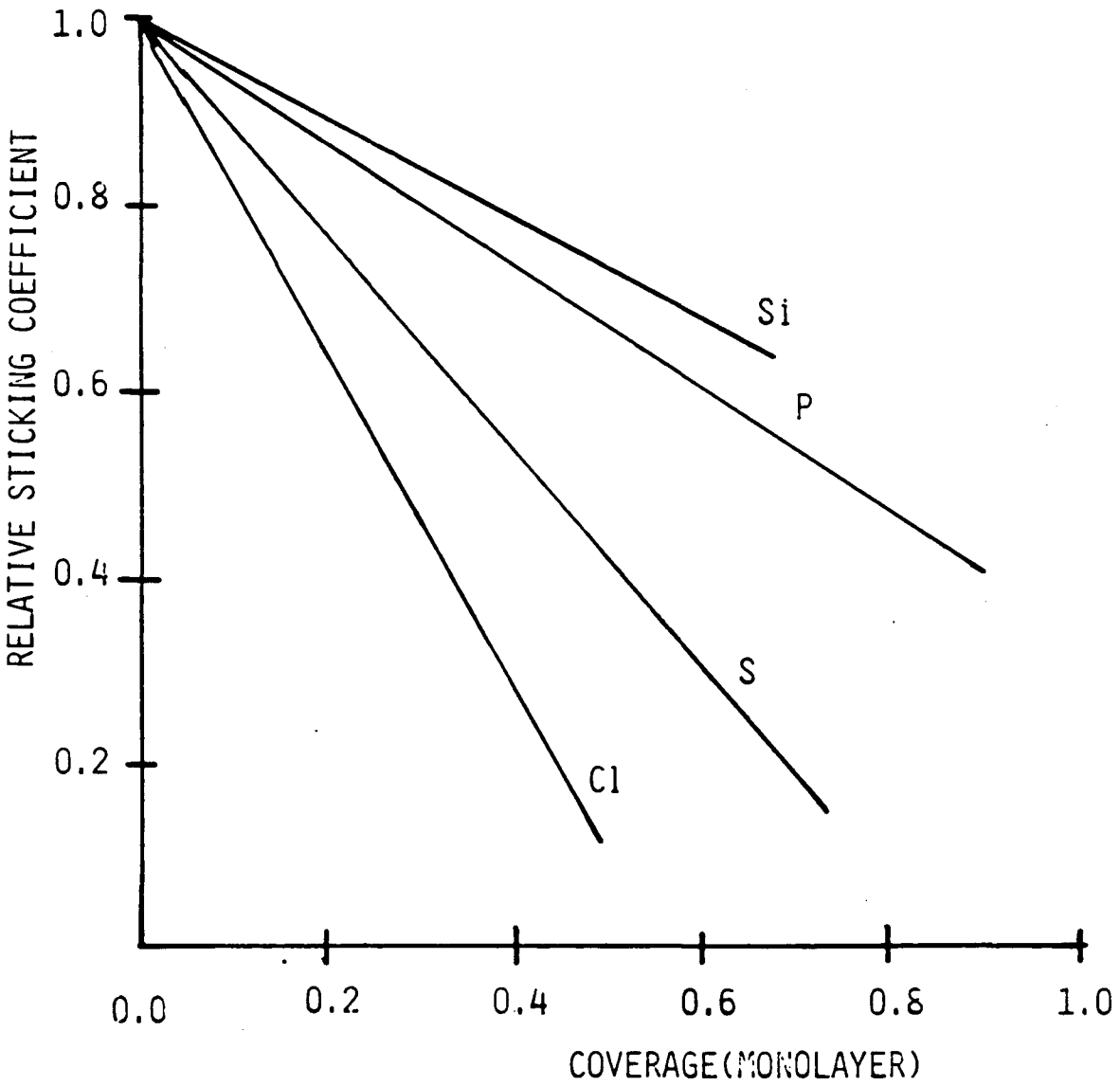
1.0
0.8
0.6
0.4
0.2
RELATIVE STICKING COEFFICIENT
Si
P
S
Cl
0.0
0.2
0.4
0.6
0.8
1.0
COVERAGE(MONOLAYER)

XBL 846-2168

molecules desorbing from the surface. The ratio of the area for an adatom at an H_2 exposure of 0.1 L to the area from the clean surface is therefore proportional to the sticking coefficient. The sticking coefficient decreases for adatom-covered surfaces and follows the trend Si > P > S > Cl (see Figure III-34).

H. Pd(100) - X - C_2H_2, where X = Si, P, S, or Cl

The thermal desorption of chemisorbed acetylene was investigated on the Pd(100), Pd(100)-Si, Pd(100)-P, Pd(100)-S, and Pd(100)-Cl surfaces. An exposure of 6.0 L was used for all of the following experiments. On clean Pd(100), reversible desorption, decomposition to carbon and hydrogen, hydrogenation of acetylene to ethylene, and cyclotrimerization of acetylene to benzene were observed (see Figure III-35). An acetylene T_{max} was observed at -95°C, with a shoulder at 25°C. The hydrogen desorption reached a maximum at 150°C, followed by a broad plateau from 220°C to 350°C. The ethylene T_{max} was observed at 30°C. A weak benzene thermal desorption maximum was observed at -25°C, and a broad one was observed from 105°C to 200°C.

Silicon has a profound influence on acetylene chemisorbed on Pd(100). The yield of both benzene and ethylene was found to increase with increasing silicon coverage. At a silicon coverage of 0.10 monolayer, a fourfold increase in the yield of ethylene was observed at T_{max} = 35°C. Two benzene thermal desorption maxima were observed, at 20°C and 200°C, with a sixfold increase in yield (see Figure III-36). Two hydrogen desorption maxima were observed, at 170°C and 370°C. Increasing the silicon coverage to 0.25 monolayer resulted in a 20-fold

Figure III-35. Thermal desorption of acetylene, 6.0 L, from Pd(100). Both ethylene and benzene formation were observed; however, the yield of benzene is significantly less than on Pd(111). Compare the benzene spectra of this figure and Figure III-1.

Figure III-36. At a silicon coverage of 0.1 monolayer, an increase in benzene yield from the thermal desorption of chemisorbed acetylene from this surface is illustrated. Comparison of the benzene traces of this figure with the previous figures demonstrates this point. Note the scale changes going from the previous figure, X40, to this figure, X10.

Figure III-37. Continued increase in the yield of benzene from chemisorbed C_2H_2 on Pd(100) at higher silicon coverages is demonstrated in this thermal desorption spectrum. Six langmuirs of acetylene were adsorbed on Pd(100) with a silicon coverage of 0.25 monolayer in this experiment.

Figure III-38. The thermal desorption of acetylene from silicon-covered Pd(100), $\theta_{Si} = 0.38$, resulted in a further increase in the yield of benzene, as compared to the previous figure. In this experiment the acetylene exposure was 6.0 L.

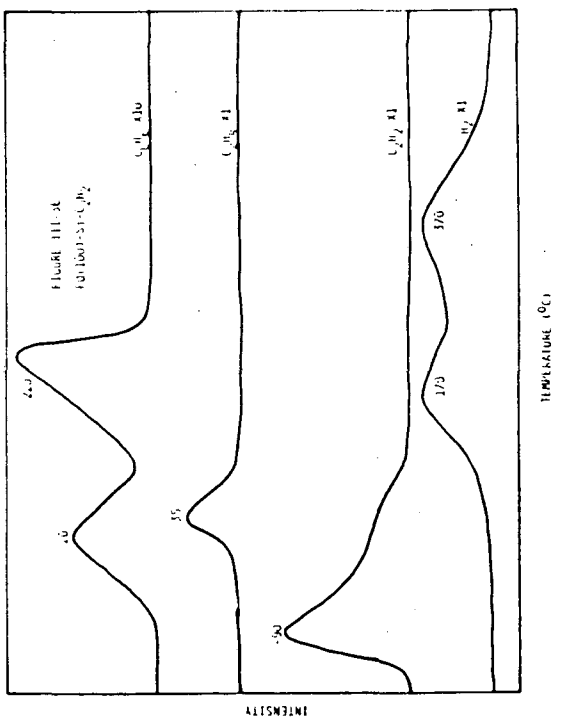

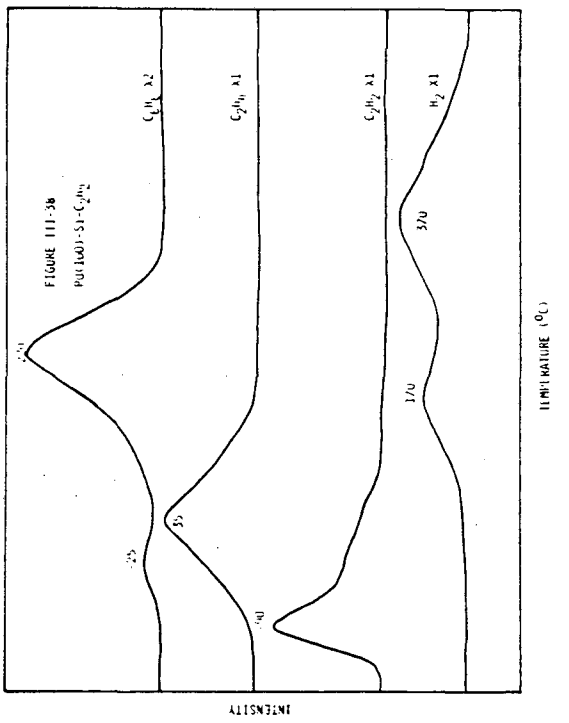

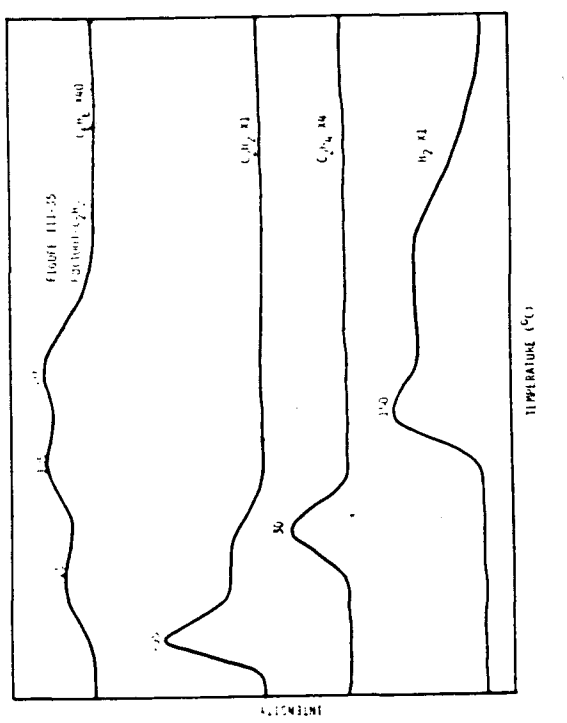

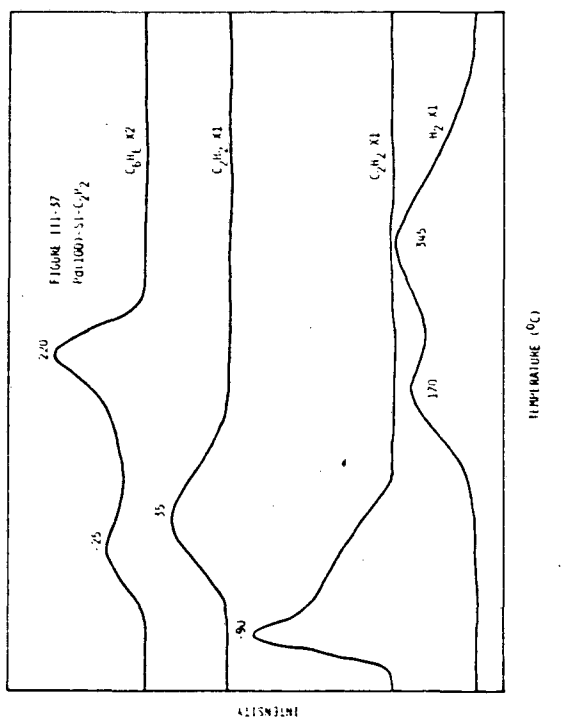

XBL 846-2195

increase in the yield of benzene, when compared to the clean surface. Two benzene thermal desorption maxima were observed, at -25°C and 220°C. An ethylene thermal desorption maximum was observed at 35°C (see Figure III-37). At a silicon coverage of 0.38 monolayer, the high temperature maximum increased (T_{max} = 220°C) with respect to the low temperature maximum (T_{max} = - 25°C). A 25-fold increase in the yield of benzene was observed (see Figure III-38).

Phosphided Pd(100) also influenced the chemistry of chemisorbed acetylene. The yield of benzene was enhanced, but not to the extent observed on the silicon-covered Pd(100). Two benzene maxima were observed, at -35°C and 80°C, on a surface with 0.17 monolayer phosphorus. The benzene yield was similar to that observed on clean Pd(100), as was the ethylene yield (T_{max} = 35°C) (see Figure III-39). Increasing the phosphorus coverage to 0.30 monolayer resulted in a threefold increase in the yield of benzene compared to the clean surface. Two benzene maxima were observed, at 100°C and 250°C. An ethylene thermal desorption maximum was observed at 35°C, with intensity increased by a factor of 2.50 as compared to the clean surface (see Figure III-40). At a phosphorus coverage of 0.40 monolayer, two benzene thermal desorption maxima were observed, at 100°C and 220°C, and the yield increased by a factor of 3.3 compared to the clean surface (see Figure III-41). An eightfold increase in the yield of benzene was observed at a phosphorus coverage of 0.55 monolayer. Two benzene maxima were observed, at 0°C and 200°C.

Figure III-39. At low phosphorus coverage, θ_P = 0.17, little change in the amount of benzene formed from chemisorbed acetylene was observed. In this thermal desorption experiment, 6.0 L of acetylene was adsorbed on the phosphorus-covered surface.

Figure III-40. The thermal desorption of acetylene from a Pd(100) surface with a phosphorus coverage of 0.31 monolayer exhibited an increase in the yield of benzene as compared to the clean surface. In the thermal desorption experiment illustrated here, the exposure of acetylene was 6.0 L.

Figure III-41. The yield of benzene is found to increase further with increasing phosphorus coverage on Pd(100). The phosphorus coverage was 0.40 monolayer, and the acetylene exposure was 6.0 L in this experiment.

Figure III-42. At a phosphorus coverage of 0.55 monolayer, a further increase in the amount of benzene desorbing from the surface is observed. Acetylene was chemisorbed with an exposure of 6.0 L.

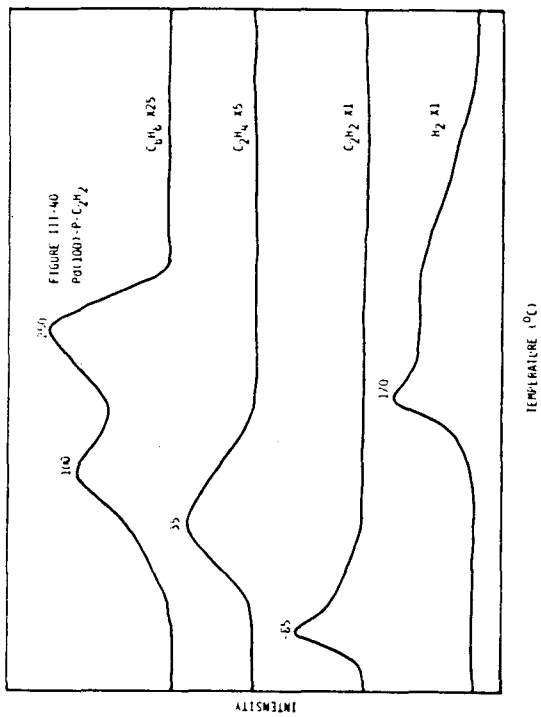
FIGURE III-40
Pd(100)-P-C_2H_2
C_6H_6 X25
C_2H_4 X5
C_2H_2 X1
H_2 X1
200
100
35
-65
170
INTENSITY
TEMPERATURE (°C)

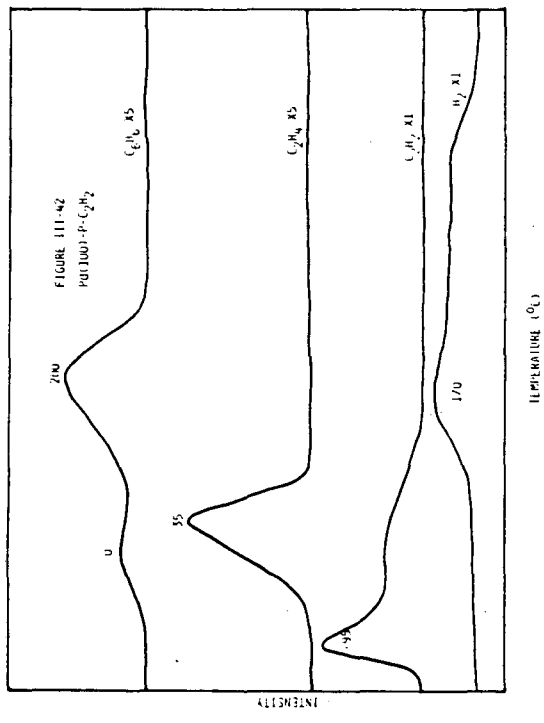
FIGURE III-42
Pd(100)-P-C_2H_2
C_6H_6 X5
C_2H_4 X5
C_2H_2 X1
H_2 X1
200
0
35
-95
170
INTENSITY
TEMPERATURE (°C)

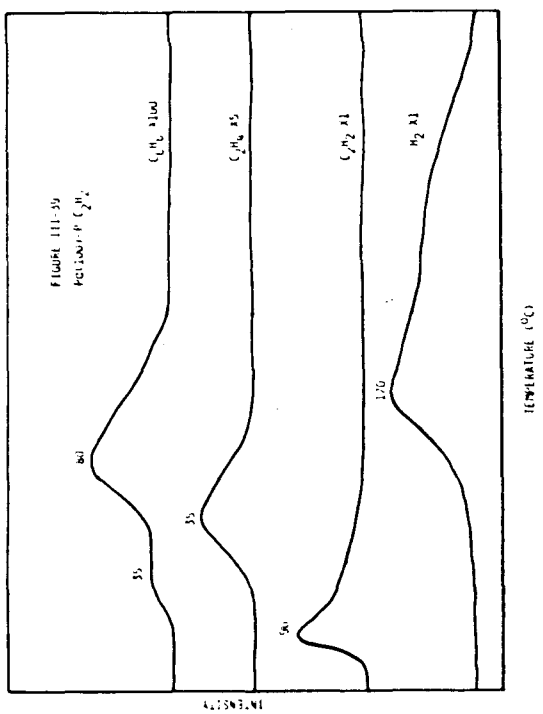
FIGURE III-39
Pd(100)-P-C_2H_2
C_6H_6 X100
C_2H_4 X5
C_2H_2 X1
H_2 X1
80
35
35
-50
170
INTENSITY
TEMPERATURE (°C)

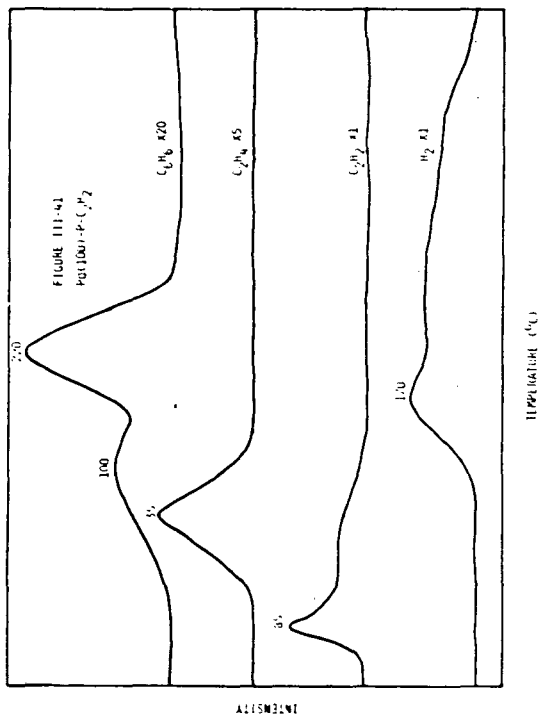
FIGURE III-41
Pd(100)-P-C_2H_2
C_6H_6 X20
C_2H_4 X5
C_2H_2 X1
H_2 X1
220
100
35
-65
170
INTENSITY
TEMPERATURE (°C)

XBL 846-2194

Ethylene desorbing from the surface increased by a factor of 3 at T_{max} = 35°C, compared to clean Pd(110) (see Figure III-42).

Sulphiding Pd(100) decreases the yield of ethylene and only slightly enhances the yield of benzene. At low sulfur coverages, the yields of benzene and ethylene were similar to that of clean Pd(100) (see Figure III-43). The amount of hydrogen desorbing from the surface also decreased; a broad desorption spectrum was observed from 165°C to 340°C. At a sulfur coverage of 0.26 monolayer, the yield of ethylene decreased by a factor of two with T_{max} = 30°C. The yield of benzene increased, with an increase in the low temperature end of the broad desorption spectrum from 100°C to 240°C (see Figure III-44).

At a sulfur coverage of 0.42 monolayer, relatively high temperature reversibly bound acetylene was observed. On clean and silicon- and phosphorus-covered surfaces only a low temperature acetylene thermal desorption maximum (~-90°C) was observed. On this surface, along with a low temperature maximum, two other maxima, at 90°C and 165°C, were also observed. Two poorly resolved benzene maxima were found, at -25°C and 165°C (see Figure III-45).

Chlorine was found to enhance the yield of ethylene and benzene, however, again the effect was much less than that observed for silicon. At a chlorine coverage of 0.14, ethylene desorbed at maximum rate at 35°C and benzene desorbed at 60°C and 270°C. The yield of benzene increased by a factor of 2.2, and that of ethylene increased by a factor of 1.8 (see Figure III-46). Increasing the chlorine coverage to 0.30 (T_{max} = 30°C) did not change the ethylene significantly.

Figure III-43. Sulfur did not increase the yield of benzene from acetylene chemisorbed on Pd(100). The thermal desorption of 6.0 L of acetylene from a sulfur-covered Pd(100) surface, $\theta_S = 0.16$, is shown. Comparison of the benzene trace of this figure with that obtained on a clean surface (see Figure III-35) shows little or no change.

Figure III-44. Increasing the sulfur coverage, $\theta_S = 0.26$, did not increase the yield of benzene from the thermal desorption of acetylene chemisorbed on Pd(100). The acetylene exposure in this experiment was 6.0 L.

Figure III-45. The yield of benzene from chemisorbed C_2H_2, 6.0 L, did not change on a Pd(100) surface with a sulfur coverage of 0.42 monolayer. However, the thermal desorption spectrum shown in this figure illustrates the poisoning of the hydrogenation reaction due to the lack of ethylene desorption. In contrast to the (111) and (110) surfaces, sulfur affected the thermal desorption of acetylene at temperatures greater than 50°C. Three acetylene thermal desorption maxima are shown, at -90°C, 90°C, and 165°C.

Figure III-46. Chlorine on Pd(100) increased the yield of reactively formed benzene in the thermal desorption of chemisorbed acetylene. In the thermal desorption experiment illustrated in this figure, the chlorine coverage was 0.14 monolayer, and the acetylene exposure was 6.0 L.

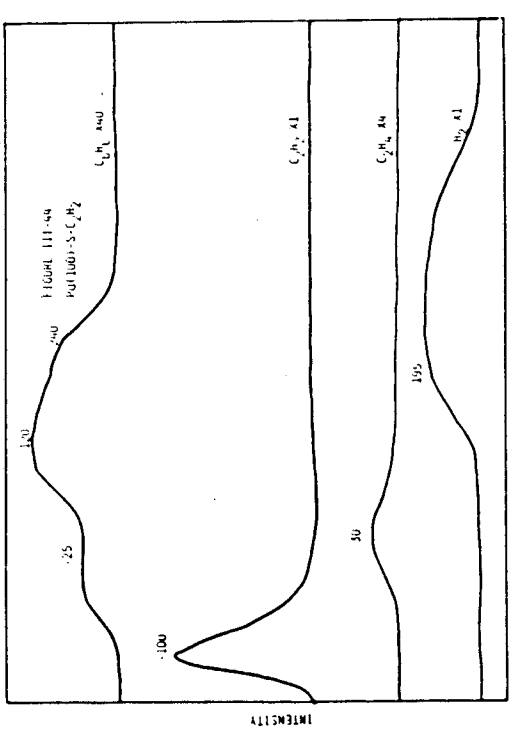
FIGURE III-46
Pd(100)-Cl-C_2H_2
C_6H_6 X10
C_2H_2 X2
C_2H_2 X1
H_2 X1
INTENSITY
TEMPERATURE (°C)

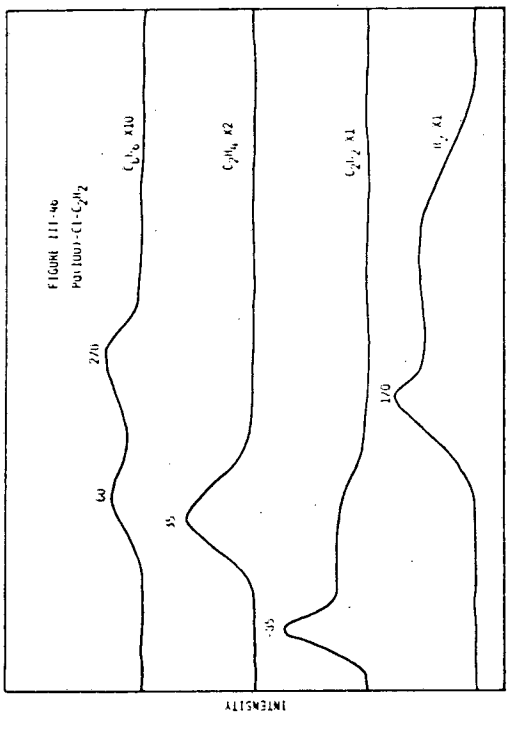
FIGURE III-46
Pd(100)-S-C_2H_2
C_6H_6 X40
C_2H_2 X1
C_2H_4 X4
H_2 X1
INTENSITY
TEMPERATURE (°C)

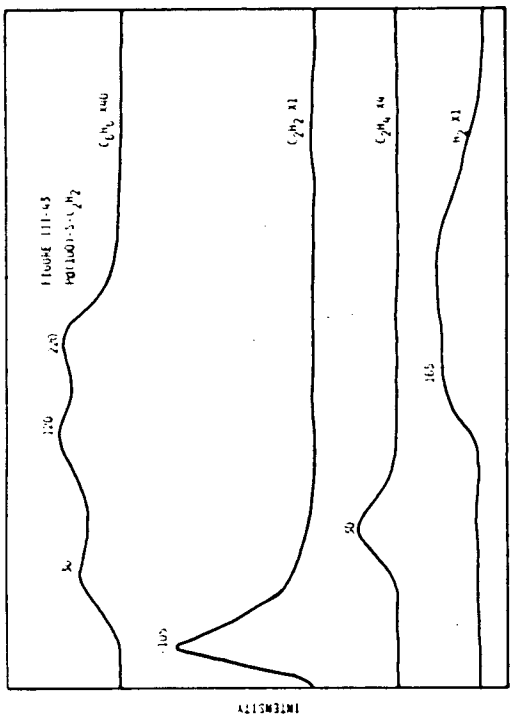
FIGURE III-45
Pd(100)-S-C_2H_2
C_6H_6 X40
C_2H_2 X1
C_2H_4 X4
H_2 X1
INTENSITY
TEMPERATURE (°C)

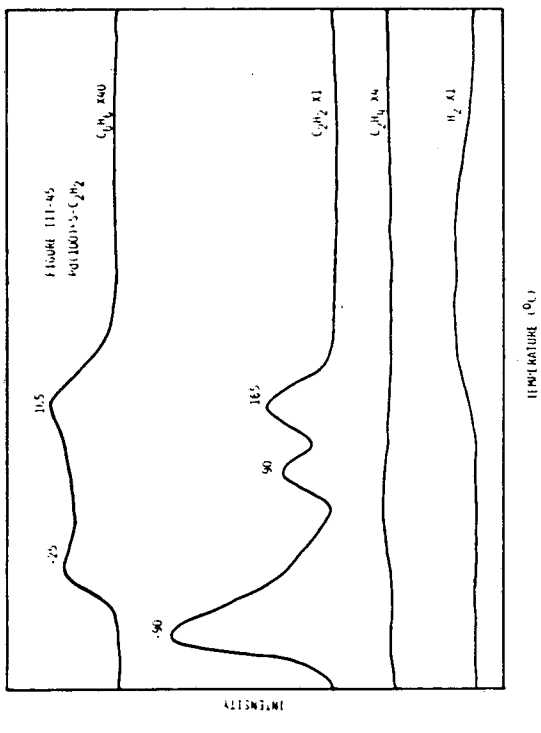
FIGURE III-45
Pd(100)-S-C_2H_2
C_6H_6 X40
C_2H_2 X1
C_2H_4 X4
H_2 X1
INTENSITY
TEMPERATURE (°C)

XBL 846-2193

Two benzene thermal desorption maxima were observed, at 50°C and 220°C. The yield of benzene increased by a factor of five as compared to the clean surface (see Figure III-47).

I. Pd(100) - X - H_2 - C_2H_2, where X = Si, P, S, or Cl

Hydrogenation of acetylene on Pd(100) was investigated on clean Pd(100) and on surfaces covered with silicon, phosphorus, sulfur, or chlorine. In these thermal desorption experiments, H_2 (3.0 L) was adsorbed followed by C_2H_2 (4.0 L). On clean Pd(100), preadsorbed H_2 completely supressed the formation of benzene. Two hydrogen thermal desorption maxima were observed, at 25°C and 160°C, with an ethylene T_{max} at 15°C (see Figure III-48). On a silicon-covered Pd(100) surface, θ_{Si} = 0.3, the ethylene yield increased by a factor of 2.6 at T_{max} = 0°C. Benzene formation was also observed, with T_{max} = 230°C (see Figure III-49). On a phosphided surface, θ_P = 0.44, the yield of ethylene also increased as compared to the clear covered surface, but not to the extent observed on the silicided surface. An ethylene thermal desorption maximum was observed at 0°C, with an increase of a factor of 1.3. Benzene was also observed, with T_{max} = 220°C (see Figure III-50). On sulfur-covered Pd(100), θ_S = 0.43, no ethylene or benzene was observed. Three acetylene thermal desorption maxima were observed, at -95°C, 100°C, and 160°C (see Figure III-51). On chlorine-covered Pd(100), θ_{Cl} = 0.30, small amounts of ethylene at T_{max} = 60°C and benzene at T_{max} = 75°C were observed (see Figure III-52).

Figure III-47. At a chlorine coverage of 0.30 monolayer on Pd(100), an increase in the amount of benzene desorbing from chemisorbed acetylene was observed. The thermal desorption spectrum is the result of the adsorption of 6.0 L of acetylene.

Figure III-48. Hydrogenation of acetylene to ethylene was affected by sequential adsorption of hydrogen and acetylene on Pd(100). Preadsorption of hydrogen was also found to suppress the trimerization of acetylene to benzene. Similar results were observed on Pd(111) (see Figure III-9).

Figure III-49. Silicon was found to increase the yield of ethylene in the thermal desorption of hydrogen and acetylene from Pd(100). At a silicon coverage of 0.30 monolayer, benzene formation was also observed.

Figure III-50. The thermal desorption spectrum shown in this figure is for a surface state formed by a sequential adsorption of hydrogen, 3.0 L, and acetylene, 4.0 L, on phosphorus-covered Pd(100), θ_P = 0.44. In this experiment, the yield of ethylene was found to increase as compared to the clean surface.

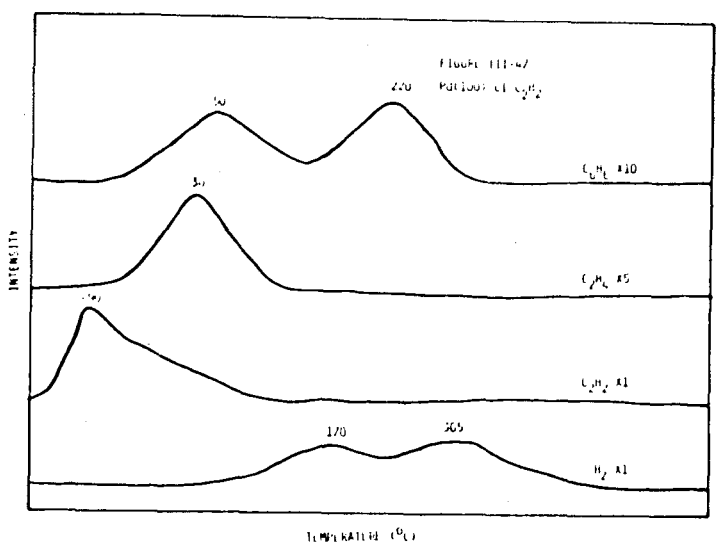
INTENSITY
50
220
C_6H_6 x10
50
C_2H_4 x5
-60
C_2H_2 x1
170
365
H_2 x1
TEMPERATURE (°C)

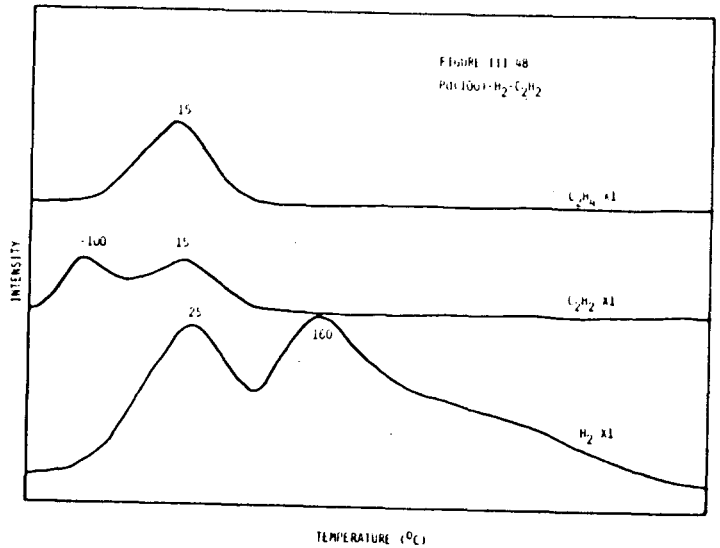
INTENSITY
15
C_2H_4 x1
-100
15
C_2H_2 x1
25
160
H_2 x1
TEMPERATURE (°C)

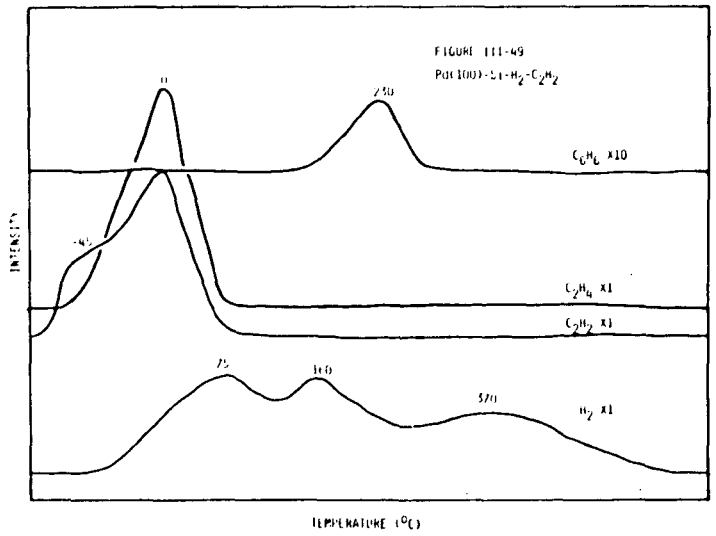
INTENSITY
0
250
C_6H_6 x10
-45
C_2H_4 x1
C_2H_2 x1
75
160
370
H_2 x1
TEMPERATURE (°C)

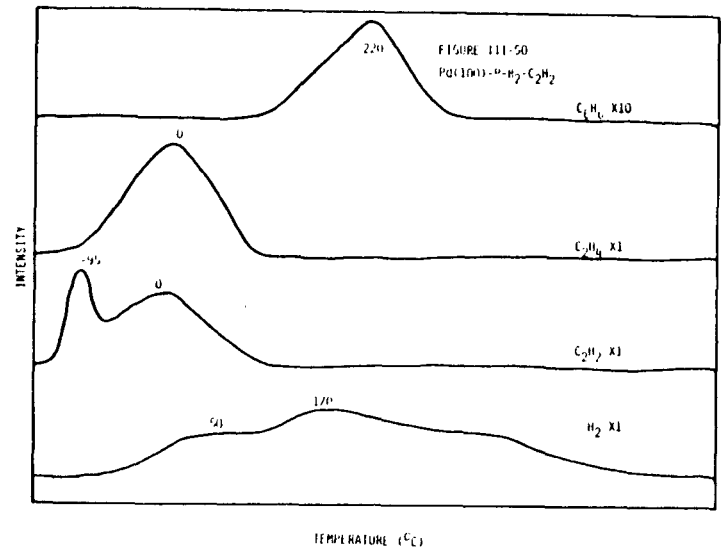
INTENSITY
220
C_6H_6 x10
0
C_2H_4 x1
-95
0
C_2H_2 x1
50
170
H_2 x1
TEMPERATURE (°C)

XBL 846-2192

Figure III-51. The presence of sulfur on Pd(100) completely suppressed the hydrogenation of acetylene. The thermal desorption spectrum of a surface state formed by adsorption of 3.0 L of H_2 and 4.0 L of C_2H_2 from sulfur-covered Pd(100), θ_S = 0.43, is shown.

Figure III-52. Chlorine was found to inhibit the hydrogenation of acetylene on Pd(100). The thermal desorption of H_2 and C_2H_2 from a surface with chlorine coverage of 0.30 monolayer shows little ethylene desorption.

Figure III-53. Sequential adsorption of acetylene, 6.0 L, and trimethylsilane, 4.0 L, on clean Pd(100) resulted in the formation of the hydrosilation product, vinyltrimethylsilane. Trimerization of acetylene to benzene and hydrogenation to ethylene are competing reactions with hydrosilation.

Figure III-54. The amount of vinyltrimethylsilane desorbing from Pd(100) increased in the presence of silicon. The thermal desorption spectrum of acetylene, 6.0 L, and trimethylsilane, 4.0 L, from silicon-covered Pd(100), θ_{Si} = 0.24, is shown.

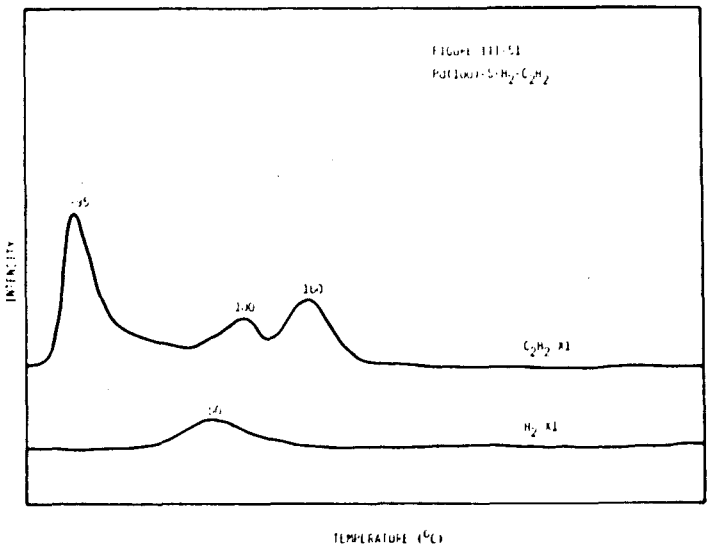
INTENSITY
TEMPERATURE (°C)
C_2H_2 X1
H_2 X1

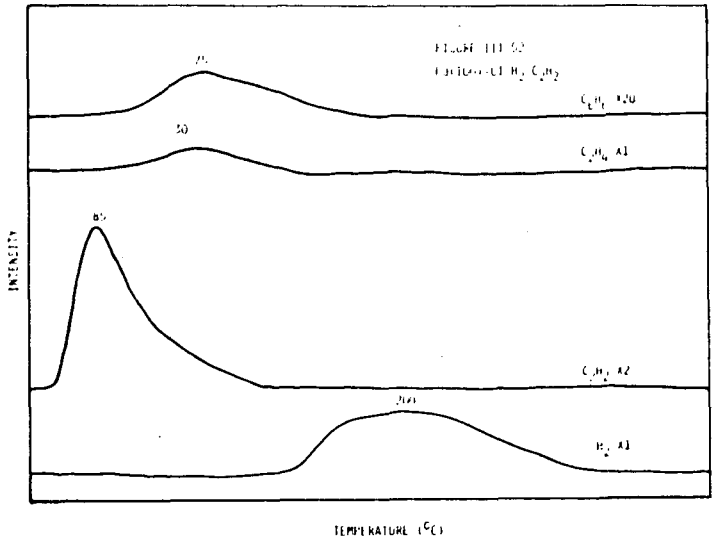
INTENSITY
TEMPERATURE (°C)
C_6H_6 X20
C_2H_4 X1
C_2H_2 X2
H_2 X1

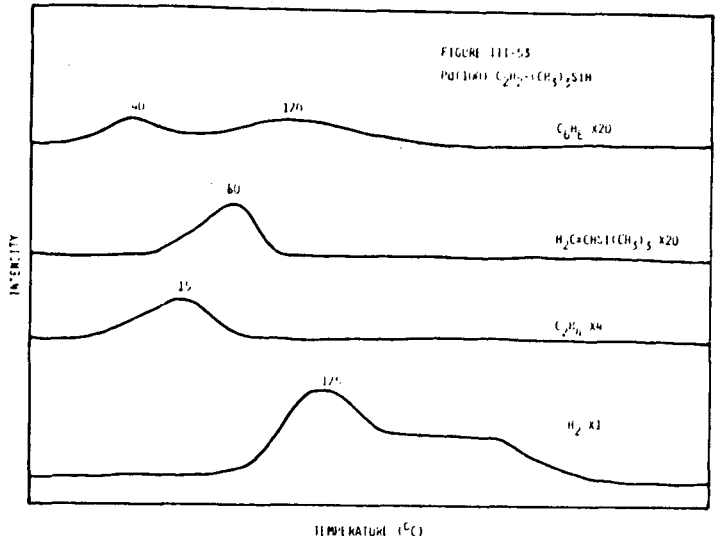
INTENSITY
TEMPERATURE (°C)
C_6H_6 X20
H_2C=CHSi$(CH_3)_3$ X20
C_2H_4 X4
H_2 X1

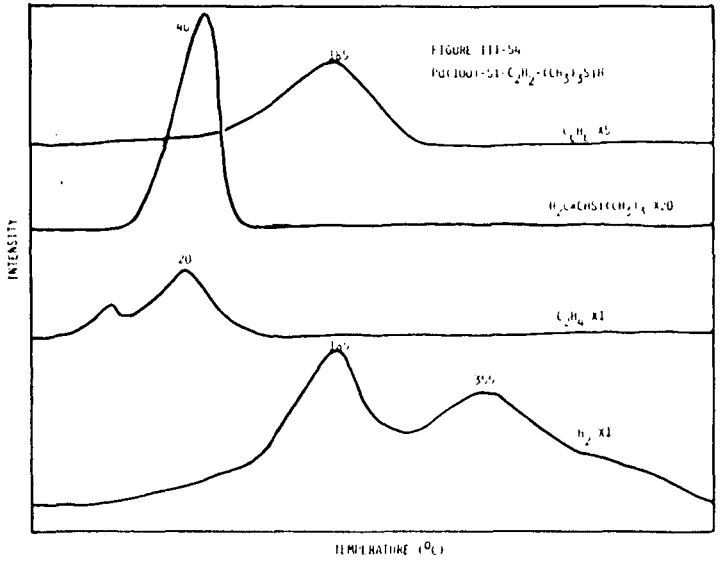
INTENSITY
TEMPERATURE (°C)
C_6H_6 X5
H_2C=CHSi$(CH_3)_3$ X20
C_2H_4 X1
H_2 X1

XBL 846-2191

J. Pd(100) - X - C_2H_2 - $(CH_3)_3SiH$, where X = Si, P, S, or Cl

The hydrosilation of acetylene with trimethylsilane was investigated on clean Pd(100), and on silicon-, phosphorus-, sulfur-, and chlorine-covered Pd(100). This reaction was performed by sequential adsorption of acetylene (6.0 L) and trimethylsilane (4.0 L) on the desired surface. Several products were observed in the subsequent thermal desorption spectrum. Ethylene, T_{max} = 15°C, benzene, T_{max} = -40°C and 170°C, and vinyltrimethylsilane, T_{max} = 80°C, were the products on clean Pd(100). A hydrogen thermal desorption maximum was observed at 170°C, followed by a plateau-like tail from 255°C to 375°C (see Figure III-53). On silicon-covered Pd(100), the yield of vinyltrimethylsilane increased by a factor of four. The temperature of the thermal desorption maximum of vinyltrimethylsilane was 40°C (see Figure III-54). The benzene and ethylene yield also increased, with thermal desorption maxima at 185°C and 20°C, respectively. Phosphided Pd(100), θ_P = 0.37, also exhibited an increased yield of vinyltrimethylsilane, T_{max} = 60°C. The yield increased by a factor of 3.5. Ethylene and benzene yields also increased as compared to the clean surface (see Figure III-55). A small increase in the yield of vinyltrimethylsilane (a factor of 1.5) was observed on sulfur-covered Pd(100), θ_S = 0.42. The yield of ethylene, T_{max} = 25°C, decreased, and the benzene yield also slightly increased (see Figure III-56). On chlorine-covered Pd(100), θ_{Cl} = 0.16, the yield of vinyltrimethylsilane, T_{max} = 20°C, was similar to

Figure III-55. Phosphiding Pd(100), θ_P = 0.37, also increased the yield of vinyltrimethylsilane in the hydrosilation reaction of acetylene with trimethylsilane. Hydrogenation and trimerization of acetylene are competing with hydrosilation. The exposures of acetylene and trimethylsilane were 6.0 L and 4.0 L, respectively.

Figure III-56. The presence of sulfur, θ_S = 0.42, did not substantially alter the yield of vinyltrimethylsilane. Comparing the thermal desorption spectrum shown in this figure with that in Figure III-53 illustrates this point. Exposures of 6.0 L and 4.0 L were used for acetylene and trimethylsilane, respectively.

Figure III-57. The thermal desorption of sequentially adsorbed acetylene, 6.0 L, and trimethylsilane, 4.0 L, from chlorine-covered Pd(100), θ_{Cl} = 0.16, is shown. Chlorine did not change the yield of trimethylsilane.

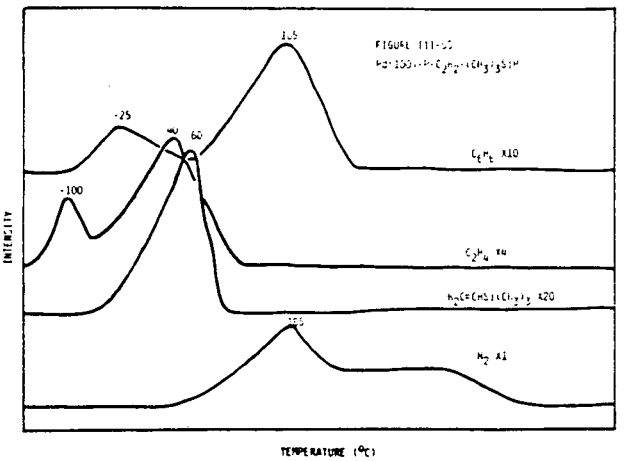
INTENSITY
TEMPERATURE (°C)

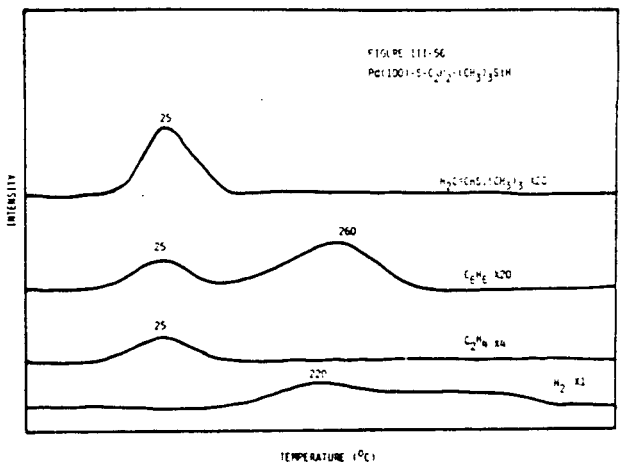
INTENSITY
TEMPERATURE (°C)

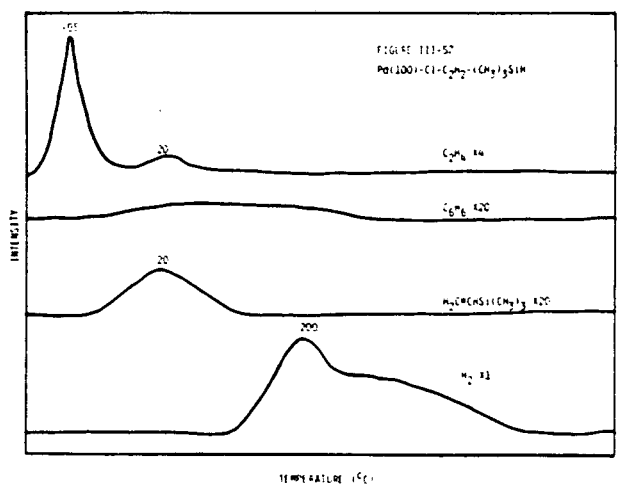
INTENSITY

XBL 846-2176

Figure III-58. The relative sticking coefficient of hydrogen as a function of adatom coverage is shown. Silicon, in contrast to phosphorous, sulfur, and chlorine, increased the sticking coefficient of hydrogen, whereas the other three elements decreased the sticking coefficient. The following trend was observed for the sticking coefficient at a given coverage: Si > P > S > Cl.

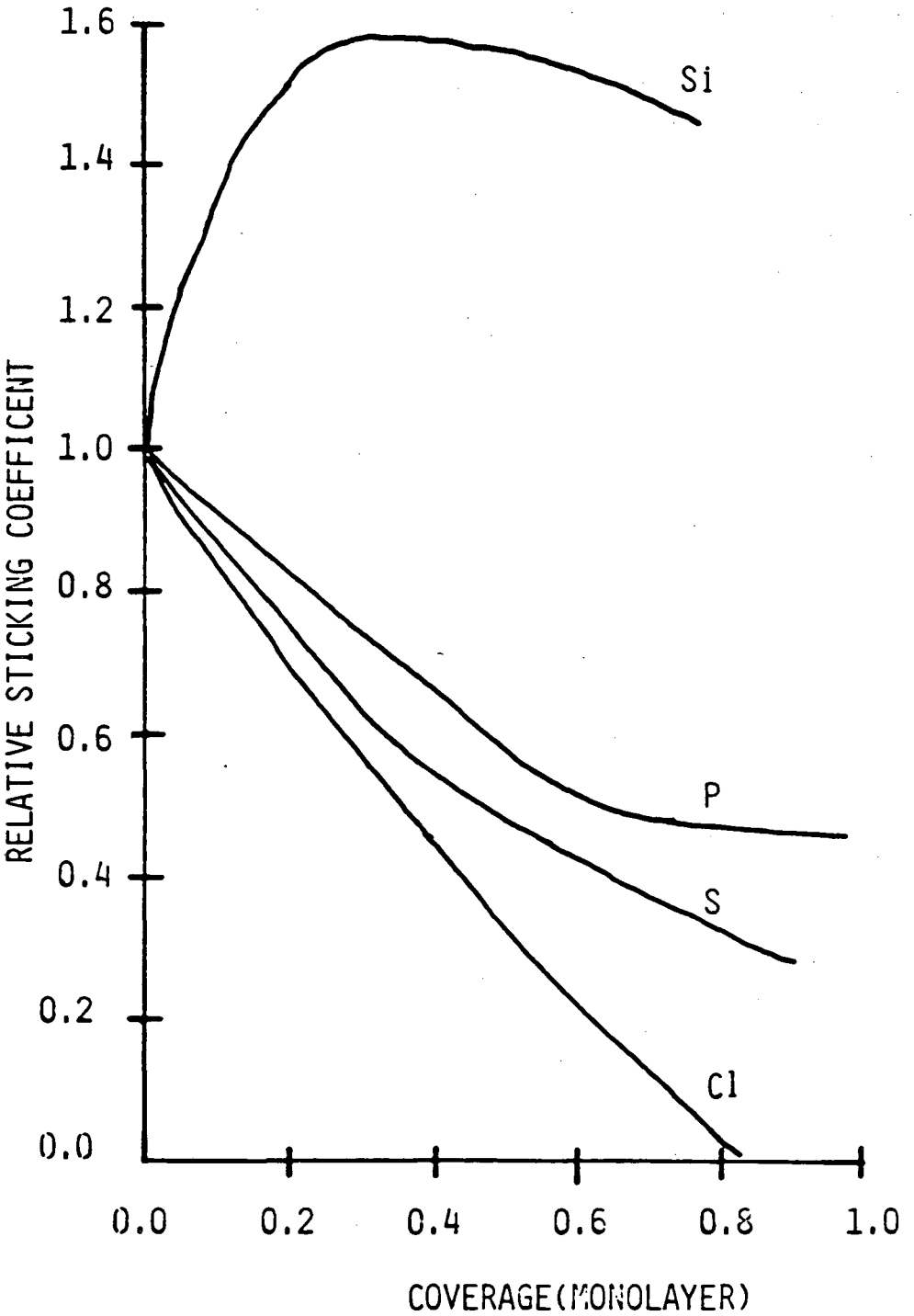
1.6
1.4
1.2
1.0
0.8
0.6
0.4
0.2
0.0
RELATIVE STICKING COEFFICENT
Si
P
S
Cl
0.0
0.2
0.4
0.6
0.8
1.0
COVERAGE(MONOLAYER)

XBL 846-2167

that observed on the clean surface. The yields of both benzene and ethylene were less than those observed on the clean surface (see Figure III-57).

K. Pd(100) - X -H_2, where X = Si, P, S, or Cl

The relative sticking coefficient of hydrogen was measured on clean Pd(100), and on silicon-, phosphorus-, sulfur-, and chlorine-covered Pd(100). The same method was used as on the Pd(111) surface. An increase in the sticking coefficient of hydrogen on silicon-covered Pd(100) was observed, while a decrease was observed for phosphorus-, sulfur-, and chlorine-covered Pd(100) (see Figure III-58).

L. Pd(100) - X - C_6H_6, where X = Si, P, S, or Cl

The chemisorption of benzene was studied on the clean, silicided, phosphided, sulphided, and chlorided Pd(100) surface. In these experiments a benzene exposure of 2.0 L was used. On clean Pd(100), a hydrogen thermal desorption maximum was observed at 295°C, with a high temperature shoulder of 390°C. Two benzene maxima were observed, at -40°C and 220°C (see Figure III-59). Silicon increased the amount of reversibly bound benzene. At a silicon coverage of 0.18 monolayer, an increase in the high temperature benzene maximum at 220°C was observed (see Figure III-60A). Increasing the silicon coverage to 0.36 monolayer, a further increase in the high temperature maximum, T_{max} = 185°C, was observed (see Figure III-60B). At low phosphorus coverages, θ_P = 0.10, two benzene maxima were observed, at -60°C and 250°C. The low temperature maximum increased slightly as compared to

Figure III-59. At an exposure of 2.0 L, both reversible and irreversible chemisorption was observed in the thermal desorption spectrum of benzene from Pd(100). The reversibly bound benzene desorbs in two maxima, at -40°C and 220°C.

Figure III-60. The thermal desorption of benzene, 2.0 L exposure, is shown from silicon-covered Pd(100). The fraction of reversibly bound benzene increased with silicon coverage. At a silicon coverage of 0.18 monolayer (Figure III-60A), a small increase in benzene desorption was observed. However, at a silicon coverage of 0.36 monolayer (Figure III-60B), a dramatic increase was observed.

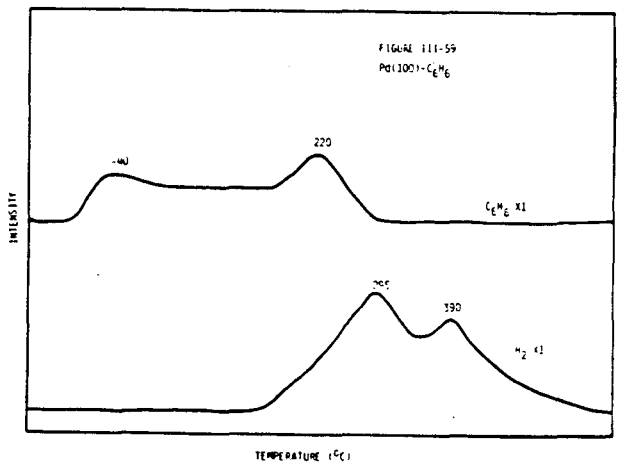
FIGURE III-59
Pd(100)-C_6H_6
INTENSITY
220
C_6H_6 X1
330
H_2 X1
TEMPERATURE (°C)

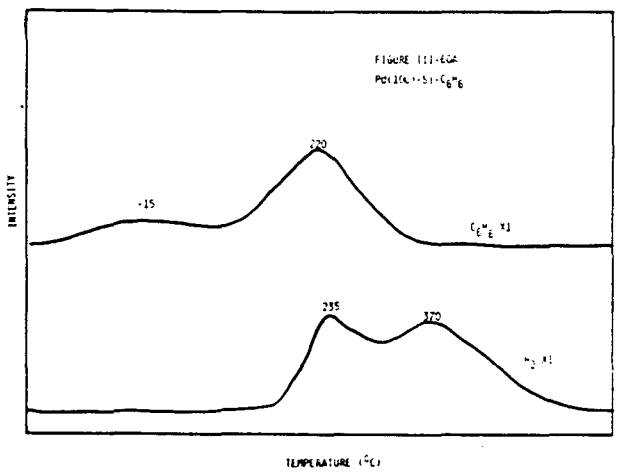
INTENSITY
C_6H_6 X1
TEMPERATURE (°C)

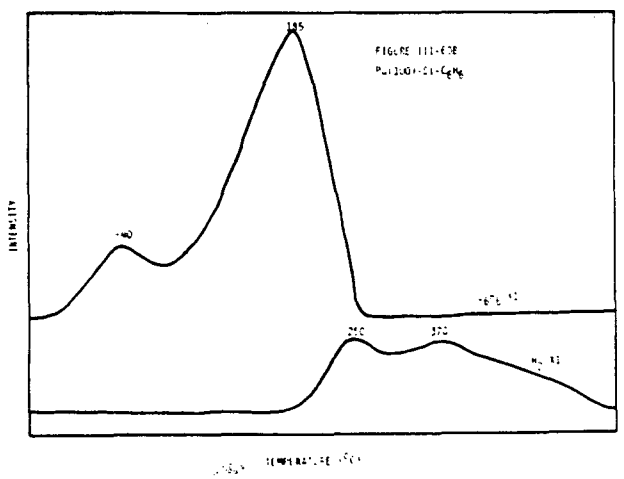
INTENSITY
H_2 X1

XBL 846-2175

Figure III-61. Phosphiding Pd(100) also increases the fraction of reversibly bound benzene observed in the thermal desorption spectrum. Illustrated are three thermal desorption spectra of benzene, 2.0 L exposure, from Pd(100) at phosphorus coverages of 0.10 monolayer (Figure III-61A), 0.28 monolayer (Figure III-61B), and 0.42 monolayer (Figure III-61C).

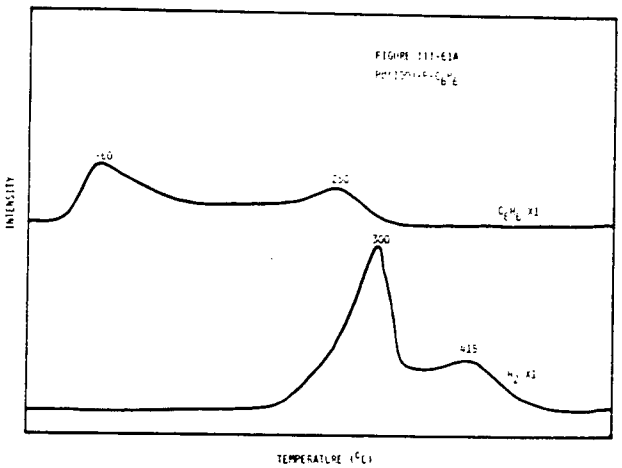
INTENSITY
300
415
TEMPERATURE (°C)

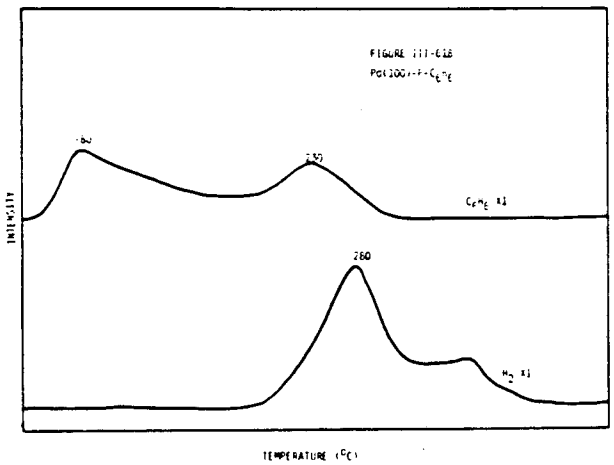
INTENSITY
280
TEMPERATURE (°C)

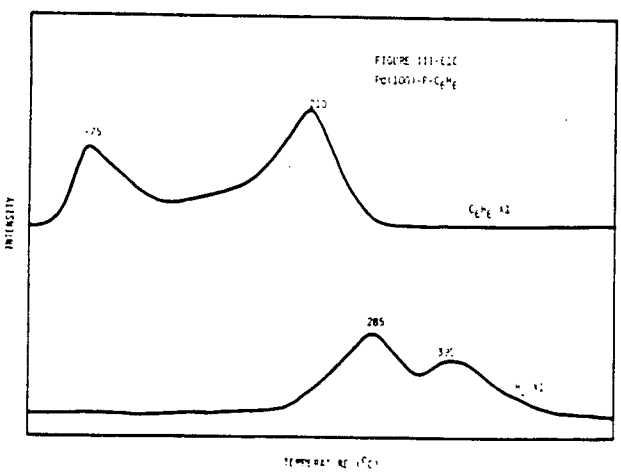
INTENSITY
285

XBL 846-2174

the clean surface (see Figure III-61A). At a phosphorus coverage of 0.28 monolayer, an increase in both the low temperature, T_{max} = 80°C, and the high temperature, T_{max} = 230°C, maxima was observed (see Figure III-61B). At a phosphorus coverage of 0.42 monolayer, an increase in the high temperature maximum was observed, T_{max} = 210°C (see Figure III-61C). As observed on silicided and phosphided Pd(100), the amount of reversible desorption of benzene increased on sulphided Pd(100). Two benzene maxima were observed, at -50°C and ~200°C on a surface with a sulfur coverage of 0.29 monolayer (see Figure III-62A). Increasing the sulfur coverage results in a further increase in the fraction of reversibly bound benzene. However, in contrast to silicon- and phosphorus-covered Pd(100), where an increase was observed in the high temperature maximum, an increase is observed in the low temperature maximum. At a sulfur coverage of 0.40 monolayer, benzene maxima were observed at -20°C, -35°C, and—in broad plateau-like desorptions--from 10°C to 100°C and 160°C to 285°C (see Figure III-62B). On chlorine-covered Pd(100), θ_{Cl} = 0.20, two benzene maxima were observed, at -70°C and 160°C (see Figure III-63A). By increasing chlorine coverage to 0.35, an increase the amount of reversible desorption was observed, T_{max} = -85°C and 135°C (see Figure III-63B).

M. Pd(100) - X - C_2H_4, where X = Si, P, S, or Cl

Ethylene chemisorption was investigated on clean and adatom-covered surfaces of Pd(100). At an exposure of 0.5 L, two ethylene thermal desorption maxima were observed, at -10°C and 40°C, and a hydrogen

Figure III-62. Sulfur also increased the amount of benzene desorbing intact from Pd(100). The thermal desorption spectra of benzene from two different sulfur-covered surfaces are displayed. Figure III-62A shows the spectrum at 0.29 monolayer of sulfur, and Figure III-62B shows the spectrum at 0.40 monolayer. In Figure III-62B note the increase of benzene desorbing at low temperatures, in contrast to silicon- and phosphorus-covered Pd(100), where benzene desorbed primarily at high temperatures.

Figure III-63. The presence of chlorine on Pd(100) also increased the portion of benzene desorbing intact. Displayed in this figure are thermal desorption spectra of benzene from surfaces with chlorine coverages of 0.20 monolayer (Figure III-63A) and 0.35 monolayer (Figure III-63B). Chlorine increased the desorption of benzene at both low and high temperatures. At 0.35 monolayer of chlorine, desorption of benzene is nearly quantitative.

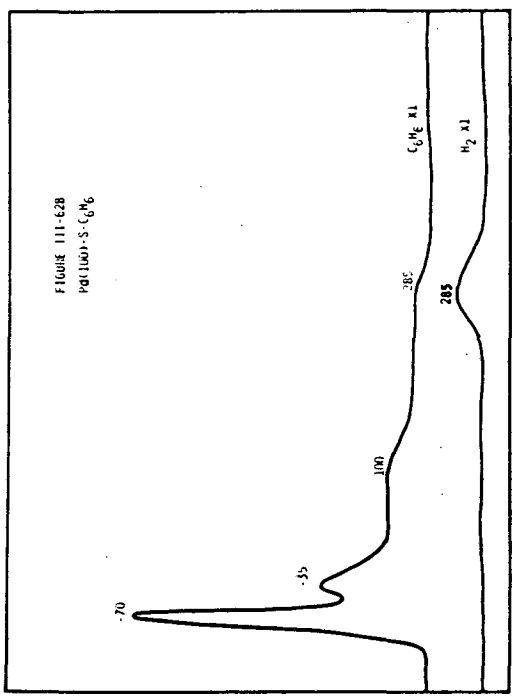
FIGURE III-62B
Pd(100)-S-C_6H_6
C_6H_6 X1
H_2 X1
70
55
100
285
285
INTENSITY
TEMPERATURE (^oC)

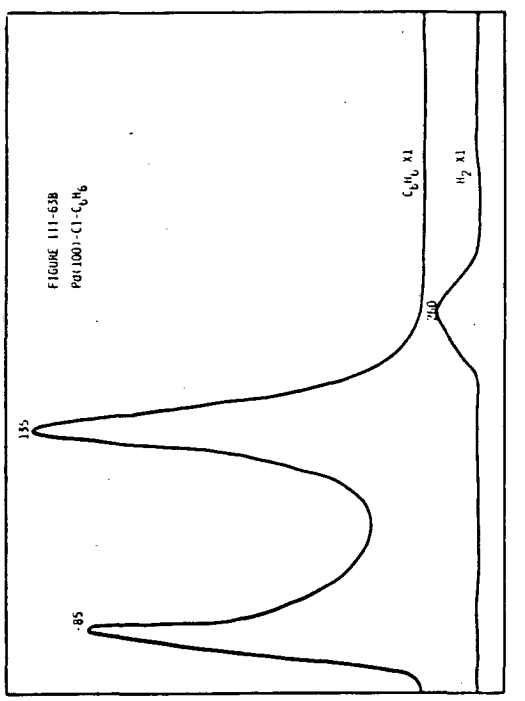
FIGURE III-63B
Pd(100)-Cl-C_6H_6
C_6H_6 X1
H_2 X1
85
135
240
INTENSITY
TEMPERATURE (^oC)

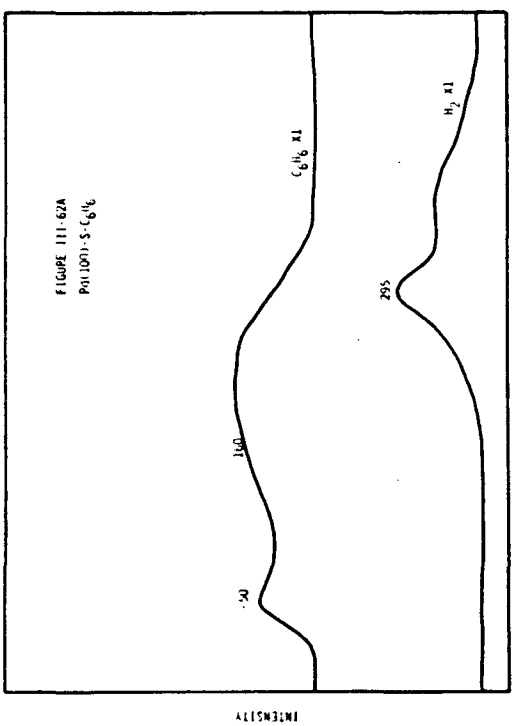
FIGURE III-62A
Pd(100)-S-C_6H_6
C_6H_6 X1
H_2 X1
50
150
295
INTENSITY
TEMPERATURE (^oC)

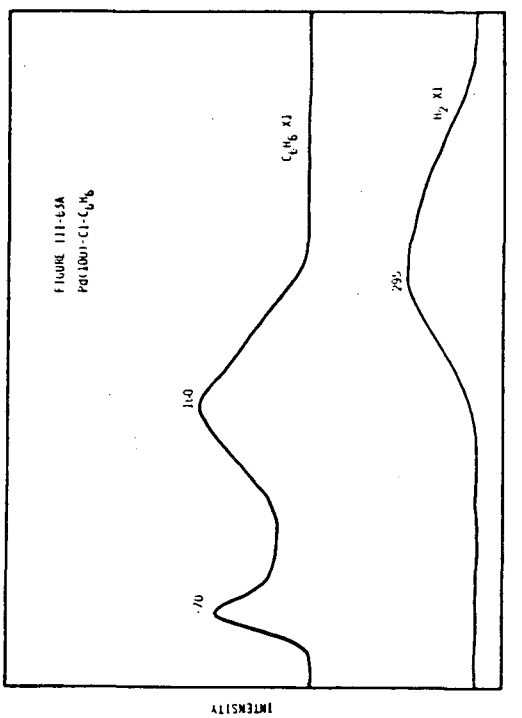
FIGURE III-63A
Pd(100)-Cl-C_6H_6
C_6H_6 X1
H_2 X1
70
140
295
INTENSITY
TEMPERATURE (^oC)

XBL 846-2190

Figure III-64. Chemisorption of ethylene on clean Pd(100) was found to be partially reversible. Shown in this figure is the thermal desorption spectrum of ethylene from Pd(100) at two exposure levels, 0.5 L (Figure III-64A) and 2.0 L (Figure III-64B). At 2.0 L, the desorption of ethylene is primarily molecular.

Figure III-65. Silicon increases the fraction of ethylene reversibly bound on Pd(100). Illustrated in this figure is the thermal desorption of ethylene, 0.5 L exposure, from two different silicon-covered surfaces. With increasing silicon coverage, 0.27 monolayer in Figure III-65A and 0.46 monolayer in Figure III-65B, the fraction of ethylene desorbing intact increases.

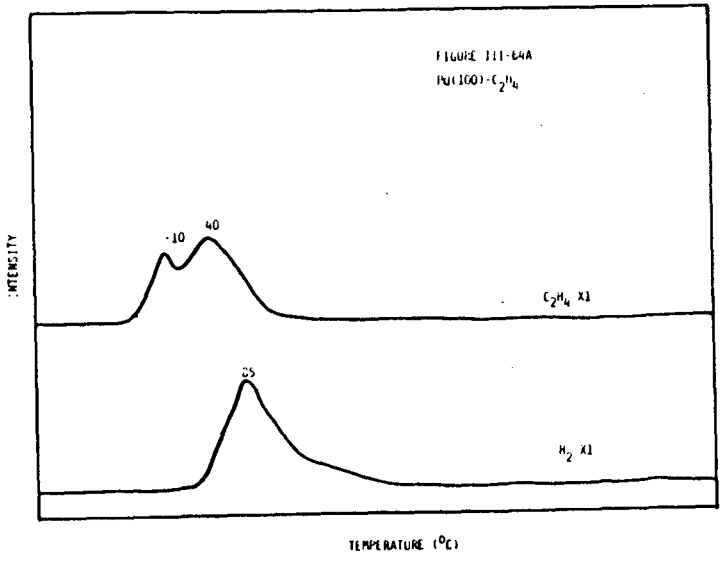
FIGURE III-64A
Pd(100)-C_2H_4
INTENSITY
-10
40
C_2H_4 X1
25
H_2 X1
TEMPERATURE (°C)

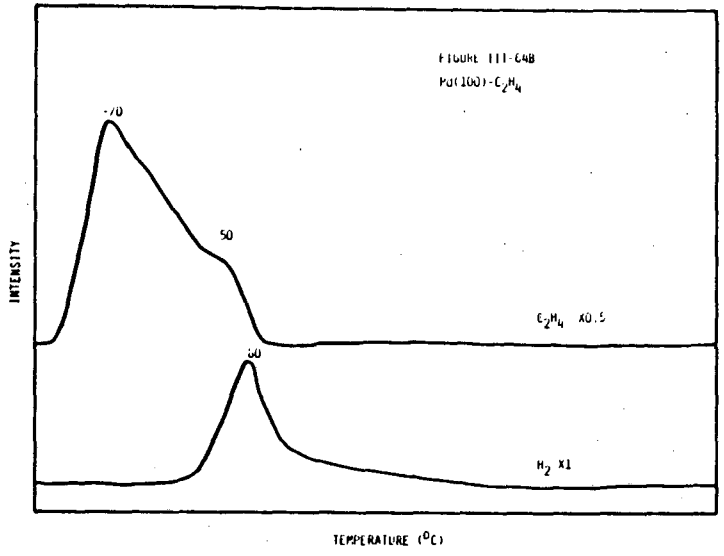
FIGURE III-64B
Pd(100)-C_2H_4
INTENSITY
50
C_2H_4 X0.5
50
H_2 X1
TEMPERATURE (°C)

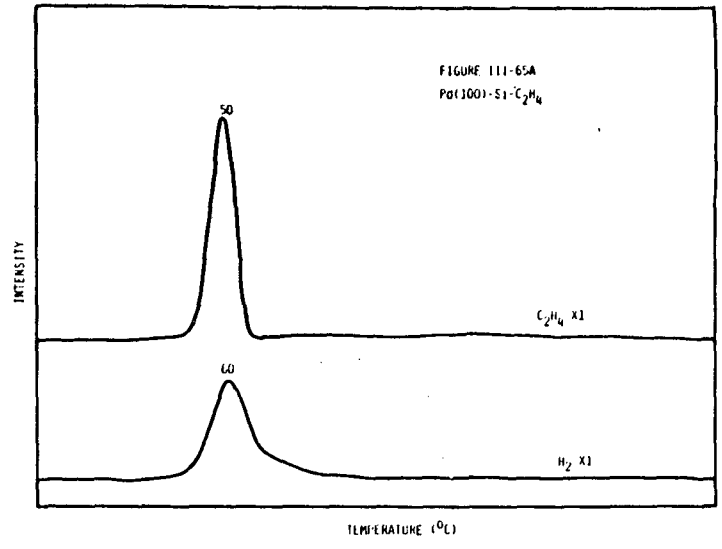
FIGURE III-65A
Pd(100)-Si-C_2H_4
INTENSITY
50
C_2H_4 X1
60
H_2 X1
TEMPERATURE (°C)

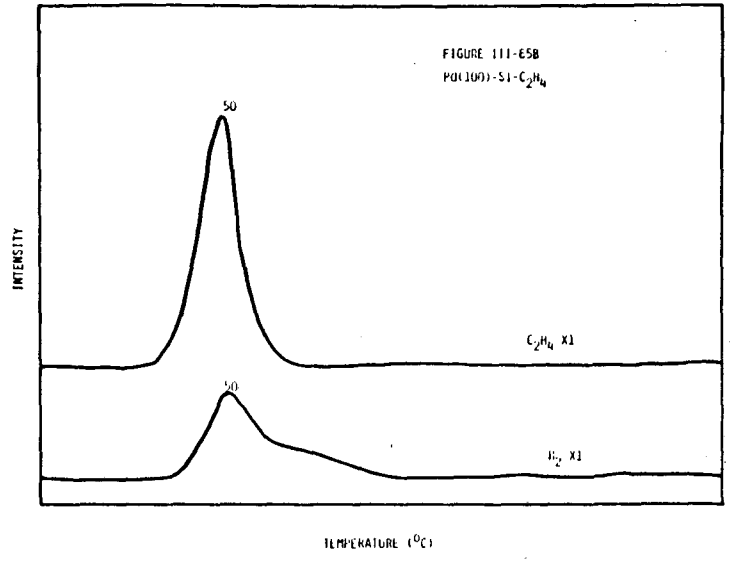
FIGURE III-65B
Pd(100)-Si-C_2H_4
INTENSITY
50
C_2H_4 X1
50
H_2 X1
TEMPERATURE (°C)

XBL 846-2189

Figure III-66. Thermal desorption of ethylene from phosphorus-covered Pd(100), θ_P = 0.43. Two spectra are shown, at exposures of 0.5 L (Figure III-66A) and 1.0 L (Figure III-66B). Ethylene chemisorption is completely reversible in both experiments.

Figure III-67. Sulphiding Pd(100), θ_S = 0.42, results in quantitative desorption of ethylene. Two ethylene exposures, 0.5 L and 1.0 L, are shown in the spectra in Figures III-67A and III-67B, respectively.

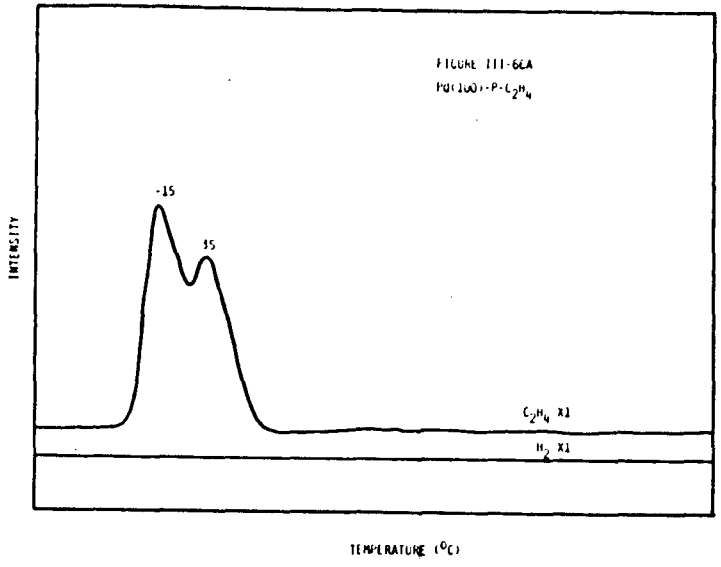
FIGURE III-66A
Pd(100)-P-C_2H_4
-15
35
C_2H_4 X1
H_2 X1
INTENSITY
TEMPERATURE (^{0}C)

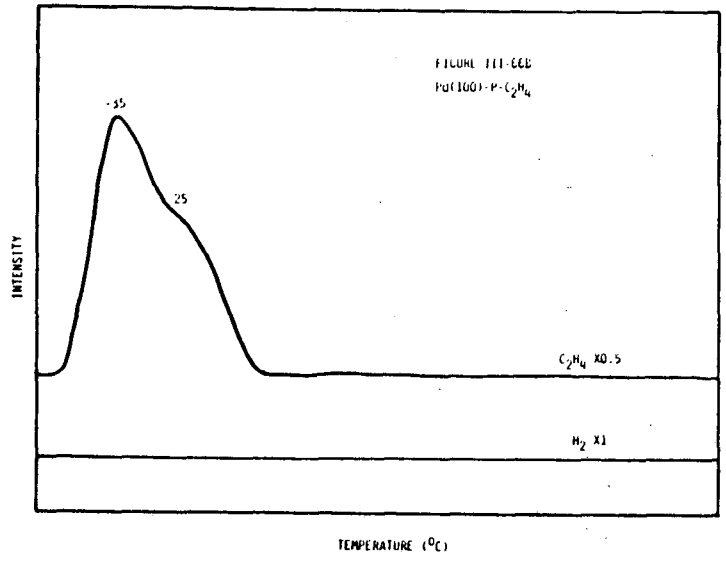
FIGURE III-66B
Pd(100)-P-C_2H_4
-35
25
C_2H_4 X0.5
H_2 X1
INTENSITY
TEMPERATURE (^{0}C)

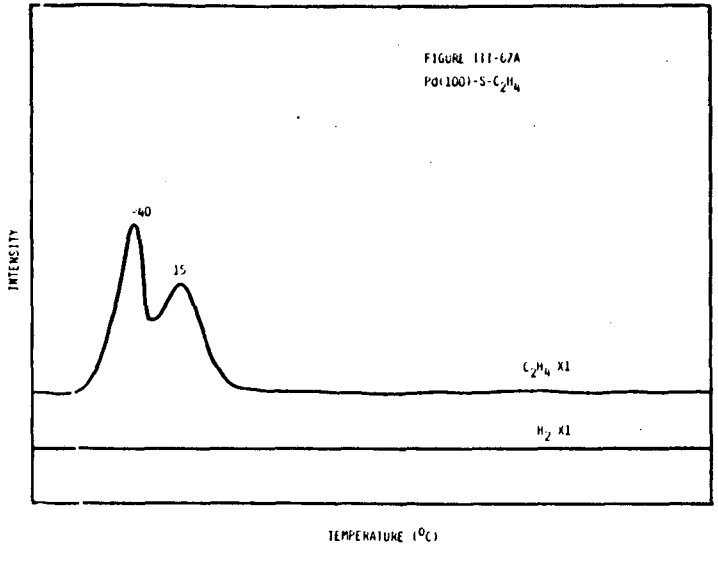
FIGURE III-67A
Pd(100)-S-C_2H_4
-40
35
C_2H_4 X1
H_2 X1
INTENSITY
TEMPERATURE (^{0}C)

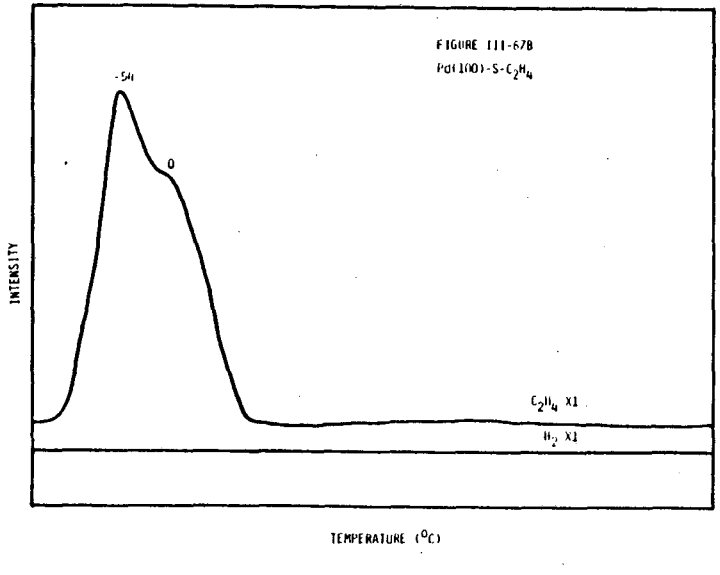
FIGURE III-67B
Pd(100)-S-C_2H_4
-50
0
C_2H_4 X1
H_2 X1
INTENSITY
TEMPERATURE (^{0}C)

XBL 846-2188

Figure III-68. At a chlorine coverage of 0.27 monolayer, the thermal desorption of ethylene from Pd(100) is nearly quantitative. The exposure of ethylene was 1.0 L.

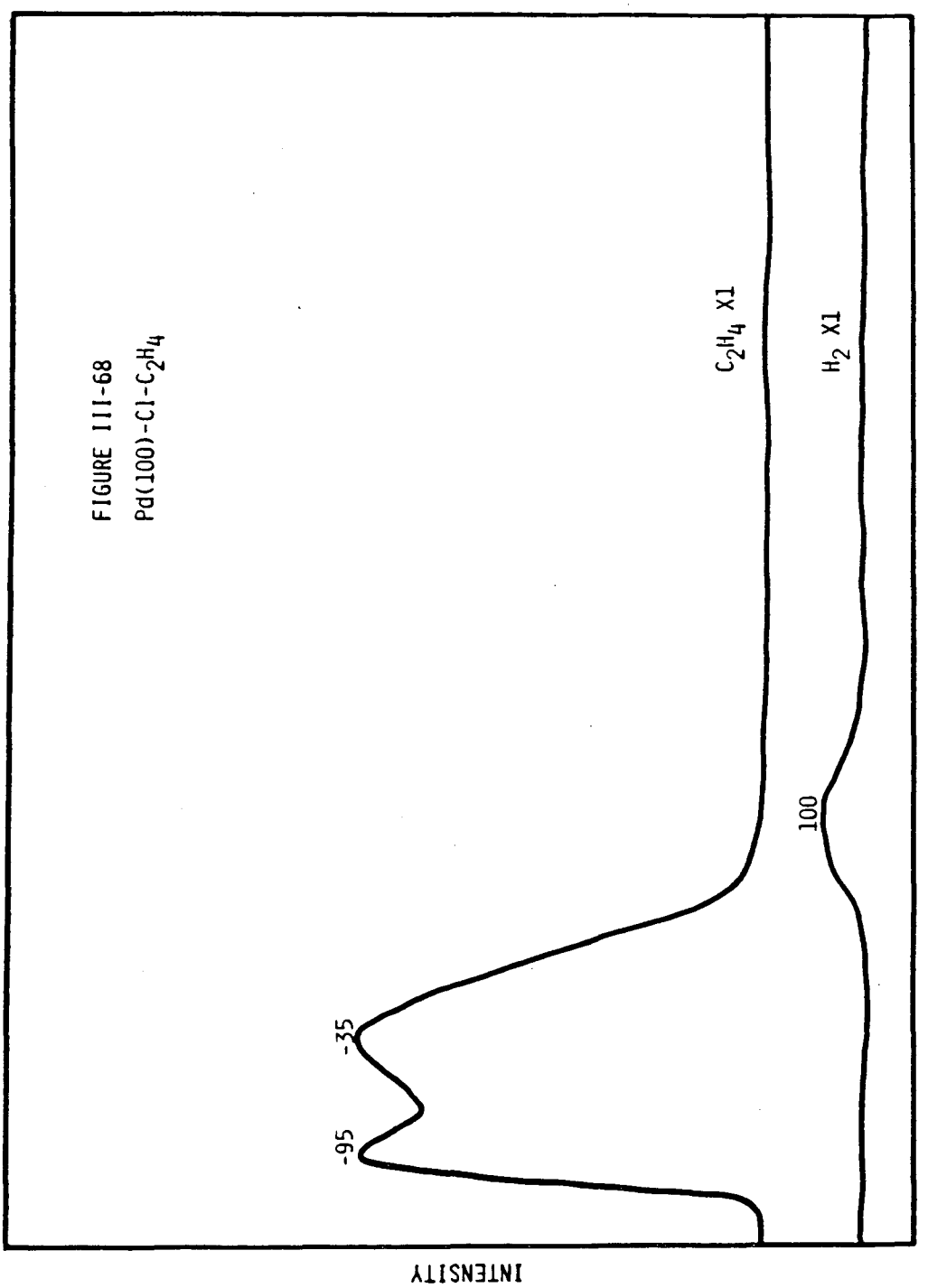
FIGURE III-68
Pd(100)-Cl-C_2H_4
C_2H_4 X1
H_2 X1
-35
-95
100
INTENSITY
TEMPERATURE (^oC)

XBL 846-2166

maximum was observed at 55°C (see Figure III-64A). Increasing the exposure resulted in an increase in the reversible desorption. A broad ethylene desorption consisting of two poorly resolved maxima at -20°C and 50°C was observed. No increase in the hydrogen maximum of 80°C was observed (see figure III-64B). The presence of any of the adatoms increased the fraction of reversibly bound ethylene. On a silicon-covered Pd(100) surface, $\theta_S = 0.27$, an ethylene thermal desorption maximum at 50°C was observed, with a hydrogen maximum at 60°C (see Figure III-65A). At a silicon coverage of 0.46 monolayer, the yield of reversibly bound ethylene increased further (see Figure III-65B). On phosphorus-covered Pd(100), $\theta_P = 0.43$, only reversible desorption of ethylene was observed, with maxima at -15°C and 35°C (see Figures III-66A and III-66B). On sulfur-covered Pd(100), $\theta_S = 0.42$, only reversible desorption was also observed. Two maxima were observed, at -40°C and 15°C (see Figures III-67A and III-67B). Ethylene chemisorption was also largely reversible on chlorine-covered Pd(100), $\theta_{Cl} = 0.27$. Two ethylene maxima were observed, at -95°C and -35°C (see Figure III-68).

N. Pd(110) - X - C_2H_2, where X = Si, P, S, or Cl

Thermal desorption of acetylene, C_2H_2, chemisorbed at -150°C from Pd(110) results in (a) reversible chemisorption, (b) decomposition to hydrogen and Pd(110)-C, (c) hydrogenation of acetylene to ethylene, and (d) cyclotrimerization of acetylene to benzene (see Figure III-69). Reversibly bound C_2H_2 desorbed with a thermal desorption maximum at -100°C and a long tail extending to 220°C. A broad H_2 maximum was

Figure III-69. Chemisorption of acetylene, 4.0 L, on Pd(110) yielded both ethylene and benzene in a subsequent thermal desorption spectrum. Comparing this figure with Figure III-1 reveals the fact that the yield of benzene is much less on the (110) surface than on the (111) surface.

Figure III-70. The amount of benzene desorbing from chemisorbed acetylene on Pd(110) increased in the presence of silicon. Illustrated in this figure is the thermal desorption spectrum of 4.0 L of acetylene from Pd(110) with a silicon coverage of 0.15 monolayer.

Figure III-71. The yield of reactively formed benzene is found to further increase at higher silicon coverages, $\theta_{Si} = 0.37$. Comparing the benzene trace in this figure with that in the previous figure, the increased yield is evident. The yield of ethylene decreased when compared to clean Pd(100) (see Figure III-69). In this thermal desorption experiment an acetylene exposure of 4.0 L was used.

Figure III-72. At a phosphorus coverage of 0.10 monolayer, a slight increase in the yield of benzene from acetylene chemisorbed on Pd(110) was observed. Displayed in this figure is the thermal desorption spectrum of acetylene, 4.0 L, from this phosphorus-covered Pd(110) surface.

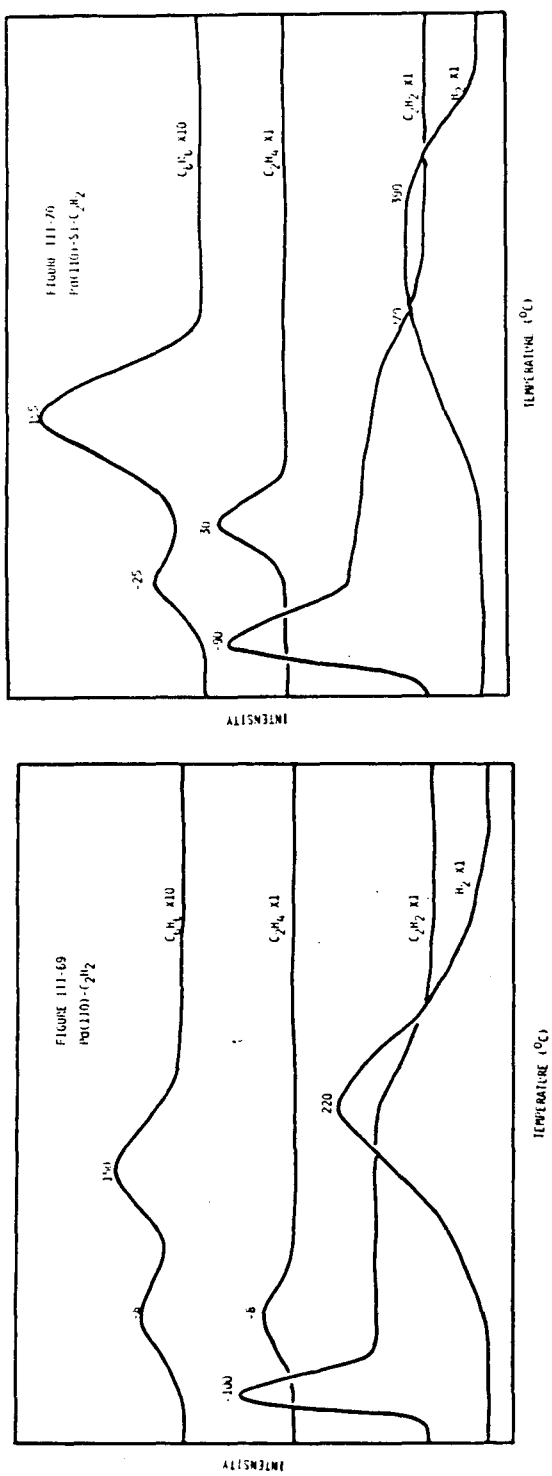
FIGURE III-69
Pd(110)-C_2H_2
C_6H_6 X10
C_2H_4 X1
C_2H_2 X1
H_2 X1
-78
150
-6
-130
220
INTENSITY
TEMPERATURE (°C)
FIGURE III-70
Pd(110)-Si-C_2H_2
C_6H_6 X10
C_2H_4 X1
C_2H_2 X1
H_2 X1
-25
-90
30
165
270
390
INTENSITY
TEMPERATURE (°C)
FIGURE III-71
Pd(110)-Si-C_2H_2
C_6H_6 X10
C_2H_4 X1
C_2H_2 X1
H_2 X1
145
-15
-90
40
570
INTENSITY
TEMPERATURE (°C)
FIGURE III-72
Pd(110)-P-C_2H_2
C_6H_6 X10
C_2H_4 X1
C_2H_2 X1
H_2 X1
165
0
-100
0
220
INTENSITY
TEMPERATURE (°C)

XBL 846-2187

observed at 220°C. Ethylene was found to desorb at -8°C. Two weak benzene maxima were observed, at -8°C and 150°C. The formation was further probed by a chemical displacement reaction. Acetylene was adsorbed on Pd(110) at 25°C. As soon as trimethylsilane was introduced into the chamber, benzene was detected in the mass spectrometer.

The yield of both ethylene and benzene from chemisorbed acetylene increased on silicon-covered Pd(110). At a silicon coverage of 0.15 monolayer ($\theta_{Si} = 0.15$), two benzene thermal desorption maxima were observed, at -25°C and 185°C (see Figure III-70). The intensity of the high temperature benzene maxima increased by a factor of two compared to the clean surface. An ethylene T_{max} was observed at 30°C, with an increase of 2.5 compared to the clean surface. The yield of H_2 was found to decrease, characterized by a broad maximum from 270°C to 390°C. At a silicon coverage of 0.37, the yield of benzene from acetylene increased further, while the yield of ethylene decreased (see Figure III-71). Two benzene maxima were observed, at -15°C and 185°C. The 185°C maximum increased by a factor of ~3.5 Ethylene was found to desorb at 40°C, with an intensity similar to that of the clean surface. Hydrogen desorbed in a broad plateau from 120°C to 240°C, followed by a broad maximum at 370°C. The ethylene yield was decreased further at this silicon coverage.

Phosphiding Pd(110) also increased the yield of benzene and ethylene formed from chemisorbed acetylene. At low phosphorus coverages, $\theta_P = 0.10$, the thermal desorption of acetylene is similar

Figure III-73. The yield of benzene from the trimerization of acetylene continued to increase at larger phosphorus coverages. The thermal desorption spectrum of chemisorbed acetylene, 4.0 L, from a phosphorus-covered Pd(110) surface, $\theta_P = 0.20$, is shown.

Figure III-74. A continued increase was observed in the amount of benzene formed from the trimerization of acetylene on a Pd(110) surface with 0.34 monolayer of phosphorus. The thermal desorption of 4.0 L of acetylene from this surface shows an increase in the amount of benzene desorbing at high temperatures.

Figure III-75. Benzene formed from the trimerization of acetylene was found to desorb primarily at high temperatures on a Pd(110) surface with a phosphorus coverage of 0.42 monolayer. The thermal desorption spectrum shown in the figure arises from the adsorption of 4.0 L of acetylene.

Figure III-76. At low sulfur coverages, no significant changes in the thermal desorption of acetylene from Pd(110) are observed. Displayed in this figure is the thermal desorption spectrum of acetylene, 4.0 L exposure, from a Pd(110) surface with 0.07 monolayer of sulfur.

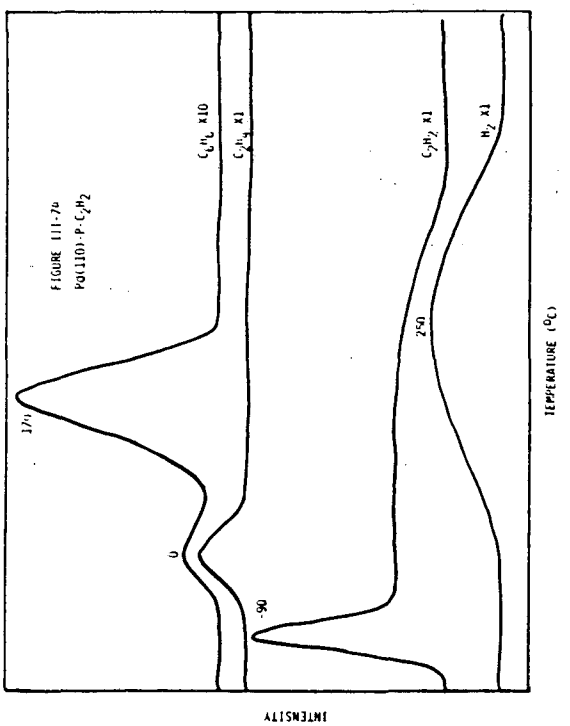
FIGURE III-74
Pd(110)-P-C_2H_2
C_2H_2 X10
C_2H_4 X1
C_2H_2 X1
H_2 X1
-90
0
170
250
INTENSITY
TEMPERATURE (°C)

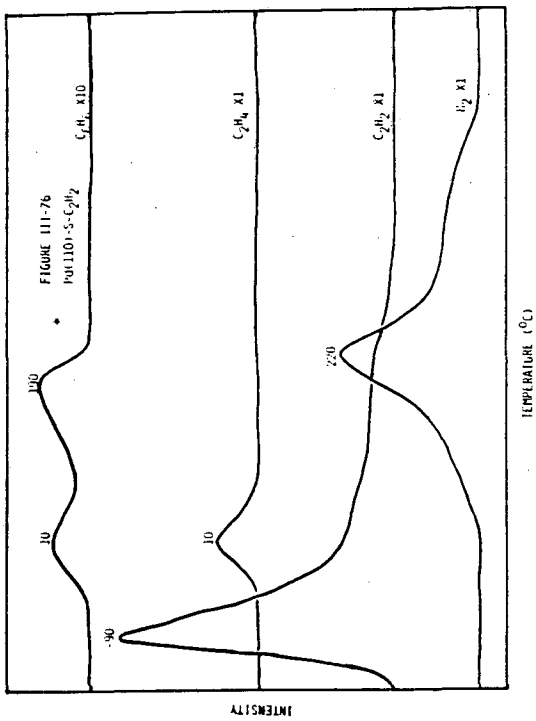
FIGURE III-76
Pd(110)-S-C_2H_2
C_2H_2 X10
C_2H_4 X1
C_2H_2 X1
H_2 X1
-90
10
100
220
INTENSITY
TEMPERATURE (°C)

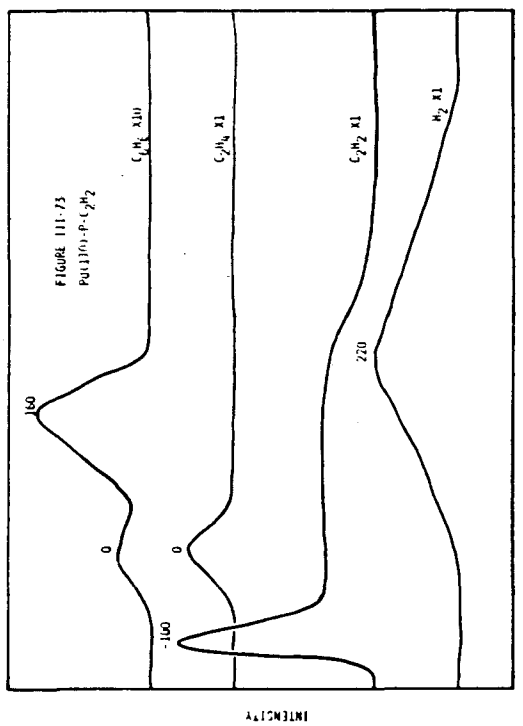
FIGURE III-73
Pd(110)-P-C_2H_2
C_2H_2 X10
C_2H_4 X1
C_2H_2 X1
H_2 X1
-100
0
160
220
INTENSITY
TEMPERATURE (°C)

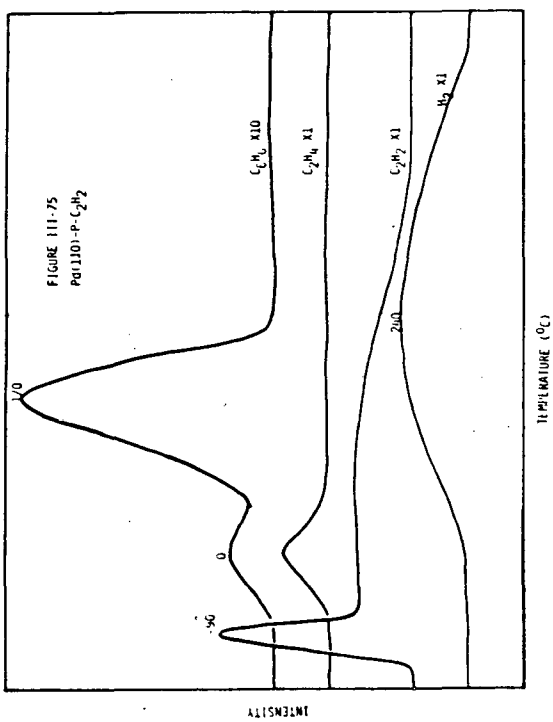
FIGURE III-75
Pd(110)-P-C_2H_2
C_2H_2 X10
C_2H_4 X1
C_2H_2 X1
H_2 X1
-90
0
110
240
INTENSITY
TEMPERATURE (°C)

XBL 846-2186

to that of a clean surface (see Figure III-72). Benzene desorption was found to increase at a phosphorus coverage of 0.20 monolayer. The low temperature maximum (T_{max} = 0°C) decreased slightly, while the high temperature maximum (T_{max} = 160°C) increased by a factor of 1.6. Ethylene desorbed at 0°C, with an increase of 1.5 (see Figure III-73). At a phosphorus coverage of 0.34 monolayer, two benzene thermal desorption maxima, at 0°C and 170°C, were observed. The high temperature maximum increased by a factor of three as compared to the clean surface. Ethylene desorbed at 0°C with a twofold increase (see Figure III-74). A nearly fourfold increase in the yield of benzene was observed at a phosphorus coverage of 0.42 (see Figure III-75). No further increase in the yield of ethylene was observed. A decrease in the amount of H_2 desorbing from the surface was observed.

On sulfur-covered Pd(110), the yield of ethylene in the thermal desorption of chemisorption was found to decrease with increased sulfur coverage. At a sulfur coverage of ~0.07 monolayer, the thermal desorption spectrum of chemisorbed acetylene is similar to that obtained on clean Pd(110) (see Figure III-76). Increasing the sulfur coverage to 0.15 monolayer results in a slight increase in the yield of benzene, while the yield of ethylene decreased by a factor of 1.25 (see Figure III-77). No ethylene was observed to desorb from a surface with a sulfur coverage of 0.35 monolayer. Two benzene thermal desorption maxima were observed, at 10°C and 150°C; the intensity of the 10°C maximum increased with respect to the high temperature maximum

Figure III-77. A slight increase in the yield of benzene was observed at higher sulfur coverage. This figure represents the thermal desorption of 4.0 L of acetylene from a Pd(110) surface with 0.14 monolayer of sulfur.

Figure III-78. At a sulfur coverage of 0.35 monolayer, an increase in the yield of benzene formed from the trimerization of acetylene on Pd(110) at low temperatures was observed. An increase in the benzene maximum of 0°C was observed. An acetylene exposure of 4.0 L was used in this experiment.

Figure III-79. A further increase was observed in the yield of reactively formed benzene at low temperatures on Pd(110) with 0.42 monolayer of sulfur present. The thermal desorption spectrum of 4.0 L of sulfur is shown.

Figure III-80. Chlorine suppressed both the hydrogenation and trimerization of acetylene on Pd(110). Illustrated is the thermal desorption spectrum of 4.0 L of acetylene from a surface with 0.34 monolayer of chlorine.

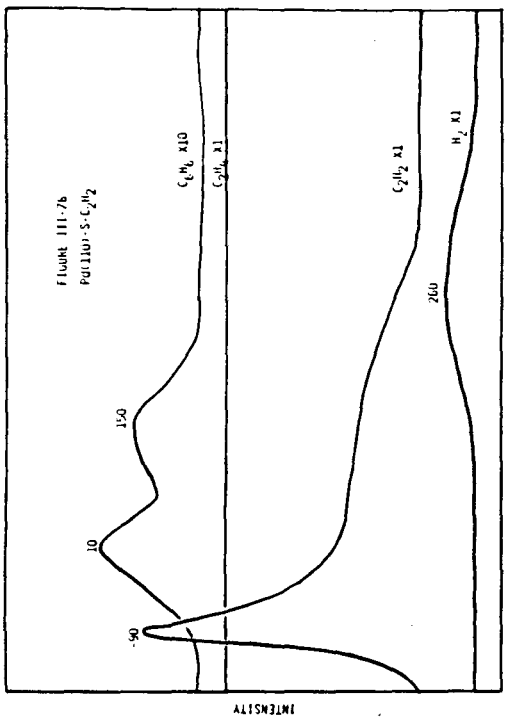
FIGURE III-76
Pd(110)-S-C_2H_2
C_6H_6 X10
C_2H_4 X1
C_2H_2 X1
H_2 X1
-90
10
150
260
INTENSITY
TEMPERATURE (°C)

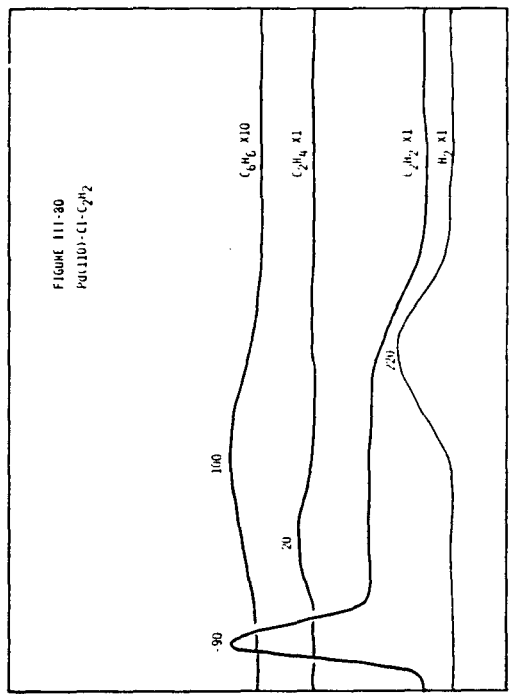
FIGURE III-80
Pd(110)-Cl-C_2H_2
C_6H_6 X10
C_2H_4 X1
C_2H_2 X1
H_2 X1
-90
100
20
220
INTENSITY
TEMPERATURE (°C)

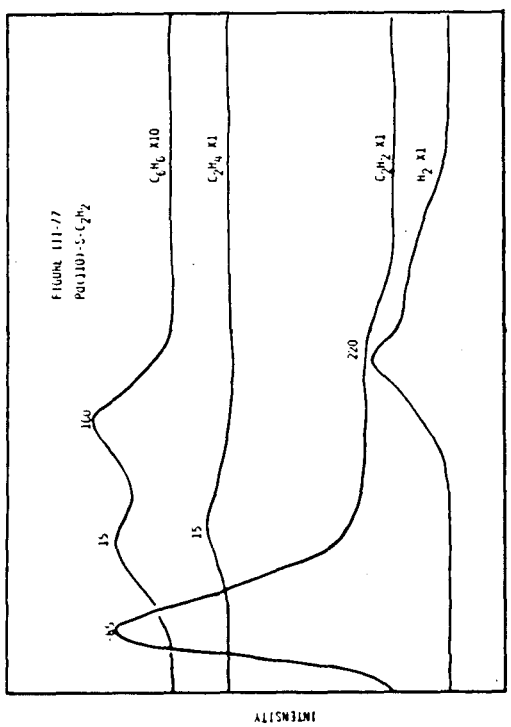
FIGURE III-77
Pd(110)-S-C_2H_2
C_6H_6 X10
C_2H_4 X1
C_2H_2 X1
H_2 X1
-90
15
160
15
220
INTENSITY
TEMPERATURE (°C)

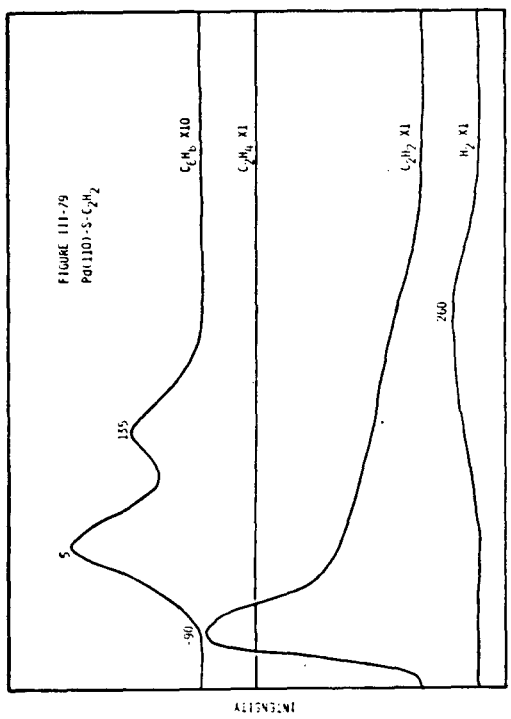
FIGURE III-79
Pd(110)-S-C_2H_2
C_6H_6 X10
C_2H_4 X1
C_2H_2 X1
H_2 X1
-90
5
155
260
INTENSITY
TEMPERATURE (°C)

XBL 846-2185

Figure III-81. The hydrogenation of acetylene on Pd(110) was affected by sequential adsorption of hydrogen, 3.0 L, and acetylene, 4.0 L. The thermal desorption spectrum of the above surface state is shown. The hydrogenation of acetylene on Pd(111) and Pd(100) completely suppressed the trimerization of acetylene; however, trimerization was evident on Pd(110).

Figure III-82. Silicon increased the amount of both ethylene and benzene in the thermal desorption of hydrogen and acetylene from Pd(110). Displayed in this figure is the thermal desorption spectrum of the surface state formed by the sequential adsorption of 3.0 L of H_2 and 4.0 L of C_2H_2 on silicon-covered Pd(110), $\theta_{Si} = 0.20$.

Figure III-83. The yield of ethylene did not increase in the hydrogenation of acetylene on phosphorus-covered Pd(110). The thermal desorption of 3.0 L of H_2 and 4.0 L of C_2H_2 from phosphorus-covered Pd(110), $\theta_P = 0.50$, is shown.

Figure III-84. Sulfur suppressed the hydrogenation of acetylene on Pd(110). At a sulfur coverage of 0.48 monolayer, a decrease in ethylene desorption is shown. The exposure of hydrogen was 3.0 L and of acetylene was 4.0 L in this experiment.

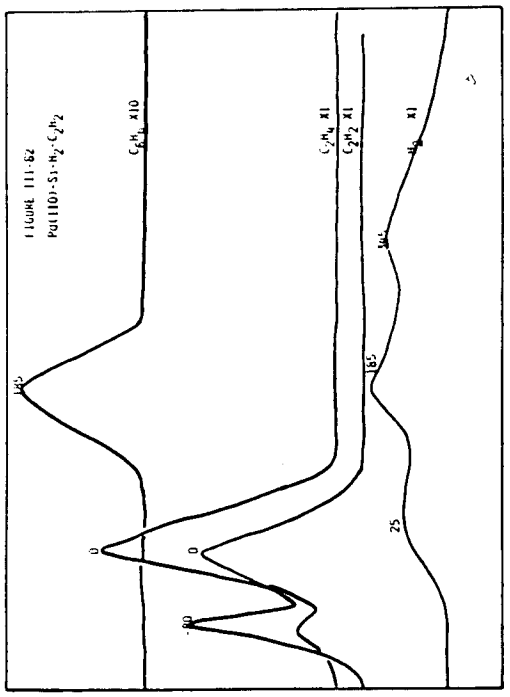
FIGURE III-82
Pd(110)-S1-H2-C2H2
C6H6 X10
C2H4 X1
C2H2 X1
H2 X1
0
-80
185
0
185
25
INTENSITY
TEMPERATURE (°C)

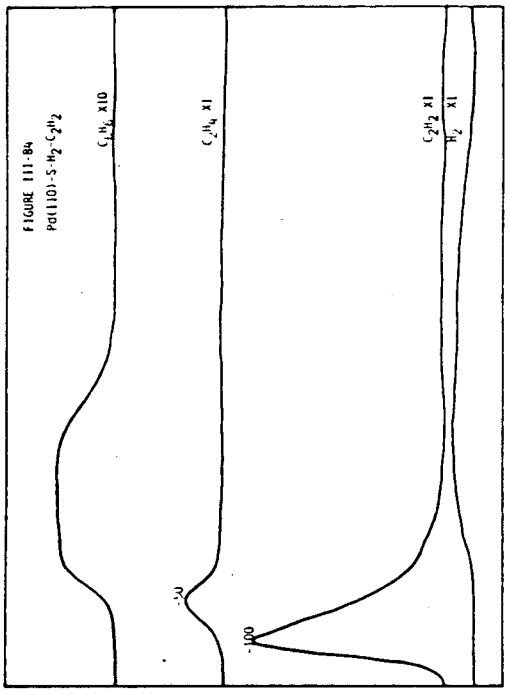
FIGURE III-84
Pd(110)-S-H2-C2H2
C6H6 X10
C2H4 X1
C2H2 X1
H2 X1
-100
INTENSITY
TEMPERATURE (°C)

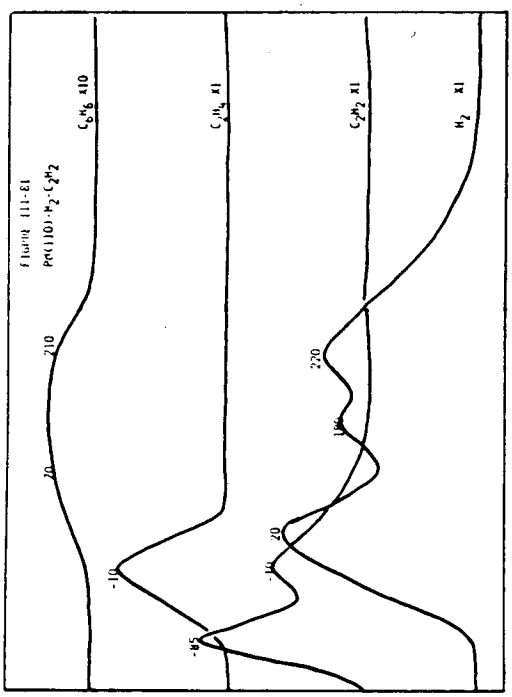
FIGURE III-81
Pd(110)-H2-C2H2
C6H6 X10
C2H4 X1
C2H2 X1
H2 X1
20
210
-10
-85
270
185
20
INTENSITY
TEMPERATURE (°C)

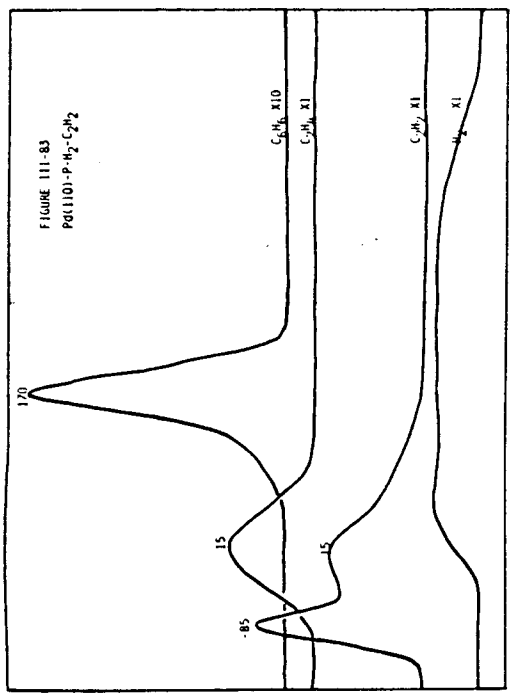
FIGURE III-83
Pd(110)-P-H2-C2H2
C6H6 X10
C2H4 X1
C2H2 X1
H2 X1
170
15
-85
15
INTENSITY
TEMPERATURE (°C)

XBL 846-2184

Figure III-85. The hydrogenation of acetylene was suppressed on chlorine-covered Pd(110), $\theta_{Cl} = 0.37$. Comparing the thermal desorption spectrum in this figure with that of clean Pd(110), Figure III-81, the decrease in yield is apparent. Hydrogen, 3.0 L, and acetylene, 4.0 L, were adsorbed on this surface.

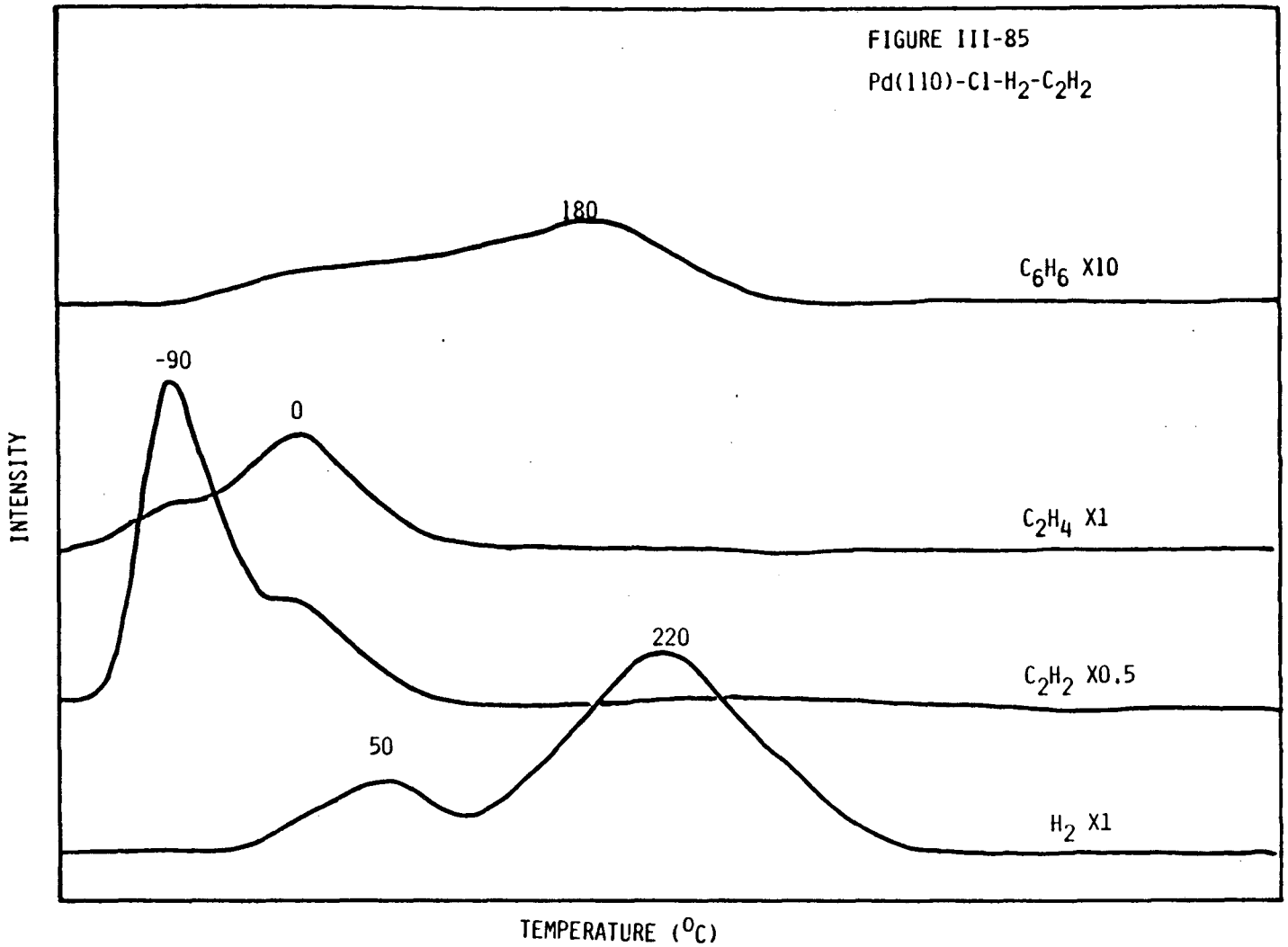
FIGURE III-85
Pd(110)-Cl-H2-C2H2
180
C6H6 X10
-90
0
C2H4 X1
220
C2H2 X0.5
50
H2 X1
INTENSITY
TEMPERATURE (°C)

XBL 846-2165

(see Figure III-78). At a sulfur coverage of 0.42 monolayer, the yield of benzene in the low temperature maximum increases further (see Figure III-79).

On chlorine-covered Pd(110), the decomposition of acetylene, hydrogenation, and trimerization were suppressed. At a chlorine coverage of 0.34 monolayer, a weak ethylene desorption was observed at 20°C, and a weak broad benzene desorption center was observed at approximately 100°C (see Figure III-80).

O. Pd(110) - X - H_2 - C_2H_2, where X = Si, P, S, or Cl

The hydrogenation of acetylene was investigated on clean Pd(110) and on silicon-, phosphorus-, sulfur-, and chlorine-covered Pd(110). In these experiments, approximately 3.0 L of hydrogen was adsorbed, followed by adsorption of 4.0 L of acetylene. On clean Pd(110) an increase in the yield of ethylene was observed compared to adsorption of C_2H_2 alone. An ethylene T_{max} was observed at -10°C, and a broad benzene maximum was observed from 70°C to 210°C (see Figure III-81). Silicided Pd(110) resulted in an increase in the yield of ethylene as compared to a clean surface. At a silicon coverage of 0.20 monolayer, a twofold increase in the yield of ethylene was evident, along with an increase in the yield of benzene at T_{max} = 185°C (see Figure III-82).

On a surface covered with 0.50 monolayer of phosphorus, a 25 percent decrease in the ethylene yield was observed, as compared to the clean surface. The benzene yield increased by a factor of ~2.0 (θ_S = 0.5), at T_{max} = 170°C (see Figure III-83). Sulphided Pd(110)

(θ_S = 0.5) resulted in a 2.5-fold decrease in the ethylene yield. A broad benzene maximum was observed from -15°C to 120°C (see Figure III-84). Similar results were obtained on chlorine-covered Pd(110). At a chlorine coverage of 0.37 monolayer, an ethylene T_{max} was observed at 0°C, with an intensity 50 percent of that observed on a clean Pd(110) surface. A broad benzene maximum was observed with a T_{max} at 180°C (see Figure III-85).

P. Pd(110) - X - D_2 - C_2H_2, where X = Si, P, S, and Cl

To further probe the mechanism of hydrogenation of acetylene on clean Pd(110) and adatom-covered surfaces, the hydrogenation reactions were performed using deterium. On clean Pd(110) the predominate species was the ethylene containing two deuteriums, $C_2H_2D_2$. None of the adatoms studied--Si, P, S, and Cl--significantly altered this result (see Figures III-86 through III-90).

Q. Pd(110) - X - C_2H_2 - $(CH_3)_3SiH$, where X = Si, P, S, or Cl

The hydrosilation of acetylene with trimethylsilane, $(CH_3)_3SiH$, was investigated as function of adatom. In these experiments 4.0 L of acetylene was adsorbed, followed by 4.0 L of $(CH_3)_3SiH$. On clean Pd(110), the thermal desorption spectrum of the above surface state yielded a compete mixture of products. Among the products were ethylene, benzene, and vinyltrimethylsilane, the hydrosilation product. A broad ethylene thermal desorption maximum was observed at -40°C. Two benzene maxima were observed, at -40°C and 100°C. Vinyltrimethylsilane was observed to have a T_{max} at 25°C (see Figure III-91). On silicon-covered Pd(110), θ_{Si} = 0.25, the yield of vinyltrimethylsilane

Figure III-86. Reaction of D_2 with C_2H_2 on Pd(110) yielded $C_2H_2D_2$ as the major product. In the thermal desorption spectrum shown in this figure, D_2 and C_2H_2 were sequentially adsorbed at exposures of 3.0 L and 4.0 L, respectively.

Figure III-87. $C_2D_2H_2$ was the predominant ethylene observed in the thermal desorption spectrum of D_2 and C_2H_2 from silicon-covered Pd(110), $\theta_{Si} = 0.15$. The thermal desorption spectrum shown in this figure arises from the adsorption of 3.0 L of D_2 and 4.0 L of C_2H_2.

Figure III-88. Phosphorus did not alter the distribution of the ethylenes formed from the reaction of D_2 and C_2H_2 on Pd(110). Displayed in this figure is the thermal desorption spectrum of 3.0 L of D_2 and 4.0 L of C_2H_2 from phosphorus-covered Pd(110), $\theta_P = 0.50$. $C_2H_2D_2$ was the major product.

Figure III-89. Although sulfur suppresses the hydrogenation of acetylene, $C_2H_2D_2$ was still the predominant ethylene from the reaction of D_2 and C_2H_2 on Pd(110). The thermal desorption spectrum in this figure arises from a sulfur-covered Pd(110) surface, $\theta_S = 0.50$, with D_2, 3.0 L, and C_2H_2, 4.0 L, adsorbed on it.

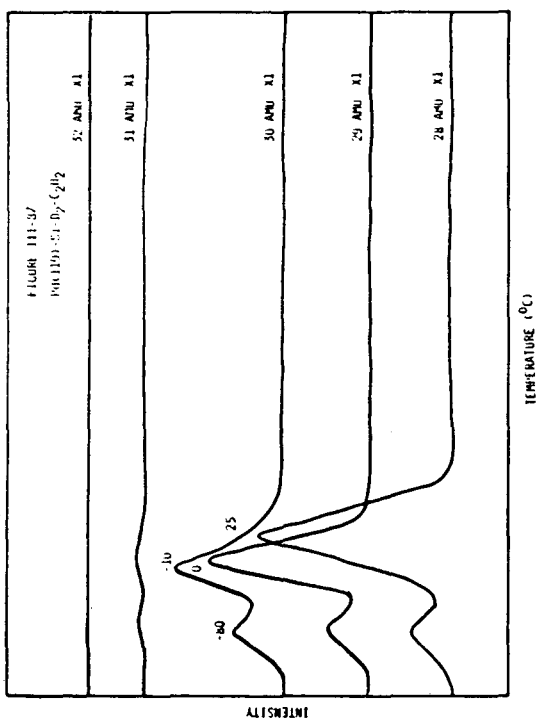
FIGURE III-87
Pd(110)-S1-D2-C2H2
52 AMU X1
51 AMU X1
30 AMU X1
29 AMU X1
28 AMU X1
-80
-10
0
25
INTENSITY
TEMPERATURE (°C)

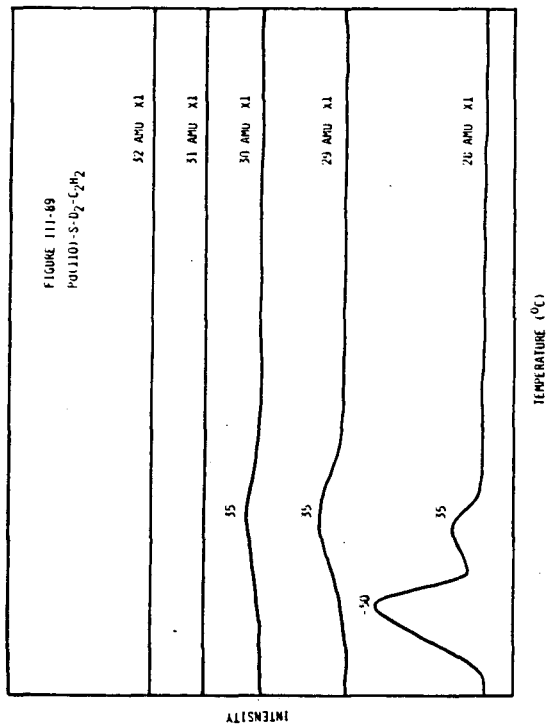
FIGURE III-89
Pd(110)-S-D2-C2H2
52 AMU X1
51 AMU X1
30 AMU X1
29 AMU X1
28 AMU X1
-50
55
35
55
INTENSITY
TEMPERATURE (°C)

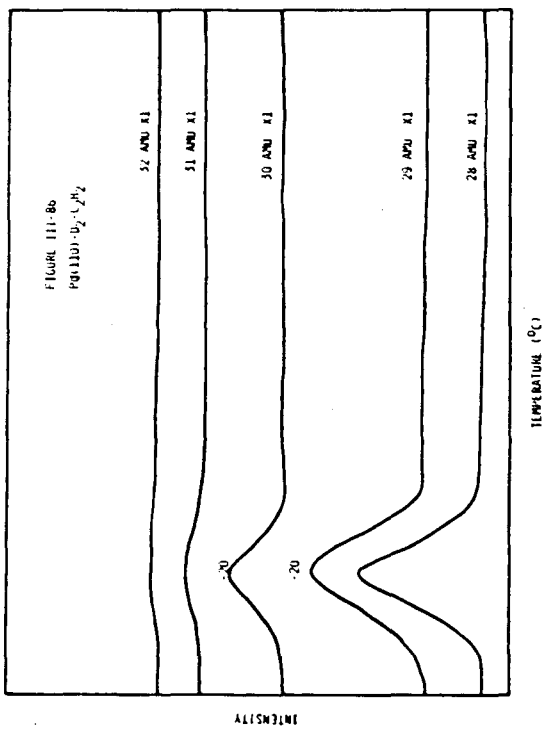
FIGURE III-86
Pd(110)-D2-C2H2
52 AMU X1
51 AMU X1
30 AMU X1
29 AMU X1
28 AMU X1
-20
-20
INTENSITY
TEMPERATURE (°C)

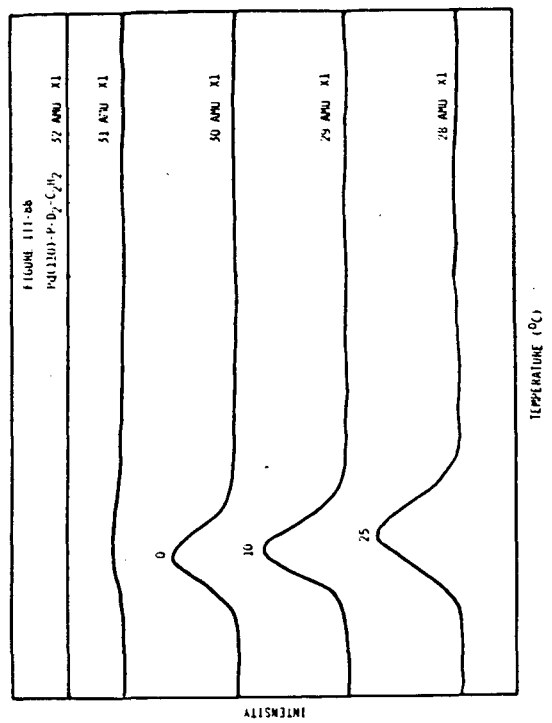
FIGURE III-88
Pd(110)-P-D2-C2H2
52 AMU X1
51 AMU X1
30 AMU X1
29 AMU X1
28 AMU X1
0
10
25
INTENSITY
TEMPERATURE (°C)

XBL 846-2183

Figure III-90. Hydrogenation of acetylene was suppressed by the presence of chlorine on Pd(110). From the thermal desorption spectrum shown in this figure, it appears that $C_2H_2D_2$ is the major product. The chlorine coverage was 0.37 monolayer, and the D_2 and C_2H_2 exposures were 3.0 L and 4.0 L, respectively.

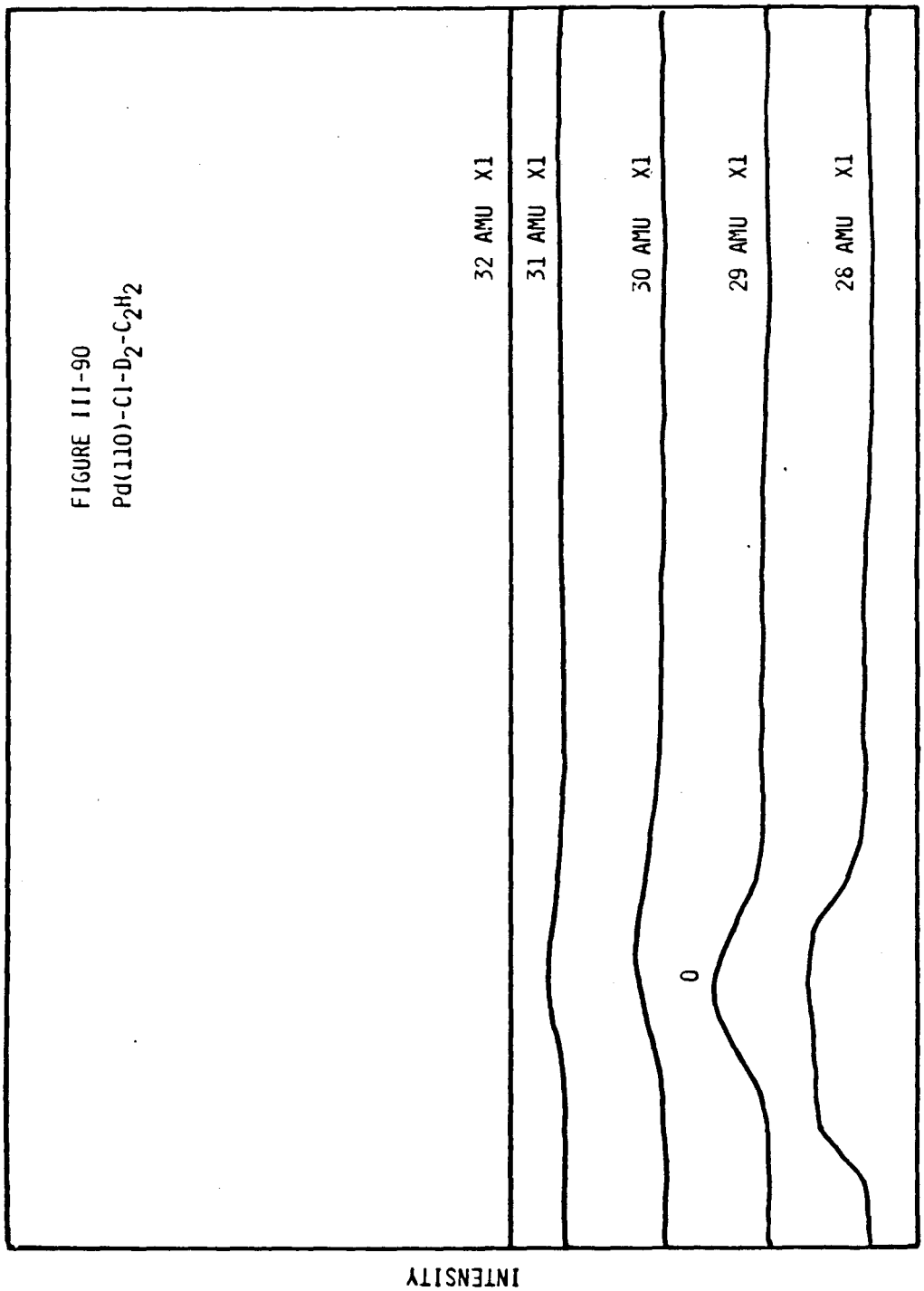

FIGURE III-90
Pd(110)-Cl-D_2-C_2H_2

XBL 846-2164

remained unchanged; however, increases at a single maximum and two poorly resolved maxima were observed at -30°C and 35°C (see Figure III-92). Increased yields of benzene (T_{max} = -25°C and 160°C) and ethylene (T_{max} = 35°C) were also observed. On phosphorus-covered Pd(110), θ_P = 0.50, the yield of vinyltrimethylsilane increased by a factor of 2.3, with a single maximum at 50°C. An increase in the yield of both ethylene (T_{max} = 0°C) and benzene (T_{max} = 170°C) was also observed (see Figure III-93). Sulphided Pd(110) resulted in an increased yield of vinyltrimethylsilane by a factor of 3.2 (T_{max} = 0°C). Trimethysilane was observed with desorption maxima at -100°C, -80°C, and 50°C. A decrease in the yield of both ethylene and benzene was observed (see Figure III-94). On chlorine-covered Pd(110), θ_{Cl} = 0.40, vinyltrimethylsilane yield increased by a factor of two (T_{max} = 50°C). The ethylene and benzene yield was comparable to that of the clean surface (see Figure III-95).

R. <u>Pd(110) - X - H_2, where X = Si, P, S, or Cl</u>

The relative sticking coefficient of H_2 on clean and adatom-covered surfaces was determined using thermal desorption spectroscopy. The area under the H_2 thermal desorption curve at 0.1 L was determined. The ratio of the area under the H_2 thermal desorption curve on the adatom-covered surface to the area from the clean surface at 0.1 L exposure is defined as the relative sticking coefficient. A plot of sticking coefficient versus adatom coverage is shown in Figure III-96. Phosphorus was found to have the least impact on the sticking coefficient.

Figure III-91. The hydrosilation of acetylene with trimethylsilane was affected on Pd(110). Vinyltrimethylsilane, the hydrosilation product, desorbed in the thermal desorption of the surface state formed by sequential adsorption of acetylene, 4.0 L, and trimethylsilane, 4.0 L, on Pd(110). Benzene and ethylene also desorbed.

Figure III-92. Silicon did not increase the yield of vinyltrimethylsilane formed in the thermal desorption of acetylene and trimethylsilane from Pd(110). However, increased ethylene and benzene desorption was observed on this silicon-covered surface, $\theta_{Si} = 0.25$. The exposures of acetylene and trimethylsilane were both 4.0 L in this experiment.

Figure III-93. Phosphiding Pd(110), $\theta_P = 0.50$, increased the yield of vinyltrimethylsilane from the thermal desorption of acetylene and trimethylsilane from this surface. The increase is evident when the vinyltrimethylsilane trace in this figure is compared with the vinyltrimethylsilane trace in Figure III-91. Four-langmuir exposures were used for both acetylene and trimethylsilane.

Figure III-94. Increased vinyltrimethylsilane desorption was observed in the thermal desorption spectrum of acetylene and trimethylsilane from sulfur-covered Pd(110). The sulfur coverage was 0.50 monolayer, and the exposure of both acetylene and trimethylsilane was 4.0 L.

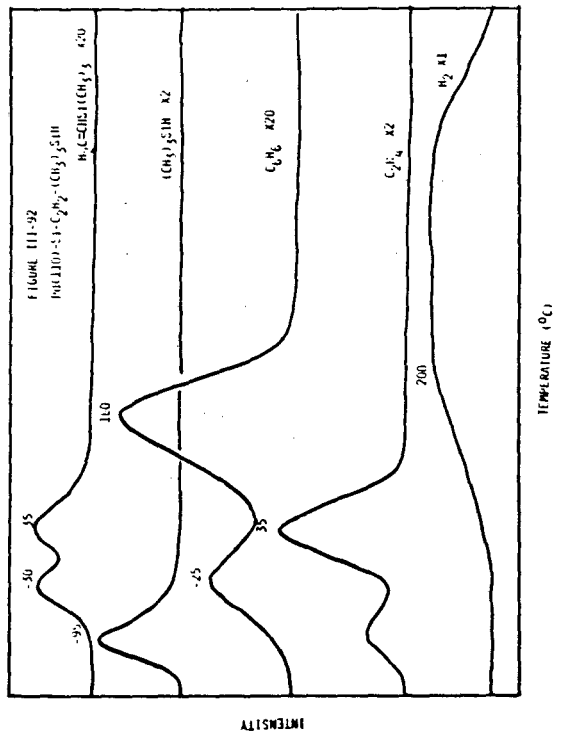
FIGURE III-92
Pd(111)-S-C2H2-(CH3)2SiH
H2C=CHSi(CH3)3 X20
(CH3)2SiH X2
C6H6 X20
C2H4 X2
H2 X1
-50
-95
55
110
-25
35
200
INTENSITY
TEMPERATURE (°C)

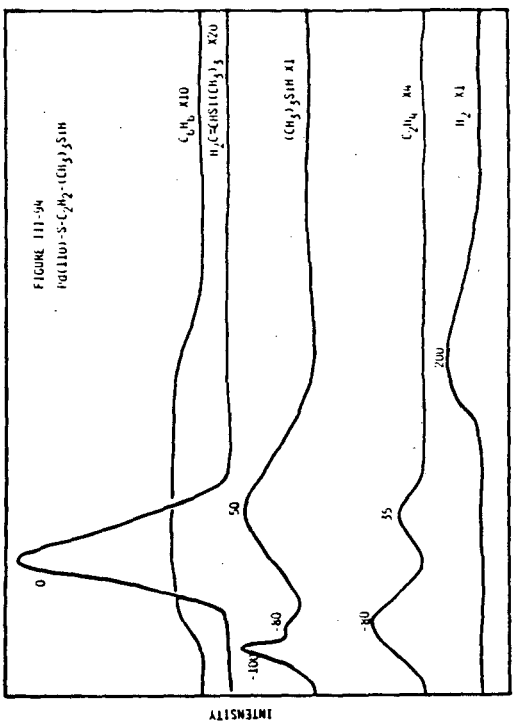
FIGURE III-94
Pd(111)-S-C2H2-(CH3)2SiH
C6H6 X10
H2C=CHSi(CH3)3 X20
(CH3)2SiH X1
C2H4 X4
H2 X1
0
-100
50
-80
35
-30
200
INTENSITY
TEMPERATURE (°C)

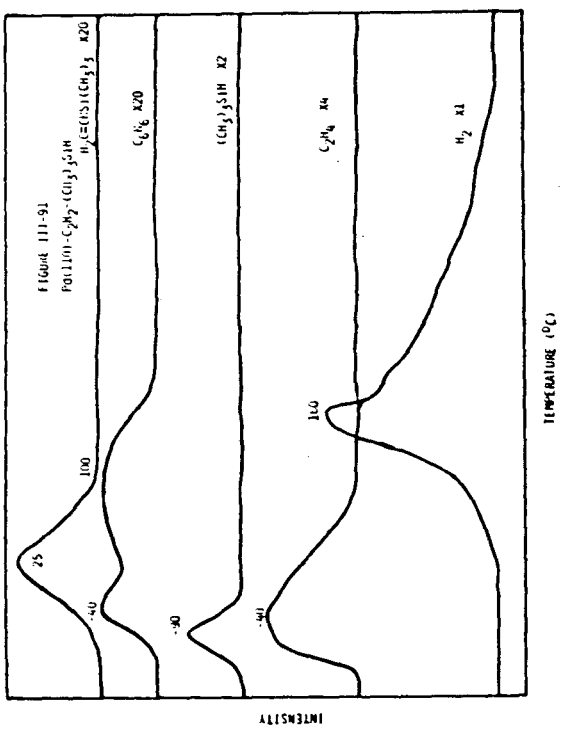
FIGURE III-91
Pd(111)-C2H2-(CH3)2SiH
H2C=CHSi(CH3)3 X20
C6H6 X20
(CH3)2SiH X2
C2H4 X4
H2 X1
25
100
-40
-90
-91
110
INTENSITY
TEMPERATURE (°C)

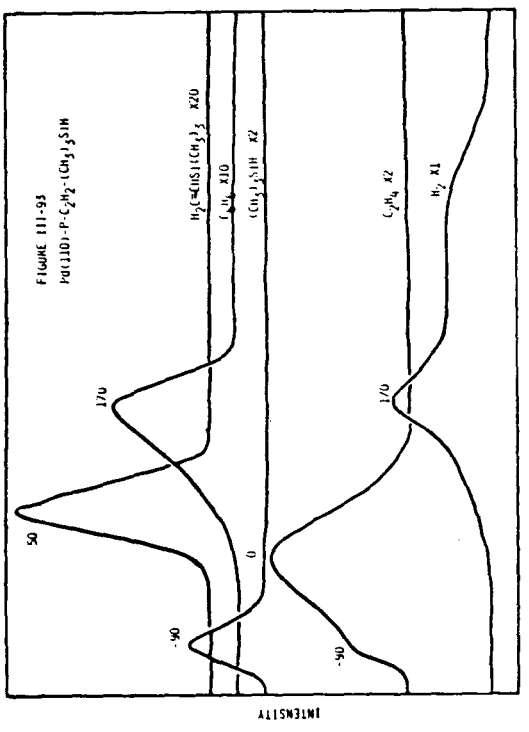
FIGURE III-93
Pd(111)-P-C2H2-(CH3)2SiH
H2C=CHSi(CH3)3 X20
C2H4 X10
(CH3)2SiH X2
C2H4 X2
H2 X1
50
170
-90
0
-90
170
INTENSITY
TEMPERATURE (°C)

XBL 846-2182

Figure III-95. The thermal desorption spectrum in this figure demonstrates that the presence of chlorine also increases the yield of vinyltrimethylsilane from acetylene and trimethylsilane. In this experiment, acetylene, 4.0 L, and trimethylsilane, 4.0 L, were sequentially adsorbed on a chlorine-covered Pd(110) surface, θ_{Cl} = 0.40.

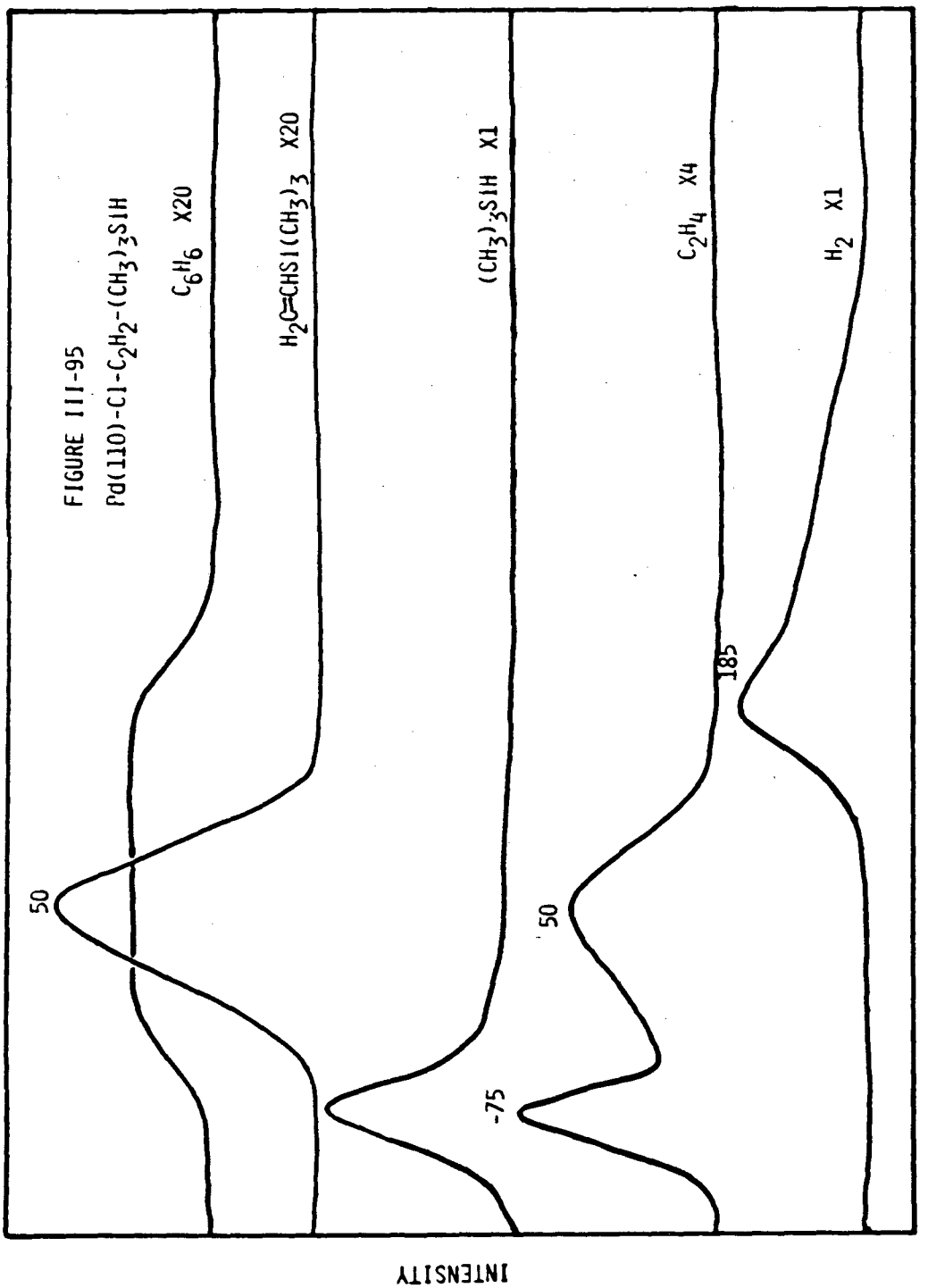
FIGURE III-95
Pd(110)-Cl-C2H2-(CH3)3SiH
C6H6 X20
H2C=CHSi(CH3)3 X20
(CH3)3SiH X1
C2H4 X4
H2 X1
50
-75
50
185
INTENSITY
TEMPERATURE (°C)

XBL 846-2162

Figure III-96. A plot of the relative sticking coefficient of H_2 on Pd(110) versus adatom coverage in monolayers is shown. The adatoms studied were Si, P, S, and Cl. In contrast to the (111) and (100) surfaces, where the correlation between electronegativity and decreased sticking coefficient was observed, no such trend was observed on this surface.

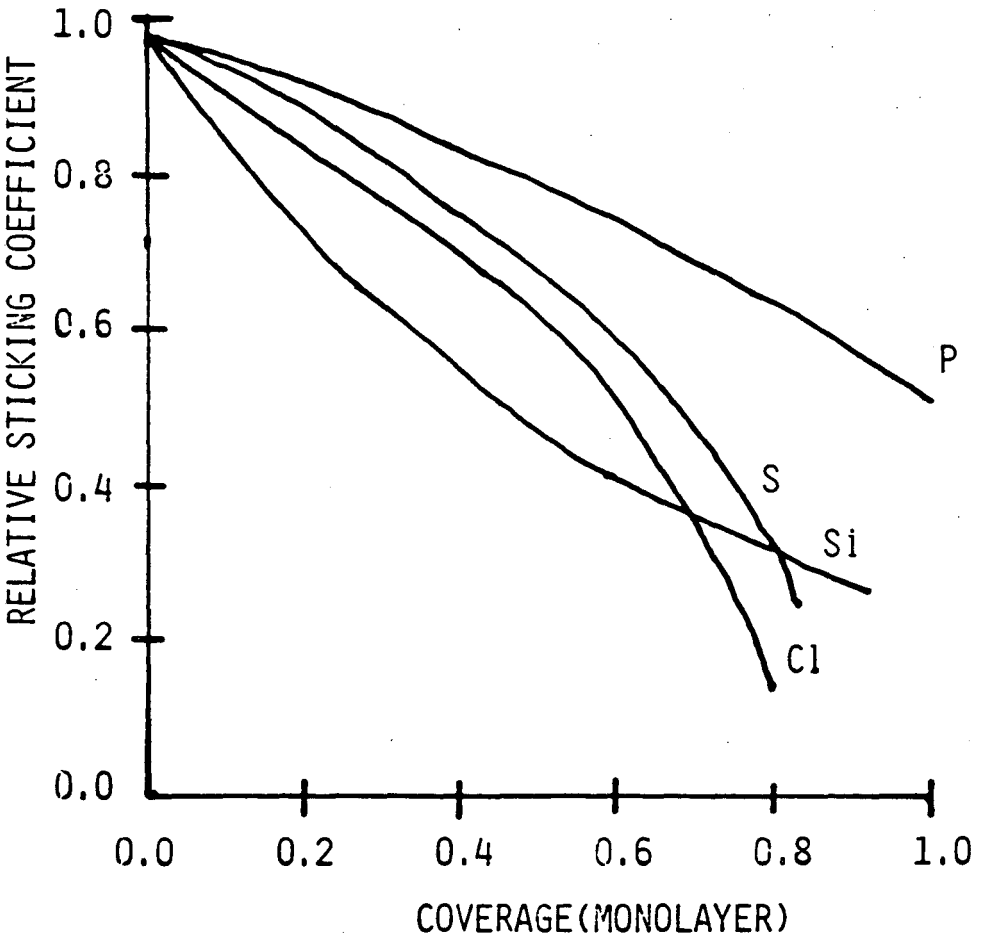
RELATIVE STICKING COEFFICIENT
1.0
0.8
0.6
0.4
0.2
0.0
0.0
0.2
0.4
0.6
0.8
1.0
COVERAGE(MONOLAYER)
P
S
Si
Cl

XBL 846-2163

S. Pd(110) - X - C_2H_4, where X = Si, P, S, or Cl

Chemisorption of ethylene on clean Pd(110) was largely irreversible at low exposures (0.5 L). Two hydrogen thermal desorption maxima were observed, at 50°C and 170°C. Ethylene was found to have two small maxima, at -120°C and 50°C (see Figure III-97A). At higher exposures, the amount of hydrogen desorption did not increase significantly (T_{max} = 50°C and 185°C). The molecular desorption did increase with an increase at the high temperature maximum at 40°C (see Figure III-97B). At 4.0 L exposure, a continued increase in the reversible desorption was observed, with T_{max} at -80°C and -15°C (see Figure III-97C). On silicon-covered Pd(110), θ_{Si} = 0.2, chemisorption was largely reversible at low exposures (0.5 L). An intense ethylene maximum was observed at 25°C, and a weak hydrogen maximum was observed at 40°C (see Figure III-98). Similar behavior was observed on phosphorus-, sulfur-, and chlorine-covered Pd(110). At 0.5 L exposure, ethylene thermal desorption maxima were observed at 20°C and 0°C for surfaces with 0.5 monolayer of phosphorus (see Figure III-99) and 0.4 monolayer of sulfur (see Figure III-100), respectively. On chlorine-covered Pd(110), θ_{Cl} = 0.31, two C_2H_4 maxima were observed, at -80°C and 75°C, along with two hydrogen maxima, at 75°C and 135°C (see Figures III-101A and III-101B).

T. Pd(110) - X -C_6H_6, where X = Si, P, S, or Cl

At an exposure of 1.0 L, both reversible and irreversible chemisorption were observed for benzene, C_6H_6, on Pd(110). Two

Figure III-97. Thermal desorption spectra of ethylene from Pd(110) are shown. At low exposures, 0.5 L (Figure III-97A), the chemisorption of ethylene is largely irreversible. In Figure III-97B, an equal distribution between reversible and irreversible chemisorption is observed at an exposure of 1.0 L. At 4.0 L (Figure III-97C), a further increase in the fraction of reversibly bound ethylene is observed.

Figure III-98. The presence of silicon on Pd(110), $\theta_{Si} = 0.20$, increases the fraction of ethylene reversibly bound. Shown is the thermal desorption spectrum of 0.5 L of ethylene from this surface. It is evident from this spectrum that the ethylene desorption is nearly quantitative.

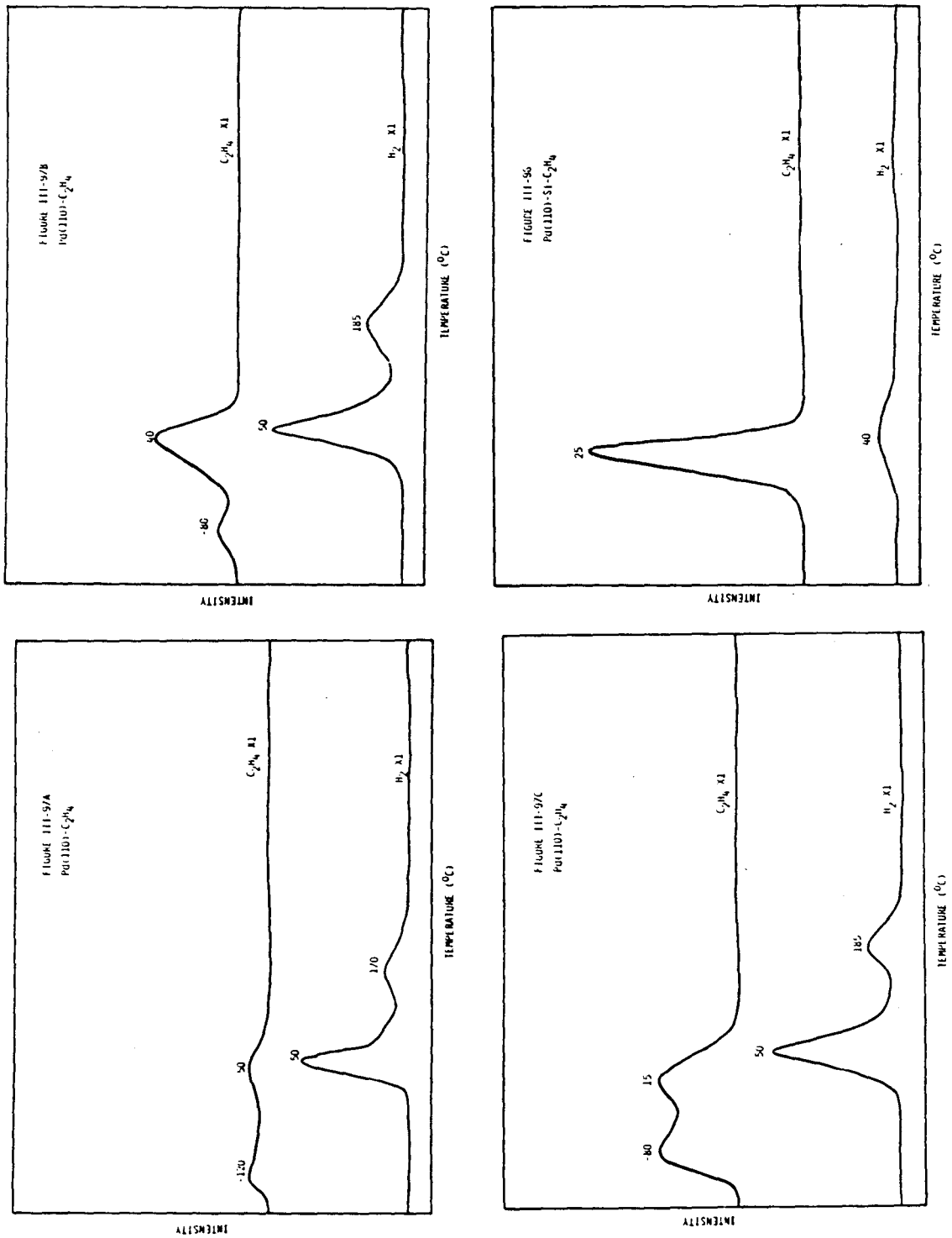
FIGURE III-96
Pd(110)-Si-C_2H_4
C_2H_4 X1
H_2 X1
25
40
INTENSITY
TEMPERATURE (°C)
FIGURE III-97A
Pd(110)-C_2H_4
C_2H_4 X1
H_2 X1
-120
50
50
110
INTENSITY
TEMPERATURE (°C)
FIGURE III-97B
Pd(110)-C_2H_4
C_2H_4 X1
H_2 X1
-90
40
50
185
INTENSITY
TEMPERATURE (°C)
FIGURE III-97C
Pd(110)-C_2H_4
C_2H_4 X1
H_2 X1
-80
15
50
185
INTENSITY
TEMPERATURE (°C)

XBL 846-2181

Figure III-99. At a phosphorus coverage of 0.50 monolayer, the desorption of ethylene from Pd(110) is nearly quantitative. The thermal desorption spectrum of 0.5 L of ethylene from this surface is shown.

Figure III-100. Sulphiding Pd(110) increased the fraction of reversible chemisorption of ethylene. The thermal desorption of 0.5 L of ethylene is nearly quantitative at a sulfur coverage of 0.40 monolayer.

Figure III-101. Thermal desorption of ethylene from chlorine-covered Pd(110) is shown. At a chlorine coverage of 0.31 monolayer and an ethylene exposure of 0.5 L, nearly quantitative desorption is observed (Figure III-101A). At higher ethylene exposures, 1.0 L, and similar chlorine coverage, $\theta_{Cl} = 0.25$, a further increase in reversible chemisorption is observed (Figure III-101B).

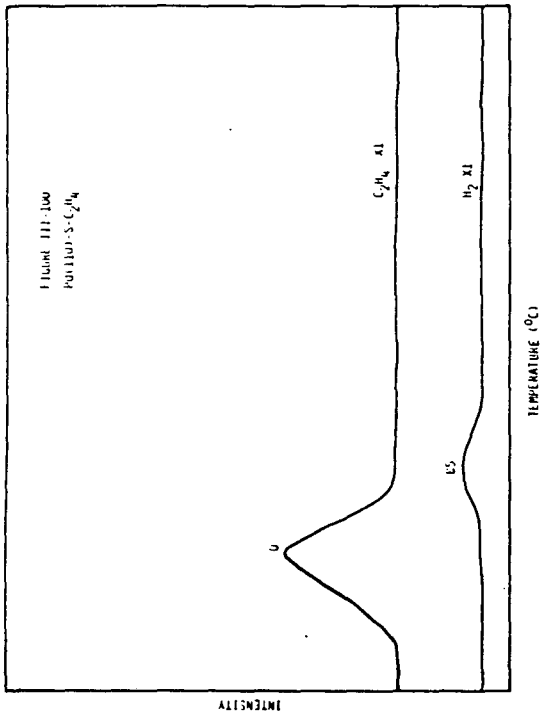
Figure III-100
Pd(110)-S-C_2H_4
C_2H_4 X1
H_2 X1
0
125
INTENSITY
TEMPERATURE (°C)

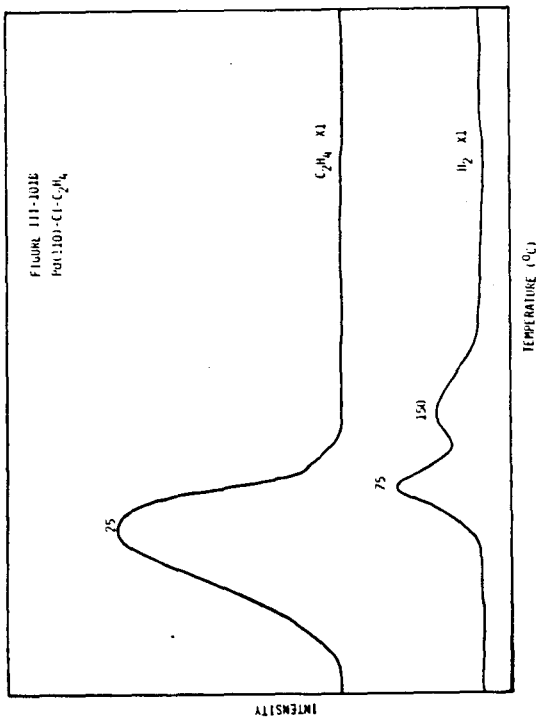
Figure III-101B
Pd(110)-Cl-C_2H_4
C_2H_4 X1
H_2 X1
25
75
150
INTENSITY
TEMPERATURE (°C)

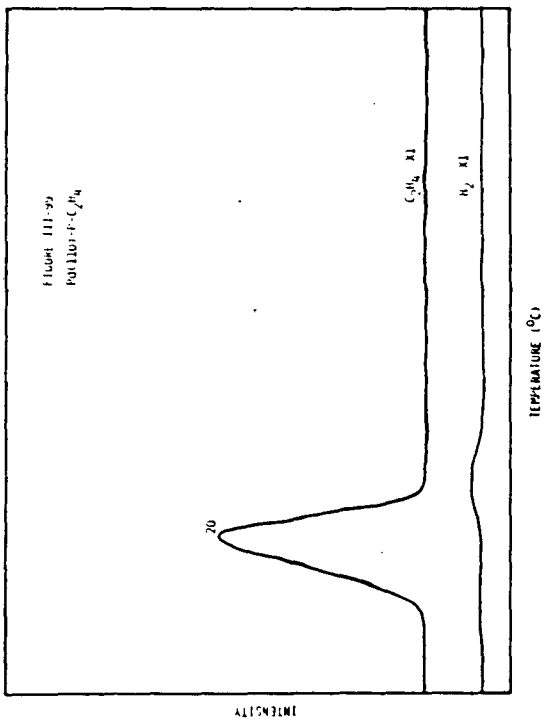
Figure III-99
Pd(110)-F-C_2H_4
C_2H_4 X1
H_2 X1
20
INTENSITY
TEMPERATURE (°C)

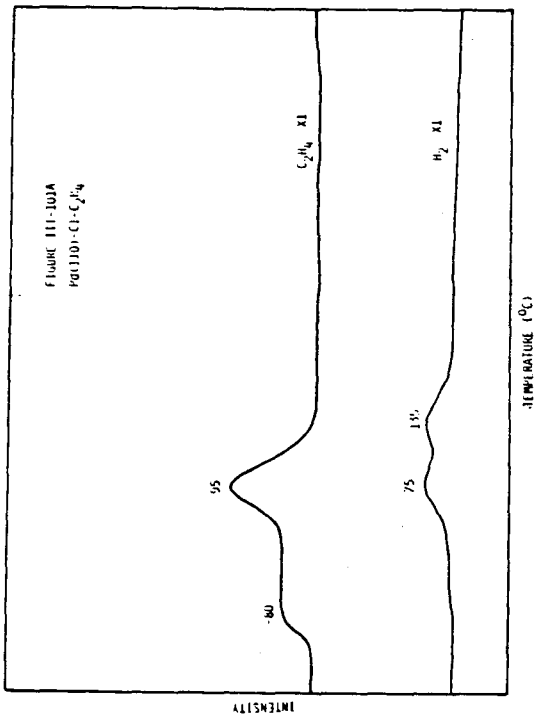
Figure III-101A
Pd(110)-Cl-C_2H_4
C_2H_4 X1
H_2 X1
-80
55
75
INTENSITY
TEMPERATURE (°C)

XBL 846-2180

benzene T_{max} were observed, at -25°C and 150°C, and an H_2 T_{max} was observed at 185°C (see Figure III-102). At the same exposure (1.0 L) on a silicon-covered Pd(110) surface, $\theta_{Si} = 0.25$, the fraction of benzene reversibly chemisorbed increases. A weak H_2 T_{max} was observed at ~220°C. The high temperature maximum (T_{max} = 170°C) increased by a factor of 5.6 compared to the clean surface (see Figure III-103). Similar results were observed on phosphided Pd(110). At a phosphorus coverage of 0.48 monolayer, two maxima were observed, at -50°C and 185°C. The 185°C maximum increased by a factor of 5.3. A weak H_2 maximum at 200°C was also observed (see Figure III-104). On sulfur-covered Pd(110), $\theta_S = 0.47$, at an exposure of 1.0 L benzene chemisorption was found to be fully reversible. A benzene maximum at -25°C with a long tail extending to 220°C was observed (see Figure III-105). At a chlorine coverage of 0.16 monolayer, both reversible and irreversible chemisorption were observed. An H_2 T_{max} was observed at 210°C. Benzene desorbed at a maximum rate of -25°C, with a broad plateau from 60°C to 210°C (see Figure III-106A). The fraction of reversible bound benzene increased at a chlorine coverage of 0.30. Two benzene maxima were observed, at -25°C and 200°C. A sharp H_2 maximum was observed at 240°C (see Figure III-106B).

Figure III-102. Chemisorption of benzene on Pd(110) exhibited both reversible and irreversible behavior. Two benzene maxima, at -25°C and 150°C, are evident at a benzene exposure of 1.0 L.

Figure III-103. Siliciding Pd(110), θ_P = 0.25, increased the amount of benzene desorbing intact from Pd(110). Illustrated is the increased molecular desorption of benzene in the 170°C maximum. The exposure of benzene was 1.0 L in this experiment.

Figure III-104. The presence of phosphorus on Pd(110) also increased the fraction of reversibly bound benzene. The thermal desorption spectrum of benzene from phosphorus-covered Pd(110), θ_P = 0.48, is shown. The exposure of benzene was 1.0 L, which resulted in an increased intensity in the high temperature benzene maximum.

Figure III-105. Benzene desorbed primarily at low temperatures on sulfur-covered Pd(110), θ_S = 0.47. Quantitative desorption of benzene is evident in the thermal desorption spectrum displayed in this figure.

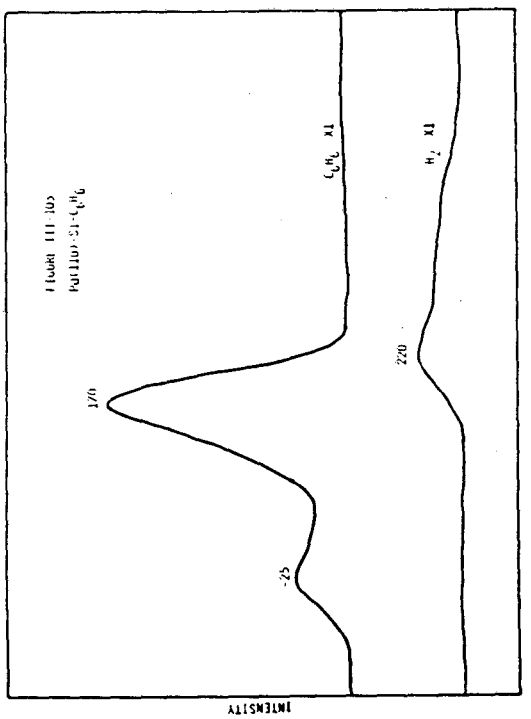
FIGURE III-103
Pd(110)-S-C_6H_6
C_6H_6 X1
H_2 X1
-25
170
270
INTENSITY
TEMPERATURE (°C)

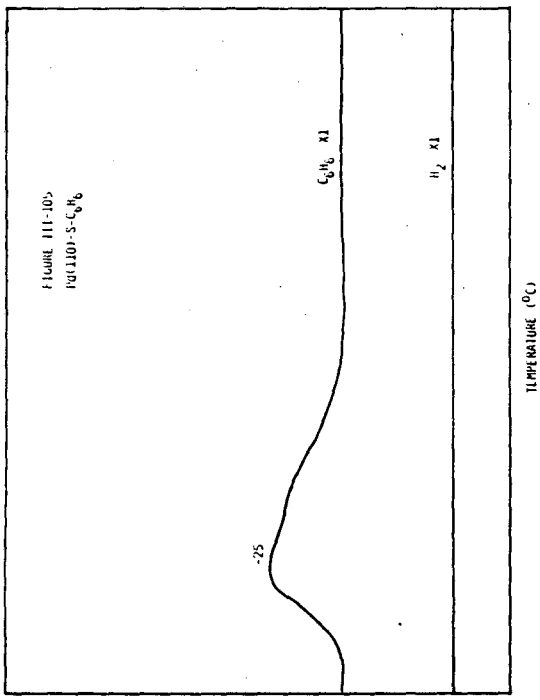
FIGURE III-105
Pd(110)-S-C_6H_6
C_6H_6 X1
H_2 X1
-25
INTENSITY
TEMPERATURE (°C)

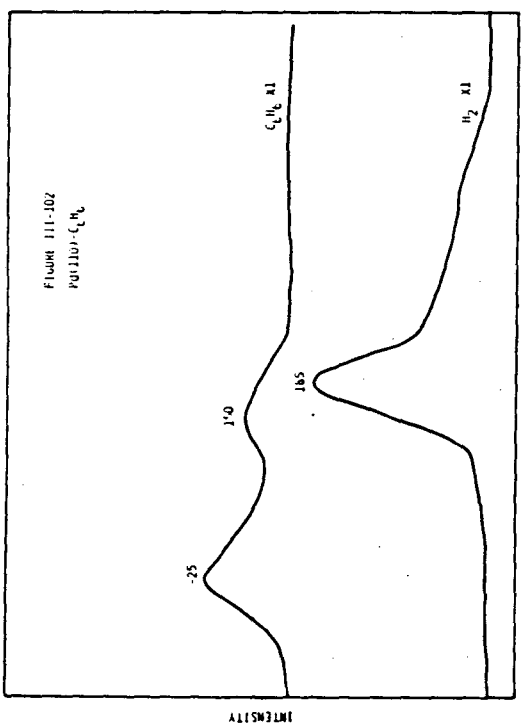
FIGURE III-102
Pd(110)-C_6H_6
C_6H_6 X1
H_2 X1
-25
140
185
INTENSITY
TEMPERATURE (°C)

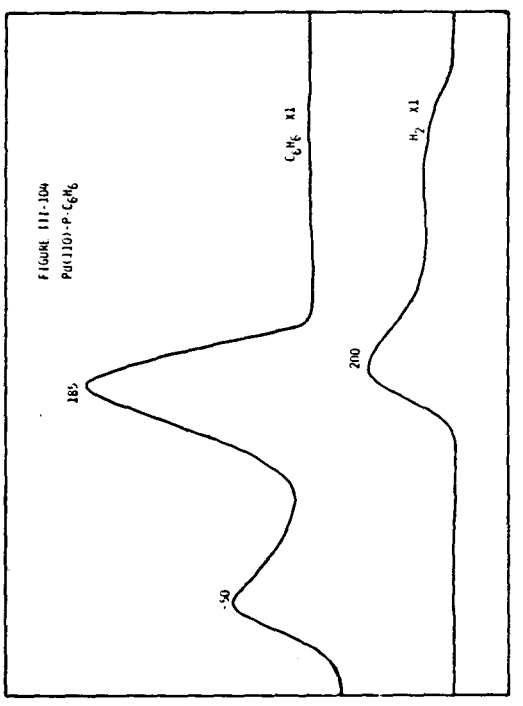
FIGURE III-104
Pd(110)-P-C_6H_6
C_6H_6 X1
H_2 X1
-50
185
200
TEMPERATURE (°C)

XBL 846-2179

Figure III-106. The thermal desorption of benzene, 1.0 L, from two different chlorine-covered Pd(110) surfaces is shown. At a chlorine coverage of 0.16 monolayer (Figure III-106A), little change was observed. In Figure III-106B, the chlorine coverage is 0.30 monolayer, and an increase in reversible desorption of benzene was observed in the 210°C maximum

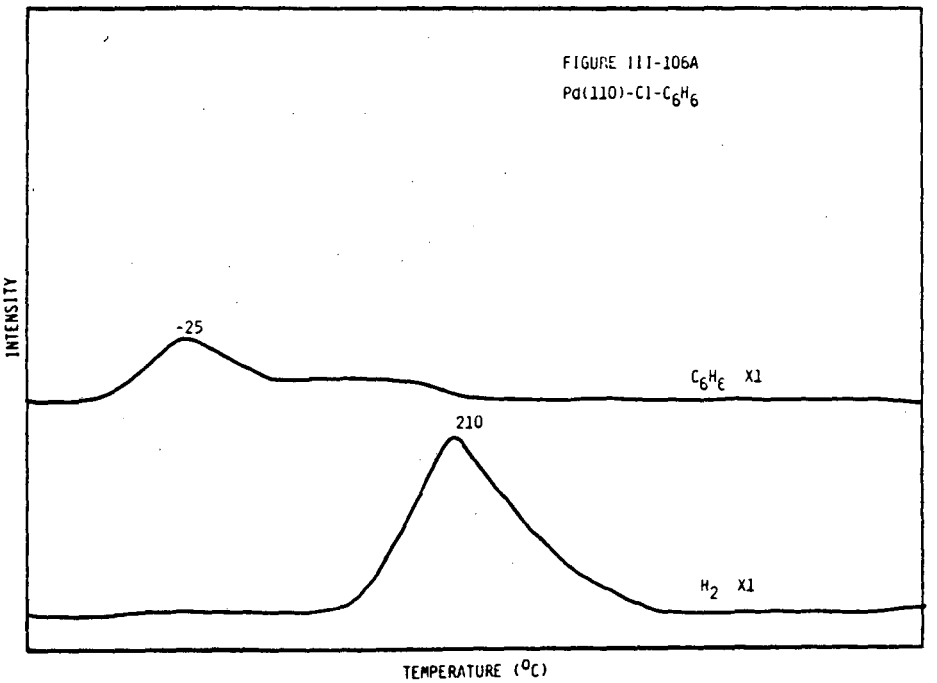
FIGURE III-106A
Pd(110)-Cl-C_6H_6
INTENSITY
-25
C_6H_6 X1
210
H_2 X1
TEMPERATURE (^oC)

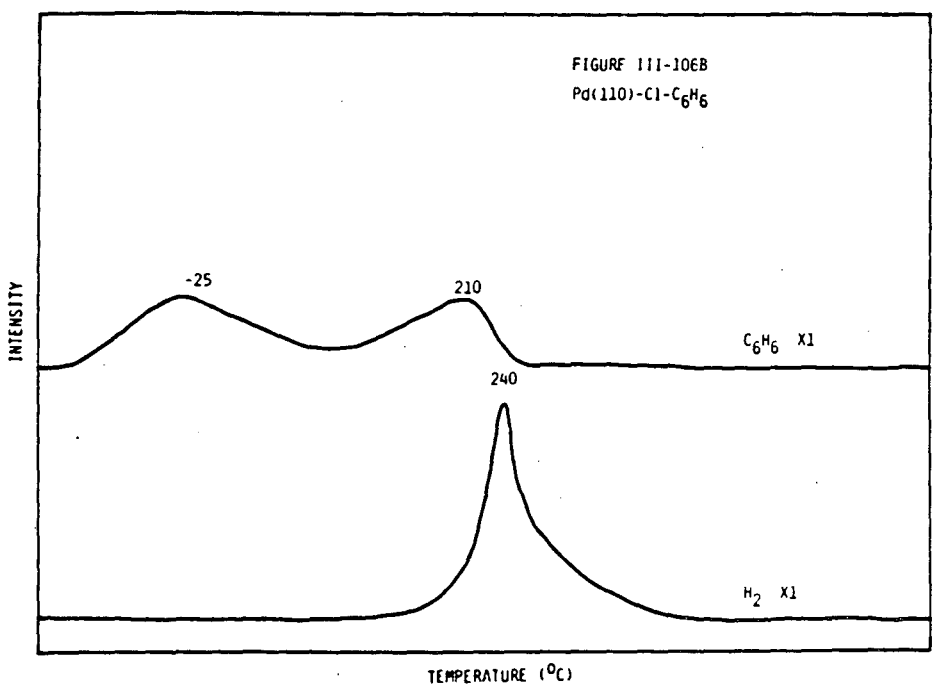
FIGURE III-106B
Pd(110)-Cl-C_6H_6
INTENSITY
-25
210
C_6H_6 X1
240
H_2 X1
TEMPERATURE (^oC)

XBL 846-2170

DISCUSSION

Acetylene chemisorbed on palladium single-crystal surfaces exhibits complex chemistry such as decomposition to hydrogen and carbon, molecular desorption, hydrogenation to ethylene, and trimerization to benzene. The reactions of coadsorbed acetylene with other reagents such as hydrogen and trimethylsilane were also catalyzed by these surfaces. Both chemisorption of acetylene and products formed from its thermal desorption (H_2, C_2H_4, and C_6H_6), as well as the catalytic reactions of acetylene (hydrogenation and hydrosilation) were found to be sensitive to both surface crystallography (structure) and composition. The influence of these variables on the trimerization will be discussed first, followed by their effect on hydrogenation and hydrosilation, and, finally, on the chemisorption of hydrogen, ethylene, and benzene.

Cyclotrimerization of acetylene was found to be most facile on clean Pd(111), followed by Pd(100) and Pd(110). The first step in the formation of benzene on the (111) surface may be the chemisorption of three acetylenes around the threefold hollow. This site may provide a template or the proper geometry to bring these acetylene molecules into a favorable bonding configuration. The acetylene would be chemisorbed at the bridging position (twofold sites) between two palladium atoms. The LEED pattern for acetylene on Pd(111) has been reported to be $\sqrt{3} \times \sqrt{3}$ R 30°C.[3b] This structure is consistent with the above mechanism. The other two clean surfaces, the (100) and the (110), do not have sites favorable for benzene formation; but

nonetheless benzene is formed but in reduced yields. The fact that benzene is formed at all on these two surfaces suggests that the above mechanism may not be the only mechanism.

Metallocycle formation has been shown to be an intermediate in the trimerization of acetylene using cobalt, rhodium, and iridium complexes.[4] If trimerization of acetylene occurred through a mechanism similar to this, then formation of benzene can be rationalized on the (100) and (110) surfaces.

The influence of the four adatoms studied--Si, P, S, and Cl--on the trimerization on the (111) surface will be discussed next. To facilitate the discussion of the results of this study, some of the relevant properties of the adatoms will be considered first.

The four adatoms decrease in size with increased atomic number, but the decrease is slight, with a 1.17-Å atomic radius for silicon and an 0.91-Å radius for chlorine. Palladium is substantialy larger; its atomic radius is 1.38Å. Van der Waals radii fall in the narrow range of ~1.95Å to 1.80Å. Hence, substantial differences in the adatom effects cannot be ascribed to size or steric factors. Also, surface structure should tend not to vary significantly with adatoms. All four adatoms and also hydrogen should tend to reside at the three-fold sites of the close-packed palladium surface. The only structural data available for the Pd(111) surface are for chlorine-,[5] and hydrogen-covered[6] surfaces. LEED studies were attempted on silicon, phosphorus, and sulfur, but no order patterns have been observed to date. Although specific structural data are not available for these

adatoms on Pd(111), there is data available for Ni(111)-S and Pt(111)-S,[7] and sulfur is generally found in the threefold hollows. The only bond energy data available are for the Pd-Si bond[8] (74.9 kcal/mole).

Electronegativity is one empirical parameter that differs significantly for the four adatoms. Electronegativity increases smoothly in going from silicon to chlorine (this holds in all electronegativity scales). The values from the Allred-Rachow Scale are Si:1.74, P:2.06, S:2.44, and Cl:2.83. These can be compared with values of 1.35 and 2.20 for palladium and hydrogen.

The influence of the four adatoms generally increases with increasing electronegativity on the (111) surface. Silicon had little impact; but the more electronegative elements--P, S, and Cl--had a significant influence on the trimerization process, as evident by the changes in the thermal desorption spectra of reactively formed benzene. Before considering these spectra, the origins of the two benzene thermal maxima observed in the trimerization of acetylene will be discussed. Other workers[3b] have postulated that the genesis of these two maxima at -25°C and 220°C arises from the configuration of benzene on the (111) surface. The low temperature maximum, the more weakly bound benzene, arises from the molecule in "tilted" configuration. In this configuration the plane containing the six carbon atoms is not parallel to the surface. Benzene bound in a π fashion, parallel to the surface, is thought to be the origin of the high temperature

maximum. Both of these configurations have precedent in the organometallic literature.[9] Triosmium clusters have been reported where the plane of the C_6 ring and the plane of the three osmium atoms interact at an angle of 70°. There are numerous examples of η^6, π-bound benzene complexes. In most of these complexes the benzene is bound to a single metal atom; however, a palladium complex exists where the benzene is bound to two metal atoms.

The changes observed in the trimerization on phosphorus-, sulfur-, and chlorine-covered surfaces are difficult to interpret completely in terms of this model. Phosphorus increases the yield of benzene in both the low temperature region ("tilted benzene") and the high temperature region (π bound). Sulfur, on the other hand, increases the yield of benzene in the low temperature region, whereas chlorine has the opposite effect and increases the benzene yield in the high temperature region.

The mobility, both across the surface and into the bulk, may be important. Silicon, like carbon, appears to readily diffuse into the bulk on Pd(111). No evidence is avilable for diffusion into the bulk from the other three adatoms; however, the mobility should increase from phosphorus to chlorine. Chlorine is the weakest bound of the adatoms. It is found to thermally desorb from Pd(111)[5] at T_{max} = 600°C, whereas sulfur and phosphorus do not. If sulfur remains in the threefold sites, one might expect to observe benzene at low temperature. If chlorine has sufficient mobility, it may either allow acetylene to occupy three sites for the formation of π-bound benzene

or allow benzene already formed to occupy these sites. The changes in the spectrum as a result of phosphorus adsorption are not easily explained in terms of this model.

The low yields of benzene from chemisorbed acetylene on Pd(100) and Pd(110) were found to be enhanced by the presence of adatoms. The presence of silicon and phosphorus on Pd(100) dramatically increased the yield of reactively formed benzene, while sulfur and chlorine did not. The origin of this effect may be the ability of the adatoms to coordinate to this surface. Normally tetravalent silicon or trivalent phosphorus may interact electronically with the fourfold hollow. They may act to electronically smooth the (100) surface, which could facilitate the trimerization reaction.

On Pd(110), silicon and phosphorus were found to be beneficial for the trimerization reaction. Again, silicon and phosphorus may interact electronically more strongly on the even more open (110) surface. The experiments here do not define the mechanism of trimerization. However, their formation can be influenced by these adatoms. Further investigation into the nature of the chemisorbed species, using a variety of surface spectroscopies, should lead to a fuller understanding of complex interactions of structure and composition on the trimerization process.

The hydrogenation and trimerization of acetylene were substantially influenced by preadsorbed hydrogen on palladium surfaces. On Pd(111), the presence of preadsorbed hydrogen completely suppressed trimerization of acetylene while increasing the yield of ethylene. Reversing

the order of adsorption--that is, acetylene followed by hydrogen--did not substantially alter the trimerization or hydrogenation reactions. Hydrogen adsorbed dissociatively on transition metal surfaces,[10] and on Pd(111) hydrogen occupies the threefold hollow. Hydrogenation and trimerization may compete for the same acetylene species. The suppression of the trimerization may be a kinetic phenomenon, that is, the hydrogenation reaction is a faster reaction than the trimerization. Sites of adsorption of hydrogen are probably blocked by acetylene adsorption, so hydrogen adsorbed on acetylene-covered Pd(111) has little influence.

The presence of adatoms was also found to influence the hydrogenation reaction of acetylene. On Pd(111), silicon and phosphorus did not substantially alter the yield of ethylene. Sulfur and chlorine were found to be detrimental. On both sulfur- and chlorine-covered surfaces, significant amounts of benzene were observed. The inhibition or poisoning of the hydrogenation lies in the ability of the sulfur- and chlorine-covered surfaces to adsorb hydrogen. The sticking coefficient of hydrogen was found to decrease dramatically on these surfaces; therefore, no hydrogen is available for hydrogenation.

To further probe the mechanism of the hydrogenation of acetylene on Pd(111), the reaction was investigated using deuterium. On clean Pd(111), the major product was the formation of ethylene containing two deuteriums, $C_2H_2D_2$. These experiments cannot distinguish which isomer is formed. On palladium-supported catalysts the cis

$C_2D_2H_2$ was the predominant species observed.[11] An important question here is what acetylene surface species is involved in the hydrogenation reaction. Other workers have investigated chemisorbed acetylene on Pd(111) using surface spectroscopies. Gates and Kesmodel claim to have observed thermal evolution of small amounts of vinyldiene, $>C = CH_2$, but primarily ethyldyne, $\equiv C-CH_3$, at 300°C on Pd(111).[2d] At low temperatures, C_2H_2 is found to be bound in a manner where the carbon–carbon bond is parallel to the surface. The formation of $C_2D_2H_2$ suggests that ethyldyne is not an important intermediate in the formation of ethylene. Although H–D exchange has been observed for ethyldyne on Pt(111),[12] it seems unlikely that $C_2H_2D_2$ would be the predominant product from this process. These results indicate that hydrogenation proceeds through cis addition of hydrogen across an acetylene bond with the carbon–carbon bond parallel to the surface.

On Pd(100), preadsorbed hydrogen also completely inhibited trimerization of acetylene while enhancing hydrogenation. The presence of silicon enhanced the yield of ethylene on Pd(100) substantially. The origin of this result may be the result of two phenomena. Silicon increased the fraction of reversibly bound ethylene, as did phosphorus, sulfur, and chlorine. Silicon, however, also increased the sticking coefficient of hydrogen, where phosphorus, sulfur, and chlorine did not. The increased sticking coefficient means more hydrogen is available for the reaction, combined with decrease in the decomposition of ethylene. This enhancement of the ethylene formation is to be expected.

The superstepped (110) surface exhibited unusual behavior when acetylene was adsorbed on a hydrogen-covered surface. In contrast to the atomically flat (111) and (100) surfaces, where trimerization of acetylene was completely suppressed, it was not on the (110) surface. Hydrogen is found to have unusual chemisorption properties on Pd(110). The formation of a subsurface hydrogen has been observed on this surface.[13] On silicon-covered Pd(110), the yield of both ethylene and benzene increased, suggesting that on this surface sites of hydrogenation and trimerization may be different. Phosphorus was found to decrease the yield of ethylene, as did sulfur and chlorine. However, the trimerization reaction was enhanced by phosphorus and largely unaffected by sulfur and chlorine. Although the presence of adatoms increased the amount of reversibly bound ethylene as observed on the (111) and (100) surfaces, the sticking coefficient of H_2 did not follow the same trends as the other surfaces; that is, the more electronegative elements decreased the sticking coefficient of H_2 the most.

The hydrosilation of acetylene by trimethylsilane was found to occur on all palladium surfaces. Palladium is usually regarded as a poor catalyst for hydrosilation.[14] One might have expected to observe hydrosilation, however, if hydrogenation occurred, because these reactions are thought to have similar enthalpies.[15] One interesting difference is the experimental protocol for hydrosilation, as compared to hydrogenation. While preadsorbed hydrogen affected hydrogenation, preadsorbed trimethylsilane did not. Reversing the

order of adsorption--that is, acetylene followed by trimethylsilane--did result in hydrosilation. This behavior may be the result of the larger trimethylsilane blocking sites of acetylene chemisorption. Alternatively, when hydrosilation is performed using homogeneous catalysts in the presence of an excess of the silane, one usually observes the formation of the product where two moles of the silane add across the unsaturated carbon-carbon bond. The formation of the product was not observed; however, its chemisorption may be irreversible and its subsequent desorption not detectable.

On Pd(111), phosphorus had the largest impact of all of the adatoms on the hydrosilation reaction. The yield of vinyltrimethylsilane increased by a factor of five. This promotion by phosphorus is consistent with results of Tsuji et al.[16] An increase in the catalytic activity of both palladium complexes and metallic palladium was observed in the presence of triphenylphosphine. On the (100) surface, silicon and phosphorus enhanced the yields; while on the (110) surface, phosphorus, sulfur, and chlorine were beneficial.

The mechanism of hydrosilation is a complex question. Several reactions are also competing for chemisorbed acetylene on these surfaces. The lower yields of the hydrosilation as compared to hydrogenation are most certainly due to the great steric demands of the trimethylsilane.

The sticking coefficient of H_2 on Pd(111) was found to decrease with adatom coverage. The more electronegative elements were found to have a larger effect. Since all atoms are of similar size, the

decrease in sticking coefficient is related to electron phenomena. Similar results were obtained with hydrogen on clean and phosphrous-, sulfur-, and chlorine-covered Ni(100).[17] The sticking coefficient of H_2 on Pd(111) was found to be unity, and the decrease is to be expected.[18] On Pd(100), the same trend was observed; however, silicon increased the sticking coefficient. This does not mean the sticking coefficient of hydrogen becomes greater then unity, because the sticking coefficient on clean Pd(100) is estimated to be ~0.5. This increase may be the result of the interaction between hydrogen, silicon, and the palladium surface. This type of complex has precedent in the organometallic literature. For example, $W_2(CO)_8H_2\{Si(C_2H_5)_2\}_2$ contains a hydrogen-bridged transition metal bond.[19]

The presence of the four adatoms investigated--silicon, phosphorus, sulfur, and chlorine--was found to influence the chemisorption of benzene on all three low Miller-index surfaces of palladium. On all surfaces, both reversible and irreversible chemisorption was observed. Preadsorbed adatoms decreased the amount of irreversibly bound benzene. On clean Pd(111), two benzene maxima were observed, at -15°C and 250°C, and a hydrogen maximum was observed at 275°C. If these adatoms adsorb in the threefold hollows, then the site of adsorption of the irreversibly bound benzene may be these sites. The adsorption of adatoms generally results in the increase in the amount of reversibly bound benzene desorbing at high temperatures.

CONCLUSION

In this chapter, the trimerization of acetylene on palladium single-crystal surfaces has been demonstrated. Furthermore, on clean surfaces this reaction has been found to be sensitive to surface structure or crystallography. The close-packed Pd(111) surface has been shown to produce optimum yields of benzene from acetylene.

The catalytic behavior of palladium single-crystal surfaces can be substantially modified by the presence of various adatoms--silicon, phosphorus, sulfur, and chlorine. Surfaces such as Pd(100) and Pd(110), which exhibited low activity for trimerization of acetylene when clean, were found to be extremely active when modified with silicon or phosphorus.

The selectivity of palladium single-crystal surfaces can also be modified by adatoms. For example, on Pd(111), hydrogenation and trimerization of acetylene were competing reactions. Sulphiding this surface made it extremely selective. Hydrogenation of acetylene was suppressed while trimerization was enhanced.

These studies offer insights into the mechanisms of reaction of hydrocarbons on real transition metal catalysts. These catalysts are found to be sensitive to their structure and composition. Palladium single-crystal studies have demonstrated that they are outstanding models for determining which surface structures and surface compositions are catalytically most active.

REFERENCES

1. (a) J. E. Germain, Catalytic Conversion of Hydrocarbons, Academic Press, New York, 1969. (b) P. N. Rylander, Catalytic Hydrogenation over Platinum Metals, Academic Press, New York, 1967.

2. (a) T. E. Fischer, S. R. Kelemen, and H. P. Bonzel, Surf. Sci. 1977, 64, 157-175; (b) J. E. Demuth, Surf. Sci. 1979, 84, 315-328; (c) J. E. Demuth, Surf. Sci. 1979, 80, 367-387; (d) J. E. Demuth, Chem. Phys. Lett. 1977, 45, 12-17; (e) T. E. Fischer and S. R. Kelemen, Surf. Sci. 1978, 74, 47-53; (f) W. J. Lo, Y. W. Chung, L. L. Kesmodel, P. C. Stair, and G. A. Somorjai, Solid State Commun. 1977, 22, 335-337; (g) A. E. Morgan and G. A. Somorjai, J. Chem. Phys. 1969, 51, 3309-3320; (h) L. L. Kesmodel, P. C. Stair, R. C. Baetzold, and G. A. Somorjai, Phys. Rev. Lett. 1976, 36, 1316-1319; (i) P.C. Stair and G. A. Somorjai, J. Chem. Phys. 1977, 66, 2036-2044; (j) L. L. Kesmodel, R. C. Baetzold, and G. A. Somorjai, Surf. Sci. 1977, 66, 299-320; (k) L. L. Kesmodel, L. H. Dubois, and G. A. Somorjai, Chem. Phys. Lett. 1978, 56, 267-271; (l) L. L. Kesmodel, L. H. Dubois, and G. A. Somorjai, J. Chem. Phys. 1979, 70, 2180-2188; (m) H. Ibach, H. Hopster, and B. Sexton, Appl. Phys. 1977, 14, 21-24; (n) H. Ibach, H. Hopster, and B. Sexton, Appl. Surf. Sci. 1977, 1, 1-24; (o) H. Ibach and S. Lehwald, J. Vac. Sci. Technol. 1978, 15, 407-415; (p) A. M. Baro and H. Ibach, J. Chem. Phys. 1981, 74, 4194-4199; (q) T. E. Felter and W. H. Weinberg, Surf. Sci. 1981, 103, 265-287; (r) M. H.

Howard, S. F. A. Kettle, J. A. Oxton, D. B. Powell, N. Sheppard, and P. Skinner, J. Chem. Soc. Faraday Trans. 2 1981, 77, 397-404; (s) E. L. Muetterties, M.-C. Tsai, and S. R. Kelemen, Proc. Nat. Acad. Sci. USA 1981, 78, 6571.

3. T. M. Gentle and E. L. Muetterties, J. Phys. Chem. 1983, 87, 2469. (b) W. T. Tysoe, G. L. Nyberg, and R. M. Lambert, Surf. Sci. 1983, 135, 128. (c) W. Sesselmann, B. Woratschek, G. Ertl, and J. Kuppers, Surf. Sci. 1983, 130, 240. (d) J. A. Gates and L. L. Kesmodel, Surf. Sci. 1983, 124, 68.
4. G. W. Parshall, Homogeneous Catalysis, John Wiley and Sons, New York, 1980, p. 166.
5. W. Erley, Surf. Sci. 1980, 94, 281.
6. H. Conrad, G. Ertl, and E. E. Latta, Surf. Sci. 1974, 41, 435.
7. C. H. Bartholmew, P. K. Agrawal, and J. R. Katzer, Adv. Cat. 1982, 31, 135.
8. (a) A. Vander Auwera-Mahieu, R. Peters, N. S. McIntyre, and J. Drowart, Trans. Faraday Soc. 1970, 66, 809.
9. E. L. Muetterties, J. R. Blecke, E. J. Wucherer, and T. A. Albright, Chem. Rev. 1982, 82, 522.
10. S. O. Louie, Phys. Rev. Lett. 1979, 42, 476.
11. G. C. Bond and P. B. Wells, Adv. Catal. 1964, 15, 90.
12. J. R. Creighton, K. M. Ogle, and J. M. White, Surf. Sci. 1984, 138, L137.
13. R. J. Behm, V. Penka, M.-G. Cattania, and G. Ertl, J. Chem. Phys. 1983, 78, 7486.

14. A. J. Chalk and J. F. Harrod, J. Am. Chem. Soc. 1965, 87, 16.

15. J. L. Speier, Adv. in Organometallic Chem. 1979, 17, 407.

16. M. Hara, K. Ohno, and J. Tsuji, J. Chem. Soc. Chem. Comm. 1971, 247.

17. M. Kiskinova and D. W. Goodman, Surf. Sci. 1981, 108, 64.

18. T. J. Engel and H. Kuipers, Surf. Sci. 1979, 90, 162.

19. M. J. Bennett and K. A. Simpson, J. Am. Chem. Soc. 1976, 93, 7156.

IV. SURFACE CHEMISTRY OF BENZENE AND METHYLSUBSTITUTED BENZENE ON PALLADIUM SINGLE-CRYSTAL SURFACES

INTRODUCTION

Platinum metals, such as nickel, palladium, and platinum, are known to be catalysts for the hydrogenation of aromatic molecules.[1] The chemisorption of benzene and toluene has been investigated on nickel and platinum single-crystal surfaces in the Muetterties group by Dr. C. M. Friend[2] and Dr. M. C. Tsai,[3] respectively. In this chapter, the chemisorption of benzene and methylsubstituted derivatives of benzene on palladium single crystals will be described and discussed.

Aromatic molecules have been extremely useful probes for transition metal surface chemistry. Regioselective carbon-hydrogen bond scission was found to occur in chemisorbed toluene on Ni(100). The mechanism of this process was investigated using selectively labeled toluene, $CD_3C_6H_5$. Alaphatic carbon-hydrogen bonds were found to break before the aromatic carbon-hydrogen bonds broke.

The chemisorption of benzene on other transition metal surfaces, namely ruthenium, osmium, and iridium, has also been investigated.[4] A trend towards increased reversible chemisorption has been observed for transition metals on the right side of the periodic table.

The chemisorption of benzene; toluene; ortho-, meta-, and paraxylene; and 1,3,5-trimethybenzene has been investigated on the three low Miller-index surfaces of palladium. The mechanism of carbon-hydrogen bond scission of toluene and the xylenes has been

investigated with the chemisorption of selectively labeled molecules: toluene, $CD_3C_6H_5$; and ortho-, meta-, and paraxylene, $(CD_3)_2C_6H_4$.

RESULTS

The chemisorption of benzene and its methylsubstituted derivatives will be described in this section. Some general features of benzene chemisorption will be described first, followed by a detailed description of the chemisorption of these arenes on Pd(111), Pd(100), and Pd(110), respectively.

Benzene chemisorption on the three low Miller-index palladium surfaces was fully associative (molecular) at 20°C, as demonstrated through quantitative displacement of benzene by trimethylphosphine. Rapid heating of benzene chemisorbed on these surfaces--Pd(111), Pd(100), and Pd(110)--led to competing reactions of thermal desorption and decomposition, which were also observed on nickel[2] and platinum[3] surfaces. No reversible C-H bond breaking was evident on Pd(100) or Pd(110), in that initial chemisorption of C_6H_6-C_6D_6 mixtures did not yield $C_6H_xD_{6-x}$ molecules in the subsequent thermal desorption experiments. However, H-D exchange between chemisorbed C_6H_6 and C_6D_6 was detected on Pd(111); and all possible $C_6H_xD_{6-x}$ molecules were observed in the thermal desorption maximum at 250°C, but not in the low temperature maximum at 40°C. The extent of exchange, however, was low, less than 10 percent. No ordered pattern was observed in LEED experiments of benzene chemisorption on Pd(110). A 2 x 2 R45° structure has been reported for benzene

chemisorbed on Pd(100).[4] No ordered LEED pattern was observed for benzene on Pd(111). The presence of silicon, phosphorus, sulfur, and chlorine adatoms on all three surfaces suppressed the thermal decomposition process. The results of these experiments are presented and discussed in chapter III of this thesis.

A. Pd(111)

Benzene undergoes both reversible and irreversible chemisorption on Pd(111). The fraction of reversibly bound benzene increases with exposure. At low exposures (~1.0 L), benzene undergoes irreversible chemisorption, as characterized by a hydrogen thermal desorption maximum, T_{max}, at 270°C (see Figure IV-1A). This maximum has both low and high temperature shoulders. After this experiment, the surface was clean as determined by AES. In the decomposition process, surface carbon is formed; however, it diffuses into the bulk at ~400°C.[5] Two small benzene thermal desorption maxima were observed, at -15°C and 250°C. Increasing the exposure (2.0 L) results in the growth of benzene thermal desorption maxima. Two maxima are observed, at -40°C and 240°C (see Figure IV-1B). A hydrogen T_{max} is observed at 275°C. At higher exposures (3.0 L), the benzene thermal desorption maxima continue to increase, T_{max} = -40°C and 220°C. The hydrogen thermal desorption maximum at 280°C is approximately the same intensity as in the previous experiment (see Figure IV-1C).

Toluene exhibited a much higher degree of irreversible chemisorption than benzene on Pd(111). At low exposures (~1.0 L), three hydrogen thermal desorption maxima were observed, at 90°C,

Figure IV-1. Benzene was found to undergo both reversible and irreversible chemisorption on Pd(111). The thermal desorption of benzene from Pd(111) is shown at three exposures, 1.0 L, 2.0 L, and 3.0 L in A, B, and C, respectively. These spectra illustrate that increased molecular desorption, reversible chemisorption, is observed at higher exposures.

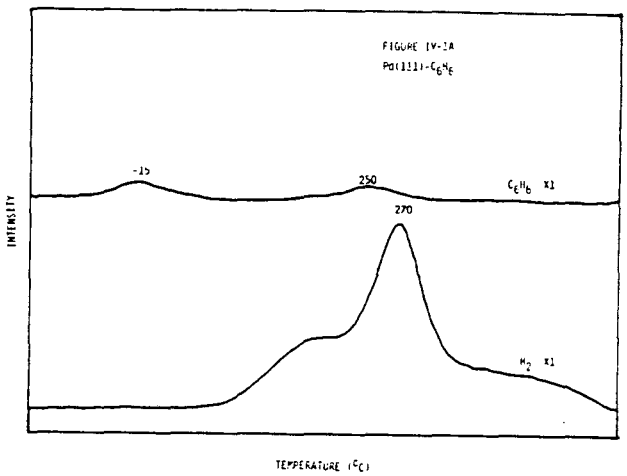
FIGURE IV-1A
Pd(111)-C6H6
-15
250
C6H6 X1
270
H2 X1
INTENSITY
TEMPERATURE (°C)

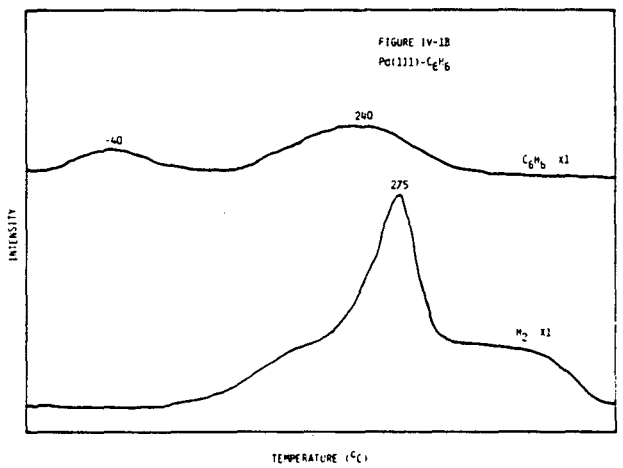
FIGURE IV-1B
Pd(111)-C6H6
-40
240
C6H6 X1
275
H2 X1
INTENSITY
TEMPERATURE (°C)

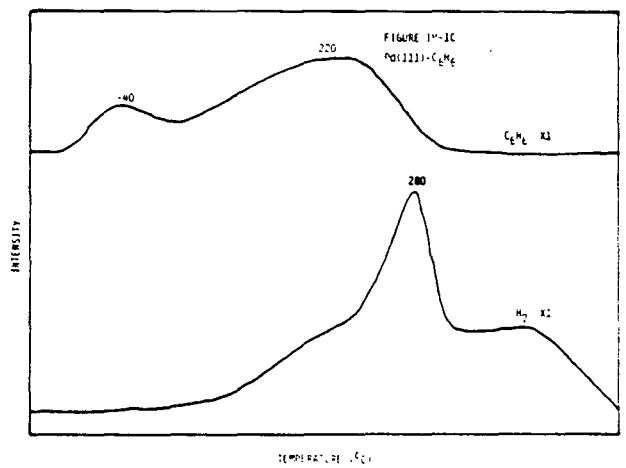
FIGURE IV-1C
Pd(111)-C6H6
-40
220
C6H6 X1
280
H2 X1
INTENSITY

XBL 846-2153

Figure IV-2. The chemisorption of toluene is largely irreversible on Pd(111). Thermal desorption spectra of toluene from Pd(111) are shown at exposures of 1.0 L, 2.0 L, and 3.0 L in A, B, and C, respectively. In all spectra, three hydrogen thermal desorption maxima were observed. The fraction of irreversibly bound toluene was much greater than that of benzene. Comparison of Figures IV-1B and IV-2B illustrates this point.

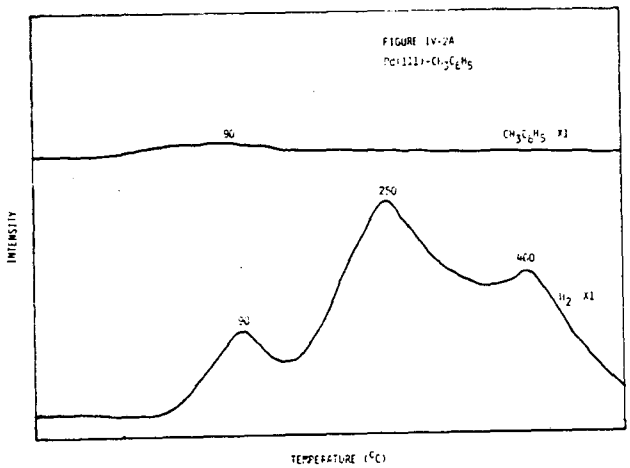
FIGURE IV-2A
Pd(111)-CH3C6H5
90
CH3C6H5 X1
250
460
H2 X1
80
INTENSITY
TEMPERATURE (°C)

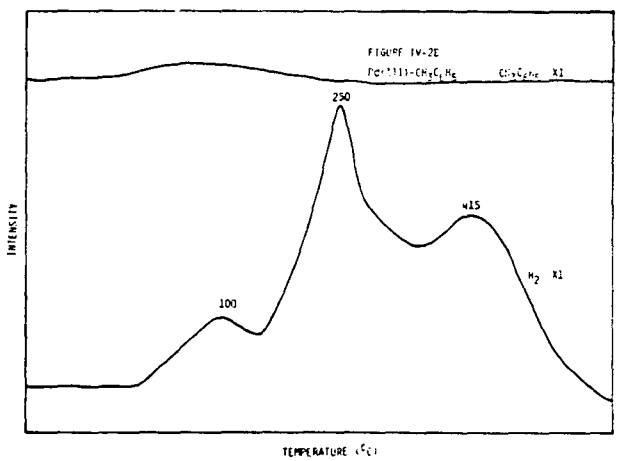
FIGURE IV-2B
250
415
H2 X1
100
INTENSITY
TEMPERATURE (°C)

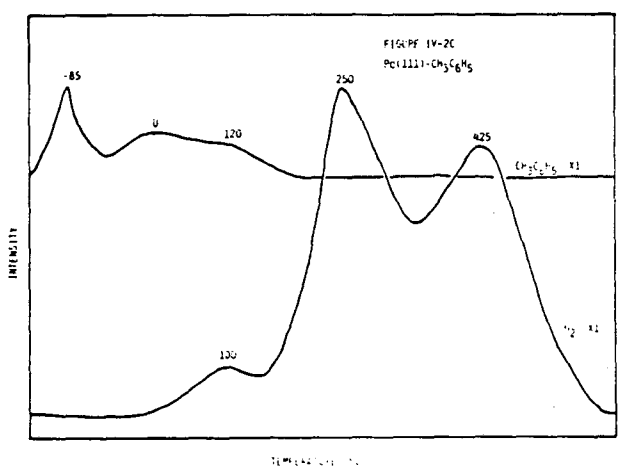
FIGURE IV-2C
Pd(111)-CH3C6H5
-85
0
120
250
425
CH3C6H5 X1
130
INTENSITY

XBL 846-2152

250°C, and 400°C. The 250°C and 400°C maxima were not well resolved (see Figure IV-2A). A very weak and broad toluene thermal desorption maximum was observed at ~90°C. Increasing the exposure further resulted in an increase in the fraction of irreversibly bound toluene, as evident by the increase in the intensity of the hydrogen thermal desorption spectrum. Three maxima were found, at 100°C, 250°C, and 415°C. The intensity of the high temperature maxima (250°C and 415°C) increased with respect to the low temperature maximum (100°C) (see Figure IV-2B). At higher exposures (3.0 L), toluene thermal desorption maxima were observed at -85°C and (a broad maximum) from 0°C to 120°C. Hydrogen was observed to desorb in maxima at 100°C, 250°C, and 425°C, with a continued increase in the high temperature maxima with respect the low temperature maximum (see Figure IV-2C).

The chemisorption of the selectively labeled toluene $CD_3C_6H_5$ was used to probe the origin of the multiple H_2 thermal desorption maxima. All three molecules—H_2, HD, and D_2—were observed in the thermal desorption spectrum. At low exposures (1.0 L), D_2 was observed in a low temperature maximum, 100°C; HD was observed in both low and high maxima, at 100°C and 240°C, respectively; and H_2 was observed in the high temperature maximum at 240°C. The H_2 maximum had a shoulder at ~350°C (see Figure IV-3A). Increasing the exposure resulted in a decrease in the amount of HD in the low temperature maximum and an increase of both H_2 and HD in the high temperature maximum (see Figures IV-3B and IV-3C).

Figure IV-3. The selectively labeled toluene $CD_3C_6H_5$ exhibited partial regiospecific C-H bond scission about thermal desorption from Pd(111). The thermal desorption spectra are at exposures of 1.0 L (A), 2.0 L (B), and 3.0 L (C). As shown in these spectra, the amount of HD in the 100°C thermal desorption maximum decreases with exposure.

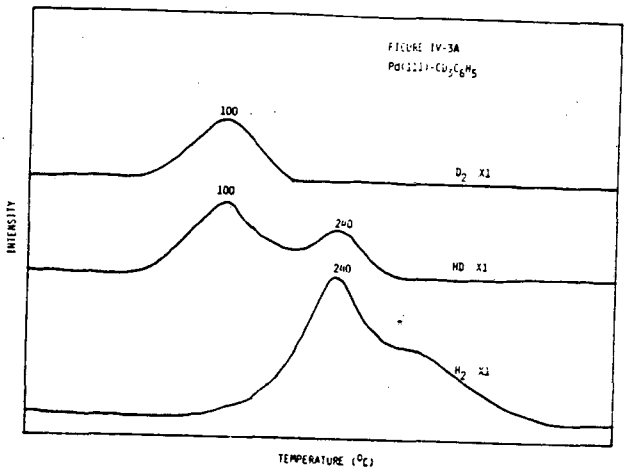
FIGURE IV-3A
Pd(111)-CD3C6H5
100
D2 X1
100
240
HD X1
240
H2 X1
INTENSITY
TEMPERATURE (°C)

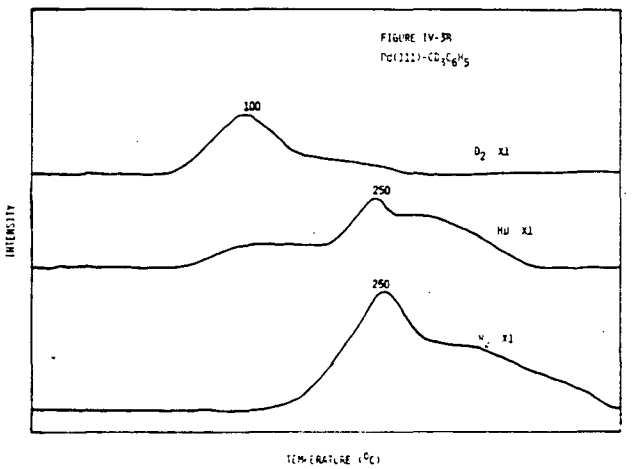
FIGURE IV-3B
Pd(111)-CD3C6H5
100
D2 X1
250
HD X1
250
INTENSITY

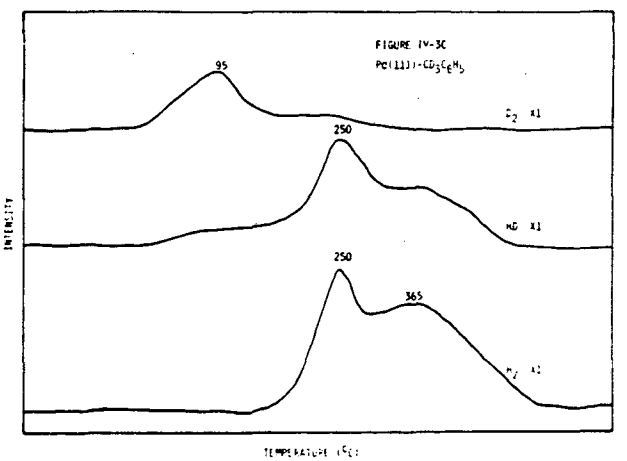
FIGURE IV-3C
Pd(111)-CD3C6H5
95
250
HD X1
250
365
INTENSITY

XBL 846-2151

The chemisorption of the three isomers of dimethylbenzene--ortho-, meta-, and paraxylenes--was also studied on Pd(111). Multiple hydrogen thermal desorption maxima were observed for all three molecules. To investigate the origin of these multiple hydrogen thermal maxima, that is, to gain insights into the mechanisms of C-H bond cleavage, chemisorption of the three partially labelled xylenes--o-$(CD_3)_2C_6H_4$, m-$(CD)_3C_6H_4$, and p-$(CD_3)_3C_6H_4$--was also investigated on Pd(111). The chemisorption of all three xylenes was found to be largely irreversible. Only weak molecular thermal desorption maxima were observed for all three isomers.

The thermal desorption spectrum of d^{10} paraxylene, $(CD_3)_2C_6D_4$, from Pd(111) exhibited three D_2 maxima, at 100°C, 270°C, and 320°C at low exposures, 1.0 L (see Figure IV-4A). At higher exposures, the high temperature D_2 maximum increased with respect to the low temperature D_2 maximum (90°C-100°C). A plateau-like high temperature maximum also appeared in the region from 350°C-460°C (see Figures IV-4B and IV-4C). Thermal desorption of metaxylene at low exposures (1.0 L) from Pd(111) resulted in three H_2 thermal maxima, at 100°C, 270°C, and 305°C (see Figure IV-5A). The 270°C and 305°C maxima were poorly resolved. At higher exposures, the high temperature maxima increased with respect to the low temperature H_2 maximum. A high temperature plateau-like maximum was also observed from 350°C to 415°C (see Figures IV-5B and IV-5C). The thermal desorption spectrum of d^{10} orthoxylene from Pd(111) exhibited four D_2 thermal desorption maxima, at 85°C, 220°C, 305°C, and 415°C, at low exposures

Figure IV-4. Chemisorption of d^{10} paraxylene was largely irreversible on Pd(111). Shown are deuterium thermal desorption spectra from chemisorbed d^{10} paraxylene. The spectra in A, B, and C are at exposures of 1.0 L, 2.0 L, and 3.0 L, respectively.

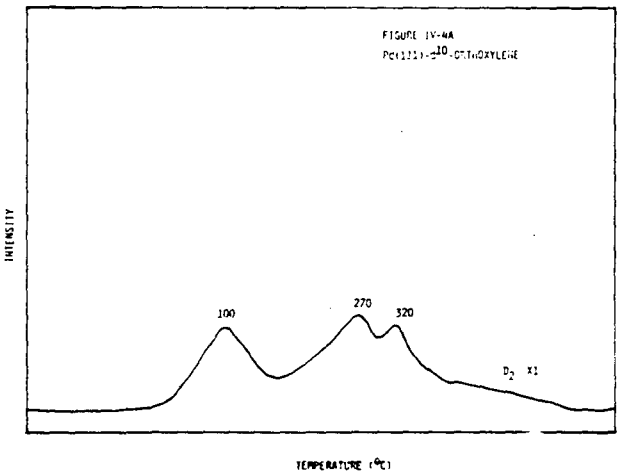
FIGURE IV-4A
Pd(111)-a^{10}-ORTHOXYLENE
INTENSITY
100
270
320
D_2 X1
TEMPERATURE (°C)

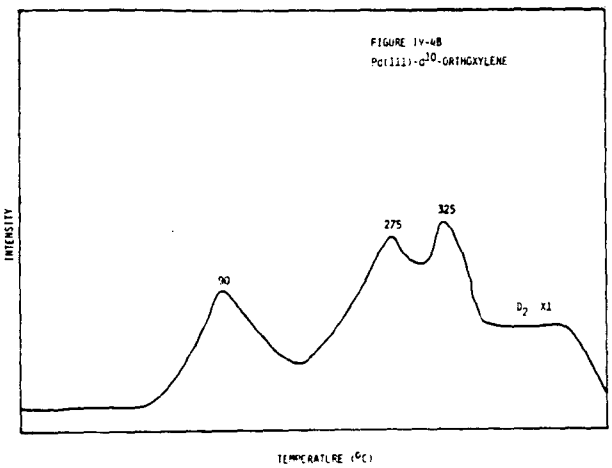
FIGURE IV-4B
Pd(111)-a^{10}-ORTHOXYLENE
INTENSITY
90
275
325
D_2 X1
TEMPERATURE (°C)

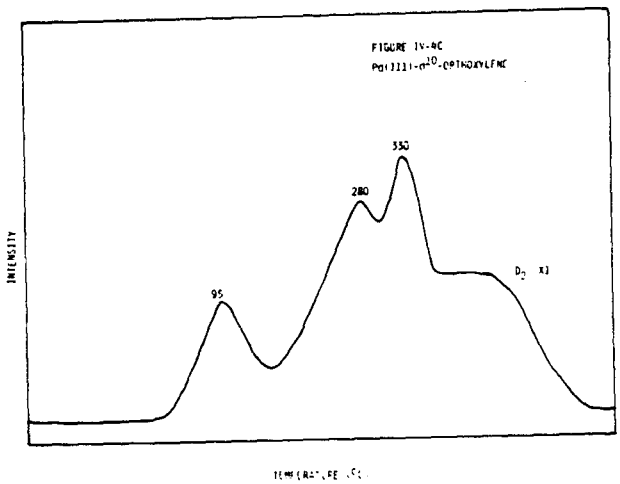
FIGURE IV-4C
Pd(111)-a^{10}-ORTHOXYLENE
INTENSITY
95
280
350
D_2 X1

XBL 846-2139

Figure IV-5. The thermal desorption spectra of metaxylene from Pd(111) demonstrate that chemisorption of metaxylene is primarily irreversible. The thermal desorption spectra shown here are for exposures of 1.0 L (A), 2.0 L (B), and 3.0 L (C).

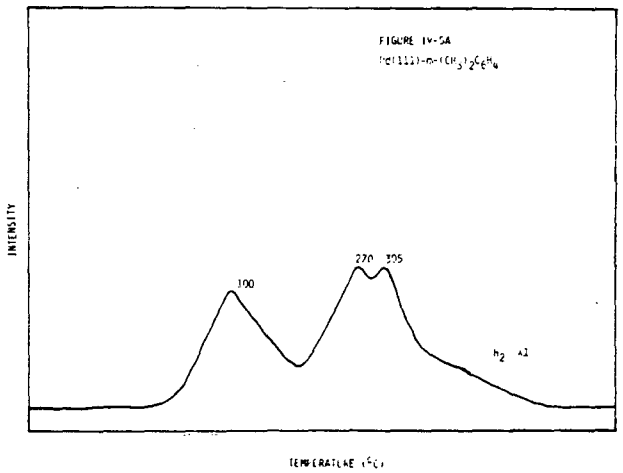
FIGURE IV-5A
Pd(111)-o-(CH3)2C6H4
INTENSITY
100
270
305
H2 X1
TEMPERATURE (°C)

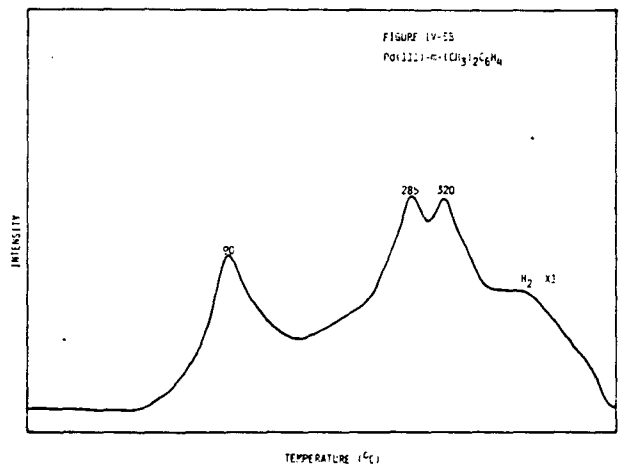
FIGURE IV-5B
Pd(111)-o-(CH3)2C6H4
INTENSITY
90
285
320
H2 X3
TEMPERATURE (°C)

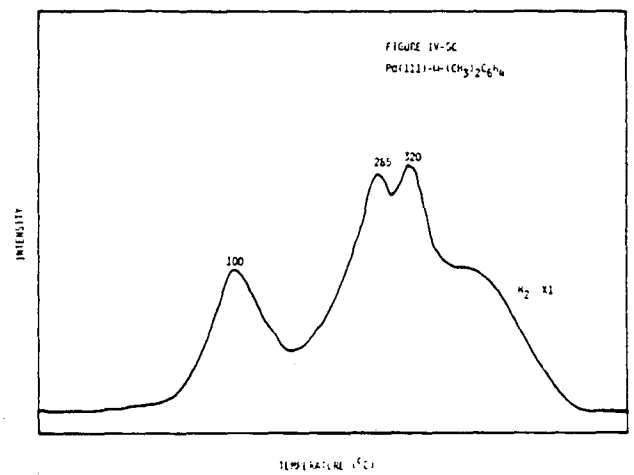
FIGURE IV-5C
Pd(111)-o-(CH3)2C6H4
INTENSITY
100
285
320
H2 X1
TEMPERATURE (°C)

XBL 846-2138

Figure IV-6. A unique deuterium thermal desorption maximum was observed at 220°C in the thermal desorption spectrum of d^{10} orthoxylene from Pd(111). The relative intensity of this maximum increases with exposure, as shown in A (1.0 L), B (2.0 L), and C (3.0 L).

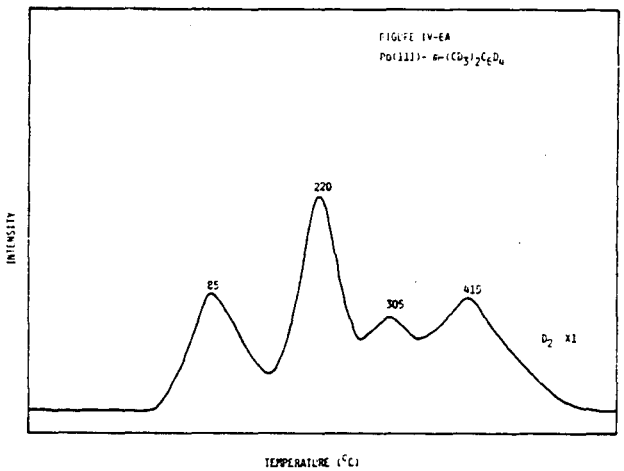
FIGURE IV-6A
Pd(111)- 6-(CD3)2C6D4
220
85
305
415
D2 X1
INTENSITY
TEMPERATURE (°C)

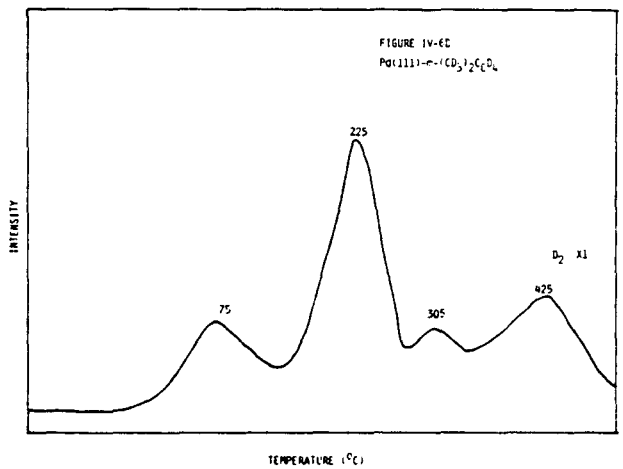
FIGURE IV-6B
Pd(111)-6-(CD3)2C6D4
225
75
305
425
D2 X1
INTENSITY
TEMPERATURE (°C)

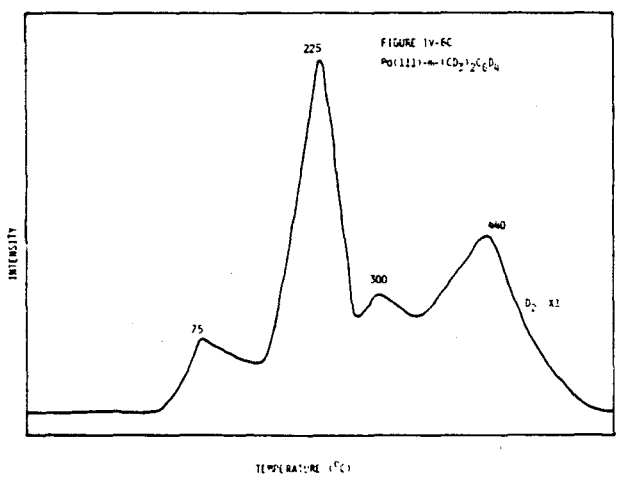
FIGURE IV-6C
Pd(111)-6-(CD3)2C6D4
225
75
300
440
D2 X1
INTENSITY
TEMPERATURE (°C)

XBL 846-2137

(1.0 L) (see Figure IV-6A). The high temperature maxima (220°C, 305°C, and 415°C) increased with respect to the low temperature maximum (75°C-85°C) with increased exposure. The H_2 maximum at 220°C is 50°C lower than the corresponding first high temperature maximum observed at 270°C in both para- and metaxylene.

The thermal desorption spectrum of para-$(CD_3)_2C_6H_4$ yielded all three molecules, H_2, HD, and D_2. At low exposures (1.0 L), D_2 and HD were observed in the low temperature maximum (90°C) and in the high temperature maxima, at 270°C and 305°C (see Figure IV-7A). H_2 was observed only in the 305°C maximum. At high exposures the desorption of HD at low temperatures decreased to the point where it was negligible, at an exposure of 3.0 L. At this exposure H_2 was observed in the 305°C maximum, which had a high temperature tail. HD was observed in the 270°C and 305°C maxima, and D_2 was observed in all three maxima (90°C, 270°C, and 305°C) (see Figure IV-7C).

Thermal desorption of meta $(CD_3)_2C_6H_4$ from Pd(111) at low exposures yielded H_2, HD, and D_2. D_2 was observed in the 110°C and 260°C maxima; HD was observed in the 110°C maximum and showed a broad maximum from 260°C-310°C. H_2 was observed in only the ~300°C maximum (see Figure IV-8A). Increasing exposure resulted in a decrease in the amount of HD in the low temperature maximum, but it did not decrease to zero, as observed for para $(CD_3)_2C_6H_4$. At high exposures D_2 was observed in three poorly resolved maxima, at 75°C, 150°C, and 260°C. HD was observed in a broad maximum from 75°C to 200°C and in a 320°C maximum with a plateau-like tail. H_2 was observed only in a broad 320°C maximum (see Figures IV-8B and IV-8C).

Figure IV-7. The selectively labeled paraxylene $(CD_3)_2C_6H_4$ exhibited partial regioselective C-H bond scission when thermally desorbed from Pd(111). As observed in the $CD_3C_6H_5$ spectrum, the amount of HD desorbing at low temperatures decreased with increasing exposures. Exposures of 1.0 L, 2.0 L, and 3.0 L were used in spectra A, B, and C, respectively.

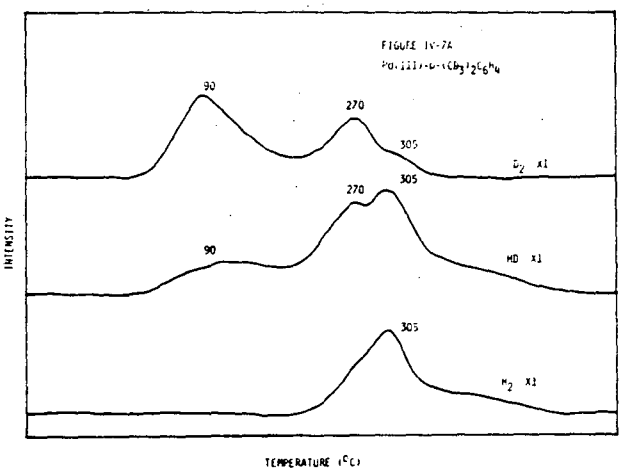
FIGURE IV-7A
90
270
305
D_2 X1
305
270
90
HD X1
305
H_2 X1
INTENSITY
TEMPERATURE (°C)

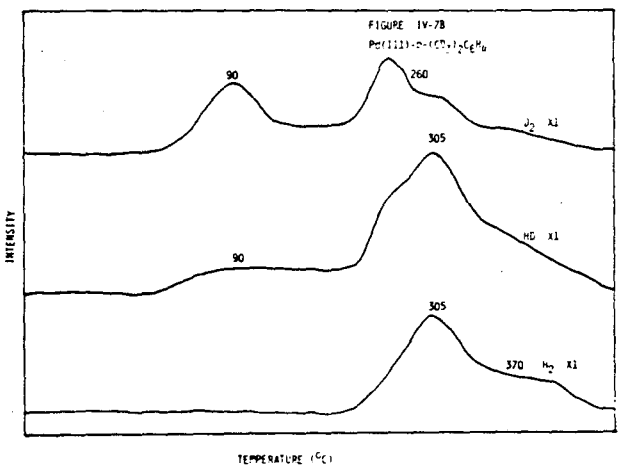
FIGURE IV-7B
90
260
D_2 X1
305
90
HD X1
305
370 H_2 X1
INTENSITY
TEMPERATURE (°C)

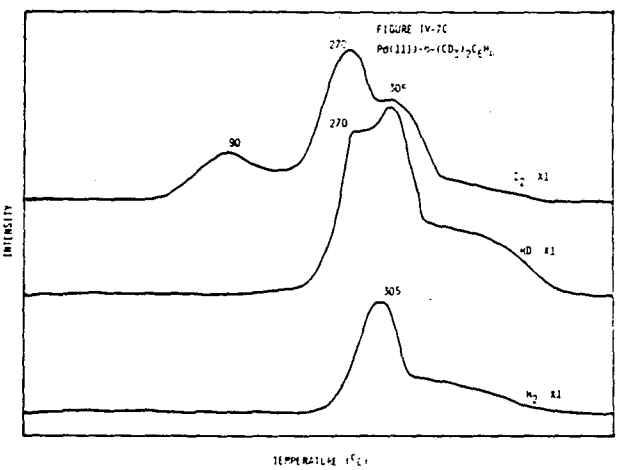
FIGURE IV-7C
270
305
270
90
D_2 X1
HD X1
305
H_2 X1
INTENSITY
TEMPERATURE (°C)

XBL 846-2136

Figure IV-8. Thermal desorption spectra of selectively labeled metaxylene $(CD_3)_2C_6H_4$ from Pd(111) exhibited incomplete regioselective C-H bond scission. Hydrogen, H_2, was found to desorb in the high temperature maxima at the three exposures, 1.0 L (A), 2.0 L (B), and 3.0 L (C).

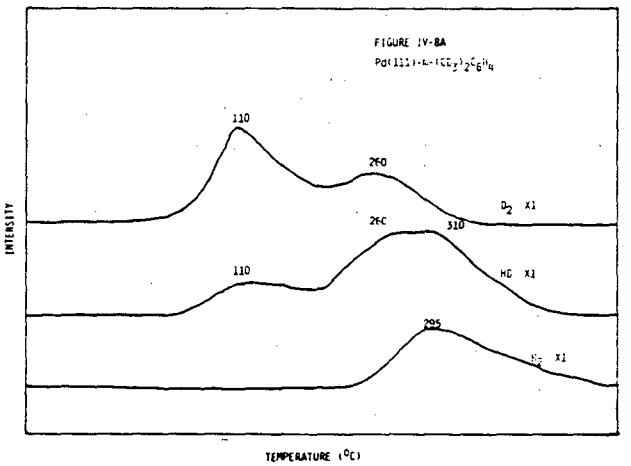
FIGURE IV-8A
110
260
D_2 X1
260
310
110
HD X1
295
INTENSITY
TEMPERATURE (°C)

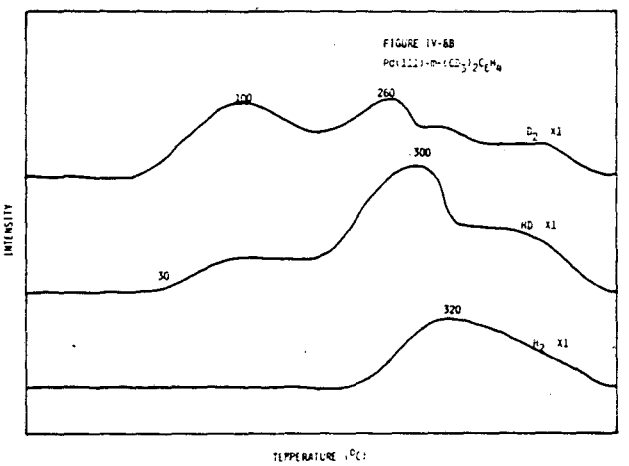
FIGURE IV-8B
100
260
D_2 X1
300
HD X1
30
320
H_2 X1
INTENSITY
TEMPERATURE (°C)

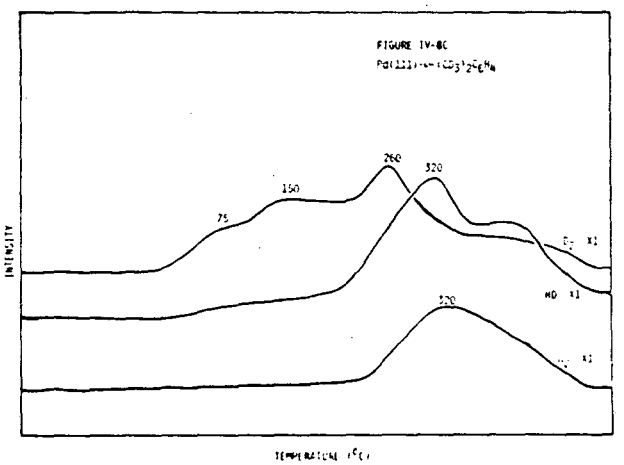
FIGURE IV-8C
260
320
150
75
D_2 X1
HD X1
220
INTENSITY

XBL 846-2135

The thermal desorption of ortho $(CD_3)_2C_6H_4$ from Pd(111) (1.0 L) is shown in Figure IV-9A. At low exposures, D_2 thermal desorption maxima were observed at 75°C and 210°C, HD maxima were observed at 75°C and 210°C, and H_2 was observed in a broad maximum at 340°C. Increasing the exposure resulted in an increase in the amount of D_2 in the 210°C maximum. Weak D_2 maxima were also observed at 60°C and 420°C. HD maxima were observed at 60°C, 210°C, 285°C, and 420°C. H_2 was observed in three maxima, at 210°C, 285°C, and 390°C (see Figures IV-9B and IV-9C).

The thermal desorption of 1,3,5-trimethylbenzene yielded two H_2 maxima at all exposures, one at 90°C and a broad maximum at ~350°C (see Figures IV-10A through IV-10C).

B. Pd(100)

Chemisorption of benzene on Pd(100) exhibited both reversible and irreversible chemisorption. At low exposures (1.0 L), a hydrogen thermal maximum with a high temperature tail was observed at 260°C (see Figure IV-11A). A weak benzene maximum was observed at 35°C, with a tail extending to 260°C. Increasing the exposure to 2.0 L resulted in an increase in the amount of hydrogen desorbing from the surface; an H_2 maximum was observed at 285°C, with a high temperature plateau-like tail (see Figure IV-11B). At high exposures (4.0 L), two benzene maxima were observed, at 45°C and 245°C, along with an H_2 maximum at 295°C with a shoulder at 390°C (see Figure IV-11C). At an exposure of 6.0 L, three poorly resolved benzene maxima, at -55°C,

Figure IV-9. The thermal desorption spectrum of selectively labeled orthoxylene $(CD_3)_2C_6H_4$ from Pd(111) shows the 210°C maximum to be populated primarily by D_2. The amount of D_2 increased in this maximum with increased exposure. The exposures used in A, B, C, and D were 1.0 L, 2.0 L, 3.0 L, and 4.0 L, respectively.

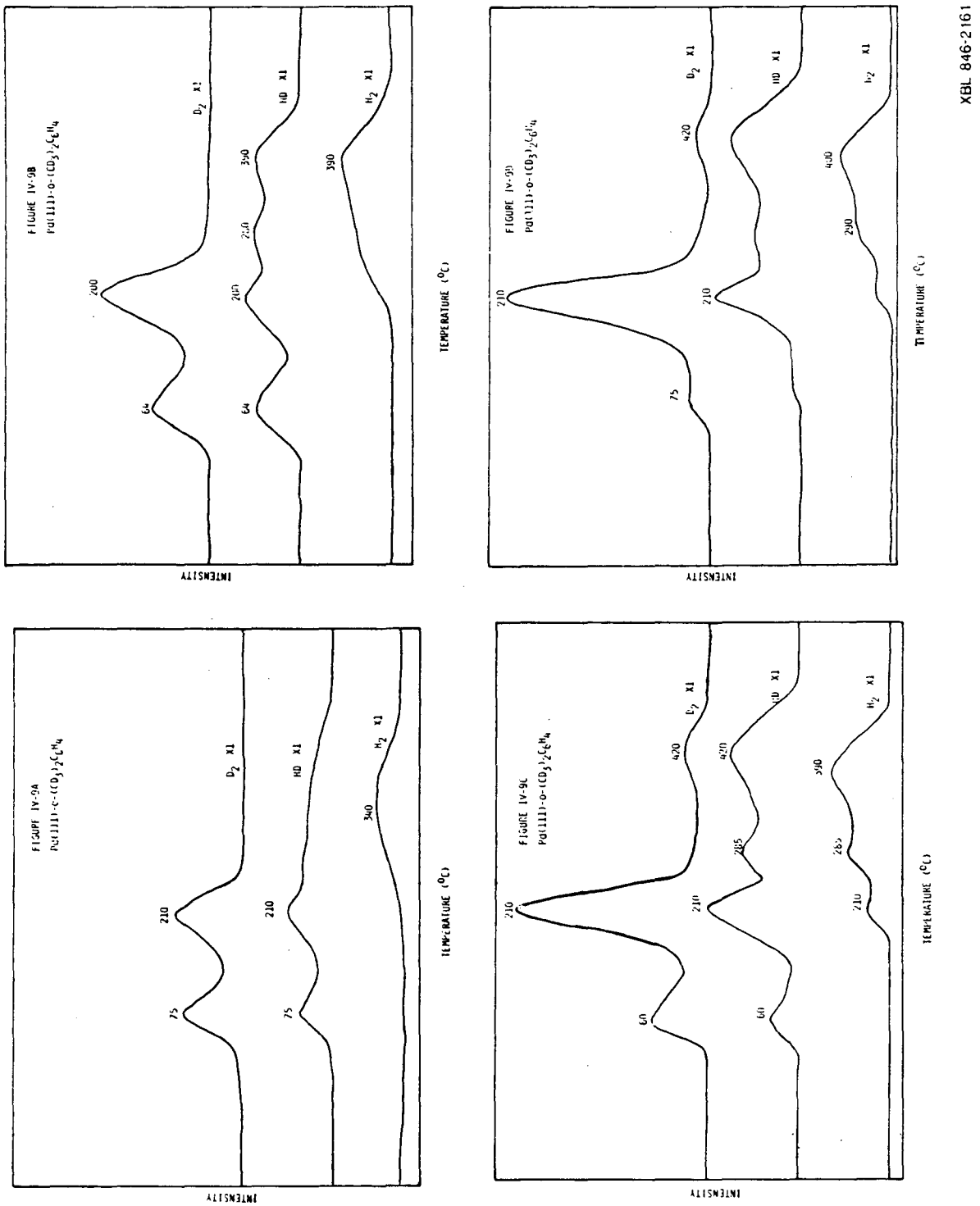
FIGURE IV-9B
Pd(111)-c-(CD3)2C6H4
D2 X1
HD X1
H2 X1
240
64
240
64
390
340
INTENSITY
TEMPERATURE (°C)
FIGURE IV-9D
Pd(111)-o-(CD3)2C6H4
D2 X1
HD X1
H2 X1
210
75
210
420
290
430
INTENSITY
TEMPERATURE (°C)
FIGURE IV-9A
Pd(111)-c-(CD3)2C6H4
D2 X1
HD X1
H2 X1
210
75
210
75
340
INTENSITY
TEMPERATURE (°C)
FIGURE IV-9C
Pd(111)-o-(CD3)2C6H4
D2 X1
HD X1
H2 X1
210
50
210
420
60
420
265
390
265
210
INTENSITY
TEMPERATURE (°C)

XBL 846-2161

Figure IV-10. The thermal desorption spectrum of 1,3,5-trimethylbenzene from Pd(111) exhibited two hydrogen thermal desorption maxima at all exposures studied. The relative intensity of the high temperature maximum increased with exposure. Exposures of 1.0 L, 2.0 L, and 3.0 L were used in A, B, and C, respectively.

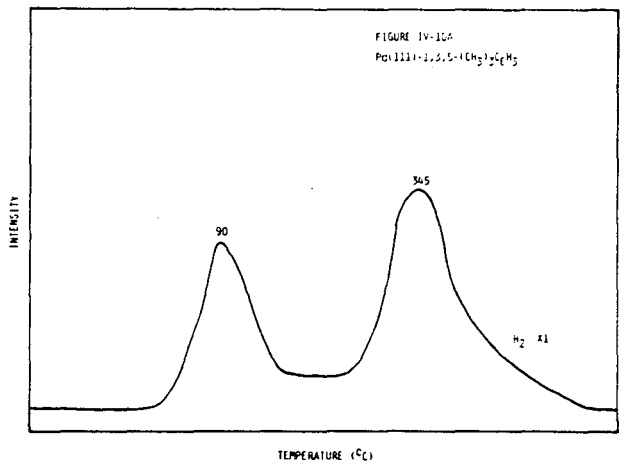
FIGURE IV-10A
Pd(111)-1,3,5-(CH3)3C6H3
345
90
H2 X1
INTENSITY
TEMPERATURE (°C)

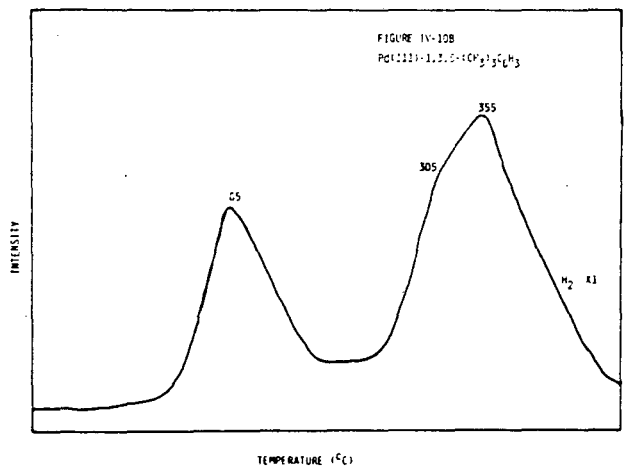
FIGURE IV-10B
355
305
65
H2 X1
INTENSITY
TEMPERATURE (°C)

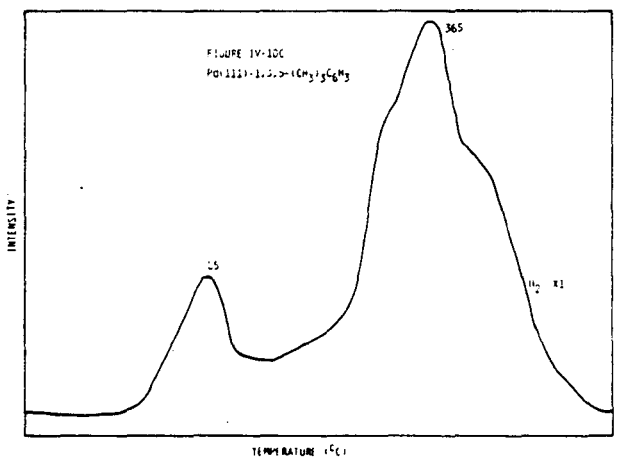
FIGURE IV-10C
Pd(111)-1,3,5-(CH3)3C6H3
365
65
H2 X1
INTENSITY
TEMPERATURE (°C)

XBL 846-2134

Figure IV-11. Chemisorption of benzene on Pd(100) was found to be partially reversible. The fraction of reversibly bound benzene increased with exposure. Thermal desorption spectra of benzene from Pd(100) are shown at four exposures, 1.0 L (A), 2.0 L (B), 4.0 L (C), and 6.0 L (D).

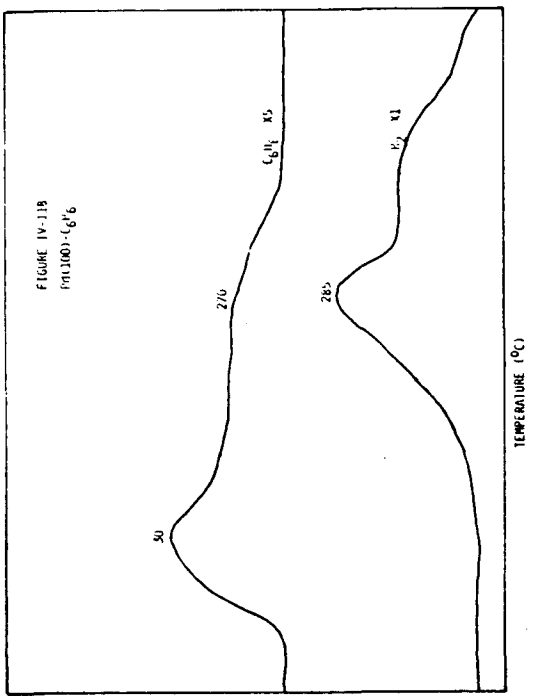
FIGURE IV-11B
Pd(100)-C_6H_6
30
270
285
C_6H_6 X5
H_2 X1
TEMPERATURE (°C)
INTENSITY

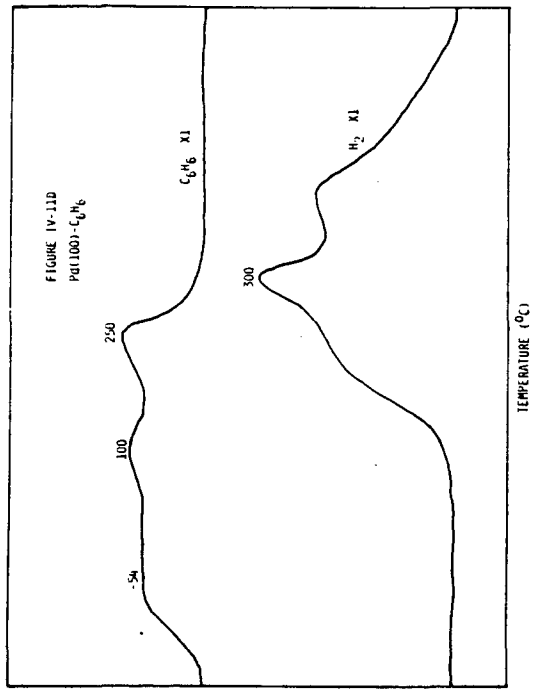
FIGURE IV-11D
Pd(100)-C_6H_6
-94
100
250
300
C_6H_6 X1
H_2 X1
TEMPERATURE (°C)
INTENSITY

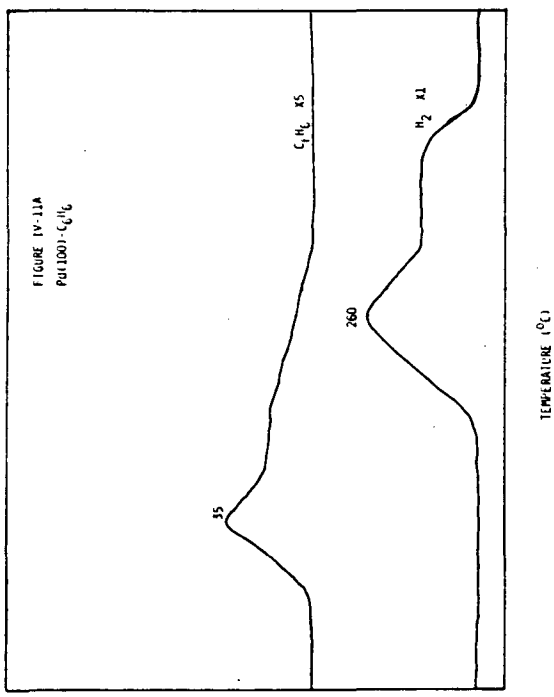
FIGURE IV-11A
Pd(100)-C_6H_6
35
260
C_6H_6 X5
H_2 X1
TEMPERATURE (°C)
INTENSITY

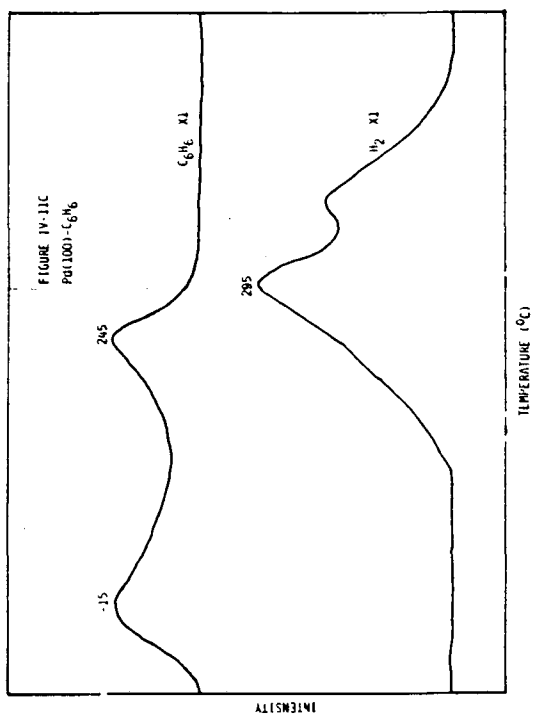
FIGURE IV-11C
Pd(100)-C_6H_6
-15
245
295
C_6H_6 X1
H_2 X1
TEMPERATURE (°C)
INTENSITY

XBL 846-2160

100°C, and 250°C, were observed, along with a hydrogen maximum at 300°C, which had a high temperature shoulder at 390°C (see Figure IV-11D).

Chemisorption of toluene on Pd(100) also exhibited both reversible and irreversible behavior; however, the amount of irreversible chemisorption is increased as compared to benzene. Three hydrogen thermal desorption maxima were observed, at 80°C, 200°C, and 300°C, at an exposure of 1.0 L (see Figure IV-12A). A weak toluene maximum was observed at 25°C. At higher exposures the high temperature maxima increased with respect to the low temperature maximum (see Figures IV-12B and IV-12C).

The thermal desorption of $CD_3C_6H_5$ from Pd(100) yielded all three molecules—H_2, HD, and D_2—at low exposures (1.0 L) (see Figure IV-13A). D_2 was observed in maxima at 90°C and 230°C. HD was observed at 90°C, 230°C, and 310°C; and H_2 was observed at 230°C and 310°C. Increasing the exposure to 3.0 L resulted in a decrease in the amount of HD in the low temperature maxima (see Figure IV-13B). At high exposures (4.0 L), D_2 was observed at 120°C, 235°C, and 325°C; HD was observed at 235°C and 325°C; and H_2 was observed at 235°C and 325°C (see Figure IV-13C).

The chemisorption of the three isomers of dimethylbenzene on Pd(100) also showed both irreversible and reversible chemisorption, but primarily irreversible. At low exposures (1.0 L), the thermal desorption spectrum of d^{10} paraxylene from Pd(100) yielded two D_2 thermal desorption maxima, one at 75°C and a broad one at 300°C (see

Figure IV-12. Thermal desorption of toluene from Pd(100) exhibits both molecular desorption and decomposition to H_2 and carbon. Three hydrogen thermal desorption maxima were observed. The two high temperature maxima were more strongly populated at high exposures. The spectra shown in A, B, and C are for toluene exposures of 1.0 L, 2.0 L, and 4.0 L, respectively.

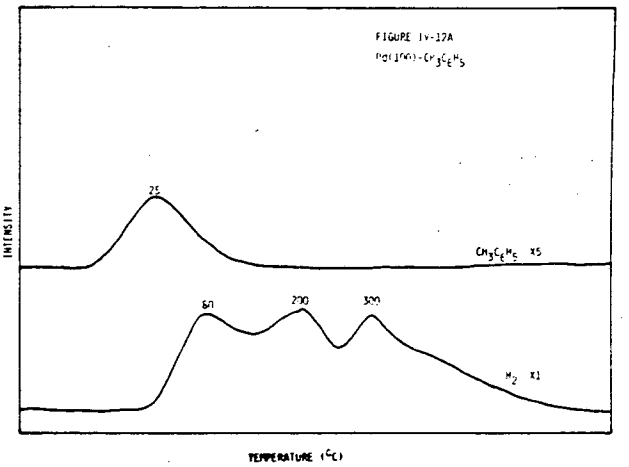
FIGURE IV-12A
Pd(100)-CH3C6H5
INTENSITY
25
CH3C6H5 X5
80
200
300
H2 X1
TEMPERATURE (°C)

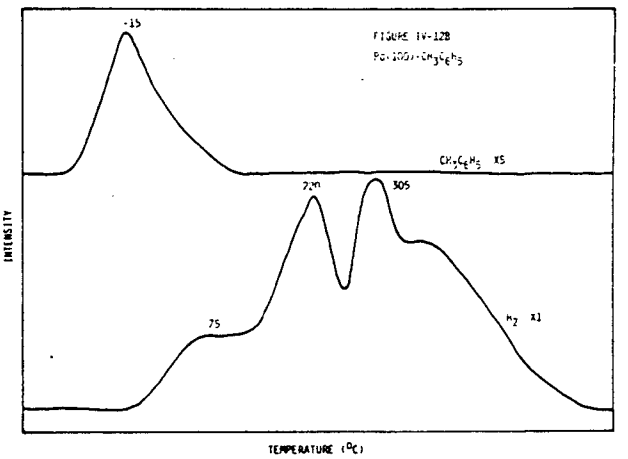
FIGURE IV-12B
Pd(100)-CH3C6H5
INTENSITY
-15
CH3C6H5 X5
220
305
75
H2 X1
TEMPERATURE (°C)

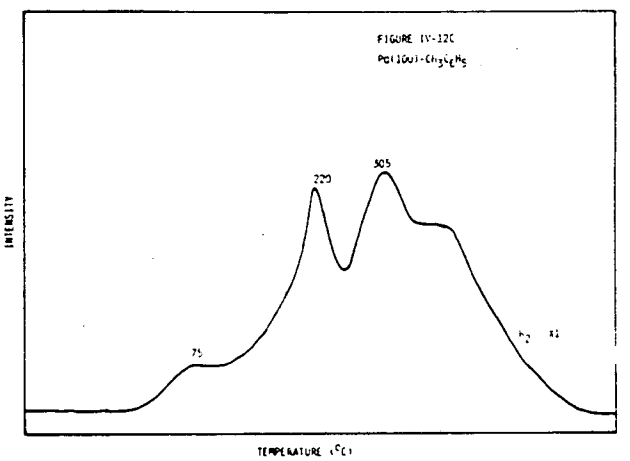
FIGURE IV-12C
Pd(100)-CH3C6H5
INTENSITY
220
305
75
H2 X1
TEMPERATURE (°C)

XBL 846-2133

Figure IV-13. The selectively labeled toluene $CD_3C_6H_5$ exhibited partial regioselective C-H bond scission upon thermal desorption from Pd(100). Hydrogen desorbed only in the high temperature maxima. The amount of HD desorbing at low temperatures decreased with exposure. The three spectra shown here, A, B, and C, are for $CD_3C_6H_5$ exposures of 1.0 L, 2.0 L, and 4.0 L, respectively.

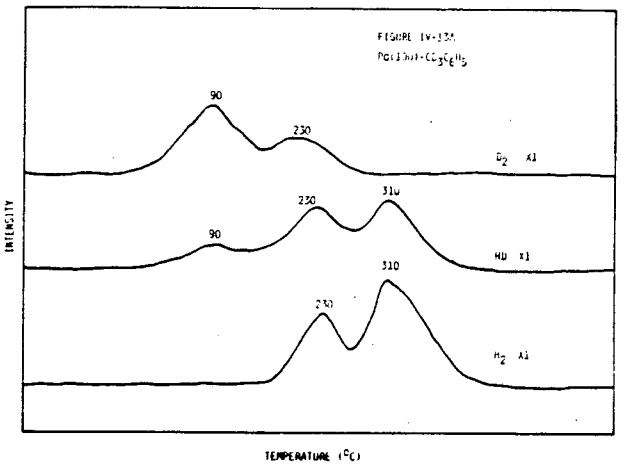
90
230
D_2 X1
230
310
90
HD X1
310
230
H_2 X1
INTENSITY
TEMPERATURE (°C)

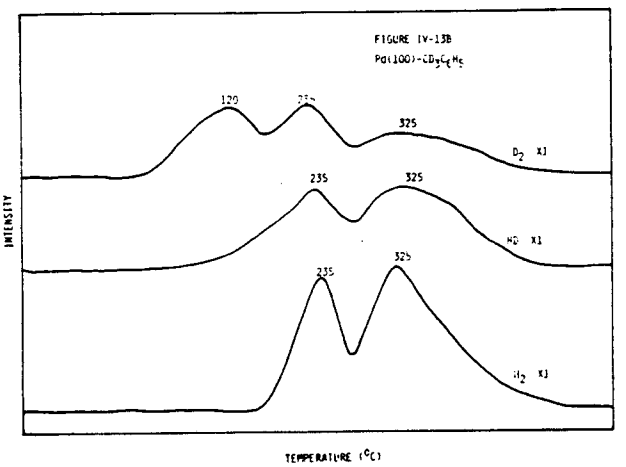
325
D_2 X1
235
325
HD X1
325
235
H_2 X1
INTENSITY
TEMPERATURE (°C)

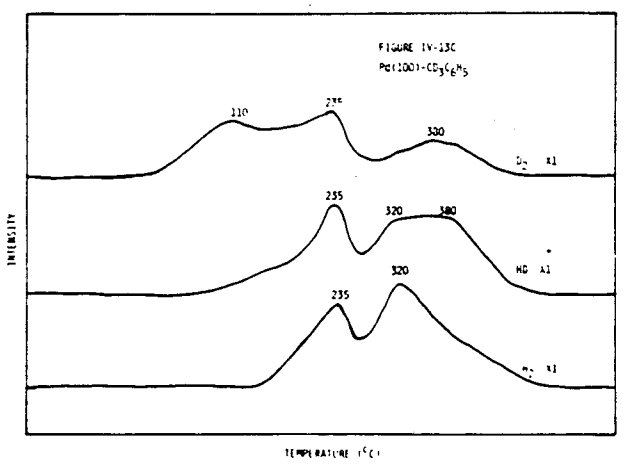
330
D_2 X1
255
320
380
HD X1
320
235
INTENSITY

XBL 846-2132

Figure IV-14. Two deuterium thermal desorption maxima were observed in the thermal desorption of d^{10} paraxylene from Pd(110). The relative intensity of the high temperature maxima increased with exposure. The following d^{10} paraxylene exposures were used: 1.0 L in spectrum A, 2.0 L in spectrum B, 3.0 L in spectrum C, and 4.0 L in spectrum D.

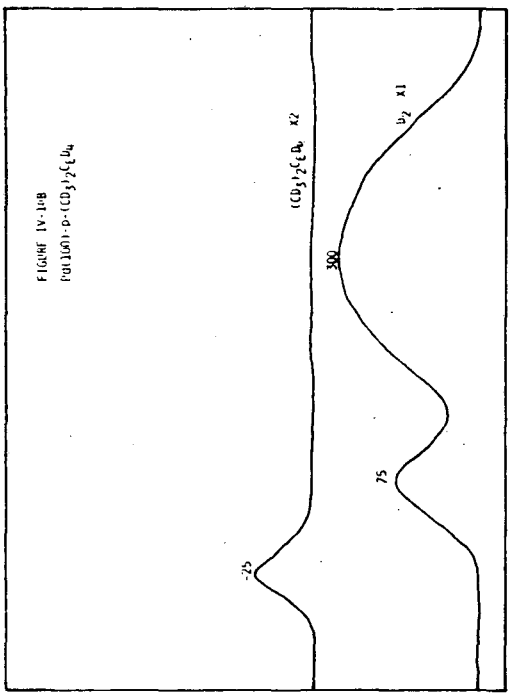
FIGURE IV-14B
Pd(100)-p-(CD3)2C6D4
INTENSITY
TEMPERATURE (°C)
-25
75
300
(CD3)2C6D4 X2
D2 X1

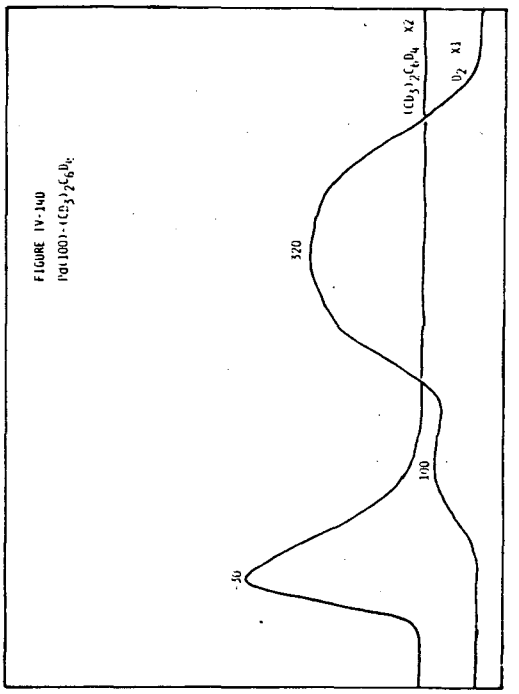
FIGURE IV-14D
Pd(100)-(CD3)2C6D5
INTENSITY
TEMPERATURE (°C)
-50
100
320
(CD3)2C6D4 X2
D2 X1

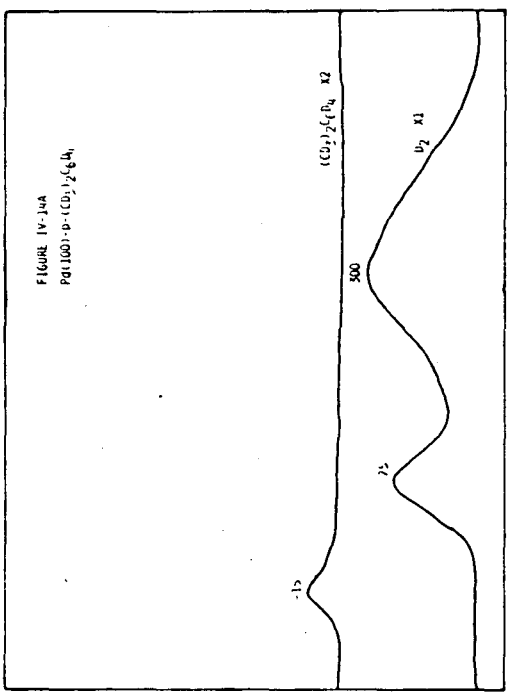
FIGURE IV-14A
Pd(100)-p-(CD3)2C6H4
INTENSITY
TEMPERATURE (°C)
-15
75
300
(CD3)2C6D4 X2
D2 X1

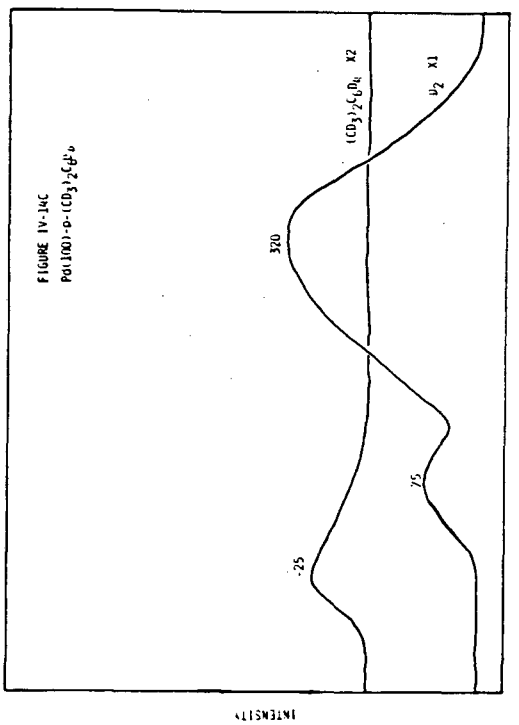
FIGURE IV-14C
Pd(100)-o-(CD3)2C6D4
INTENSITY
TEMPERATURE (°C)
-25
75
320
(CD3)2C6D4 X2
D2 X1

XBL 846-2159

Figure IV-14A). Increasing the exposure resulted in a relative increase in the high temperature maximum (see Figures IV-14B through IV-14D).

The thermal desorption of metaxylene from Pd(100) exhibited a low temperature H_2 thermal desorption maximum at 75°C, and a very broad, almost plateau-like, maximum from 210°C to 400°C (see Figure IV-15A). At an exposure of 2.0 L, two poorly resolved maxima, at 220°C and 345°C, appeared in the high temperature region (see Figure IV-15B). At higher exposures the low temperature maximum was observed as a weak broad desorption followed by a large plateau from 220°C to 390°C (see Figures IV-15C and IV-15D). Four D_2 thermal desorption maxima were observed in the thermal desorption spectrum of d^{10} orthoxylene at 1.0 L from Pd(100)--75°C, 235°C, 305°C, and 390°C (see Figure IV-16A). The 235°C maximum is the most intense of the four. Increasing the coverage resulted in a relative decrease in the intensity of the low temperature maximum, as observed in the para- and metaxylene spectra (see Figures IV-16B and IV-16C).

The thermal desorption spectrum of the selectively labeled xylenes, ortho-, meta-, and para- $(CD_3)_2C_6H_4$, were also investigated on Pd(100). Thermal desorption of para $(CD_3)_2C_6H_4$ at low exposures (1.0 L) from Pd(100) gave a broad H_2 maximum at 345°C; two HD maxima, at 60°C and 305°C; D_2 maxima at 60°C and 250°C, and a broad plateau from 300°C to 390°C (see Figure IV-17A). Increasing the exposure to 4.0 L resulted in a decrease in HD in the low temperature

Figure IV-15. Chemisorption of metaxylene on Pd(100) was largely irreversible. The relative intensity of the high temperature maxima increased at higher exposures. The thermal desorption spectra are for metaxylene exposures of 1.0 L (A), 2.0 L (B), 3.0 L (C), and 4.0 L (D).

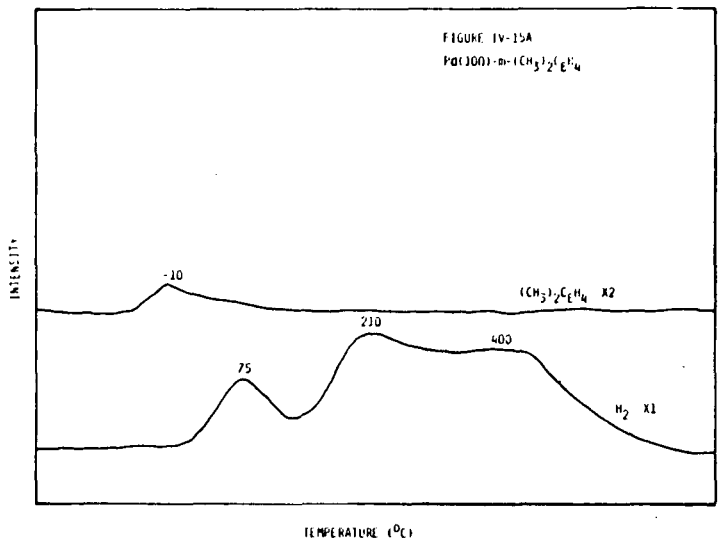
FIGURE IV-15A
Pd(100)-m-(CH3)2C6H4
INTENSITY
-10
(CH3)2C6H4 X2
210
75
400
H2 X1
TEMPERATURE (°C)

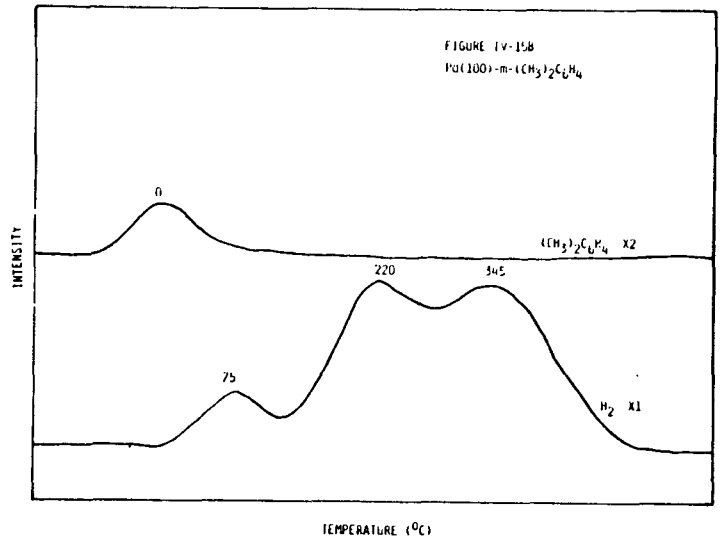
FIGURE IV-15B
Pd(100)-m-(CH3)2C6H4
INTENSITY
0
(CH3)2C6H4 X2
220
345
75
H2 X1
TEMPERATURE (°C)

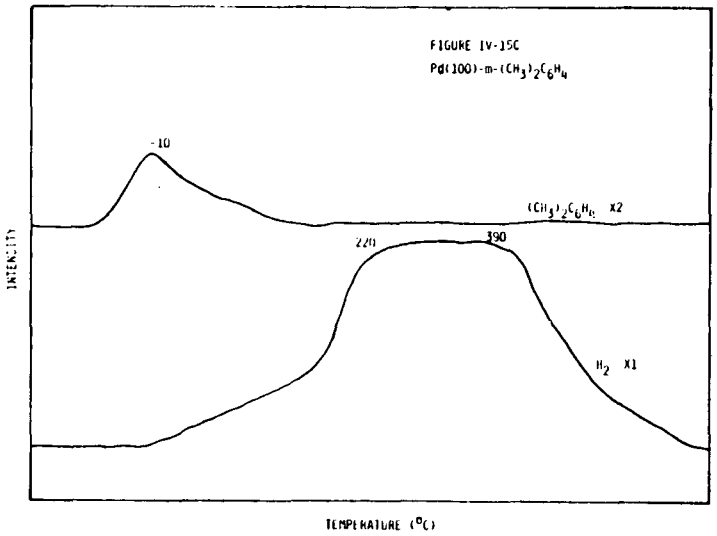
FIGURE IV-15C
Pd(100)-m-(CH3)2C6H4
INTENSITY
-10
(CH3)2C6H4 X2
220
390
H2 X1
TEMPERATURE (°C)

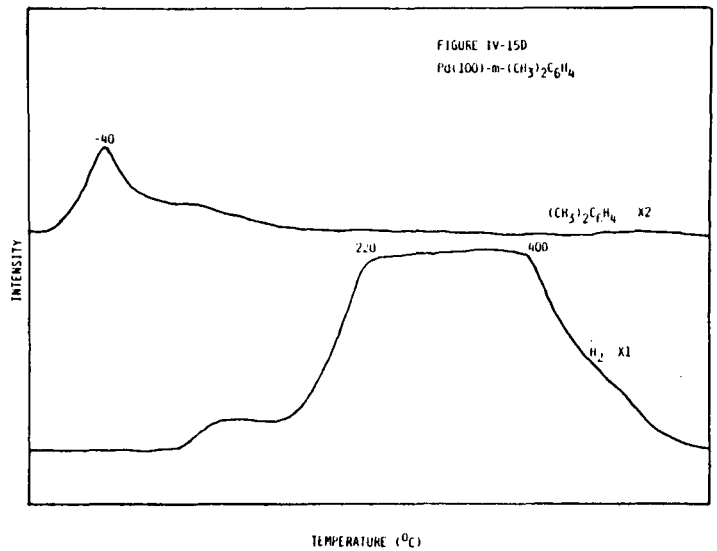
FIGURE IV-15D
Pd(100)-m-(CH3)2C6H4
INTENSITY
-40
(CH3)2C6H4 X2
220
400
H2 X1
TEMPERATURE (°C)

XBL 846-2158

Figure IV-16. The most prominent feature in the D_2 thermal desorption spectrum derived from chemisorbed d^{10} orthoxylene on Pd(100) is the 235°C maximum. The relative intensity of this maximum increased with exposure, as shown here. Orthoxylene exposures of 1.0 L, 2.0 L, and 4.0 L were used in spectra A, B, and C, respectively.

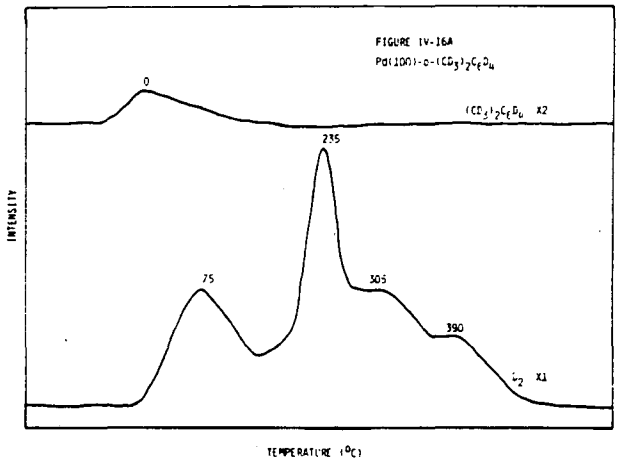
FIGURE IV-16A
Pd(100)-o-$(CD_3)_2C_6D_4$
0
$(CD_3)_2C_6D_4$ X2
235
75
305
390
D_2 X1
INTENSITY
TEMPERATURE (°C)

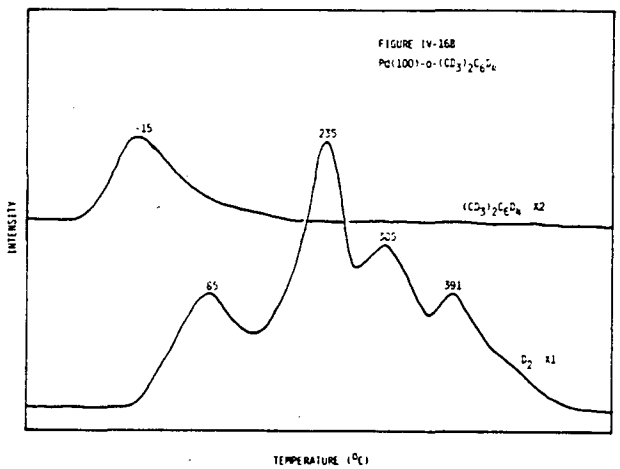
FIGURE IV-16B
Pd(100)-o-$(CD_3)_2C_6D_4$
-15
235
$(CD_3)_2C_6D_4$ X2
305
85
391
D_2 X1
INTENSITY
TEMPERATURE (°C)

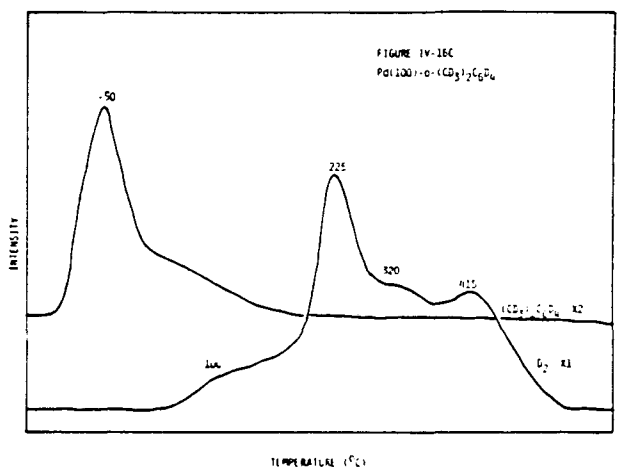
FIGURE IV-16C
Pd(100)-o-$(CD_3)_2C_6D_4$
-50
225
320
D_2 X1
INTENSITY
TEMPERATURE (°C)

XBL 846-2131

Figure IV-17. Partial regioselective C-H bond breaking was observed in the selectively labeled paraxylene $(CD_3)_2C_6H_4$ from Pd(100). HD desorption at low temperatures was found to decrease with exposure. H_2 was also found to desorb only at high temperatures. Exposures of 1.0 L (A), 2.0 L (B), 3.0 L (C), and 4.0 L (D) were used in these thermal desorption experiments.

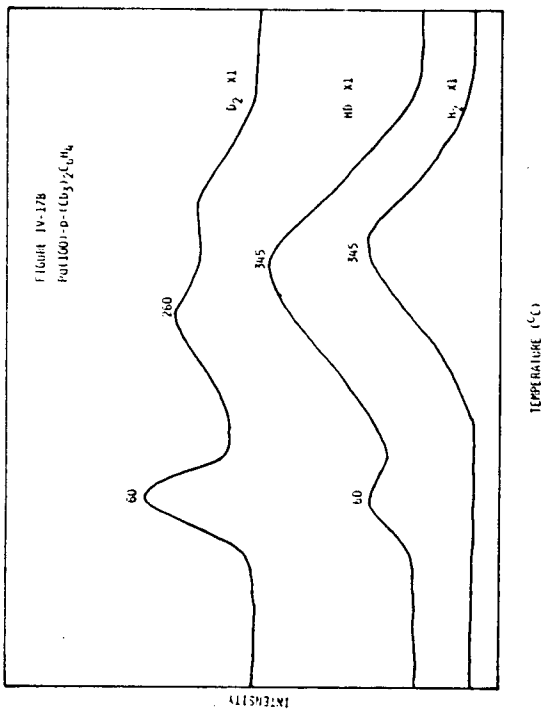
FIGURE IV-17B
Pd(100)-p-(CD3)2C6H4
D2 X1
HD X1
H2 X1
60
260
345
60
345
INTENSITY
TEMPERATURE (°C)

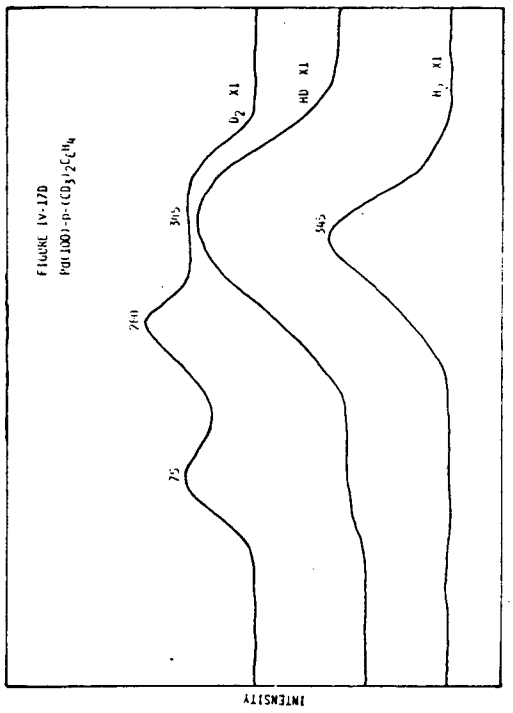
FIGURE IV-17D
Pd(100)-p-(CD3)2C6H4
D2 X1
HD X1
H2 X1
75
260
345
345
INTENSITY
TEMPERATURE (°C)

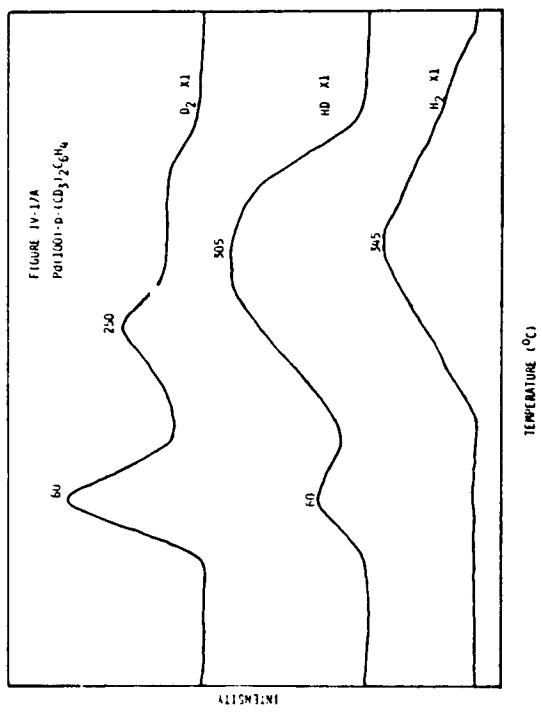
FIGURE IV-17A
Pd(100)-p-(CD3)2C6H4
D2 X1
HD X1
H2 X1
60
250
305
60
345
INTENSITY
TEMPERATURE (°C)

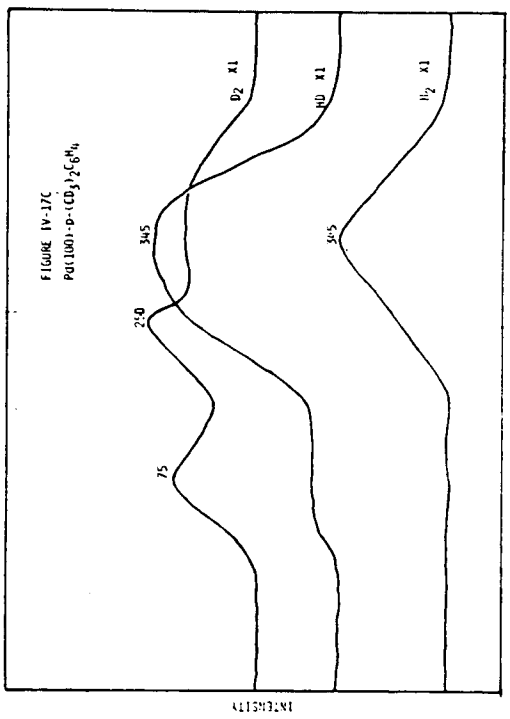
FIGURE IV-17C
Pd(100)-p-(CD3)2C6H4
D2 X1
HD X1
H2 X1
75
250
345
345
INTENSITY
TEMPERATURE (°C)

XBL 846-2157

maximum, and a decrease in the 75°C D_2 maximum with respect to the 260°C maximum. H_2 was observed only in the 345°C maximum (see Figure IV-17D).

The thermal desorption of meta $(CD_3)_2C_6H_4$ from Pd(100) yielded all three molecules--H_2, HD, and D_2. At low coverages, 1.0 L, hydrogen thermal desorption maxima were observed at 80°C, 210°C, and 300°C; HD maxima were observed at 80°C and 210°C, with a long tail extending to ~450°C; and D_2 maxima were observed at 80°C and 210°C (see Figure IV-18A). At higher coverages, H_2 was observed at 100°C and 345°C; HD was observed at 100°C, 235°C, and 345°C; and D_2 was observed at 100°C, 235°C, and 345°C (see Figures IV-18B and IV-18C). Thermal desorption of ortho $(CD_3)_2C_6H_4$ at low exposures, 1.0 L, yielded H_2 in a single maximum at 300°C; three HD maxima, at 85°C, 235°C, and 300°C; and two D_2 maxima, at 85°C and 235°C (see Figure IV-19A). At high exposures, 2.0 L, two hydrogen maxima were observed, at 270°C and 370°C; three HD maxima were observed, at 75°C, 220°C, and a broad plateau from 270°C to 370°C; and two D_2 maxima were observed, at 75°C and 220°C (see Figure IV-19B). At an exposure of 3.0 L, three D_2 maxima were observed, at 100°C, 235°C, and 390°C. HD desorbed in maxima at 100°C, 235°C, 300°C (a shoulder on the 235°C maximum), and 390°C. Two D_2 maxima were observed, at 270°C and 370°C (see Figure IV-19C).

Figure IV-18. The thermal desorption spectrum of selectively labeled $(CD_3)_2C_6H_4$ from Pd(100) showed little regioselective C-H bond scission. Thermal desorption spectra at exposures of 1.0 L, 2.0 L, and 3.0 L are shown in A, B, and C, respectively.

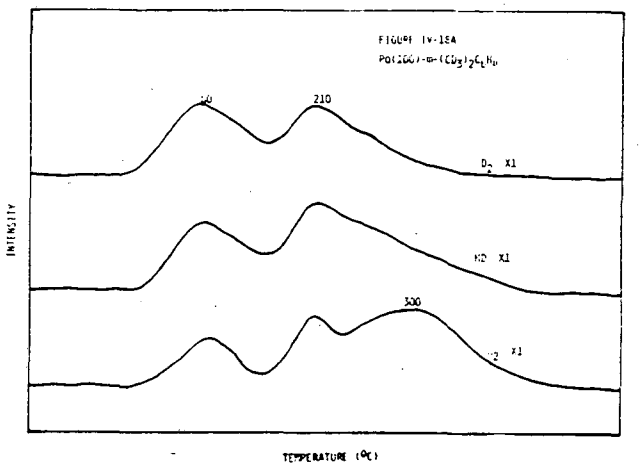
FIGURE IV-15A
210
D_2 X1
HD X1
300
INTENSITY
TEMPERATURE (°C)

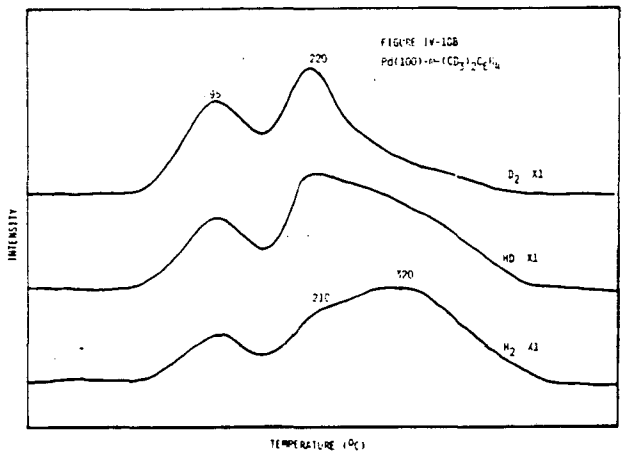
FIGURE IV-15B
220
95
D_2 X1
HD X1
320
210
H_2 X1
INTENSITY
TEMPERATURE (°C)

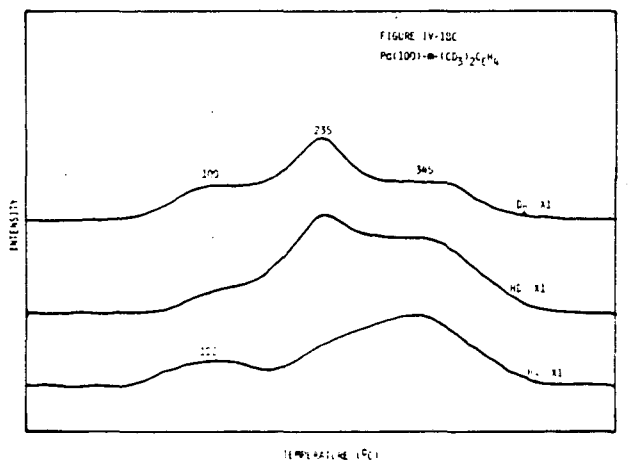
FIGURE IV-15C
235
100
345
INTENSITY

XBL 846-2130

Figure IV-19. The maximum at ~235°C was populated primarily by D_2 and HD in the thermal desorption of the selectively labeled orthoxylene $(CD_3)_2C_6H_4$ from Pd(100). H_2 desorbed only at high temperature in the three spectra shown here. Orthoxylene exposures of 1.0 L, 2.0 L, and 3.0 L were used in spectra A, B, and C, respectively.

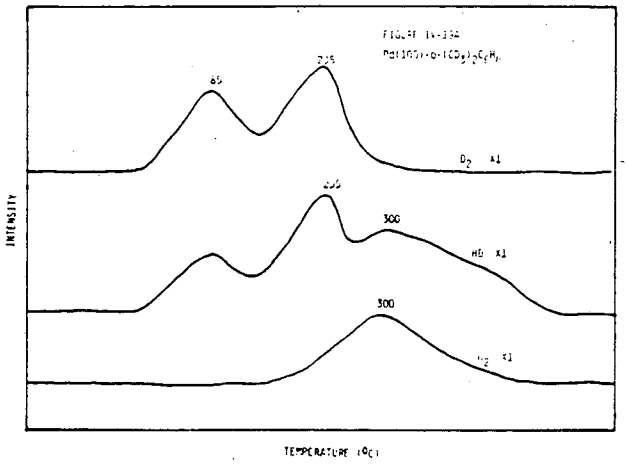
65
215
D_2 x1
200
300
HD x1
300
H_2 x1
INTENSITY
TEMPERATURE (°C)

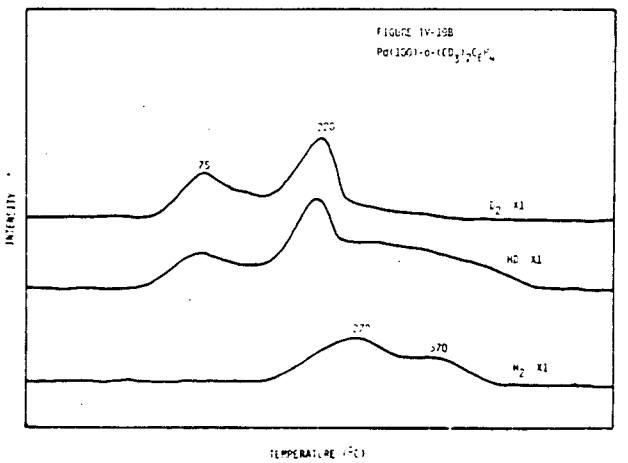
75
200
D_2 x1
HD x1
270
370
H_2 x1
INTENSITY
TEMPERATURE (°C)

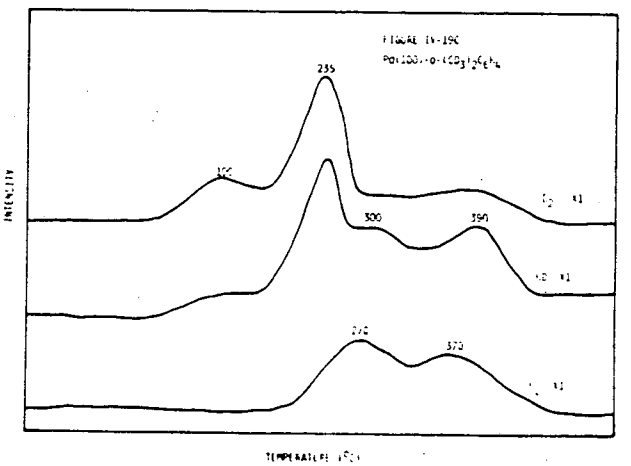
235
300
390
D_2 x1
HD x1
270
370
INTENSITY
TEMPERATURE (°C)

XBL 846-2129

C. Pd(110)

As observed on Pd(111) and Pd(100), benzene was found to exhibit both reversible and irreversible chemisorption on Pd(110). At low exposures (0.5 L), two hydrogen maxima were observed, one at 170°C and a shoulder at 250°C; a benzene maximum was observed at -39°C (see Figure IV-20A). At an exposure of 1.0 L, hydrogen maxima were observed at 170°C and 250°C, and a benzene maximum was observed at -15°C (see Figure IV-20B). At an exposure of 2.0 L, two H_2 thermal desorption maxima were observed, at 200°C and 260°C, and a benzene maximum was observed at -55°C with a broad plateau-like tail from 0°C to 150°C (see Figure IV-20C).

Chemisorbed toluene on Pd(110) (1.0 L) exhibited three hydrogen thermal desorption maxima, at 25°C, 160°C, and 270°C, and a toluene maximum at 15°C (see Figure IV-21A). At higher exposures (2.0 L), the high temperature maxima (170°C and 275°C) increased with respect to the low temperature maximum (see Figures IV-21B and IV-21C).

The selectively labeled toluene, $CD_3C_6H_5$, at low exposure, yielded the following thermal desorption spectrum: D_2 in the low temperature maximum, 50°C; HD at 50°C and 135°C; and H_2 at 170°C and 269°C (see Figure IV-22A). By increasing the exposure to 1.0 L, the amount of HD in the low temperature maximum decreased, and D_2 was observed in the high temperature maxima (see Figures IV-22B and IV-22C).

Chemisorption studies of the three isomers of dimethylbenzene--ortho-, meta-, and paraxylene--were also performed on Pd(110). At low

Figure IV-20. Benzene chemisorption on Pd(110) was found to exhibit a greater fraction of reversibility at higher exposures. At low exposures, chemisorbed benzene was largely irreversible. Thermal desorption spectra of benzene from Pd(110) at exposures of 0.5 L (A), 1.0 L (B), and 2.0 L (C) are shown here.

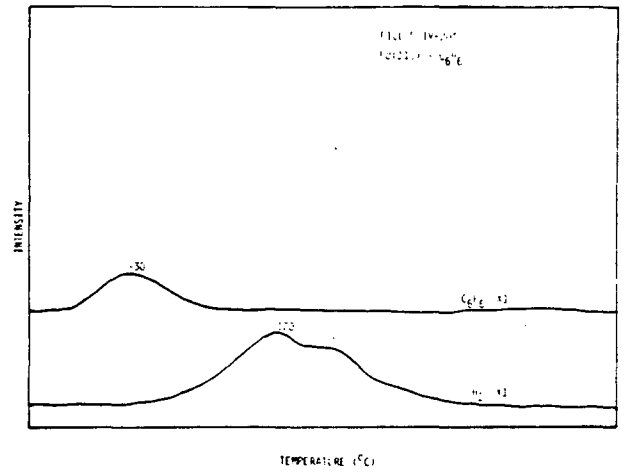
INTENSITY
-30
TEMPERATURE (°C)

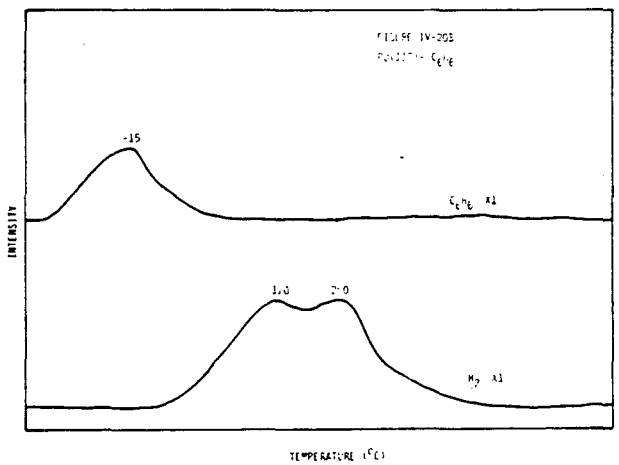
INTENSITY
-15
TEMPERATURE (°C)

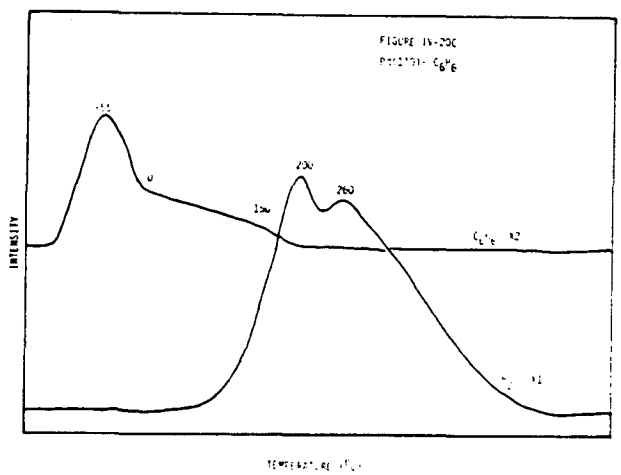
INTENSITY
230
260
TEMPERATURE (°C)

XBL 846-2128

Figure IV-21. Toluene was found to chemisorb both reversibly and irreversibly on Pd(110). Three H_2 thermal desorption maxima were observed at all exposures studied. The relative intensity of the two high temperature H_2 maxima increased with exposure. Spectra A, B, and C are derived from toluene exposures of 1.0 L, 2.0 L, and 3.0 L, respectively.

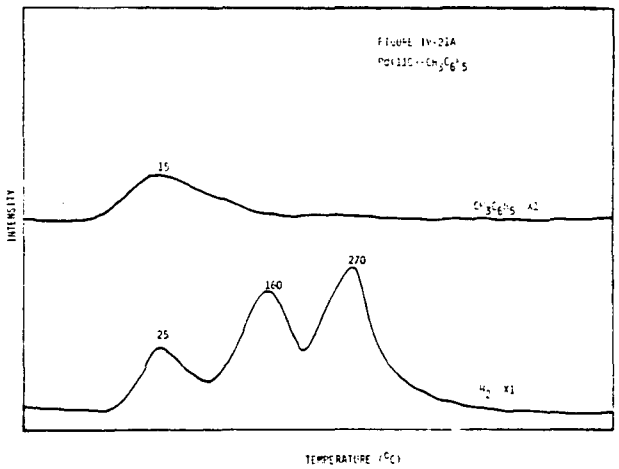
INTENSITY
15
270
160
25
TEMPERATURE (°C)

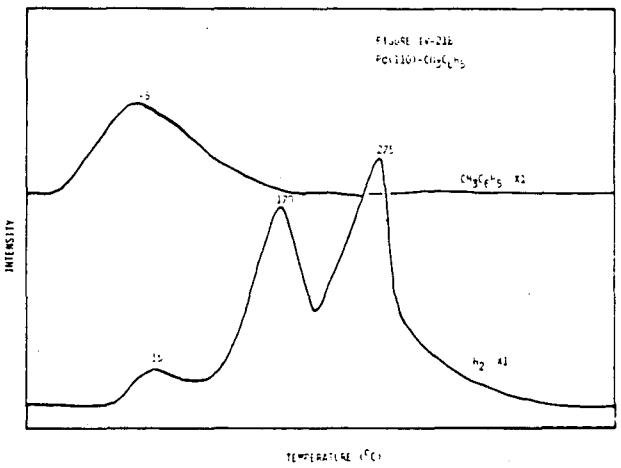
INTENSITY
TEMPERATURE (°C)

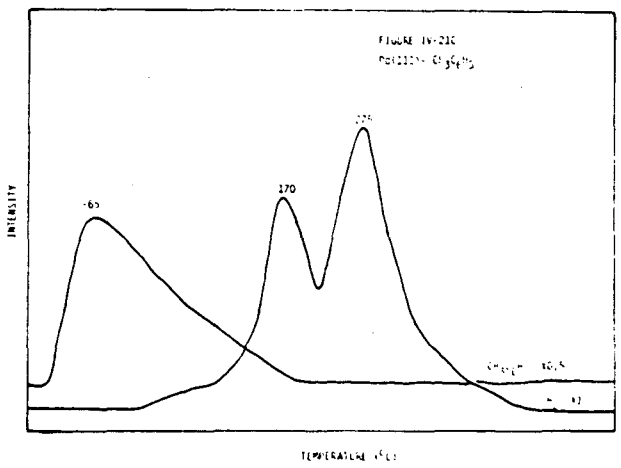
INTENSITY
170
TEMPERATURE (°C)

XBL 846-2127

Figure IV-22. Thermal desorption of $CD_3C_6H_5$ from Pd(110) exhibited incomplete regioselective C-H bond scission. At low exposure, 0.5 L, D_2 desorbed only at low temperatures and H_2 only at high temperatures. HD also desorbed at low temperatures. Increasing exposure decreased the amount of HD desorbing at low temperatures. Three thermal desorption spectra, at exposures of 0.5 L (A), 1.0 L (B), and 3.0 L (C), are shown here.

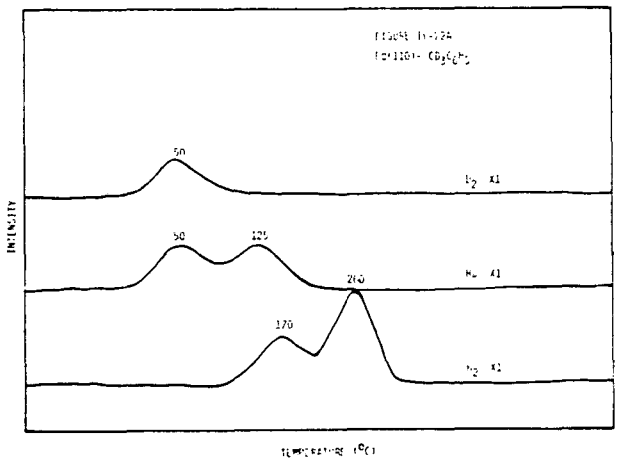
50
D_2 X1
50
125
H_2 X1
260
170
h_2 X1
INTENSITY

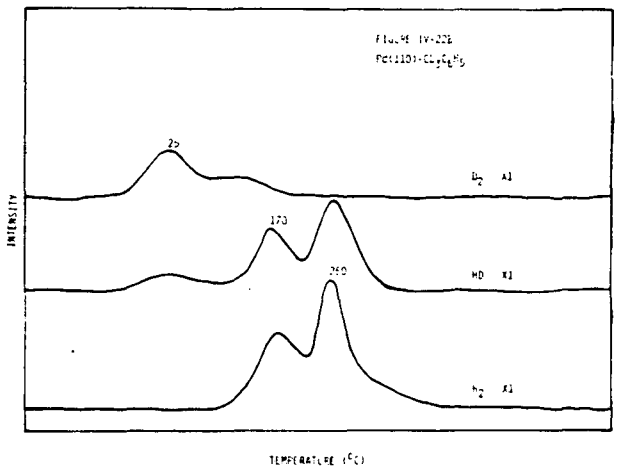
25
D_2 X1
170
HD X1
260
h_2 X1
INTENSITY

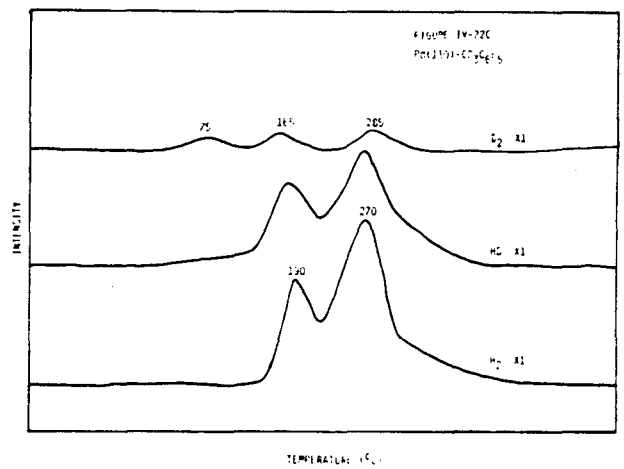
75
185
205
D_2 X1
270
HD X1
190
H_2 X1
INTENSITY

XBL 846-2126

Figure IV-23. Deuterium derived from the decomposition of d^{10} paraxylene during thermal desorption from Pd(110) desorbed in three maxima, a low temperature maximum and two high temperature maxima. The intensity of the two high temperature maxima increased with respect to the low temperature maximum with increased exposures. Spectra A, B, and C shown here correspond to exposures of 1.0 L, 2.0 L, and 3.0 L, respectively.

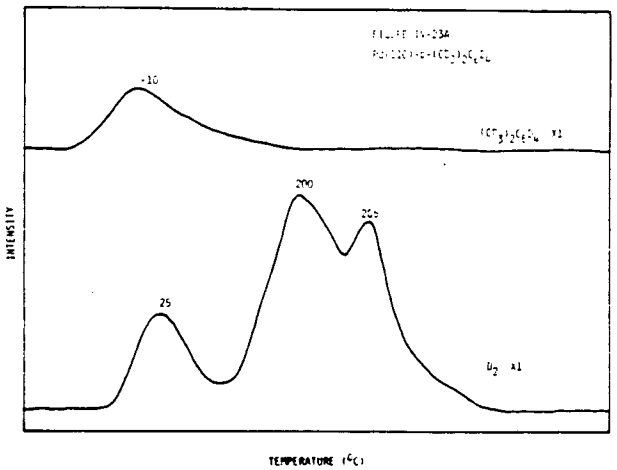
-10
200
260
25
INTENSITY
TEMPERATURE (°C)

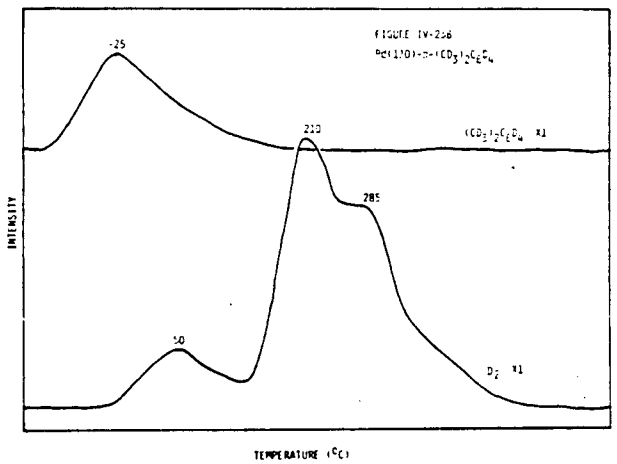
-25
210
285
50
INTENSITY
TEMPERATURE (°C)

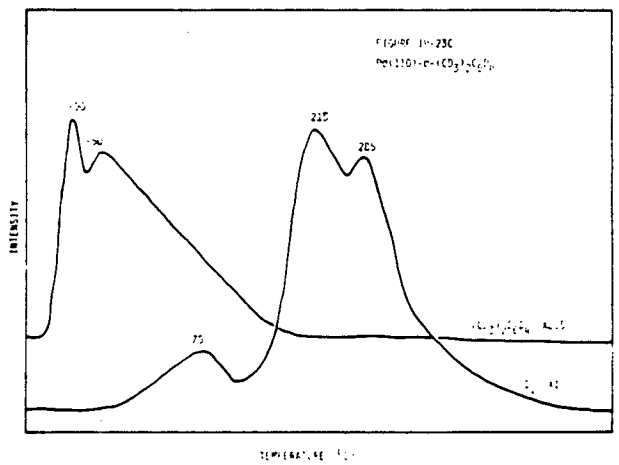
210
285
75
INTENSITY

XBL 846-2125

exposures (1.0 L), the thermal desorption spectrum of d^{10} paraxylene yielded three D_2 thermal desorption maxima, a low temperature maximum at 25°C, and two poorly resolved maxima at 200°C and 285°C (see Figure IV-23A). At an exposure of 2.0 L, the two high temperature maxima at 210°C and 285°C increased with respect to the low temperature maximum (50°C) (see Figures IV-23B and IV-23C). Metaxylene chemisorbed on Pd(110) at low exposures also yielded three hydrogen thermal desorption maxima, at 50°C, 170°C, and 285°C (see Figure IV-24A). The two high temperature maxima were more resolved in paraxylene. At higher exposures (3.0 L), the low temperature maximum appeared as a broad desorption and a decreased relative intensity with respect to the two high temperature maxima (see Figure IV-24C).

The d^{10} orthoxylene thermal desorption spectrum from Pd(110) yielded three D_2 thermal desorption maxima, at 25°C, 180°C, and 280°C (see Figure IV-25A). Resolution of these three maxima was better than in metaxylene. As observed for para- and metaxylene, the relative intensity of the low temperature hydrogen decreased at higher exposures (see Figures IV-25B and IV-25C).

The chemisorption of the selectively labelled xylenes--ortho, para, and meta $(CD_3)_2C_6H_4$--was investigated to probe the mechanism of carbon-hydrogen bond scission in these molecules. The thermal desorption spectrum of para $(CD_3)_2C_6H_4$ at low exposures (0.5 L) exhibited two H_2 thermal desorption maxima, at 190°C, and 290°C; three HD maxima, at 40°C, 190°C, and 270°C; and three D_2 maxima, at 40°C, 190°C, and 270°C (see Figure IV-26A).

Figure IV-24. Thermal desorption of metaxylene from Pd(110) at various exposures is shown here. The relative intensities of the three hydrogen thermal desorption maxima are found to be a function of exposure. The low temperature H_2 maximum decreases with exposure. Metaxylene exposures of 1.0 L, 2.0 L, and 3.0 L were used in experiments illustrated in A, B, and C, respectively.

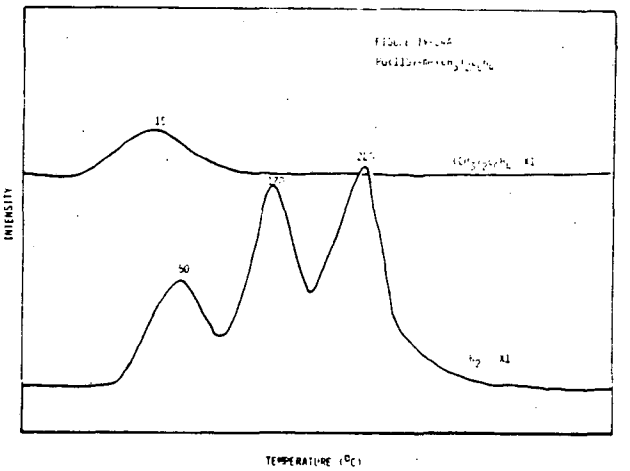
INTENSITY
TEMPERATURE (°C)

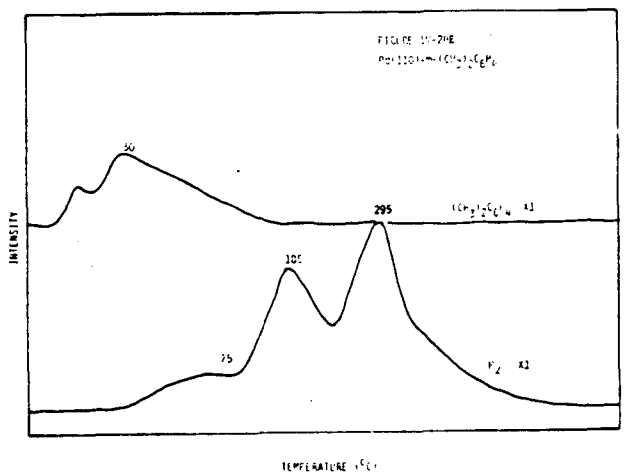
INTENSITY
295
TEMPERATURE (°C)

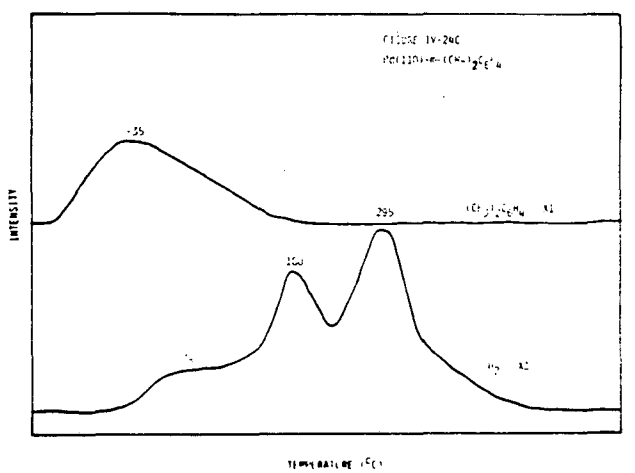
INTENSITY
295
TEMPERATURE (°C)

XBL 846-2124

Figure IV-25. The most intense D_2 thermal desorption maximum derived from the thermal desorption of d^{10} orthoxylene was the central maximum at 180°C. Spectra A, B, and C shown here correspond to experiments using d^{10} orthoxylene exposures of 1.0 L, 2.0 L, and 3.0 L, respectively.

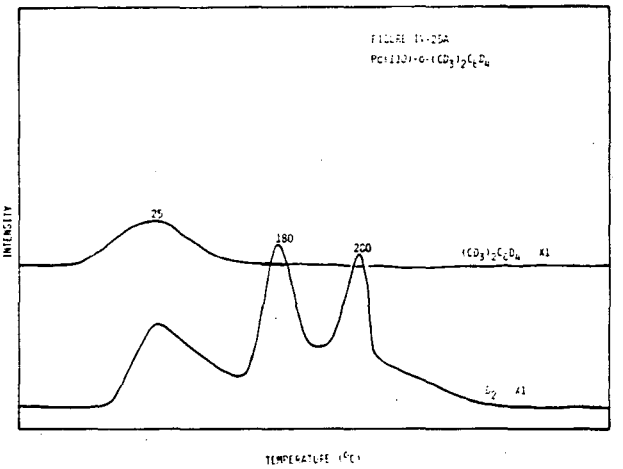
INTENSITY
25
180
200
$(CD_3)_2C_6D_4$ X1
D_2 X1
TEMPERATURE (°C)

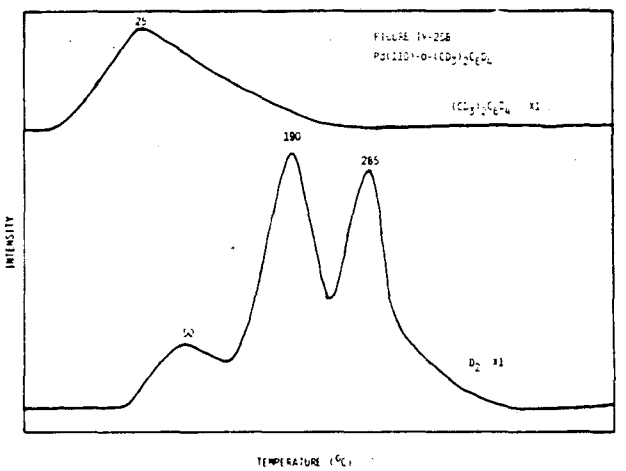
INTENSITY
25
190
265
50
$(CD_3)_2C_6D_4$ X1
D_2 X1
TEMPERATURE (°C)

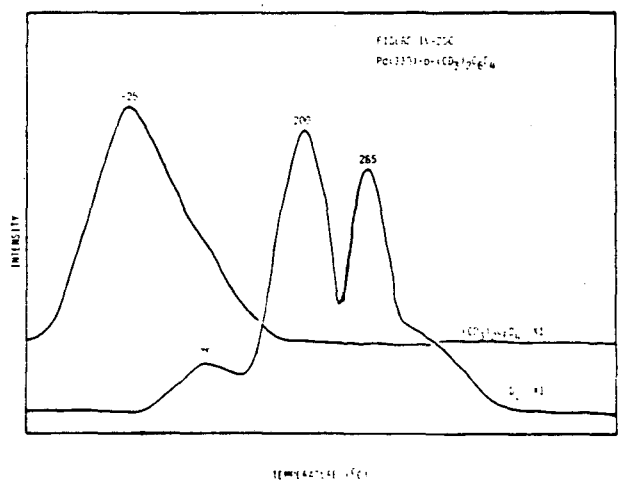
INTENSITY
25
200
265
D_2 X1

XBL 846 2123

Figure IV-26. Regioselective C-H bond scission was not complete in the thermal desorption of the selectively labeled paraxylene $(CD_3)_2C_6H_4$ from Pd(110). H_2 desorbed only at high temperatures. Exposures of 0.5 L, 1.0 L, 2.0 L, and 4.0 L were used in spectra A, B, C, and D, respectively.

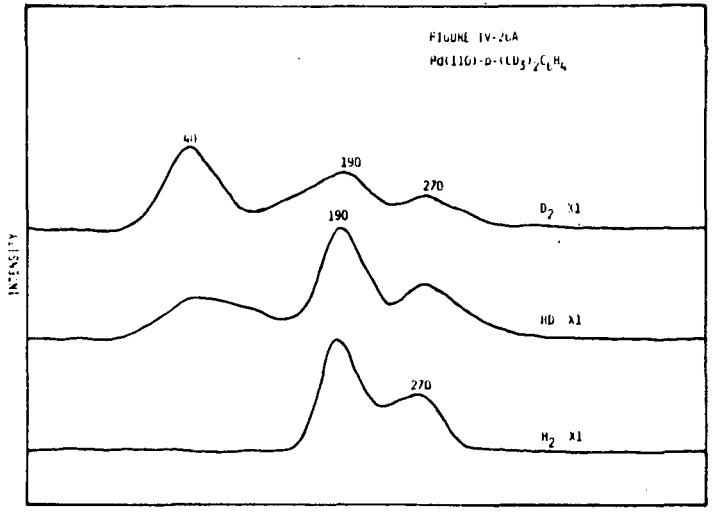
FIGURE IV-26A
Pd(110)-p-(CD3)2C6H4
40
190
270
D2 X1
190
HD X1
270
H2 X1
INTENSITY
TEMPERATURE (°C)

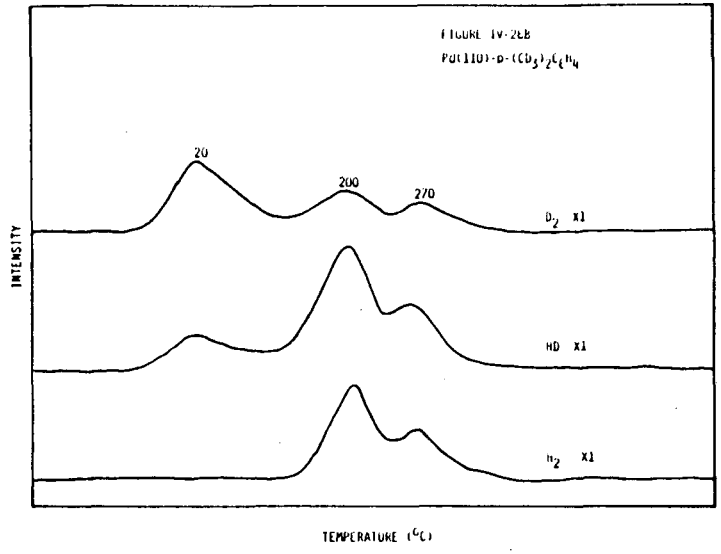
FIGURE IV-26B
Pd(110)-p-(CD3)2C6H4
20
200
270
D2 X1
HD X1
H2 X1
INTENSITY
TEMPERATURE (°C)

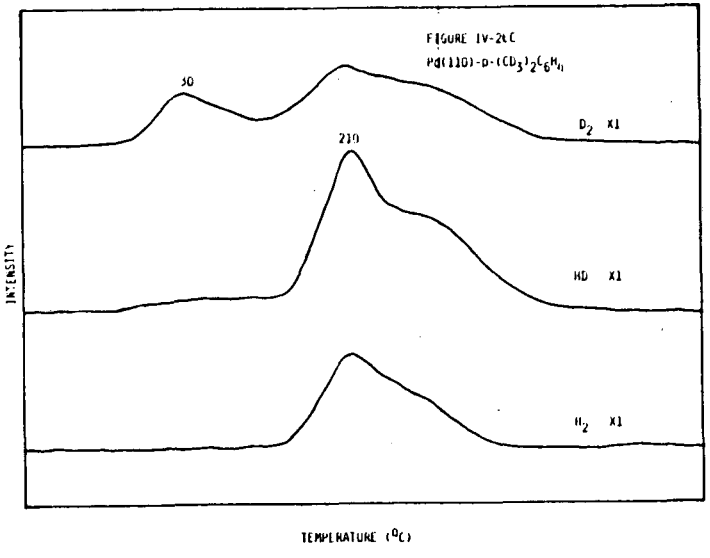
FIGURE IV-26C
Pd(110)-p-(CD3)2C6H4
50
D2 X1
210
HD X1
H2 X1
INTENSITY
TEMPERATURE (°C)

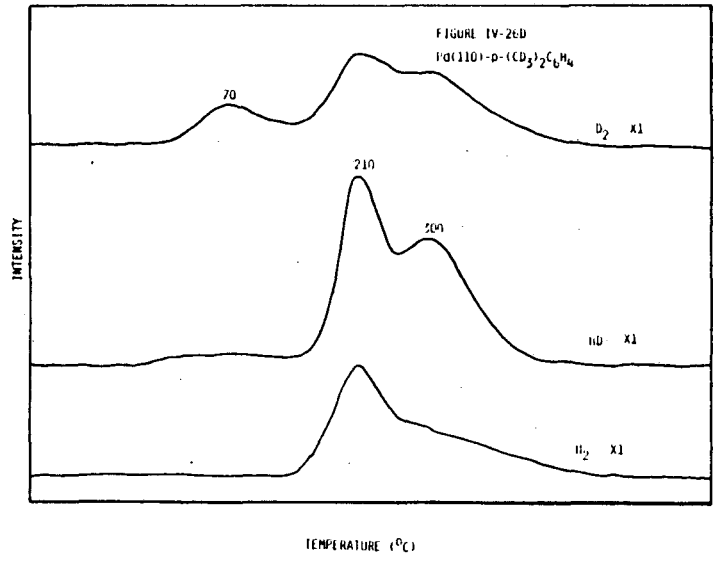
FIGURE IV-26D
Pd(110)-p-(CD3)2C6H4
70
D2 X1
210
500
HD X1
H2 X1
INTENSITY
TEMPERATURE (°C)

XBL 846-2156

Increasing the exposure resulted in a decrease in the amount of HD in the low temperature maximum (see Figures IV-26B through IV-26D). Similar trends were observed in the thermal desorption spectrum of meta $(CD_3)_2C_6H_4$. At low exposures (1.0 L), two H_2 maxima were observed, at 125°C and 280°C; three HD maxima were observed, at 20°C, 125°C, and 280°C; and three D_2 maxima were observed, at 20°C, 165°C, and 280°C (see Figure IV-27A). Deuterium was observed in three maxima, at 80°C, 180°C, and 290°C, at an exposure of 4.0 L. HD was observed in a weak broad maximum at ~80°C, and also in two high temperature maxima, at 190°C, and 290°C. Two hydrogen maxima were observed, at 180°C, and 290°C (see Figure IV-27D). Chemisorption of ortho $(CD_3)_2C_6H_4$ also yielded D_2, HD, and H_2 during the thermal desorption experiment. At low exposures (1.0 L), H_2 was observed in two high temperature maxima, at 180°C, and 270°C; HD was observed in three maxima, at 20°C, 170°C, and 270°C; and D_2 also desorbed in three maxima, at 20°C, 160°C, and 270°C (see Figure IV-28A). At higher exposures (3.0 L), a similar spectrum was observed, with increased intensity in all of the maxima (see Figure IV-28B and IV-28C).

Three H_2 thermal desorption maxima were observed from chemisorbed 1,3,5-trimethylbenzene, at 1.0 L, on Pd(110). These maxima were a weak broad maximum from 45°C to 100°C, and two intense maxima, at 170°C, and 320°C (see Figure IV-29A). At higher exposures these three maxima were also observed (see Figures IV-29B and IV-29C).

Figure IV-27. Thermal desorption spectra of the selectively labeled metaxylene $(CD_3)_2C_6H_4$ exhibited partial regioselective C-H bond scission on Pd(110). The fraction of HD desorbing at low temperatures decreased with exposure. Four thermal desorption spectra, at exposures of 1.0 L (A), 2.0 L (B), 3.0 L (C), and 4.0 L (D) are shown here.

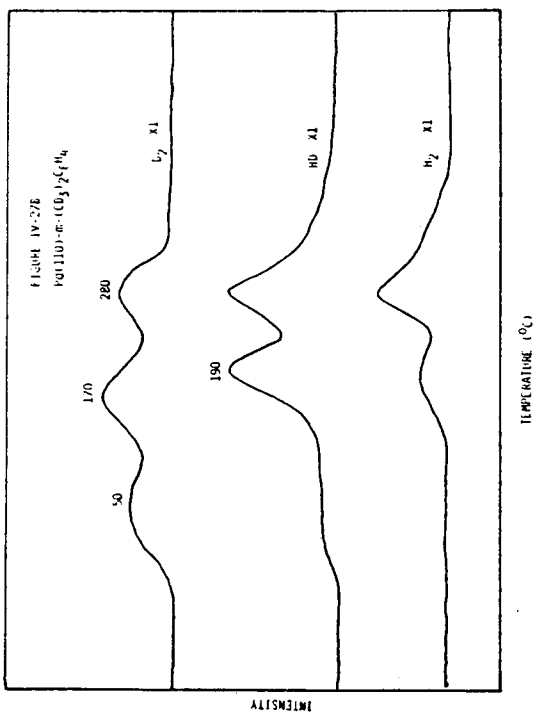
INTENSITY
TEMPERATURE (°C)
50
170
280
190
D_2 X1
HD X1
H_2 X1

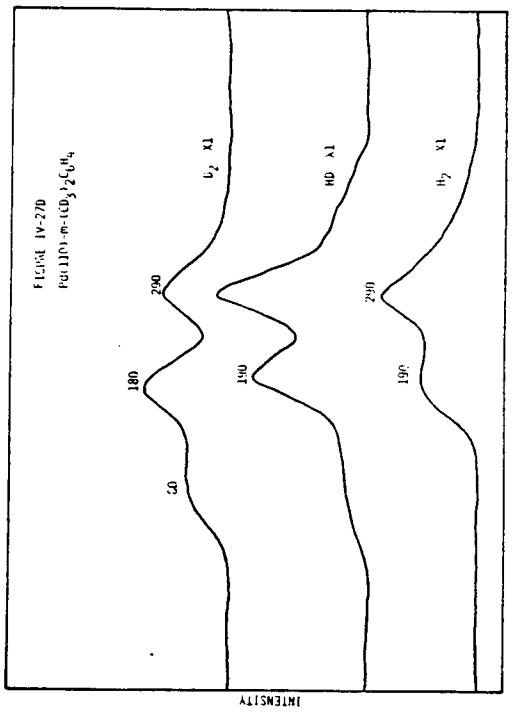
INTENSITY
TEMPERATURE (°C)
50
180
290
190
290
190
D_2 X1
HD X1
H_2 X1

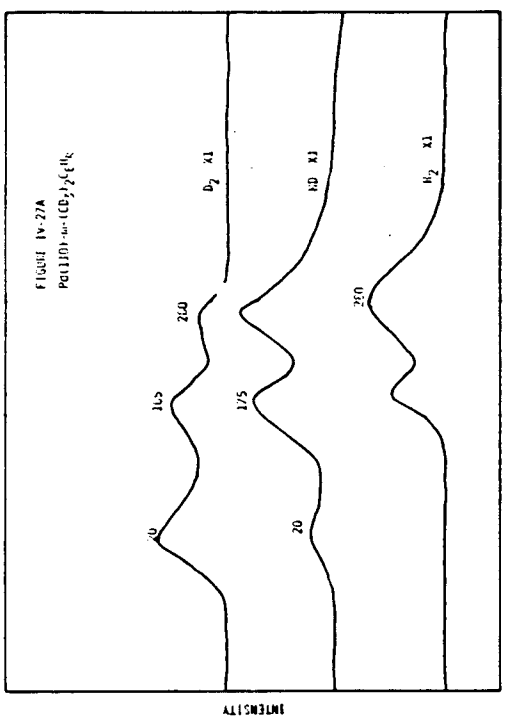
INTENSITY
TEMPERATURE (°C)
0
165
250
175
20
250
D_2 X1
HD X1
H_2 X1

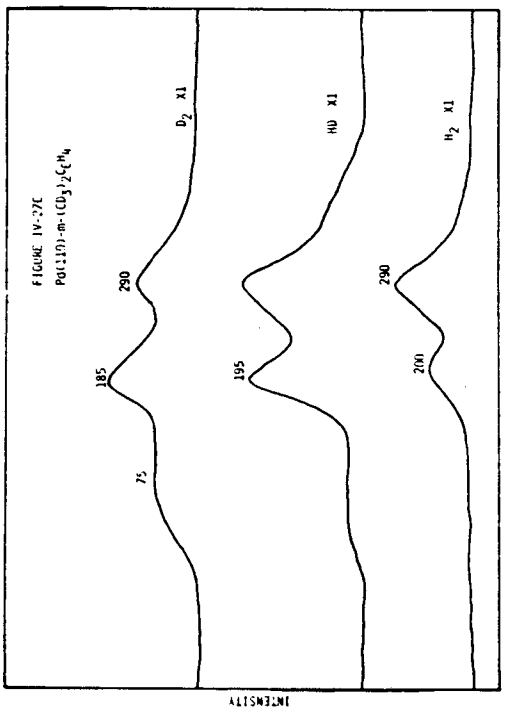
INTENSITY
TEMPERATURE (°C)
75
185
290
195
290
200
D_2 X1
HD X1
H_2 X1

XBL 846-2155

Figure IV-28. HD and D_2 were found to populate the central maximum, T_{max} = ~180°C, in the thermal desorption spectrum of the selectively labeled oxthoxylene $(CD_3)_2C_6H_4$ from Pd(110). Four orthoxylene exposures are shown here, 1.0 L (A), 2.0 L (B), 3.0 L (C), and 4.0 L (D).

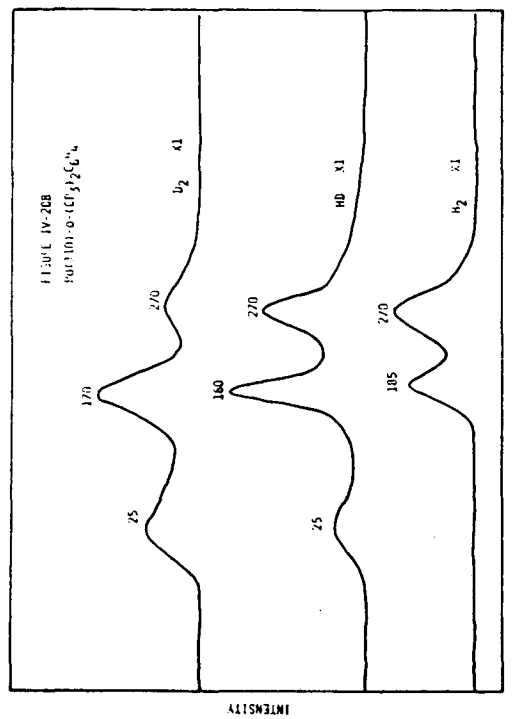
FIGURE IV-2CB
Pd(110)-o-(CD3)2C6H4
25
170
270
D2 X1
160
270
HD X1
185
270
H2 X1
INTENSITY
TEMPERATURE (°C)

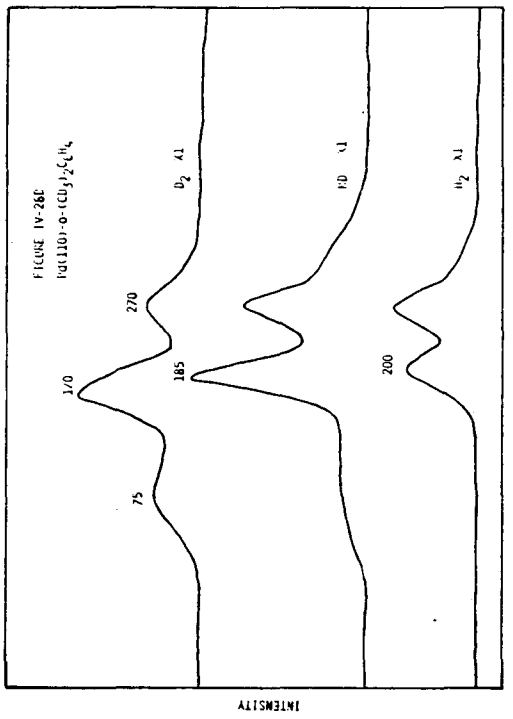
FIGURE IV-26C
Pd(110)-o-(CD3)2C6H4
75
170
270
D2 X1
185
HD X1
200
H2 X1
INTENSITY
TEMPERATURE (°C)

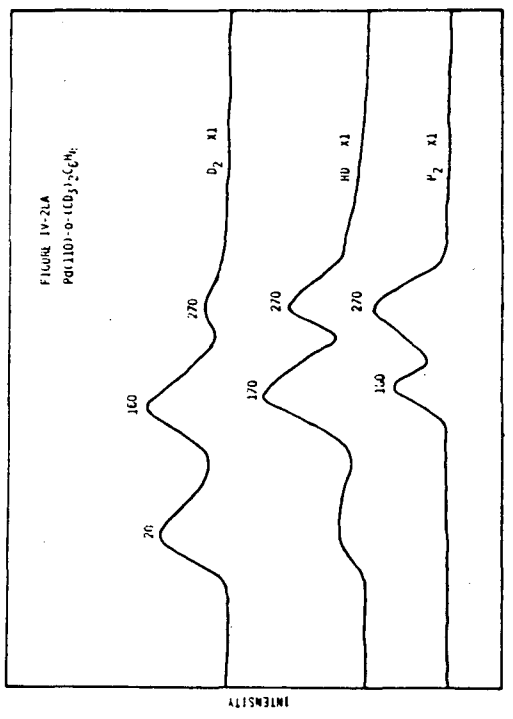
FIGURE IV-2AA
Pd(110)-o-(CD3)2C6H4
20
160
270
D2 X1
170
270
HD X1
140
270
H2 X1
INTENSITY
TEMPERATURE (°C)

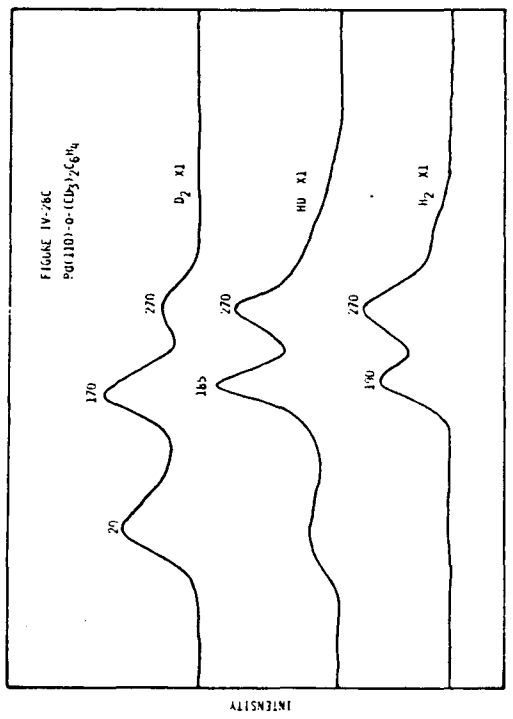
FIGURE IV-26C
Pd(110)-o-(CD3)2C6H4
20
170
270
D2 X1
165
270
HD X1
190
270
H2 X1
INTENSITY
TEMPERATURE (°C)

XBL 846-2154

Figure IV-29. Thermal desorption of 1,3,5-trimethylbenzene from Pd(110) exhibits three H_2 maxima, a weak maximum at ~60°C and two strong maxima at 170°C and 320°C. At all three exposures shown in the spectra here, 1.0 L (A), 2.0 L (B), and 3.0 L (C), all three H_2 maxima were observed.

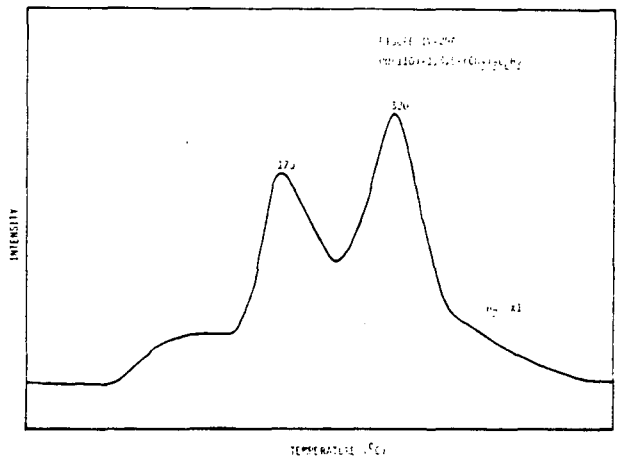
INTENSITY
320
370
TEMPERATURE (°C)

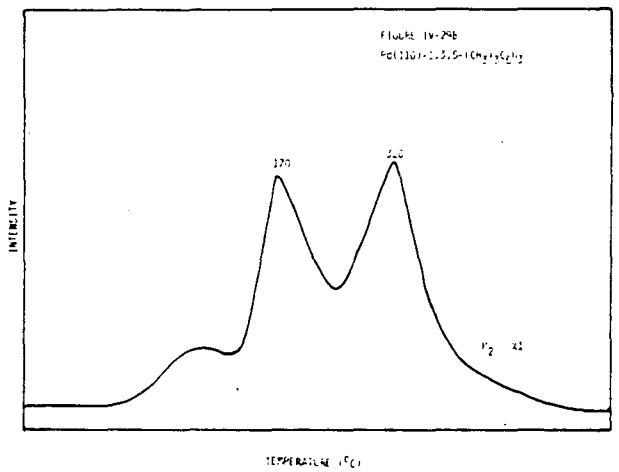
INTENSITY
370
320
TEMPERATURE (°C)

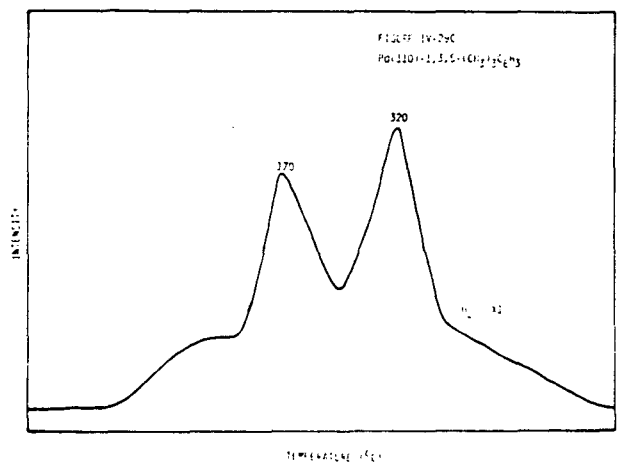
INTENSITY
320
370
TEMPERATURE (°C)

XBL 846-2122

DISCUSSION

On all three low Miller-index surfaces of palladium, the fraction of irreversible chemisorption increased with methyl substitution. Benzene exhibited the largest fraction of reversible chemisorption. Chemisorption of benzene will be discussed first, followed by toluene and the di- and trimethylsubstituted benzenes.

The results of the thermal desorption experiments imply at least two chemisorption states of benzene: a strongly and irreversibly bound state and at least one more weakly bound reversible state. On all three surfaces multiple benzene thermal desorption maxima were observed. On Pd(111), sequential adsorption of C_6H_6 and C_6D_6 was performed. In the ensuing thermal desorption experiments, the ratio of C_6H_6:C_6D_6 was experimentally indistinguishable for the low and high temperature regions. This sequential labeling procedure also failed to establish differentiable states on Pd(100) and Pd(110). Differentiable benzene chemisorption states have been observed on Pt(111).[3] On Pd(111), H-D exchange was observed for mixtures of C_6H_6:C_6D_6. Exchange was observed only in the high temperature benzene thermal desorption maximum. None was observed in the low temperature maximum. The occurrence of exchange in the high temperature maximum suggests that the orientation of the chemisorbed benzene is important for exchange to occur. If the genesis of the high temperature maximum is a π-bound benzene, then this orientation may provide proper geometry for H-D exchange to occur. Recently, high resolution electron energy loss spectroscopy of benzene on Pd(111) has

been reported.[5] These studies suggest a π-bound benzene species. Further evidence for H-D exchange involving this species was presented.

Reversible desorption of benzene and decomposition are competing processes on single-crystal surfaces of palladium. This competition is more evident when the surface is modified by the presence of adatoms such as silicon, phosphorus, sulfur, and chlorine. Adatoms on palladium single-crystal surfaces favor reversible desorption of benzene. It has been suggested that on (111) surfaces, adatoms adsorb in threefold hollows. These sites appear to be involved in the irreversible chemisorption of benzene.

The chemisorption of toluene on these surfaces was found to be more irreversible than the chemisorption of benzene. Although the initial interaction with the surface is through the π-system of the ring, there also must be significant interaction with the methyl carbon-hydrogen bonds. The thermal desorption of $CD_3C_6H_5$ on all three surfaces exhibited partial but not complete regioselective carbon-hydrogen bond scission. Lack of hydrogen at low temperatures suggests that, for the most part, aliphatic carbon-hydrogen bond scission occurs first. The presence of HD in the low temperature maximum could be the result of the reaction of deuterium with background hydrogen. An alternative explanation is that limited intramolecular exchange between the alaphatic and aromatic carbon-hydrogen bonds occurs prior to desorption of hydrogen from the surface. At higher exposures, the yield of HD in the low temperature maximum decreased. This change may be indicative of a change in

orientation of the chemisorbed molecule. At low exposures, toluene is most probably bound in a π fashion, and at high coverages the primary interactions may be through the methyl group.

The thermal desorption spectrum of the other methylsubstituted benzenes also gives insights into the mechanism of carbon–hydrogen bond scission on palladium single-crystal surfaces. The thermal desorption spectrum of the selectively labeled para- and metaxylene on Pd(111) indicates the primary interaction of a single methyl group. Orthoxylene, however, may interact through both methyl groups. The close proximity of both methyl groups may lead to the formation of a surface metallocycle. The formation of surface metallocycles has been postulated to occur in other hydrocarbon systems.[6]

It is interesting to compare the chemisorption of toluene on the single-crystal surfaces of nickel, palladium, and platinum. Complete regioselective carbon–hydrogen bond scission was observed on both Ni(100) and Ni(111), whereas only partial regioselective carbon–hydrogen bond scission was observed on Pd(111) and Pd(100). A sharp contrast exists between the chemisorption of toluene on Ni(110) and on Pd(110). On Ni(110) a single hydrogen maximum was observed at 150°C, while on Pd(110) three maxima were observed, at 15°C, 170°C, and 275°C. Nickel surfaces generally are more reactive then palladium surfaces; that is, chemisorption of unsaturated hydrocarbons tends to be more irreversible. This difference in reactivity may be enhanced on this "super-stepped" surface, resulting in a single hydrogen thermal desorption maximum on Ni(110).

The chemisorption of toluene on platinum single-crystal surfaces is similar to that of palladium. Chemisorption of toluene was not investigated on Pt(110). On the other two low Miller-index surfaces, only partial regioselective bond scission was found to occur. The trend appers to be decreased regioselectively on the atomically flat surfaces going down the column from nickel to platinum.

REFERENCES

1. P. N. Rylander, Catalytic Hydrogenation over Platinum Metals, Academic Press, New York, 1967, p. 308.
2. C. M. Friend, Ph.D. Thesis, University of California Berkeley, 1981, p. 32.
3. M. C. Tsai, Ph.D. Thesis, University of California Berkeley, 1982, p. 41.
4. P. Hoffman, K. Horn, and A. M. Bradshaw, Surf. Sci. 1981, 108, L260.
5. W. T. Tysoe, Ph.D. Thesis, Cambridge University, 1982, p. 100.
6. L. L. Kesmodel, G. D. Waddell, and J. A. Gates, Surf. Sci. 1984, 138, 464.
7. R. M. Wexler, Ph.D. Thesis, University of California Berkeley, 1983, p. 92.

V. SILANE SURFACE CHEMISTRY OF PALLADIUM

Chemisorption of cycloalkenes on transition metal surfaces are followed by a dehydrogenation process[1] that often gives chemisorbed C_nH_n species, for example, cyclohexene⟶benzene[1-3] and cyclooctadiene⟶cyclooctatetraene. Because these transformations are facile, it appeared that it might be possible to effect dehydrogenation of organosilanes as routes to compounds with Si-C bonds of multiple orders. With platinum and nickel surfaces, no dehydrogenation occurred, only gross decomposition of the organosilanes.[4] Palladium, however, has furnished dehydrogenation synthesis of silaelthylenes, silabenzene, and what appears to be silacyclobutadiene.

Compounds containing multiple bonds to silicon have been reported since the inception of organasilicon chemistry. Many of these earlier reports were inaccurate and in most cases were the result of the lack of knowledge about the polymeric nature of many organosilanes. A brief historical survey has been published by Gusel'nikov and Nametkin.[5]

Early attempts to dehydrogenate cyclic organosilicon compounds over transition metal catalysts such as palladium and platinum were unsuccessful.[6] West reported that silacyclohexenes did not dehydrogenate to form silabenzenes over palladium or platinum. The only chemistry observed was thermal cracking to hydrogen and olefins at temperatures greater than 500°C. This temperature is well above the normal operating rate of transition metal catalysts, and cracking of organosilanes should be expected.

Only in recent times have compounds containing silicon–carbon multiple bonds been reported. Schaefer[7] recently commented that the works of Chapmond and Barton[8] and Shechter[9] were the "first physical and chemical characterization of a silicon–carbon bond." He also asserted that these works transformed the preception of silaethylenes from the "unstable intermediates to reasonably well understood chemical compounds." However, Gusel'nikov[10] earlier reported the formation of silaethylenes from the pyrolysis of silacyclobutanes. The controversy over who first characterized the silicon–carbon multiple bond is outside the scope of this thesis and is better left in the hands of chemical historians. What is important is the fact that the existence of the class of compounds has been established.

There has been reported a variety of routes to these highly reactive unsaturated organosilanes. Only a few of the routes will be reviewed here. The reader is referred to other reviews for a more complete picture of this chemistry.[11] As mentioned earlier, thermal decomposition of monosilacyclobutanes[12] yields silaethylenes. A typical reaction is shown in equation one.

(1) 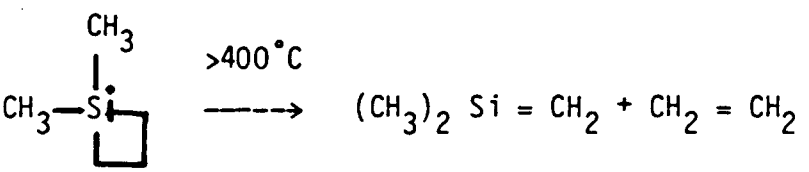

Silaethylenes are highly reactive and usually react to form dimers in the absence of a chemical trapping agent. Two isomers of these dimers

are possible: one with "head-to-tail" bonding as shown in (1) below, and the other with "head-to-head" bonding, as shown in (2) below:

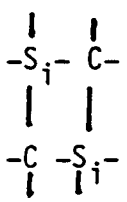

(1)

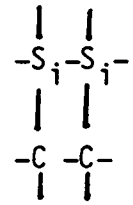

(2)

Isomer (1) is the most thermodynamically stable and is the species observed in most cases.

Acyclicorganosilanes have also been found to undergo transformations to unsaturated organosilanes under pyrolysis conditions. The following scheme was proposed for the thermal decomposition of tetramethylsilane by Fritz, Grobe, and Kummer:[13]

a) $(CH_3)_4Si \xrightarrow{\Delta} (CH_3)_3Si + CH_3\cdot$

b) $CH_3\cdot + (CH_3)_4Si \longrightarrow (CH_3)_3SiCH_2\cdot + CH_4$

c) $(CH_3)_3SiCH_2\cdot \longrightarrow [(CH_3)_2Si = CH_2] + CH_3\cdot$

Recently, using pyrolysis techniques, the aromatic compound silabenzene and substituted silabenzenes have been prepared.[14] The reaction involved the pyrolysis of substituted alkylsilacyclohexadienes. A typical reaction is shown below.

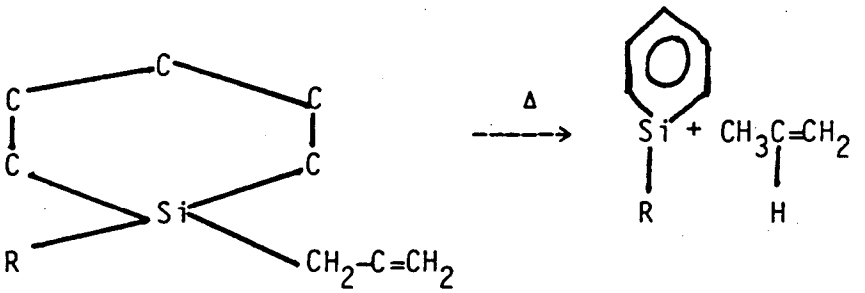

Photolysis of organosilanes has also led to the formation of silicon–carbon multiple bonds. Among the compounds known to form unsaturated organsilanes under photolysis conditions are 1,1-diphenyl-1-silacyclobutane[15] (formed 1,1-dephenyl-1-silaethylene), methylsilane[16] (formed silaethylene), tetramethylsilane[17] (formed 1,1-dimethylsilaethylene), and hexamethyldisilane[18] (formed 1,1-dimethylsilaethylene).

A variety of physical techniques have been used to characterize species containing silicon–carbon multiple bonds. The infrared spectrum of species containing silicon–carbon double bonds has been reported. In the spectrum of 1,1-dimethylsilaethylene, the Si = C double-bond stretching vibration has been assigned to the vibrational mode occurring at ~1000 cm^{-1}.[19] Mass spectrometry has been useful in the characterization of many unsaturated organosilicon compounds. Silabenzene was characterized by the observation of 94 amu in the vacuum pyrolysis of 1 allyl-silacyclohexadiene.[20] Photoelectron spectroscopy has also proved useful in the characterization of these species.[21]

The first compound, containing a silicon–carbon double bond, that was stable at room temperature has been reported by Brook et al.[22] The compound (3)

Me_3Si

$Si = C$ $Osi(CH_{23}$

Me_3Si

was characterized by I.R. NMR, mass spectrometry, and x-ray crystallography. The silicon-carbon double bond distance was found to be 1.764 Å.

It is clear that species containing silicon-carbon multiple bonds do indeed exist and can be prepared by a variety of routes. The chemistry of a variety of organosilanes on palladium single-crystal surfaces will be described in the next section, demonstrating a new route to these compounds.

RESULTS

Tetramethylsilane on Pd(110) desorbed fully and intact at -50°C (see Figure V-1), analogous to neopentane on Pd(110), which also quantitatively desorbed with a thermal desorption maximum, T_{max}, of ~60°C. In sharp contrast, trimethylsilane, after adsorption at -135°C, underwent two competing processes: (a) reversible desorption with a maximum rate at -20°C, and (b) dehydrogenation to form $(CH_3)_2Si = CH_2$, which desorbs with maximum rates at -40°C, and 90°C. The surface was free from silicon and carbon after the thermal desorption experiments, the results of which are shown in Figure V-2. The dehydrogenation process was accompanied by H_2 desorption, which also exhibited maxima at -40°C, and 90°C. Minor dimerization of silaethylene also occurred; it was characterized by a broad T_{max} at

Figure V-1. Chemisorption of tetramethylsilane on Pd(110) was found to be fully reversible. The thermal desorption spectrum shown here exhibits a single tetramethylsilane thermal desorption maximum at -50°C.

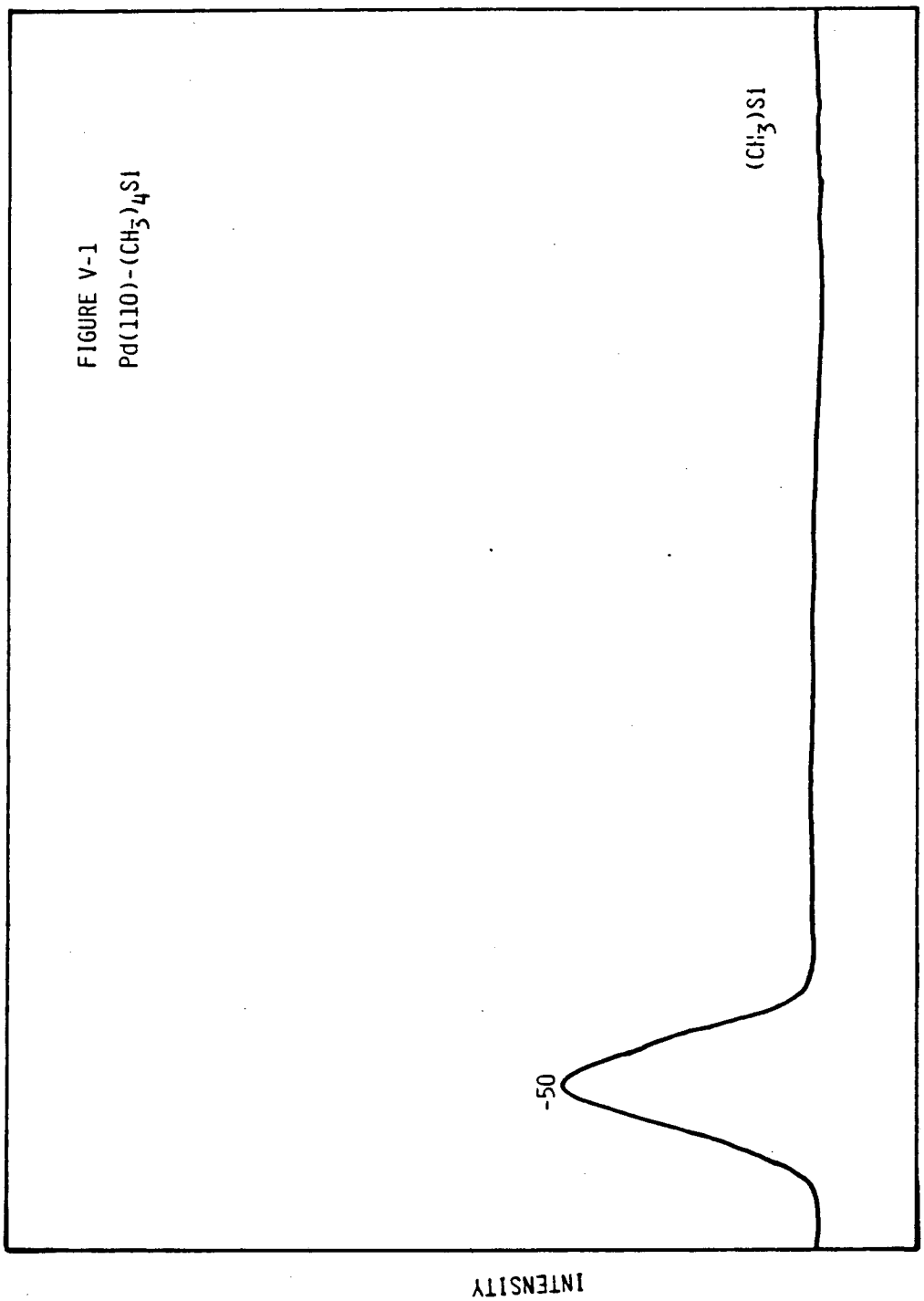

XBL 845-2058

Figure V-2. Chemisorbed trimethylsilane, $(CH_3)_3SiH$, was found to undergo several processes upon thermal desorption from Pd(110). Molecular desorption of $(CH_3)_3SiH$ was observed, with a maximum at -20°C. Dehydrogenation to form 1,1-dimethylsilaethylene and dimerization of this species was also observed.

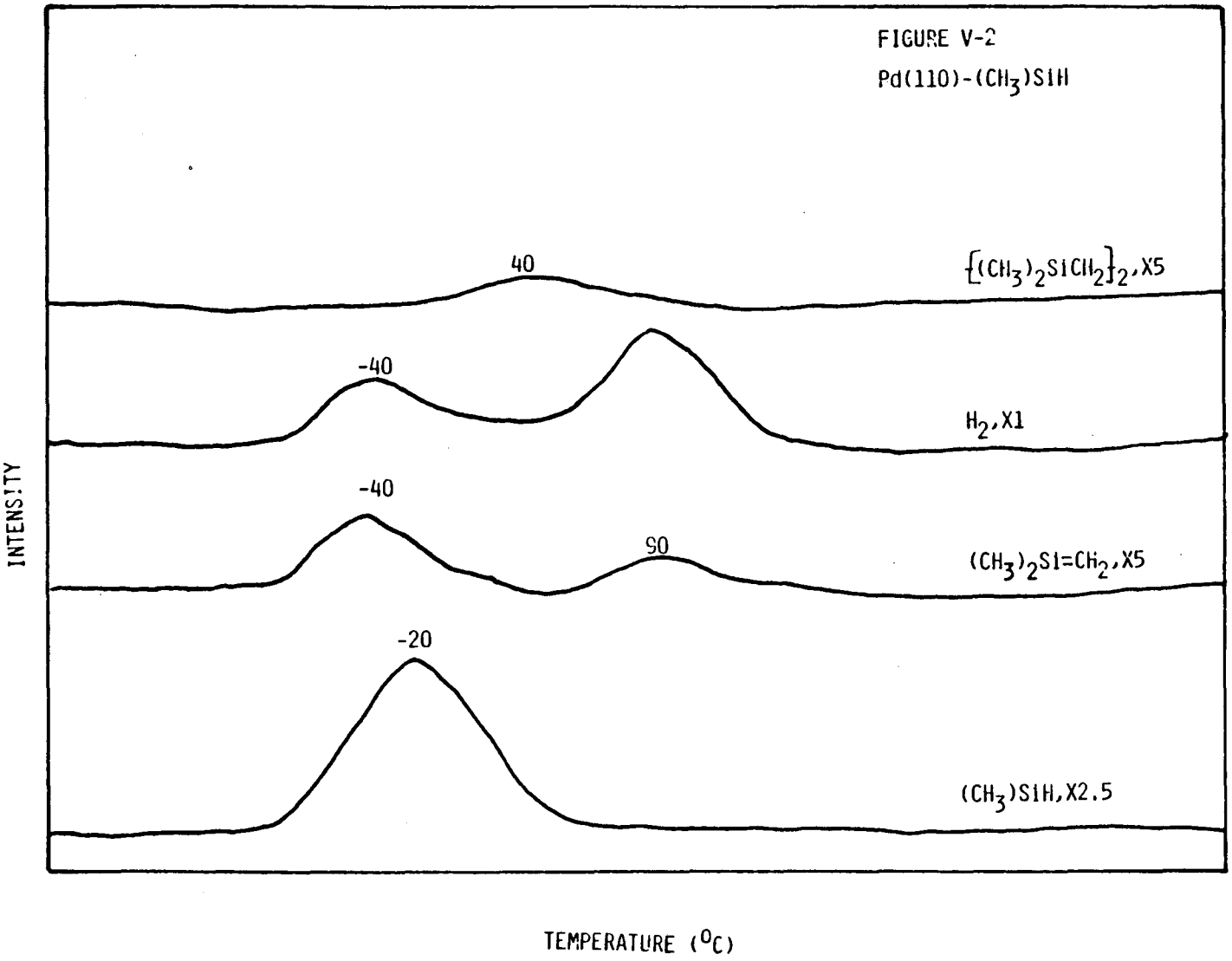
FIGURE V-2
Pd(110)-(CH3)SiH
40
{(CH3)2SiCH2}2,X5
-40
H2,X1
-40
90
(CH3)2Si=CH2,X5
-20
(CH3)SiH,X2.5
INTENSITY
TEMPERATURE (°C)

XBL 845-2059

~40°C. An unexpected feature here was desorption of silaethylene, because most alkenes and alkynes irreversibly chemisorb on clean transition metal surfaces. Consistent with the organosilicon surface chemistry, we have found acetylene and ethylene to at least partially undergo reversible chemisorption on Pd(111), Pd(100), and Pd(110).

Consistent with the chemistry observed on Pd(110), trimethylsilane was also found to undergo dehydrogenation on Pd(100). Trimethylsilane was adsorbed at -85°C, and the following products were observed in the subsequent thermal desorption experiment: (a) $(CH_3)_3SiH$ desorbing intact with a T_{max} at -25°C; (b) H_2 with a T_{max} at 90°C; and (c) $(CH_3)_2 Si = CH_2$ with a T_{max} at 90°C (see Figure V-3). Tetramethylsilane was also found to quantitatively desorb from Pd(100).

Chemical displacement reactions have been shown to be useful in probing the dehydrogenation process occurring on transition metal surfaces.[4] For example, cyclohexene adsorbed at 25°C on Pt(111) followed by exposure to a displacing agent, trimethylphosphine, results in desorption of the dehydrogenation product, benzene. This result demonstrates that dehydrogenation of cyclohexene to benzene is occurring at room temperature. Displacement of 1,1-dimethylsila-ethylene, $(CH_3)_2 Si = CH_2$, from a surface state formed by adsorption of trimethylsilane, $(CH_3)_3SiH$, on Pd(110) at 25°C with trimethylphosphine, $(CH_3)_3P$. On exposing the crystal to $(CH_3)_3P$, along with 1,1-dimethylsilaethylene, there was immediate displacement of the dimer and trimethylsilane (see Figure V-4).

Figure V-3. Thermal desorption of trimethylsilane from Pd(100) yielded the dehydrogenation product, 1,1-dimethylsilaethylene. Hydrogen and molecular desorption were also observed.

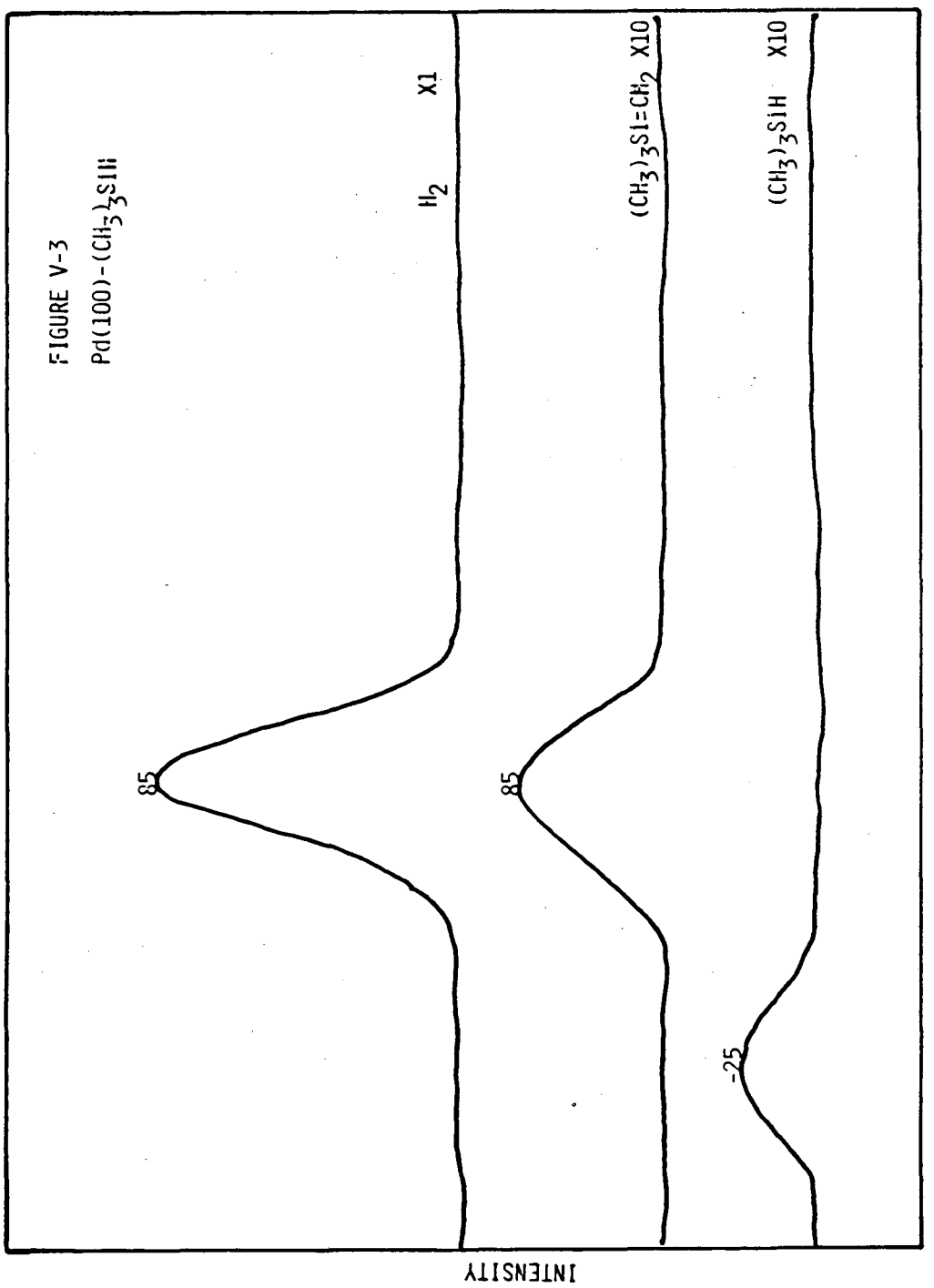
FIGURE V-3
Pd(100)-(CH3)3SiH
H2 X1
(CH3)3Si=CH2 X10
(CH3)3SiH X10
85
85
-25
INTENSITY
TEMPERATURE (°C)

XBL 845-2060

Figure V-4. Chemical displacement of 1,1-dimethylsilaethylene from trimethylsilane chemisorbed on Pd(110) was affected by trimethylphosphine. Along with 1,1-dimethylsilaethylene, its dimer and trimethylsilane were observed in the reaction at 25°C.

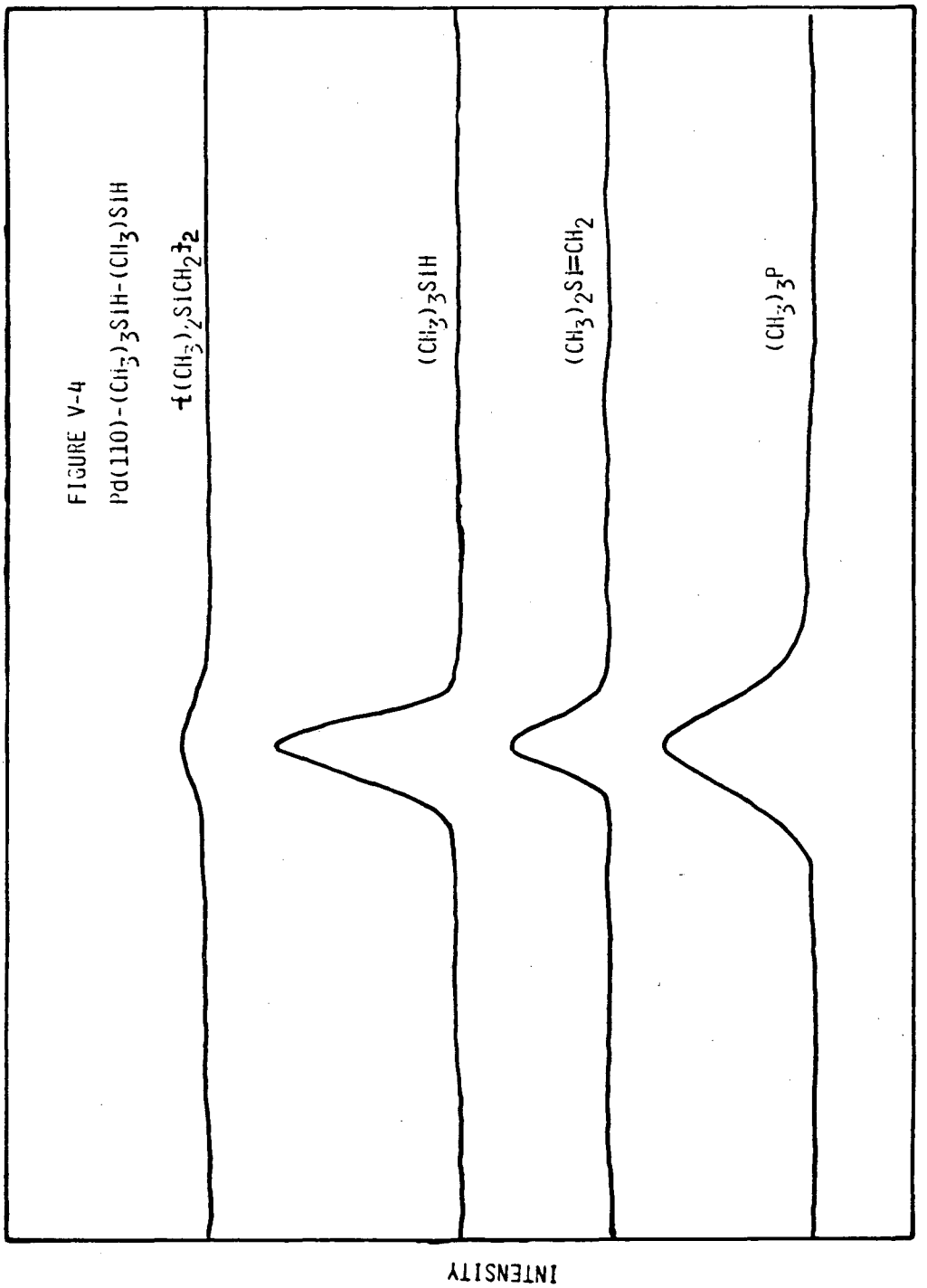
FIGURE V-4
Pd(110)-(CH3)3SiH-(CH3)SiH
↑(CH3)2SiCH2↑2
(CH3)3SiH
(CH3)2Si=CH2
(CH3)3P
INTENSITY
TIME

XBL 845-2061

1,1-dimethylsilane was also produced in the thermal desorption experiments with $(CH_3)_3SiOSi(CH_3)_3$, $(CH_3)_3SiNHSi(CH_3)_3$, and $(CH_3)_3SiN_3$ on Pd(110). All three compounds also exhibited paritially reversible chemisorption. In the azide system an additional and major product was $[(CH_3)_2SiNiN(CH_3)]_2$.

Silacyclobutane displayed complex Pd(110) surface chemistry. After adsorption at -135°C, silanes 1-4 below were observed in the subsequent thermal desorption experiment, with maxima at ~65°C, 65°C, 50°C, and 70°C, respectively.

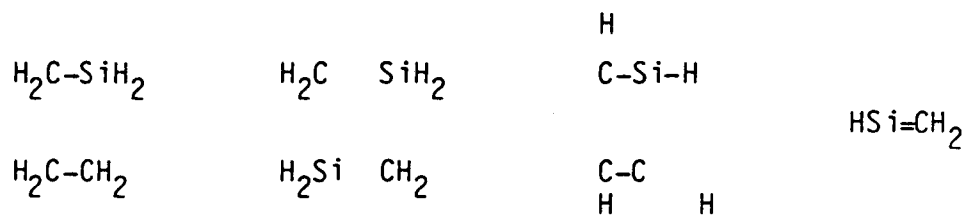

1 2 3 4

The thermal desorption spectrum is shown in Figure V-5. Ethylene and hydrogen were also observed, each with a similar T_{max} of 60-80°C. All of these species were also observed in a chemical displacement reaction at 25°C with $P(CH_3)_3$. Silacyclobutadiene is a new compound, and its characterization must be considered tentative in that it is based solely on mass spectrometric data. The parent ion was less intense than the parent-minus-one ion, as expected for a species with an Si-H bond. Ostensibly, silaethylene was the precursor to the dimer 2. Consistent with this presumption, the ratio of 4 to 2 increased when the heating rate was increased from 25°C/sec to 75°C/sec.

Figure V-5. In the thermal desorption experiment for Pd(110)-silacyclobutane (initial adsorption of -135°C), there were detectably six molecules that desorbed. Shown are the mass spectra intensities of the ion characteristic of these species, with the exception of ethylene (ethylene desorbed at ~60-80°C). In these plots, mass 2 is for H_2, mass 67 is for silacyclobutadiene, mass 86 is for $[SiH_2CH_2]_2$, and mass 44 is for the parent ion of $H_2Si{=}CH_2$ and a fragmentation ion for a silacyclobutane. The low temperature (-65°C) maximum is ascribed to silacyclobutane reversibly desorbing and the high temperature (+75°C) maximum to silaethylene. In this experiment, the heating rate was 75°C/sec. In an experiment performed with a heating rate of 25°C/sec, more dimer $[SiH_2CH_2]_2$ and less silaethylene were formed.

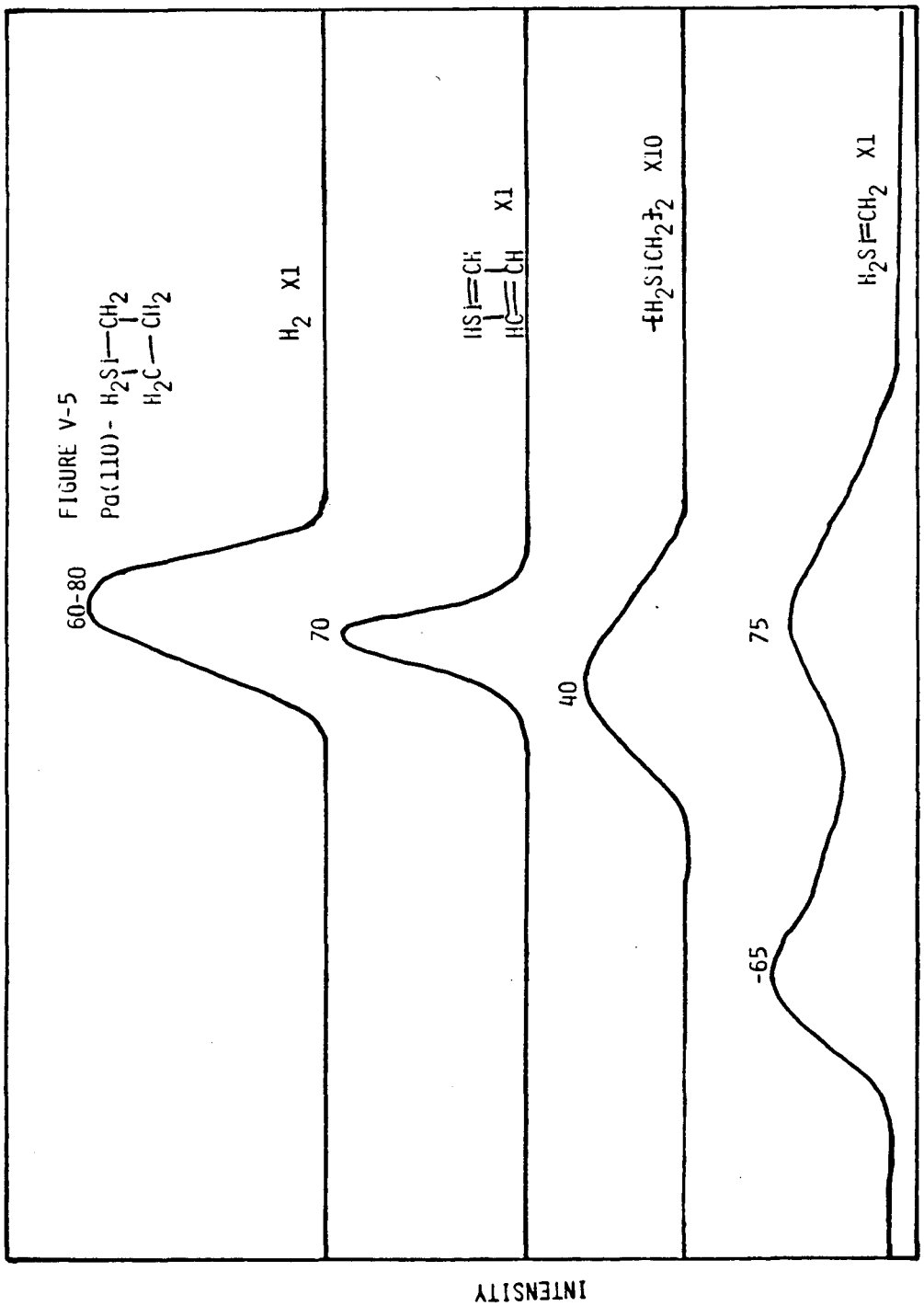
FIGURE V-5
Pd(110)- $H_2Si(CH_2)_2$
60-80
H_2 X1
70
$HSi{=}CH$ $HC{=}CH$ X1
40
$+H_2SiCH_2\frac{1}{2}_2$ X10
75
$H_2Si{=}CH_2$ X1
-65
INTENSITY
TEMPERATURE (°C)

XBL 845-2062

The dehydrogenation of cyclic olefins to form aromatic sytems has been studied on both Ni and Pt single-crystal surfaces. Pd(110) has also afforded dehydrogenations of cyclic olefins. Cyclohexene, when adsorbed on Pd(110) at -135°C, yielded benzene, with a T_{max} at 220°C (see Figure V-6). It was also observed that cyclic hydrocarbons containing a heteroatom undergo dehydrogenation to form aromatic systems. Piperidine adsorbed on Pd(110) yielded pyridine in the thermal desorption experiment. Two pyridine maxima were observed, one 115°C, and the other at 155°C (see Figure V-7). Consistent with the behavior of cyclohexene and pyridine, the organosilane silacyclohexane was dehydrogenated on Pd(110). When adsorbed at -135°C, silacyclohexane underwent two competing surface reactions, reversible desorption (T_{max} = -25°C) and dehydrogenation to form silabenzene (T_{max} = 90°C, and 190°C). Two H_2 thermal desorption maxima were observed, at 15°C and 190°C (see Figure V-8). Silabenzene was not displaced by $P(CH_3)_3$ from the surface generated from silacyclohexane adsorbed on Pd(110) at temperatures of 25°C-70°C.

Hexamethyldisilane adsorbed on Pd(100) exhibited molecular desorption, decomposition, and formation of 1,1-dimethylsilaethylene. Two hydrogen thermal desorption maxima were observed, at 90°C, and 165°C. A single hexamethyldisilane maximum was observed at -15°C. 1,1-dimethylsilaethylene formation was observed, with two desorption maxima, at -15°C, and 80°C (see Figure V-9).

Figure V-6. Dehydrogenation of cyclohexene to benzene is observed on Pd(110). The thermal desorption spectrum of chemisorbed cyclohexene, 1.0 L, from Pd(110) shows the presence of two hydrogen thermal desorption maxima, at 40°C and 220°C. The origin of the low temperature maximum is probably from the hydrogen formed in the dehydrogenation reaction. The hydrogen desorbing at high temperature is derived from the decomposition of benzene.

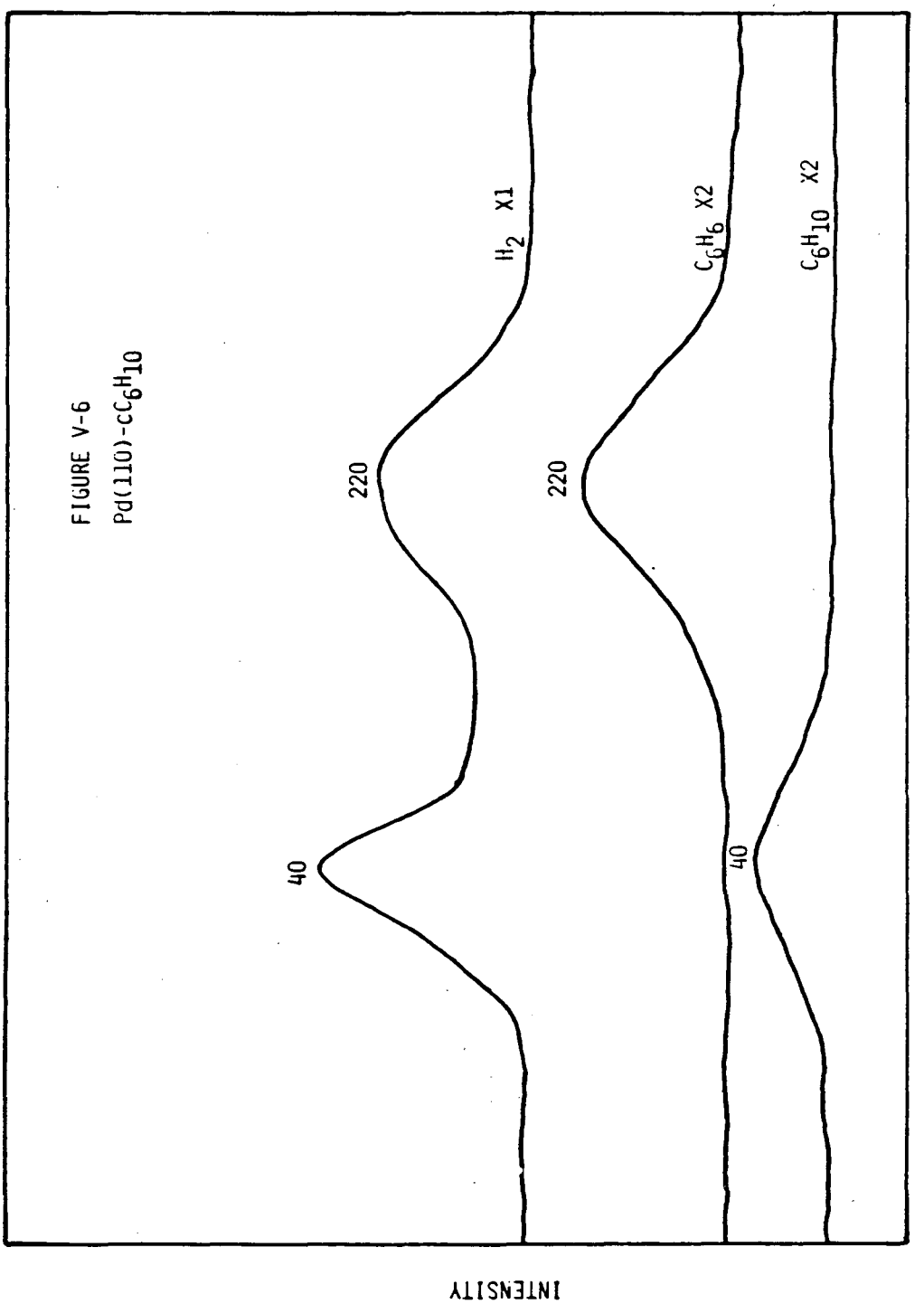
FIGURE V-6
Pd(110)-cC_6H_{10}
H_2 X1
C_6H_6 X2
C_6H_{10} X2
220
220
40
40
INTENSITY
TEMPERATURE (°C)

XBL 845-2063

Figure V-7. Pyridine formation was observed in the thermal desorption spectrum of piperidine from Pd(110). Desorption of intact piperidine and hydrogen was also observed in this experiment. A piperidine exposure of 1.0 L was used.

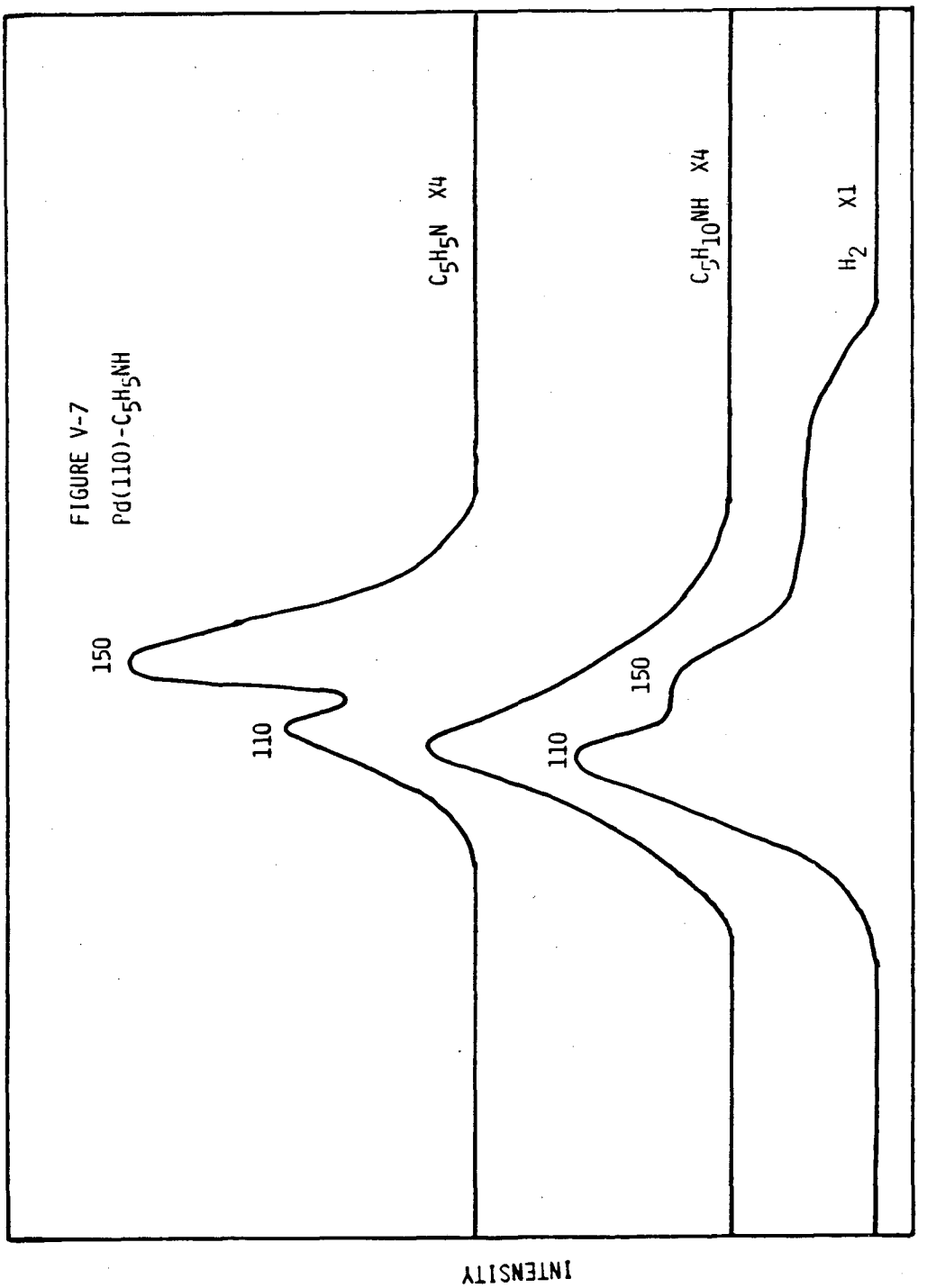
FIGURE V-7
Pd(110)-C5H5NH
C5H5N X4
C5H10NH X4
H2 X1
150
110
150
110
INTENSITY
TEMPERATURE (°C)

XBL 845-2064

Figure V-8. Formation of the aromatic molecule silabenzene, SiC_5H_6, was observed in the thermal desorption of silacyclohexane from Pd(100). At an exposure of 1.0 L, both hydrogen and silacyclohexene maxima were also observed in the thermal desorption spectrum.

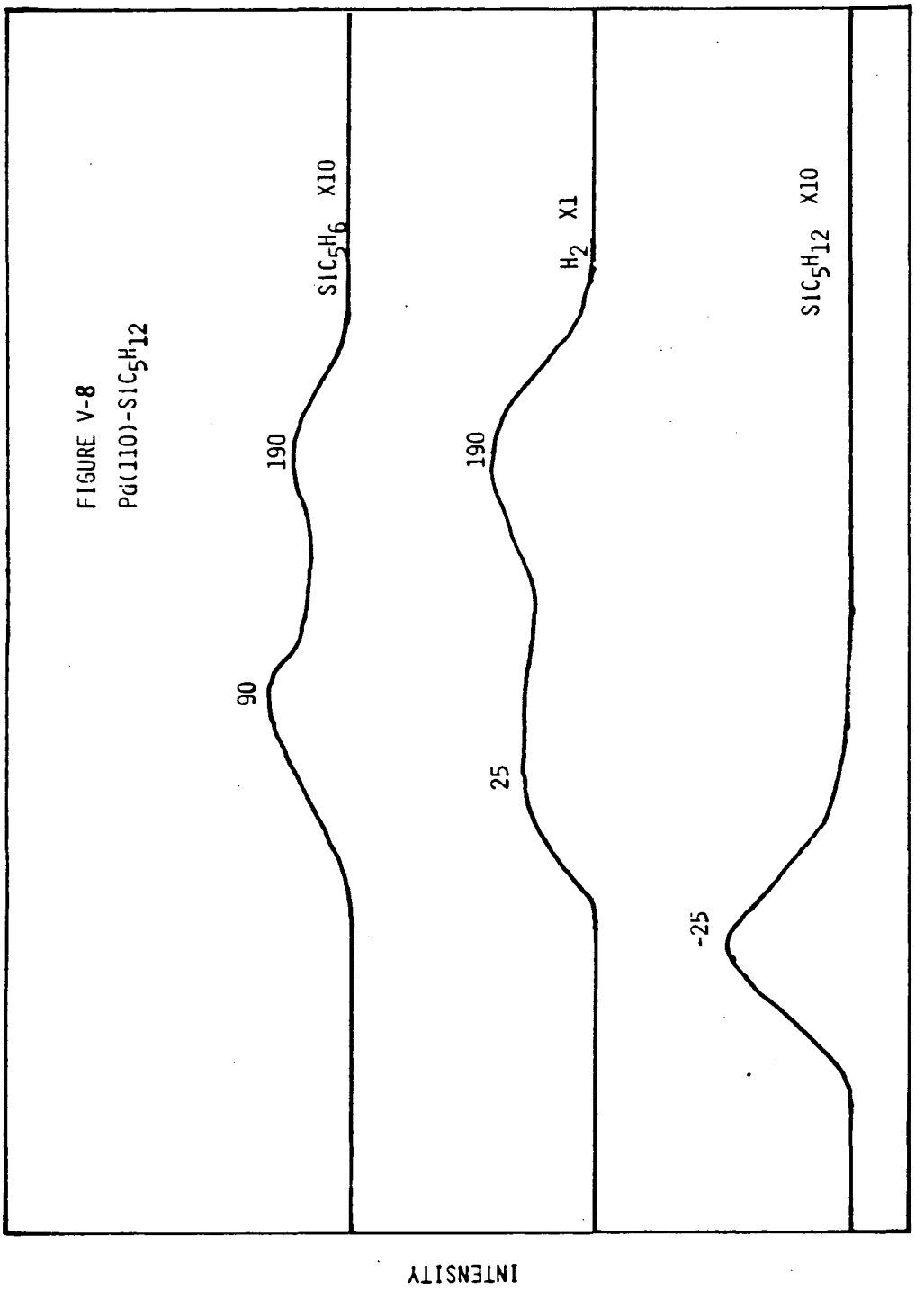
FIGURE V-8
Pd(110)-SiC5H12
SiC5H6 X10
190
90
H2 X1
190
25
SiC5H12 X10
-25
INTENSITY
TEMPERATURE (°C)

XBL 845-2065

Figure V-9. Hexamethyldisilane upon thermal desorption from Pd(110) formed 1,1-dimethylsilaethylene. Observed with the species in the thermal desorption experiment was hydrogen and intact hexamethyldisilane. An exposure of 1.0 L was used in this experiment.

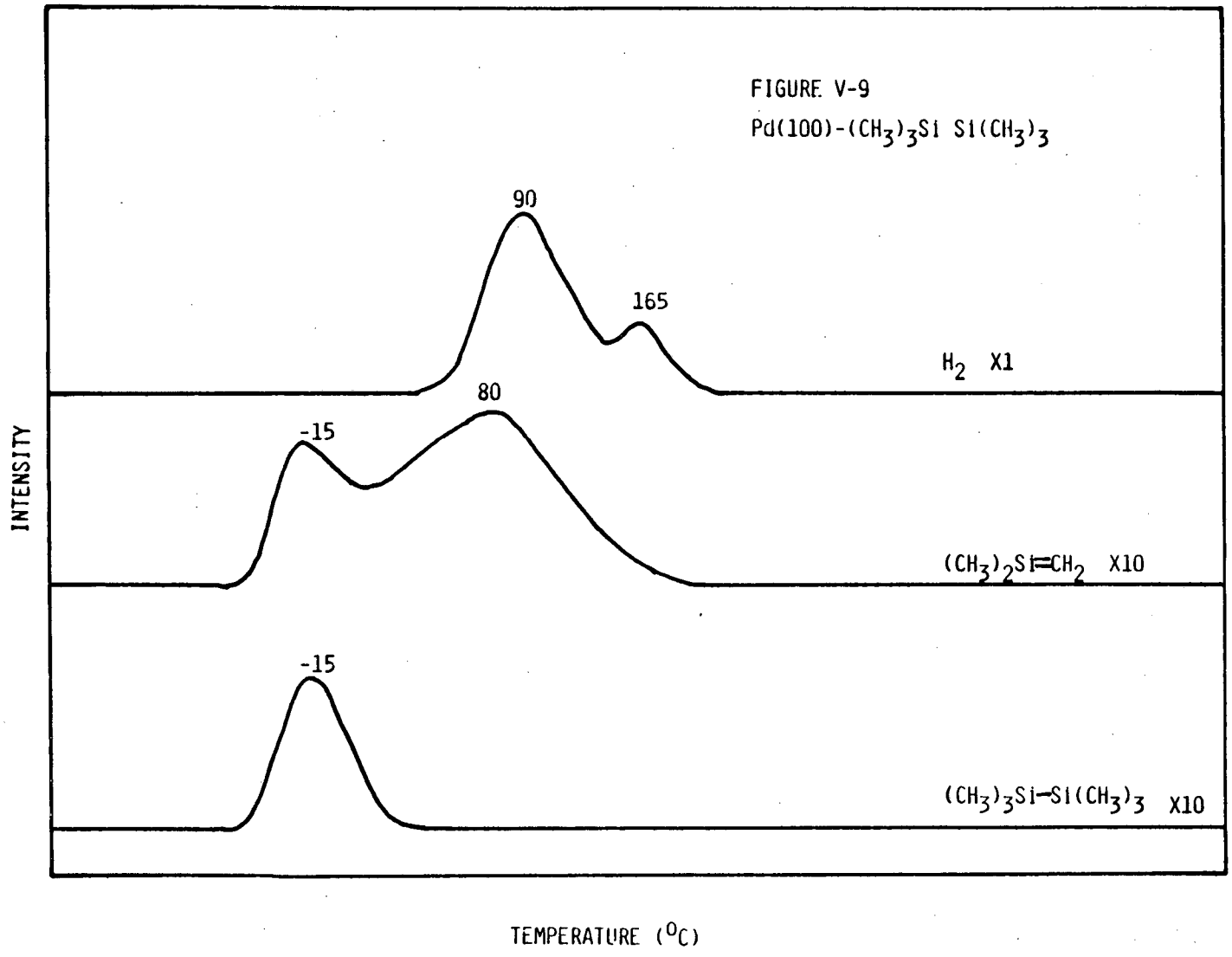
FIGURE V-9
Pd(100)-(CH3)3Si Si(CH3)3
90
165
H2 X1
80
-15
(CH3)2Si=CH2 X10
-15
(CH3)3Si-Si(CH3)3 X10
INTENSITY
TEMPERATURE (°C)

XBL 845-2066

DISCUSSION

Dehydrogenation of organosilanes on palladium single-crystal surfaces as a novel route to unsaturated organosilane has been demonstrated and found to be a facile process. This chemistry is in sharp contrast to that of saturated hydrocarbons, which quantitatively desorb from these surfaces; that is, no dehydrogenation is observed. Insights into the mechanism of dehydrogenation can be found by considering the results of the thermal desorption of tetramethylsilane $(CH_3)_4Si$, and trimethylsilane, $(CH_3)_3SiH$, and their two hydrocarbon analogs neopentane, $(CH_3)_4C$, and isobutane, $(CH_3)_3CH$. Both neopentane and tetramethylsilane undergo quantitative desorption, whereas a sharp contrast exists in the chemisorption of isobutane and trimethylsilane. Isobutane is found to quantitatively desorb, whereas trimethylsilane dehydrogenates to form 1,1-dimethylsilaethylene. It is apparent from these results that, in order for an organosilane to dehydrogenate, at least one Si-H bond must be present. The initial chemisorption state may be formed by a surface interaction of the Si-H bond through a three-center $\equiv Si\text{-}H\text{-}M_{surf.}$ bond. From this configuration, silicon-hydrogen bond scission may occur to form a surface silyl species. For example, trimethylsilane would undergo transformation to a trimethylsilyl surface intermediate. This intermediate may bring a C-H bond of the methyl group into close proximtiy, leading to C-H bond scission and subsequent Si = C bond formation. Desorption of the dehydrogenation product, 1,1-dimethylsilaethylene, from palladium

single-crystal surfaces is not totally unexpected in light of the reversible nature of the chemisorption of ethylene on these surfaces.[22]

The chemical displacement of unsaturated organosilanes gives further insights to the temperature range in which these dehydrogenations are occurring. Thermal dehydrogenations have been observed at temperatures in excess of 400°C; however, 1,1-dimethylsilaethylene has been displaced from chemisorbed trimethylsilane on Pd(110) at 25°C. This result suggests that dehydrogenation is a facile process at 25°C or less. The displacement of silaethylene and silacyclobutadiene from chemisorbed silacyclobutane indicates that both silicon-carbon and silicon-hydrogen bond scission have been affected at 25°C.

The dehydrogenation of six-membered rings provided routes to aromatic molecules. Saturated cyclic hydrocarbons, such as cyclohexane, undergo quantitative desorption. Heterocyclic molecules, such as piperidine, HNC_5H_{10}, and silacyclohexane, $HSiC_5H_{10}$, were found to dehydrogenate to pyridine and silabenzene, respectively. This chemistry is similar to that observed for cyclohexene on palladium single-crystal surfaces. Upon chemisorption, the primary interaction in both piperidine and silacyclohexane is probably through a three-centered bond, $X\text{-}H\text{-}M_{surf}$, where X is either nitrogen or silicon. As postulated for acyclicorganosilanes, the next step is X-H bond scission to form a surface species bonded through the heteroatom. This species would bring the C-H bond adjacent to the heteroatom in a

configuration where C-H bond scission is possible. The experiments performed in this chapter cannot unambigously define whether the subsequent dehydrogenation of the rings was a stepwise or a concerted process.

The nature of the chemisorbed state of silabenzene is an interesting question. Silabenzene could not be displaced from chemisorbed silacyclohexane on Pd(110). There was a simlar lack of displacement of an aromatic molecule, benzene, from cyclohexane chemisorbed on certain nickel and platinum single-crystal surfaces. Silabenzene formed on the surface may be strongly bond, or the dehydrogenation process is taking place at temperatures greater than 25°C.

CONCLUSION AND THE FUTURE

In this chapter, the facile dehydrogenation of organosilanes to form highly reactive unsaturated organosilanes has been demonstrated. Palladium single-crystal surfaces provide novel routes to those molecules. Recently, it has been demonstrated that chemistry that occurs under ultrahigh-vacuum conditions can be observed at much higher pressure on palladium surfaces.[24] In light of these results, it might be possible to prepare unsaturated organosilanes at much higher pressures on polycrystalline and supported palladium. These unsaturated organosilanes should exhibit interesting chemistry. Pyrolysis of polymeric organosilanes is known to produce ceramic materials.[25] Polymers formed from these unsaturated organosilanes may prove to have interesting properties.

REFERENCES

1. M.-C. Tsai, J. Stein, C. M. Friend, and E. L. Muetterties, J. Am. Chem. Soc. 1982, 104, 3533.

2. B. C. Gates, J. R. Katzer, and G. C. A. Schuitt, Chemistry of Catalytic Processes, McGraw Hill, New York, 1979, pp. 222-247.

3. (a) M.-C. Tsai, C. M. Friend, and E. L. Muetterties, J. Am. Chem. Soc. 1982, 104, 2539; (b) M.-C. Tsai, and E. L. Muetterties. J. Phys. Chem. 1982, 86, 5067.

4. M.-C. Tsai, C. M. Friend, A. J. Johnson, and E. L. Muetterties, unpublished data.

5. L. E. Gusel'nikov, and N. S. Nametkin, Chem. Rev. 1979, 79, 529.

6. R. West, J. Am. Chem. Soc. 1954, 76, 6012.

7. H. F. Schaefer. Accts. of Chem. Res. 1982, 15, 283.

8. O. L. Chapman, C.-C. Chang, J. Kole, M. E. Jung, J. A. Lowe, T. J. Barton, and M. L. Tumey, J. Am. Chem. Soc. 1976, 98, 7844.

9. M. R. Chedekel, M. Skoglund, R. L. Kreeger, and H. Schechter, J. Am. Chem. Soc. 1976, 98, 7846.

10. M. C. Flowers, and L. E. Gusel'nikov, J. Chem. Soc. B 1968, 419.

11. (a) L. E. Gusel'nikov, N. S. Nametkin, and V. M. Vdouin, Acc. Chem. Res. 1975, 8, 18; (b) B. Coleman, and M. Jones, Rev. Chem. Intermediates 1981, 4, 297.

12. N. S. Nametkin, V. M. Vdouin, L. E. Gusel'nikov, and V. L. Zav'yalou, Izv. Akad. Nauk. SSSR, Serkhim, 1966, p. 584.

13. G. Fritz, J. Grobe, and D. Kummer, Advan. Inorg. Chem. Radiochem. 1965, 7, 349.

14. (a) B. Solouk, P. Rosmus, H. Bock, and G. Maier, Angew. Chem. Int. Ed. Engl. 1980, 19, 51; (b) T. J. Barton, and G. T. Burns, J. Am. Chem. Soc. 1978, 100, 5246.

15. P. Boudjouk, and L. H. Summer, J. Chem. Soc. Chem. Commun. 1973, 54.

16. O. P. Strausz, K. Obi, and W. K. Duholke, J. Am. Chem. Soc. 1968, 90, 1359.

17. P. Potinger, and W. Weddle, 5th International Symposium on Organosilicon Chemistry, Karlsruhe, West Germany, 1978, p. 1232.

18. P. Boudjouk, and R. D. Koob, J. Am. Chem. Soc. 1975, 97, 6595.

19. (a) L. E. Gusel'nikov, U. U. Volkova, V. G. Avakyan, and N. S. Nametkin, J. Organomet. Chem. 1980 201, 137; (b) O. M. Mefedou, A. K. Maltsev, V. N. Khabasheku, and V. A. Koroleu. J. Organomet. Chem. 1980, 201, 123.

CHAPTER VI. SURFACE CHEMISTRY OF THIOPHENE AND METHYLSUBSTITUTED THIOPHENES ON PALLADIUM SINGLE-CRYSTAL SURFACES

INTRODUCTION

Recently, the chemisorption of heteroaromatic molecules such as thiophene[1] and pyridine[2] has been investigated on a variety of transition metal surfaces. These heteroaromatic molecules have proven to be useful probes for transition metal surface chemistry. For example, pyridine on Ni(100) was found to exhibit regiospecific carbon-hydrogen bond scission. Use of specifically labeled pyridines made it possible to gain insights into the mechanism of this reaction. An α-pyridyl was postulated as an intermediate. Further evidence for this species was obtained from near-edge x-ray absorption studies.[3] In this chapter, the chemisorption of thiophene and two methylsubstituted derivatives, 3-methylthiophene and 2,5-dimethylthiophene, was investigated on palladium single-crystal surfaces. Both surface crystallography (structure) and composition were found to influence the chemistry of these molecules. The three low Miller-index surfaces, (111), (100), and (110), were studied, as well as sulfur-covered surfaces.

Transition metals and sulphided transition metals are important hydrodesulfurization (HDS) catalysts.[4] Chianelli and Pecoraro have studied the HDS activity of a number of transition metals.[5] Maximum activity was found for osmium and ruthenium. The HDS activity of palladium was found to be less than that of osmium but more than that

of molybdenum. Molybdenum sulphides are common HDS catalysts in the petroleum industry.

High pressure reactions of thiophene on Mo(100) have been reported recently.[6] A distribution of C_4 hydrocarbons (the HDS products) was observed. Both saturated products (butane) and unsaturated products (butenes and butadiene) were found. Under ultrahigh-vacuum conditions, desulfurization of thiophene to form butadiene was observed on palladium single-crystal surfaces. The desulfurization of 2,5-dimethylthiophene leads to benzene formation under similar conditions. Thus, palladium single crystals were found to provide a unique opportunity to probe catalytic reactions that usually occur at much greater pressures.

RESULTS

A. Pd(111) - Thiophene

Thermal desorption of thiophene from clean Pd(111) at low thiophene exposures, 1.0 L, resulted in decomposition (irreversible chemisorption) and formation of butadiene. Thiophene decomposed to carbon and sulfur on the surface. This decomposition led to deposition of approximately 0.15 monolayer of sulfur, $\theta_S = 0.15$, on the surface. Two hydrogen thermal desorption maxima, T_{max}, were observed, at 175°C, and 370°C. A butadiene T_{max} was observed at 130°C (see Figure VI-1A). On sulfur-covered Pd(111) with low thiophene exposure, the following trends were observed: (a) The fraction of molecular desorption increased with increased sulfur

coverage. (b) A corresponding decrease was found in the amount of irreversible chemisorption, H_2 desorption, along with a decrease in the amount of sulfur deposited. (c) A maximum yield of butadiene occurred between 0.15 and 0.30 monolayer of sulfur.

The thermal desorption spectrum of thiophene from a Pd(111) surface with a sulfur coverage of 0.15 is shown in Figure VI-1B. Two hydrogen T_{max} were observed, at 180°C, and 340°C, along with a butadiene T_{max} at 130°C, and broad thiophene T_{max} at 90°C. After this experiment, 0.30 monolayer of sulfur remained. At a sulfur coverage of 0.30 monolayer and a thiophene exposure of 1.0 L, only one H_2 T_{max} was observed, at 370°C. A butadiene T_{max} was also observed at 120°C, along with a broad plateau-like thiophene desorption from 40°C to 85°C (see Figure VI-1C). An increase of 0.1 monolayer was observed after this experiment. Largely molecular desorption of thiophene (1.0-L exposure) from Pd(111) with a sulfur coverage of 0.40 monolayer. Three thiophene desorption maxima were observed, at -25°C, 25°C, and 100°C. No butadiene was observed. A weak hydrogen T_{max} was evident at 360°C (see Figure VI-1D). The sulfur coverage increased to 0.48 monolayer after this experiment.

On clean Pd(111) at higher thiophene exposures (4.0 L), the following species were observed in the thermal desorption spectrum: (a) thiophene, with three desorption maxima, at -95°C, -30°C, and 65°C; (b) butadiene, T_{max} = 125°C; and (c) hydrogen, which desorbed in a broad plateau from 125°C to 300°C, followed by a maximum at 415°C (see Figure VI-2).

Figure VI-1. Thermal desorption of thiophene from Pd(111) was found to be a sensitive function of sulfur coverage. All thermal desorption experiments shown here were performed with a thiophene exposure of 1.0 L. The fraction of reversibly bound thiophene increased with sulfur coverage. Desulfurization of thiophene was observed, as is evident by the presence of a butadiene thermal desorption maximum. The sulfur coverages in the four spectra (A, B, C, and D) were 0.0 monolayer or clean, 0.15 monolayer, 0.29 monolayer, and 0.43 monolayer, respectively.

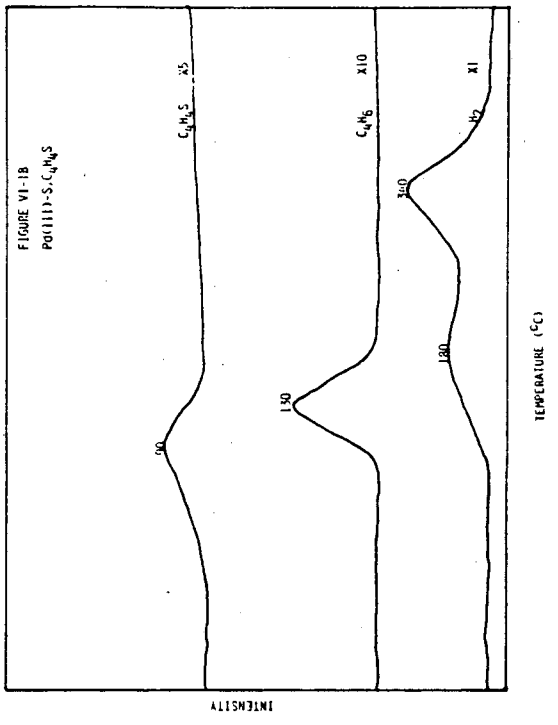
FIGURE VI-1B
Pd(111)-S.C4H4S
C4H4S X5
C4H6 X10
H2 X1
90
150
180
INTENSITY
TEMPERATURE (°C)

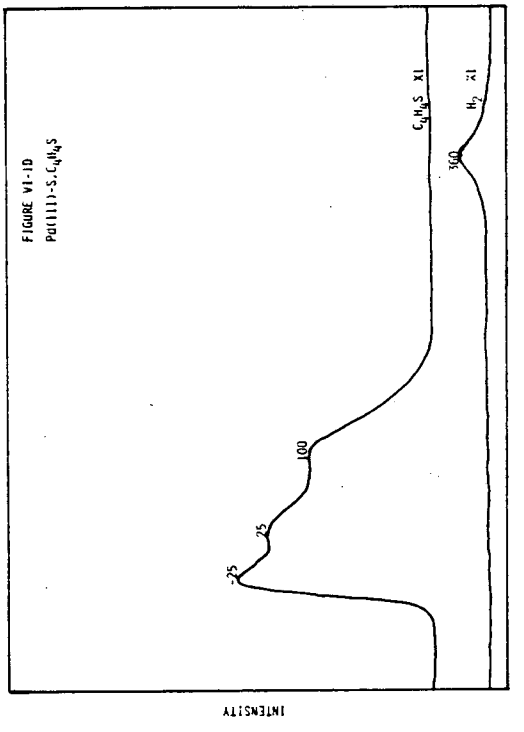
FIGURE VI-1D
Pd(111)-S.C4H4S
C4H4S X1
H2 X1
25
25
100
360
INTENSITY
TEMPERATURE (°C)

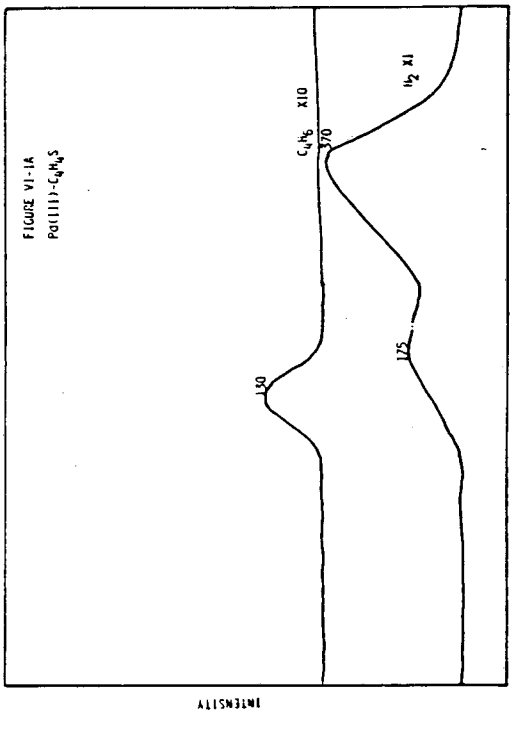
FIGURE VI-1A
Pd(111)-C4H4S
C4H6 X10
H2 X1
150
170
175
INTENSITY
TEMPERATURE (°C)

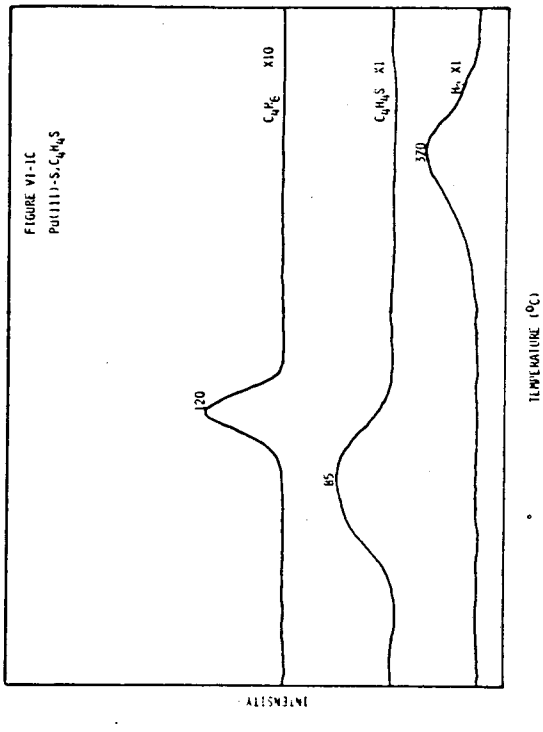
FIGURE VI-1C
Pd(111)-S.C4H4S
C4H6 X10
C4H4S X1
H2 X1
120
85
320
INTENSITY
TEMPERATURE (°C)

XBL 846-2109

Figure VI-2. At high thiophene exposures, 4.0 L, the thermal desorption spectrum from Pd(111) exhibited (a) molecular desorption, (b) desulfurization, butadiene formation, and (c) decomposition to H_2 and sulfur, $\theta_S = 0.28$, and carbon remaining on the surface.

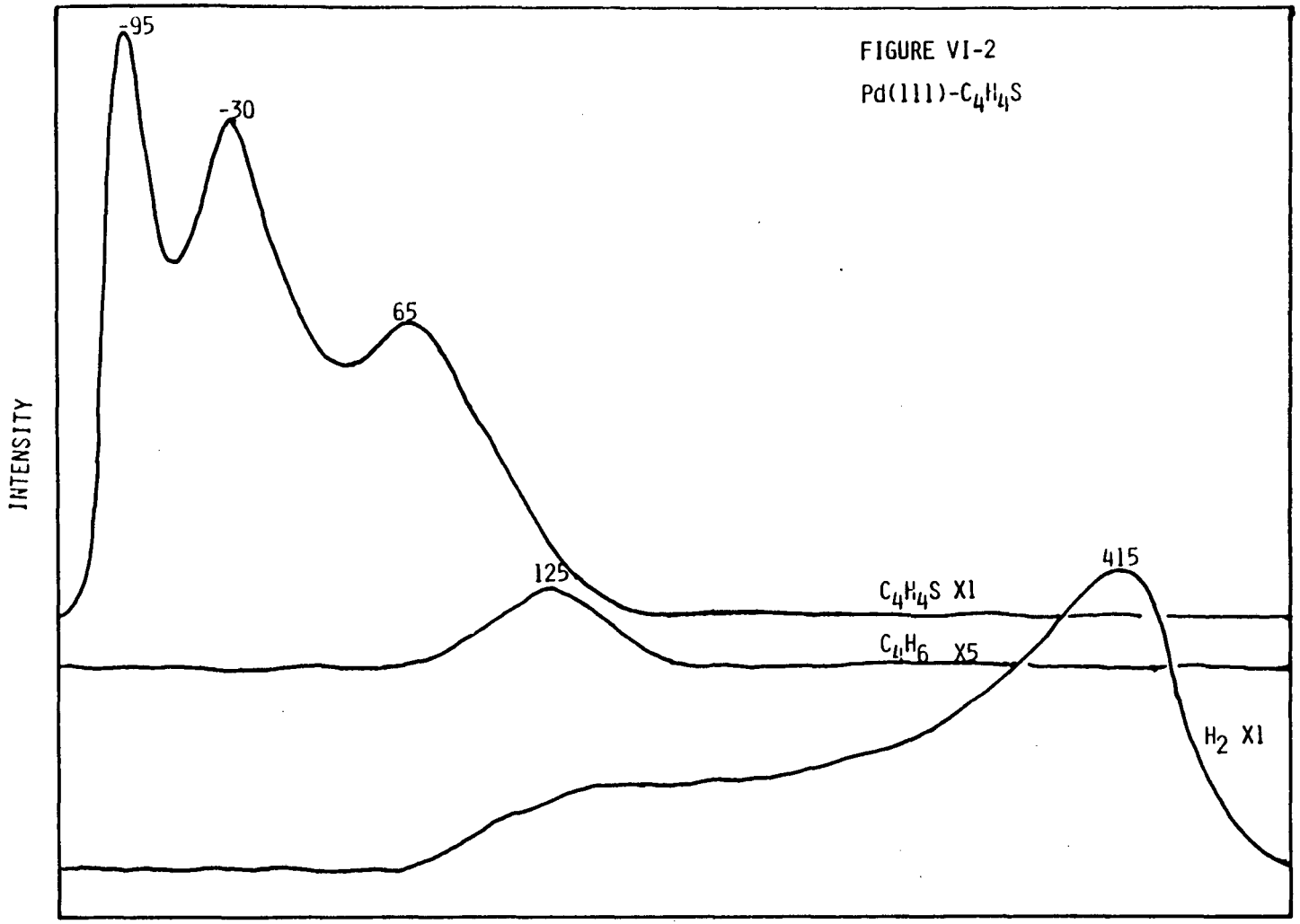

FIGURE VI-2
Pd(111)-C_4H_4S

XBL 846-2101

B. Pd(111) - 2,5-dideuterothiophene

Thermal desorption of 2,5-dideuterothiophene from clean Pd(111) yielded all three species, H_2, HD, and D_2. All three species were observed in maxima at 155°C, and 350°C (see Figure VI-3A). At a sulfur coverage of 0.30 monolayer, all three species were observed in a single maximum at 370°C (see Figure VI-3B).

Thermal desorption of a surface state prepared by sequential adsorption of deuterium followed by thiophene on sulfur-covered Pd(111), θ_S = 0.30, led to substantial deuterium incorporation in the butadiene formed. At least four deuterium atoms were incorporated into the butadiene, as shown by the signal at 58 amu ($C_4D_4H_2$).

C. Pd(111) - 3-methylthiophene

The thermal desorption spectrum of 3-methylthiophene at 1.0 L exposure is shown in Figure VI-4A. The only process observed was decomposition, as shown by three hydrogen maxima, at 75°C, 220°C, and 390°C. No molecular desorption or hydrocarbon formation was detected. After this experiment, approximately 0.15 monolayer of sulfur remained on the surface. An increase in molecular desorption of 3-methylthiophene was observed on sulfur-covered Pd(111), θ_S = 0.15 (see Figure VI-4B). A decrease in the amount of decomposition was observed. A relative decrease in the hydrogen maxima at 75°C, and 225°C with respect to the 390°C maximum was observed. A broad thiophene maximum at ~35°C was also observed. After this experiment, 0.31 monolayer of sulfur remained on the surface. At high thiophene exposures (4.0 L),

Figure VI-3. No regioselective carbon-hydrogen bond scission was observed to occur in the thermal desorption of 2,5-dideuterothiophene from clean or sulfur-covered Pd(111). Two maxima were observed for all three molecules--H_2, HD, and D_2—on clean Pd(111), as shown in A. One maximum was observed on sulfur-covered Pd(111), $\theta_S = 0.30$, which is displayed in B.

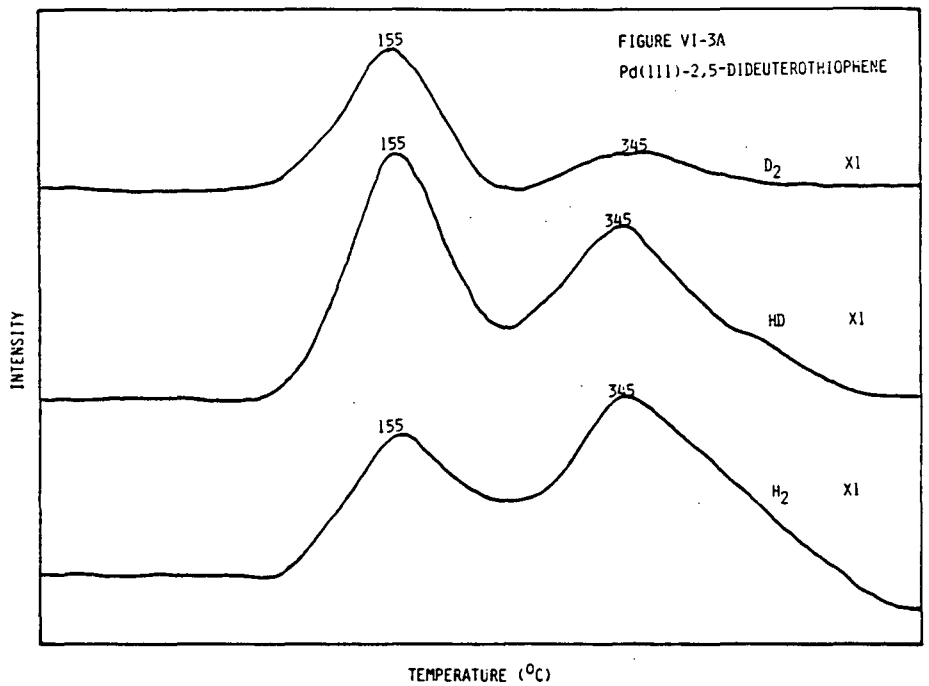
155
FIGURE VI-3A
Pd(111)-2,5-DIDEUTEROTHIOPHENE
155
345
D2
X1
345
HD
X1
345
155
H2
X1
INTENSITY
TEMPERATURE (°C)

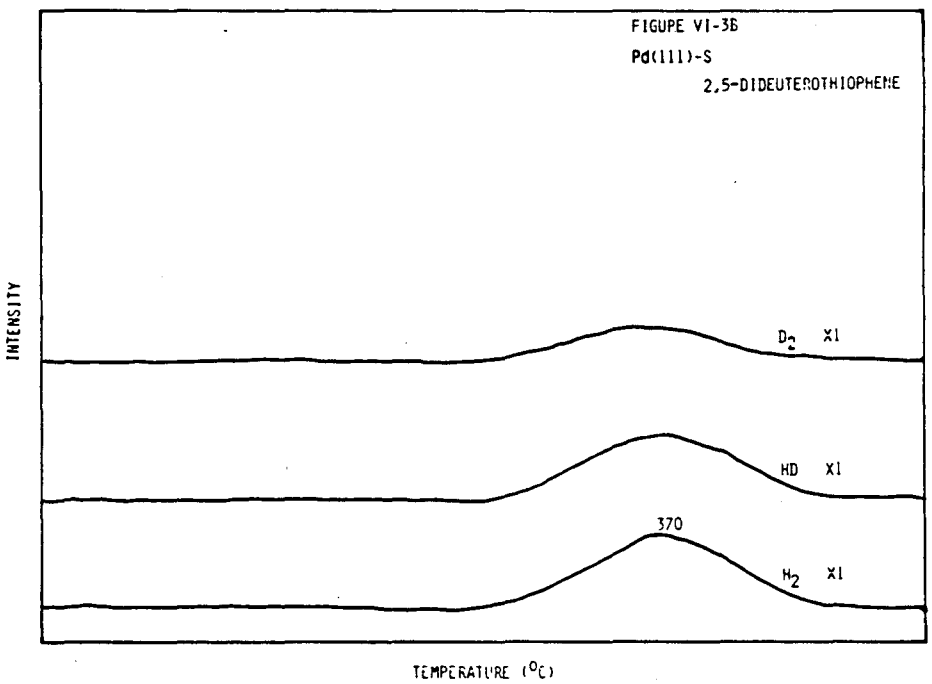
FIGUPE VI-3B
Pd(111)-S
2,5-DIDEUTEROTHIOPHENE
D2 X1
HD X1
370
H2 X1
INTENSITY
TEMPERATURE (°C)

XBL 846-2121

Figure VI-4. At an exposure of 1.0 L, 3-methylthiophene exhibits only irreversible chemisorption upon thermal desorption from clean Pd(111), as shown in A. Molecular desorption and decomposition was observed on sulfur-covered Pd(111), $\theta_S = 0.16$. No hydrocarbon desorption was observed.

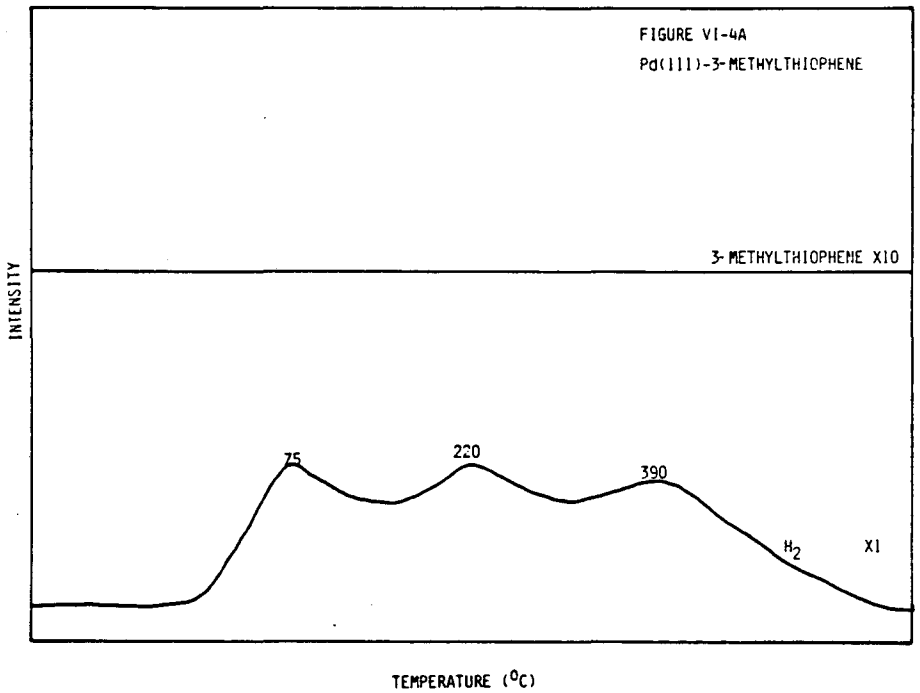
FIGURE VI-4A
Pd(111)-3-METHYLTHIOPHENE
3-METHYLTHIOPHENE X10
INTENSITY
75
220
390
H_2
X1
TEMPERATURE (°C)

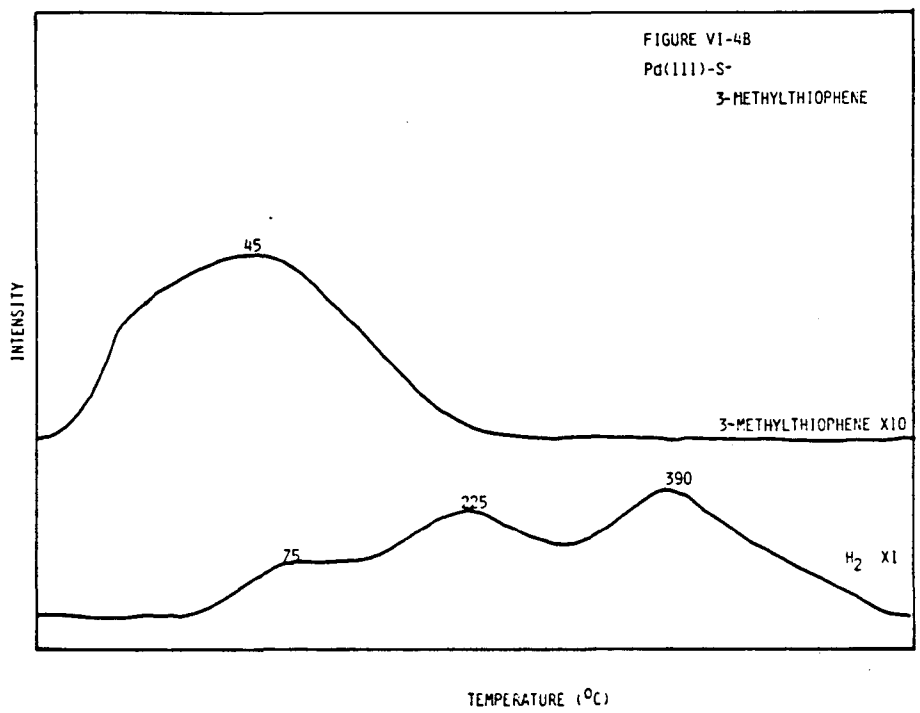
FIGURE VI-4B
Pd(111)-S-
3-METHYLTHIOPHENE
INTENSITY
45
3-METHYLTHIOPHENE X10
390
225
75
H_2 X1
TEMPERATURE (°C)

XBL 846-2120

a hydrogen maximum at 420°C with a long leading edge extending from ~100°C was observed. A 3-methylthiophene maximum at -80°C with a long tail was also observed (see Figure VI-5A). A sulfur coverage of 0.30 monolayer was observed at the conclusion of this experiment. At higher sulfur coverages, θ_S = 0.30, the yield of hydrogen decreased further (H_2 T_{max} = 405°C), and the fraction of molecule desorption increased (see Figure VI-5B).

D. Pd(111) - 2,5-dimethylthiophene

At low exposures (1.0 L), thermal desorption of 2,5-dimethylthiophene from Pd(111) results in both decomposition and benzene formation. Three hydrogen maxima were observed, at 50°C, 155°C, and 405°C. Benzene formation was evident by a desorption maximum at 225°C (see Figure VI-6A). Approximately 0.20 monolayer of sulfur remained on the surface after this experiment. On sulfur-covered Pd(111), θ_S = 0.32, the amount of decomposition decreased, and a corresponding increase in the molecular desorption was also observed. Two hydrogen thermal desorption maxima were observed, a weak one at 130°C, and a more intense one at 400°C. 2,5-dimethylthiophene maxima were observed at -70°C, and 50°C. Benzene desorption occurred in a broad plateau from 60°C to 150°C (see Figure VI-6B). At high 2,5-dimethylthiophene exposures (4.0 L), molecular desorption, benzene formation, and desorption of H_2 were observed from Pd(111). Two H_2 T_{max} were observed, at 100°C, and 410°C; 2,5-dimethylthiophene desorption maxima occurred at -75°C, and 85°C. A benzene maximum was observed at

Figure VI-5. At a 3-methylthiophene exposure of 4.0 L, both reversible and irreversible chemisorption were evident in the thermal desorption spectrum from clean Pd(111) (spectrum A). On sulfur-covered Pd(111), $\theta_S = 0.30$, increased molecular desorption was observed, as shown in spectrum B.

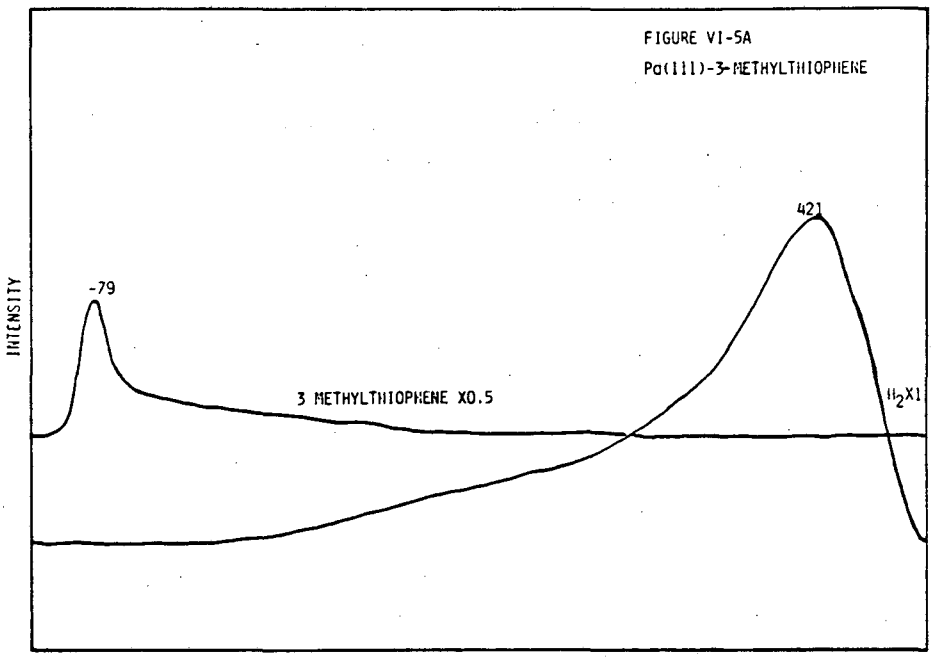
FIGURE VI-5A
Pd(111)-3-METHYLTHIOPHENE
421
-79
INTENSITY
3 METHYLTHIOPHENE X0.5
H2X1
TEMPERATURE (°C)

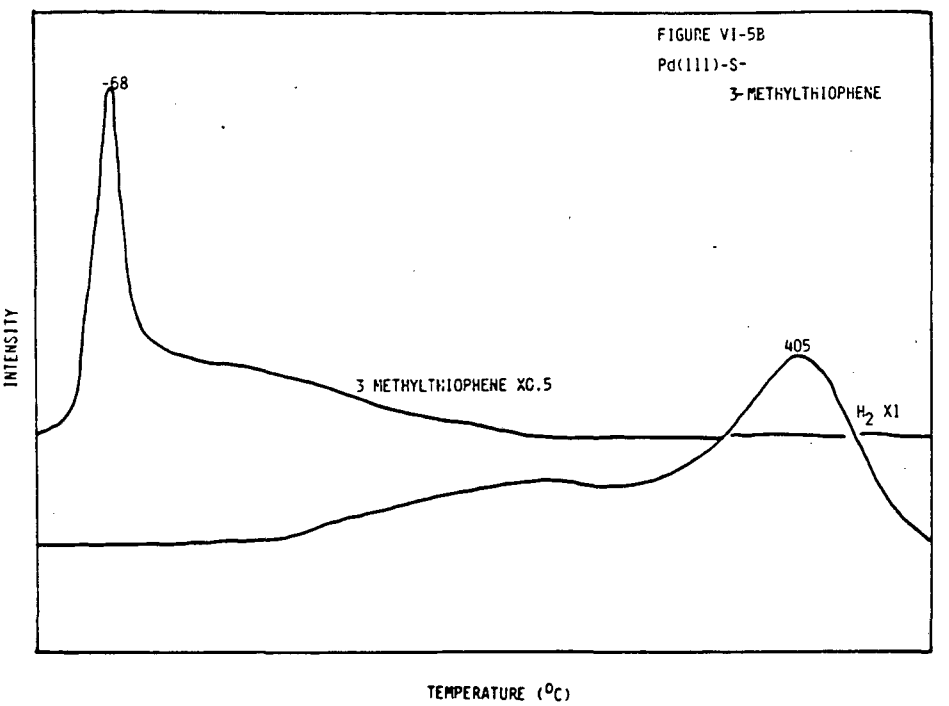
FIGURE VI-5B
Pd(111)-S-
3-METHYLTHIOPHENE
-68
405
INTENSITY
3 METHYLTHIOPHENE XC.5
H2 X1
TEMPERATURE (°C)

XBL 846-2119

Figure VI-6. Thermal desorption of 2,5-dimethylthiophene, at an exposure of 1.0 L, from Pd(111) exhibited decomposition and desulfurization. Benzene was the desulfurization product, as shown in the spectrum in A. On sulfur-covered Pd(111), $\theta_S = 0.32$, the yield of benzene decreased and molecular desorption of 2,5-dimethylthiophene was observed. This spectrum is shown in B.

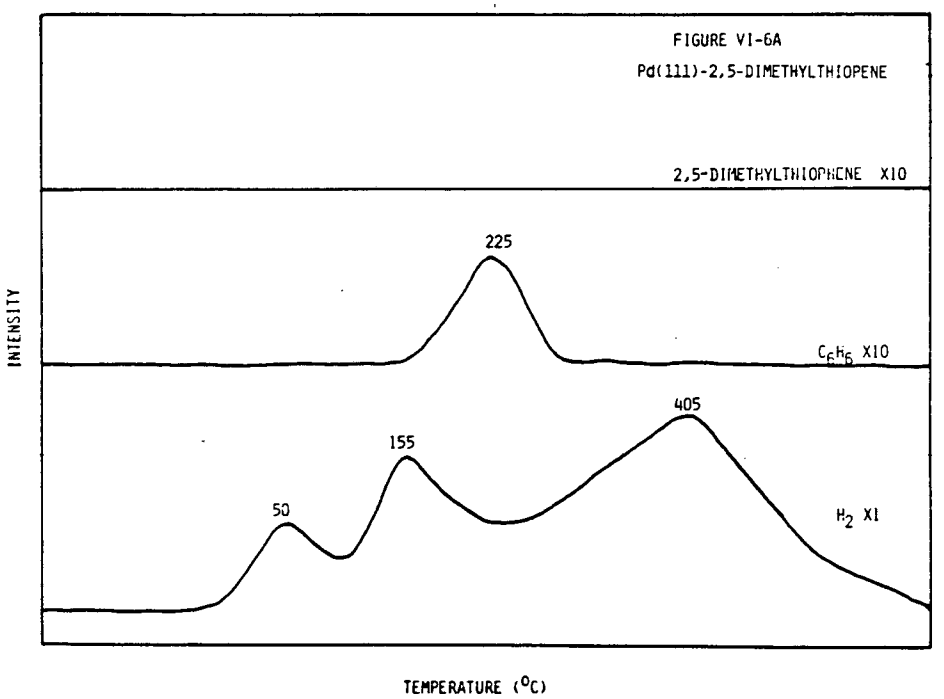
FIGURE VI-6A
Pd(111)-2,5-DIMETHYLTHIOPENE
2,5-DIMETHYLTHIOPHENE X10
225
C_6H_6 X10
405
155
50
H_2 X1
INTENSITY
TEMPERATURE (°C)

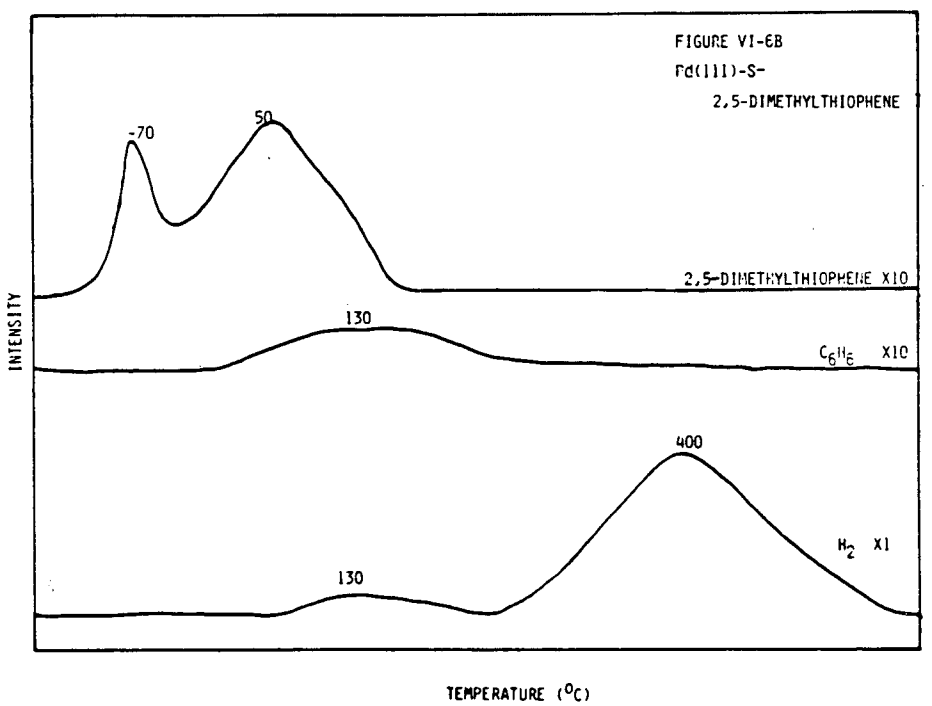
FIGURE VI-6B
Pd(111)-S-
2,5-DIMETHYLTHIOPHENE
-70
50
2,5-DIMETHYLTHIOPHENE X10
130
C_6H_6 X10
400
H_2 X1
130
INTENSITY
TEMPERATURE (°C)

XBL 846-2118

155°C (see Figure VI-7A). After desorption, 0.25 monolayer of sulfur remained on the surface. On sulfur-covered Pd(111), θ_S = 0.25, the fraction of molecular desorption increased and the yield of hydrogen decreased. A broad benzene maximum was observed from 100°C to 200°C. 2,5-dimethylthiophene desorbed at -80°C, with a long tail extending to 200°C. Hydrogen maxima were observed at 100°C, and 420°C (see Figure VI-7B).

Deuterium incorporation into benzene formed from 2,5-dimethylthiophene was observed from the surface state formed by sequential adsorption of D_2 and 2,5-dimethylthiophene. Three deuterium atoms were observed in the benzene, as evident by the signal at 81 amu ($C_6H_5D_3$) (see Figure VI-8).

E. Pd(100) - Thiophene

At low exposures (1.0 L), the thermal desorption of thiophene from Pd(100) shows reversible chemisorption (molecular desorption) and irreversible chemisorption (decomposition). No hydrocarbons were observed to desorb from the surface at the exposure. Two poorly resolved hydrogen thermal desorption maxima were observed, at 145°C, and 240°C; and a thiophene maximum was observed at 5°C (see Figure VI-9A). After this experiment, 0.15 monolayer of sulfur was observed on the surface. On sulfur-covered Pd(100), θ_S = 0.15, the fraction of reversibly bound thiophene increased (a thiophene T_{max} at -40°C of increased intensity was observed), and a corresponding decrease in

Figure VI-7. At an exposure of 4.0 L, the following processes were observed in the thermal desorption of 2,5-dimethylthiophene from Pd(111): (a) decomposition to hydrogen, with carbon and sulfur remaining on the surface; (b) desulfurization to form benzene; and (c) molecular desorption. The spectrum showing these processes is given in A. On sulfur-covered Pd(111), $\theta_S = 0.25$, the fraction of 2,5-dimethylthiophene desorbing intact increased, as shown in B.

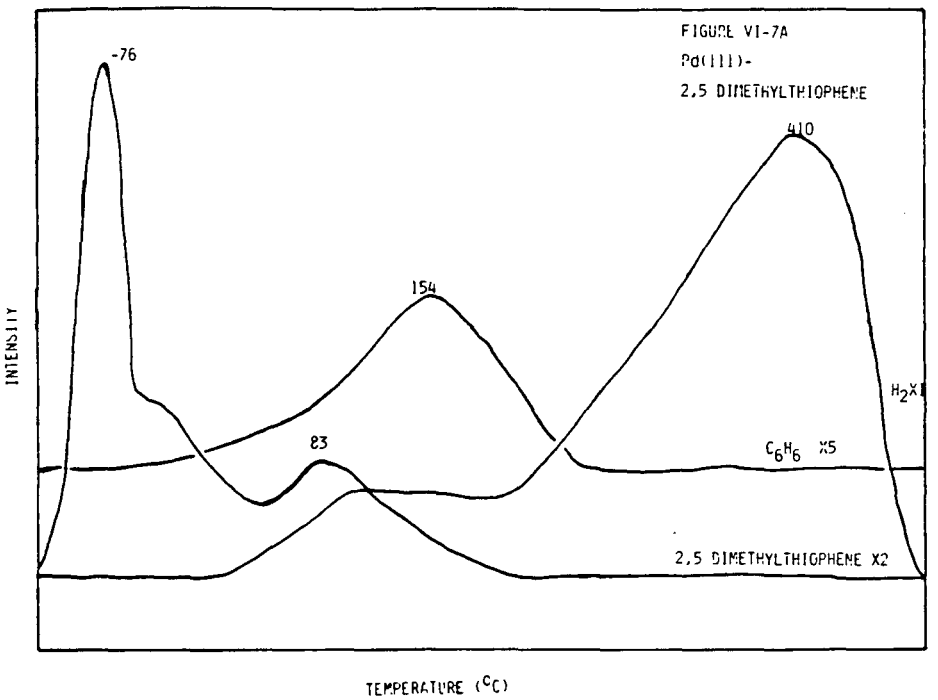
FIGURE VI-7A
Pd(111)-
2,5 DIMETHYLTHIOPHENE
-76
410
154
83
H_2 X1
C_6H_6 X5
2,5 DIMETHYLTHIOPHENE X2
INTENSITY
TEMPERATURE (°C)

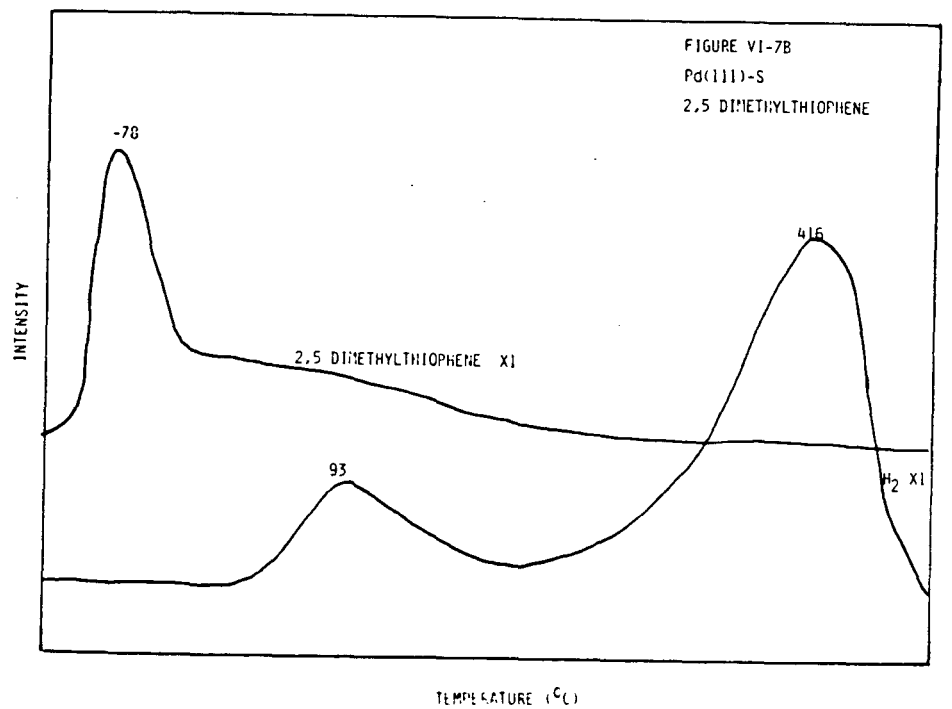
FIGURE VI-7B
Pd(111)-S
2,5 DIMETHYLTHIOPHENE
-78
416
2,5 DIMETHYLTHIOPHENE X1
93
H_2 X1
INTENSITY
TEMPERATURE (°C)

XBL 846-2117

Figure VI-8. Thermal desorption of the surface state formed by sequential adsorption of deuterium and 2,5-dimethylthiophene illustrates deuterium incorporation into the benzene formed. Shown here are traces for 78 amu, 79 amu, 80 amu, and 81 amu, corresponding to C_6H_6, C_6H_5D, $C_6H_4D_2$, and $C_6H_3D_3$, respectively.

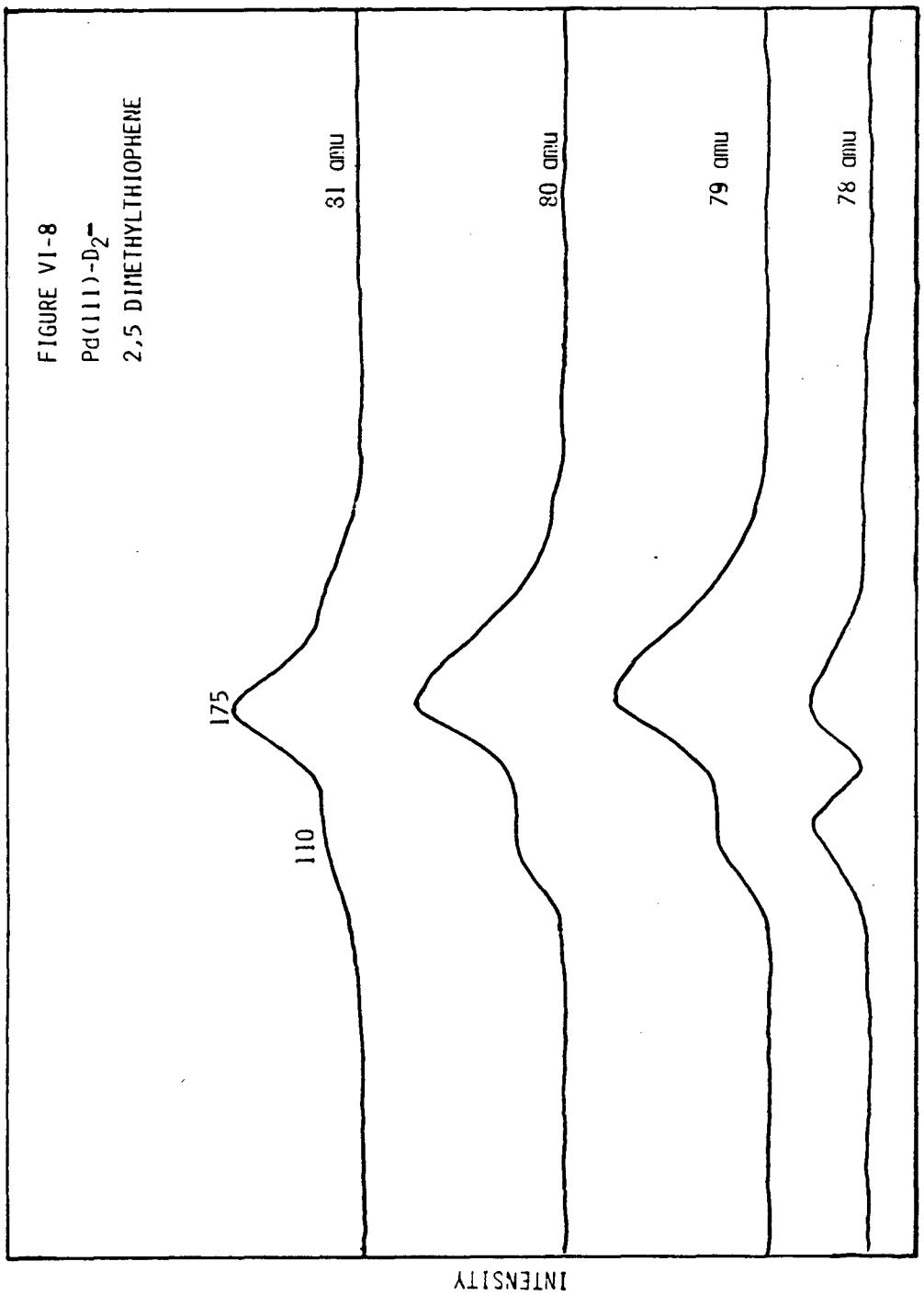
FIGURE VI-8
Pd(111)-D2-
2,5 DIMETHYLTHIOPHENE
31 amu
80 amu
79 amu
78 amu
175
110
INTENSITY
TEMPERATURE (°C)
XBL 846-2102

Figure VI-9. Thermal desorption of thiophene at low exposures, 1.0 L, from clean Pd(100) exhibited both reversible and irreversible desorption, as illustrated by the spectrum in A. No butadiene desorption was observed at this exposure. In B, the thermal desorption of 1.0 L of thiophene from a sulfur-covered Pd(100) surface, $\theta_S = 0.36$, is shown. Increased molecular desorption is evident.

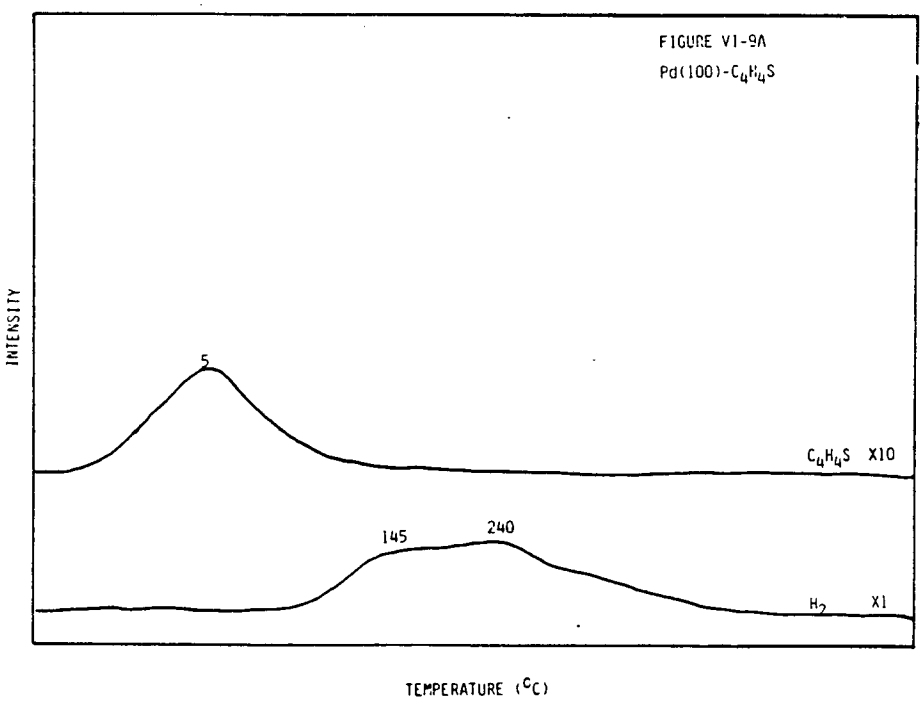
FIGURE VI-9A
Pd(100)-C4H4S
INTENSITY
5
C4H4S X10
145
240
H2 X1
TEMPERATURE (°C)

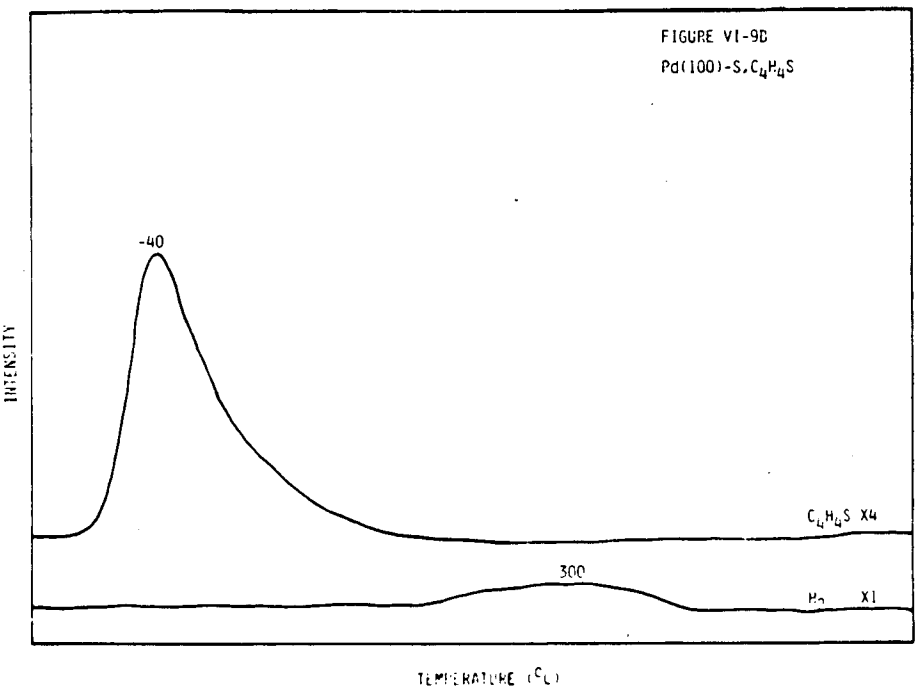
FIGURE VI-9B
Pd(100)-S,C4H4S
INTENSITY
-40
C4H4S X4
300
H2 X1
TEMPERATURE (°C)

XBL 846-2115

the fraction of irreversibly bound thiophene was observed (a single weak H_2 T_{max} was observed at 300°C) (see Figure VI-9B). At higher thiophene exposures (3.0 L), three processes were observed to occur on Pd(100): (1) reversible chemisorption; (2) irreversible chemisorption; and (3) butadiene formation. Two thiophene maxima were observed, at -65°C, and 30°C; two hydrogen maxima was observed, at 250°C, and 390°C; and a butadiene maximum was observed at 150°C (see Figure VI-10A). After this experiment, a sulfur coverage of 0.20 monolayer was observed. On sulfur-covered Pd(100), θ_S = 0.33, the fraction of reversibly bound thiophene was found to increase, T_{max} = 55°C; the yield of butadiene decreased, T_{max} = 150°C; while the fraction of irreversibly bound thiophene decreased, as evident by the decrease in the area under the curve of the hydrogen thermal desorption spectrum (see Figure VI-10B).

F. Pd(100) - 2,5-dideuterothiophene

All three species--H_2, HD, and D_2--were observed in the thermal desorption of 2,5-dideutereothiophene from Pd(100). Two maxima were observed, at 220°C, and 390°C. Both maxima were populated by H_2, HD, and D_2 (see Figure VI-11).

G. Pd(100) - 3-methylthiophene

At low exposures (1.0 L), the chemisorption of 3-methylthiophene on Pd(100) was largely reversible. Three hydrogen thermal desorption maxima were observed, at 75°C, 175°C, and 220°C (see Figure VI-12A). The intensity of the H_2 maxima followed the order 220°C > 175°C > 75°C. After this experiment, the sulfur coverage was found to be 0.14

Figure VI-10. At an exposure of 3.0 L, butadiene desorption was observed in the thermal desorption of thiophene from clean Pd(100). As shown in A, hydrogen and thiophene desorption were also observed. In B, the thermal spectrum of thiophene from sulfur-covered Pd(100) shows an increase in the fraction of thiophene desorbing intact.

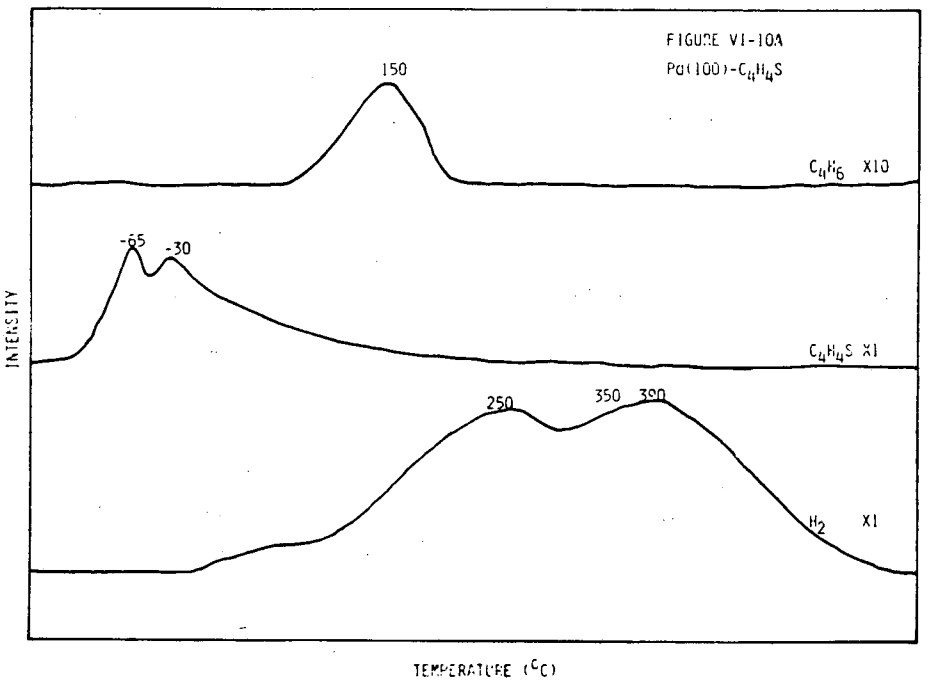
FIGURE VI-10A
Pd(100)-C_4H_4S
150
C_4H_6 X10
-65
-30
C_4H_4S X1
250
350
380
H_2 X1
INTENSITY
TEMPERATURE (°C)

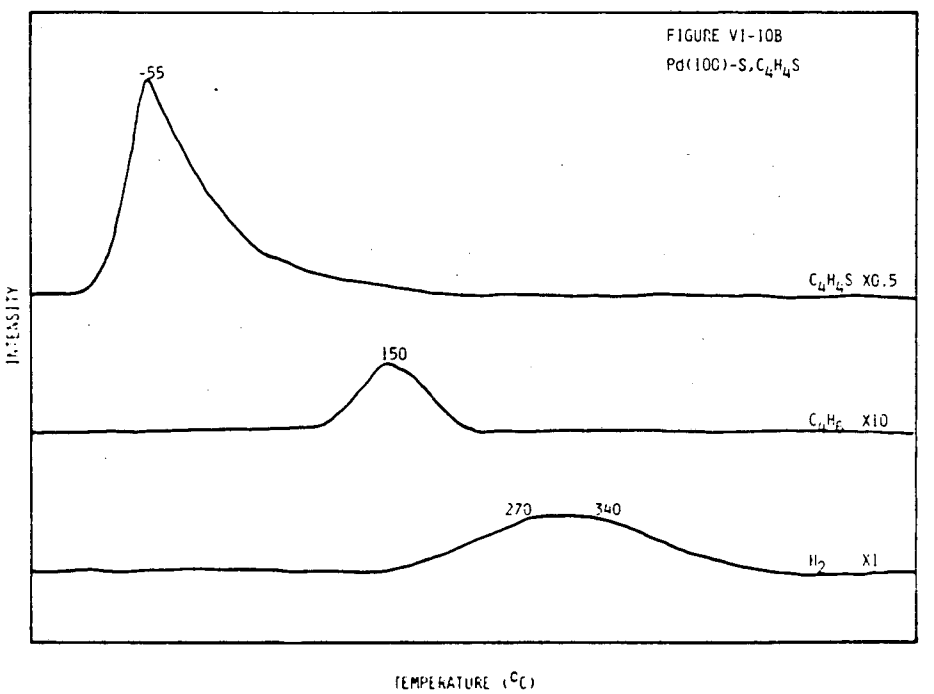
FIGURE VI-10B
Pd(100)-S,C_4H_4S
-55
C_4H_4S XG.5
150
C_4H_6 X10
270
340
H_2 X1
INTENSITY
TEMPERATURE (°C)

XBL 846-2114

Figure VI-11. No regioselective carbon–hydrogen bond scission was observed in the thermal desorption of 2,5-dideuterothiophene, 3.0 L, from Pd(100).

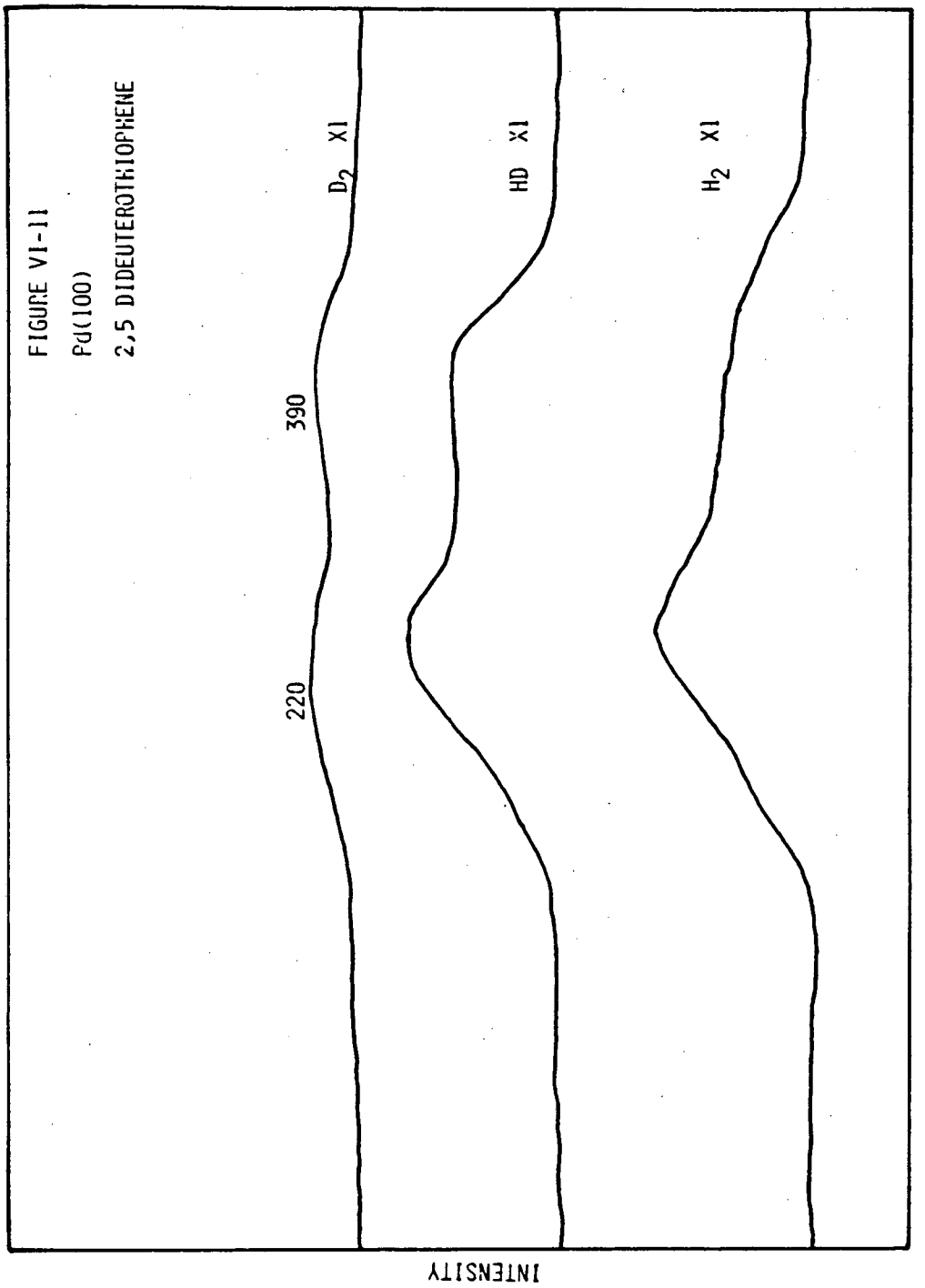
FIGURE VI-11
Pd(100)
2,5 DIDEUTEROTHIOPHENE
D_2 X1
HD X1
H_2 X1
390
220
INTENSITY
TEMPERATURE (°C)

XBL 846-2100

Figure VI-12. The thermal desorption spectrum of 3-methylthiophene from clean Pd(100) shows evidence of decomposition and molecular desorption. The spectrum in A is for a 3-methylthiophene exposure of 1.0 L. On sulfur-covered Pd(100), θ_S = 0.10, the fraction of thiophene reversibly bound increased, as illustrated in B.

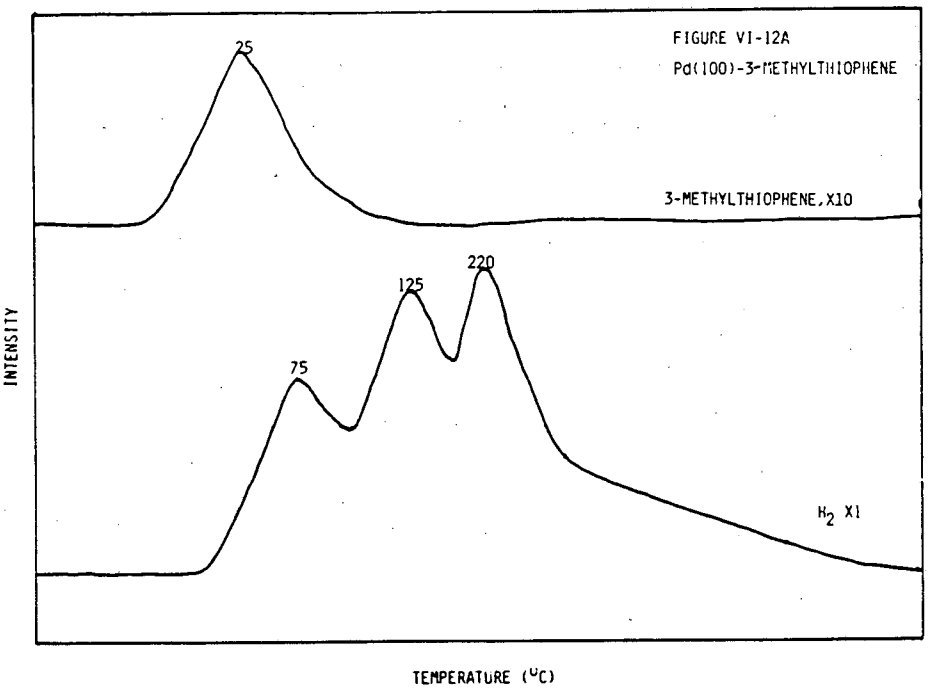
FIGURE VI-12A
Pd(100)-3-METHYLTHIOPHENE
3-METHYLTHIOPHENE, X10
25
220
125
75
INTENSITY
H_2 X1
TEMPERATURE (°C)

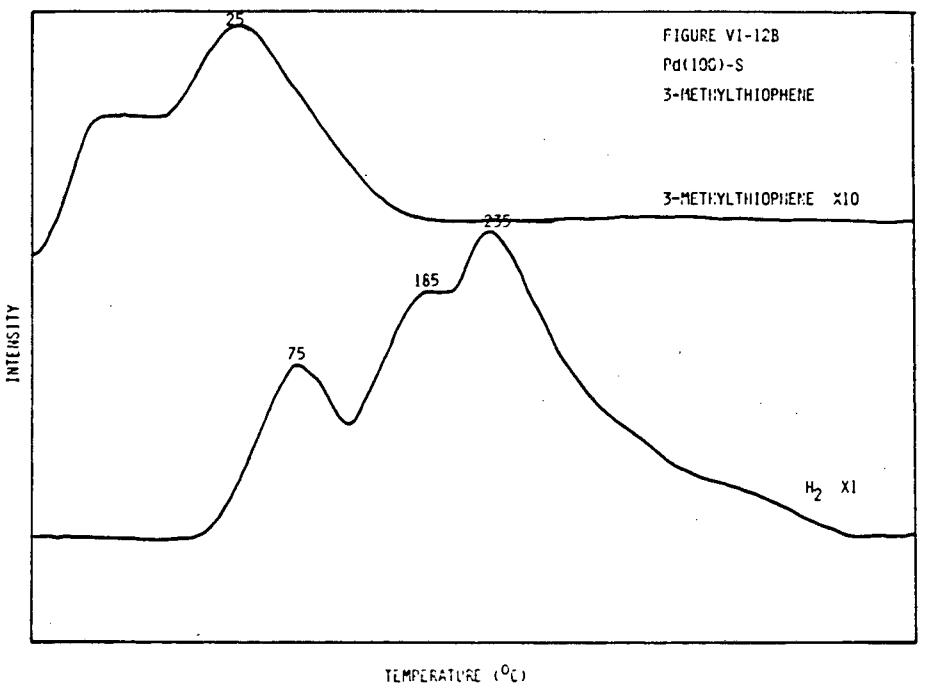
FIGURE VI-12B
Pd(100)-S
3-METHYLTHIOPHENE
3-METHYLTHIOPHENE X10
25
235
165
75
INTENSITY
H_2 X1
TEMPERATURE (°C)

XBL 846-2113

monolayer. On sulfur-covered Pd(100), θ_S = 0.14, reversible chemisorption was found to increase, along with a corresponding decrease in irreversible chemisorption. The resolution of the two high temperature hydrocarbon thermal desorption maxima decreased (see Figure VI-12B).

At high exposures (3.0 L), 3-methylthiophene exhibited increased reversible chemisorption on clean Pd(100), T_{max} = 20°C. The hydrogen thermal desorption spectrum contained three features: (1) a broad plateau-like desorption from 60°C to 90°C, (2) a maximum at 260°C, and (3) a pronounced shoulder on this maximum at 350°C (see Figure VI-13A). A sulfur coverage of 0.24 monolayer was observed after this experiment. At a sulfur coverage on Pd(100) of 0.25, a further increase in the molecular desorption of 3-methylthiophene, T_{max} = -5°C, and a decreased yield of hydrocarbon, indicated decreased irreversible chemisorption. Two hydrocarbon maxima were observed, at 260°C, and 420°C (see Figure VI-13B).

H. Pd(100) - 2,5-dimethylthiophene

At low 2,5-dimethylthiophene exposures (1.0 L), both reversible and irreversible chemisorption were observed. Three hydrocarbon thermal desorption maxima were observed, a sharp one at 75°C, a poorly resolved one at 120°C, and a broad one at 270°C. A 2,5-dimethylthiophene maximum was observed at 25°C. No benzene formation was observed at this exposure (see Figure VI-14A). A sulfur coverage of 0.14 was observed after this experiment. On sulfur-covered Pd(100), θ_S = 0.14, the fraction of 2,5-dimethylthiophene desorbing reversibly,

Figure VI-13. At an exposure of 3.0 L, increased molecular desorption is observed in the thermal desorption of 3-methylthiophene from Pd(100), as shown in A. A further increase is observed on sulfur-covered Pd(100), θ_S = 0.25, as shown in B.

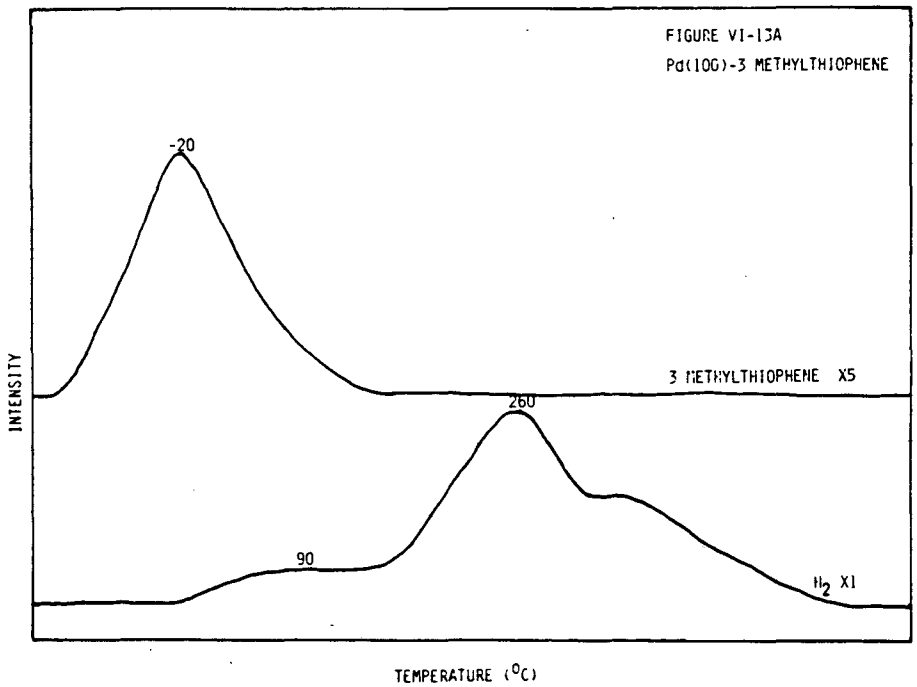
FIGURE VI-13A
Pd(100)-3 METHYLTHIOPHENE
-20
3 METHYLTHIOPHENE X5
260
90
H2 X1
INTENSITY
TEMPERATURE (°C)

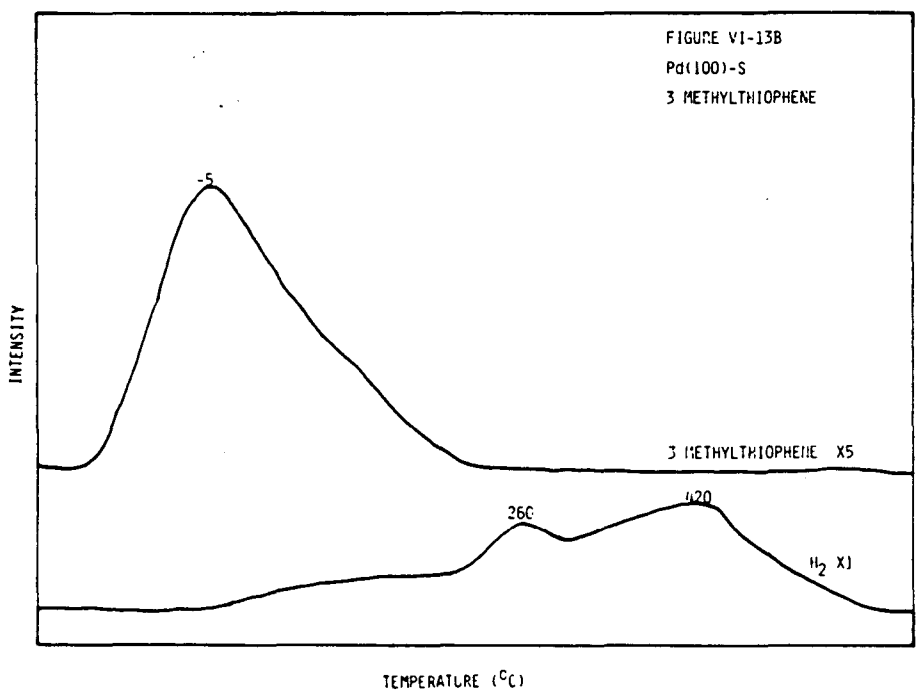
FIGURE VI-13B
Pd(100)-S
3 METHYLTHIOPHENE
-5
3 METHYLTHIOPHENE X5
260
420
H2 X1
INTENSITY
TEMPERATURE (°C)

XBL 846-2112

Figure VI-14. Chemisorption of 2,5-dimethylthiophene, at a low exposure, 1.0 L, on Pd(100) was primarily irreversible. Shown in A is the corresponding thermal desorption spectrum. At a sulfur coverage of 0.14 monolayer, an increase in the fraction of reversibly bound 2,5-dimethylthiophene was observed, as shown in B. A further increase in molecular desorption is illustrated in C at a sulfur coverage of 0.21 monolayer.

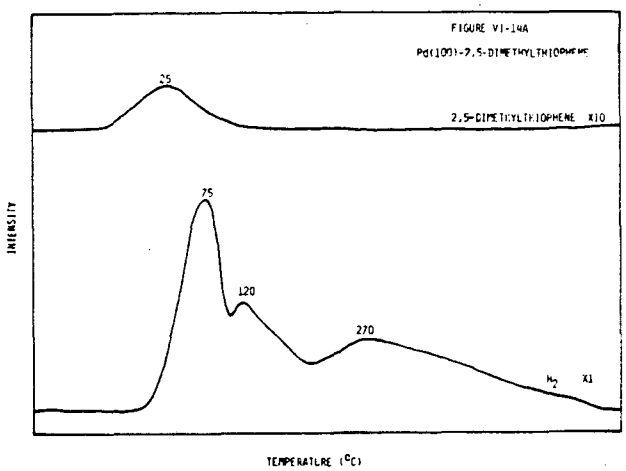
FIGURE VI-14A
25
2,5-DIMETHYLTHIOPHENE X10
75
120
270
H2 X1
INTENSITY
TEMPERATURE (°C)

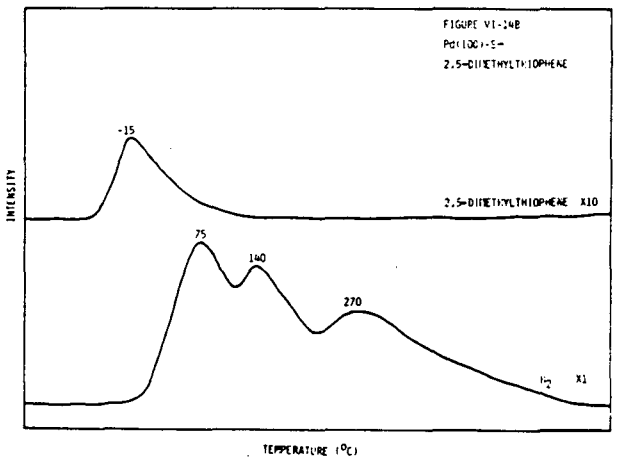
FIGURE VI-14B
-15
2,5-DIMETHYLTHIOPHENE X10
75
140
270
H2 X1
INTENSITY
TEMPERATURE (°C)

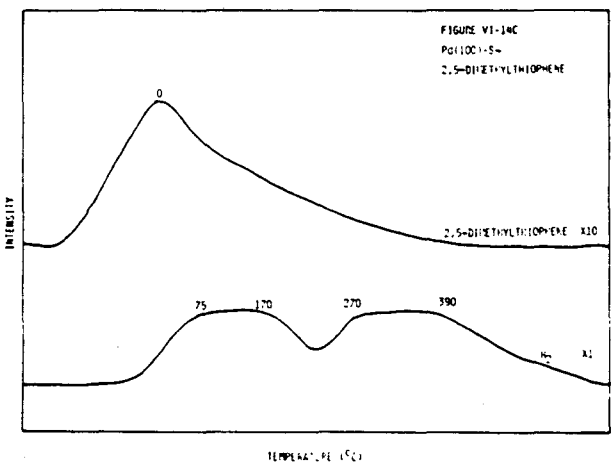
FIGURE VI-14C
0
2,5-DIMETHYLTHIOPHENE X10
75
170
270
390
H2 X1
INTENSITY

XBL 846-2108

T_{max} = -15°C, increased. The hydrocarbon thermal desorption spectrum exhibited three maxima, at 75°C, 140°C, and 270°C. The 75°C maximum decreased with respect to the other maxima (see Figure VI-14B). The sulfur coverage increased to 0.23 after this experiment. Further increasing the sulfur coverage, θ_S = 0.23, resulted in an increase in the fraction of thiophene reversibly chemisorbed on the surface, T_{max} = 0°C. Hydrogen desorbed in two plateau-like maxima, the first extending from 75°C to 170°C, and the second from 270°C to 390°C (see Figure VI-14C). At high 2,5-dimethylthiophene exposures (3.0 L), both reversible and irreversible chemisorption were observed on Pd(100). A 2,5-dimethylthiophene maximum was observed at 0°C. A benzene maximum was observed at 210°C; and three hydrogen maxima were observed, at 100°C, 170°C, and 380°C. In contrast to the low exposures, where the low temperature H_2 maximum was the most intense, the high temperature maximum, T_{max} = 380°C, was found to be the most intense (see Figure VI-15A). After this experiment, 0.25 monolayer of sulfur remained on the surface. Increased reversible chemisorption, T_{max} = -15°C, was observed on sulfur-covered Pd(100), θ_S = 0.25. The hydrogen thermal spectrum exhibited a decrease in the low temperature maximum, a broad plateau from 100°C to 200°C, and a large high temperature maximum at 440°C (see Figure VI-15B).

Figure VI-15. On clean Pd(100), benzene desorption was observed in the thermal desorption of 3.0 L of chemisorbed 2,5-dimethylthiophene. Molecular and hydrogen desorption are also shown in the spectrum in A. On sulfur-covered Pd(100), θ_S = 0.24, increased molecular desorption along with benzene desorption is illustrated in B.

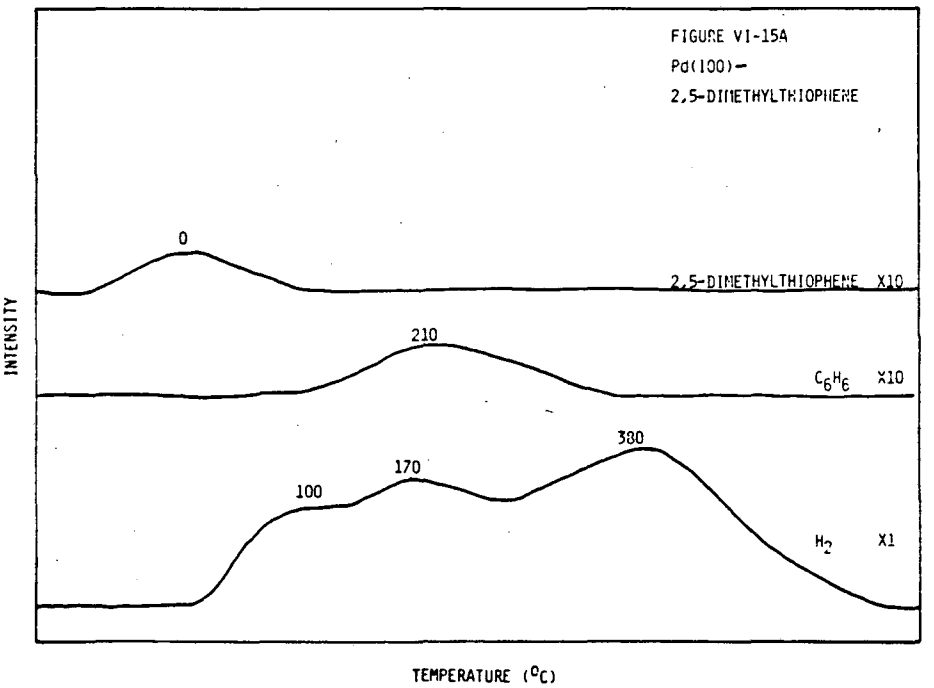
FIGURE VI-15A
Pd(100)-
2,5-DIMETHYLTHIOPHENE
0
2,5-DIMETHYLTHIOPHENE X10
210
C6H6 X10
380
170
100
H2 X1
INTENSITY
TEMPERATURE (°C)

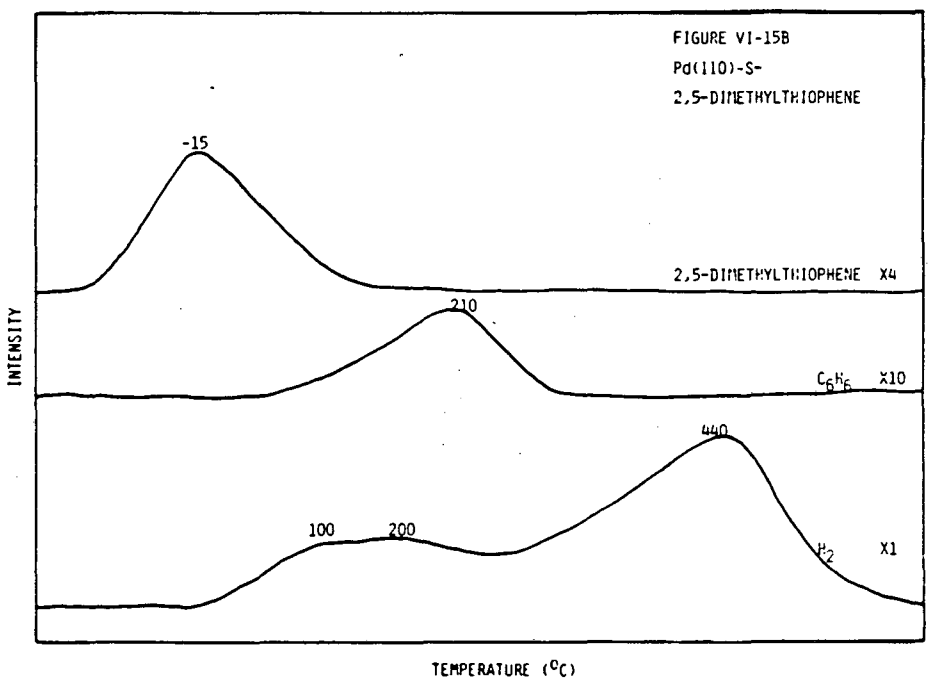
FIGURE VI-15B
Pd(110)-S-
2,5-DIMETHYLTHIOPHENE
-15
2,5-DIMETHYLTHIOPHENE X4
210
C6H6 X10
440
100
200
H2 X1
INTENSITY
TEMPERATURE (°C)

XBL 846-2111

Figure VI-16. No butadiene formation was observed in the thermal desorption spectrum of thiophene, 1.0 L, from Pd(110), as shown in A. Hydrogen desorption and molecular desorption were evident. On sulfur-covered Pd(110), the desorption of thiophene became more quantitative, with increased sulfur coverage. Shown in B and C are spectra at sulfur coverages of 0.10 monolayer and 0.30 monolayer, respectively.

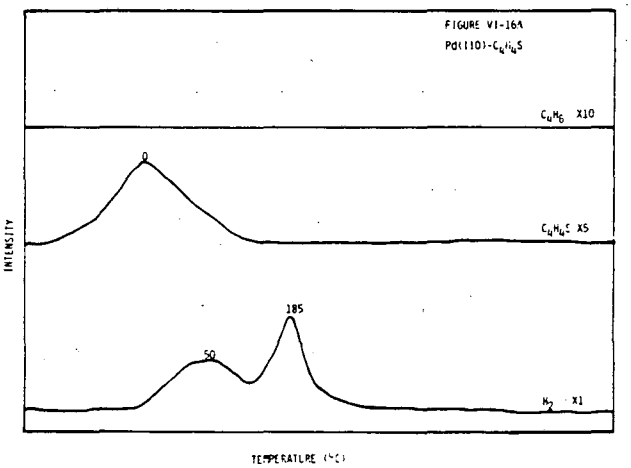
FIGURE VI-16A
Pd(110)-C_4H_4S
C_4H_6 X10
0
C_4H_4S X5
185
50
H_2 X1
INTENSITY
TEMPERATURE (°C)

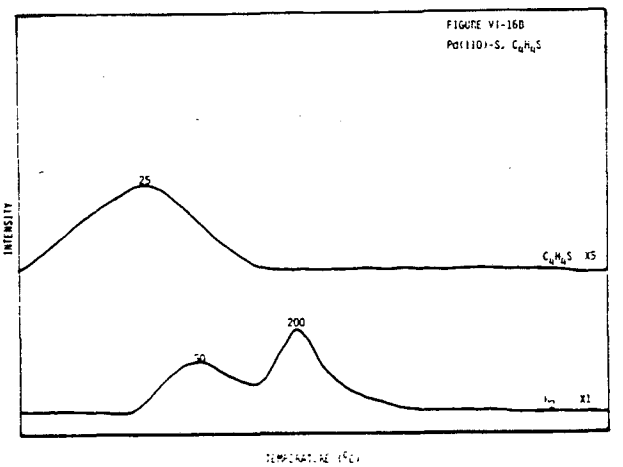
FIGURE VI-16B
Pd(110)-S, C_4H_4S
25
C_4H_4S X5
200
50
X1
INTENSITY

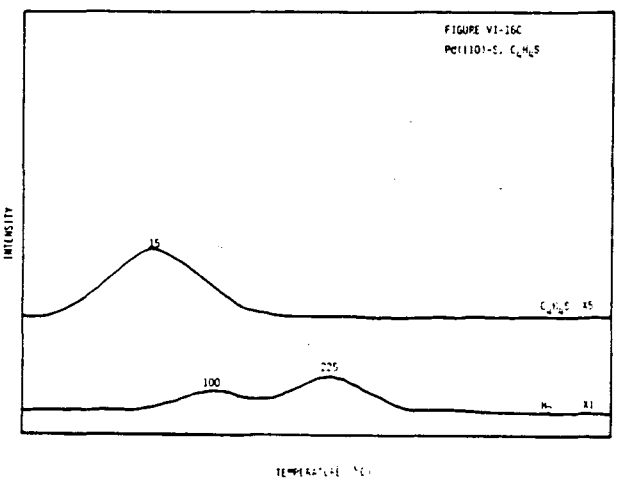
FIGURE VI-16C
Pd(110)-S, C_4H_4S
15
100
X1
INTENSITY

XBL 846-2107

I. Pd(110) - Thiophene

At low exposures (1.0 L), thiophene was observed to undergo both reversible and irreversible chemisorption on Pd(110). Two hydrogen thermal desorption maxima were observed, at 50°C, and 185°C. A single thiophene maximum was observed at 0°C (see Figure VI-16A). At a sulfur coverage of 0.10 monolayer, an increase was observed in the fraction of thiophene desorbing intact from the surface, T_{max} = 25°C, and a decrease was observed in the two hydrogen thermal desorption maxima, at 50°C, and 200°C (see Figure VI-16B). At higher sulfur coverages, θ_S = 0.30, a further decrease was observed in the hydrogen thermal desorption maxima at 100°C, and 225°C. A thiophene maximum was observed at 15°C (see Figure VI-16C). At higher thiophene exposure (3.0 L), along with reversible and irreversible chemisorption, butadiene was found to desorb from clean Pd(110) (see Figure VI-17A). A single hydrogen thermal desorption maximum was observed at 270°C; two thiophene maxima were observed, at -50°C, and 50°C; and a butadiene maximum was observed at 150°C. On sulfur-covered Pd(110), θ_S = 0.28, an increase in the fraction of reversibly bound thiophene was observed, with two maxima observed, at -70°C, and 50°C. A decrease in the hydrogen thermal desorption maximum at 270°C was observed. Decreased butadiene desorption was also observed (see Figure VI-17B). After this experiment, the sulfur coverage increased to 0.38 monolayer. At a sulfur coverage of 0.38 monolayer, chemisorption of thiophene on Pd(110) was largely reversible, with three thermal desorption maxima,

Figure VI-17. Butadiene desorption was observed in the thermal desorption of 3.0 L of thiophene from Pd(110), as illustrated in the spectrum in A. Increased molecular desorption and decreased butadiene desorption were observed on surfaces with sulfur coverages of 0.28 monolayer (B) and 0.38 monolayer (C).

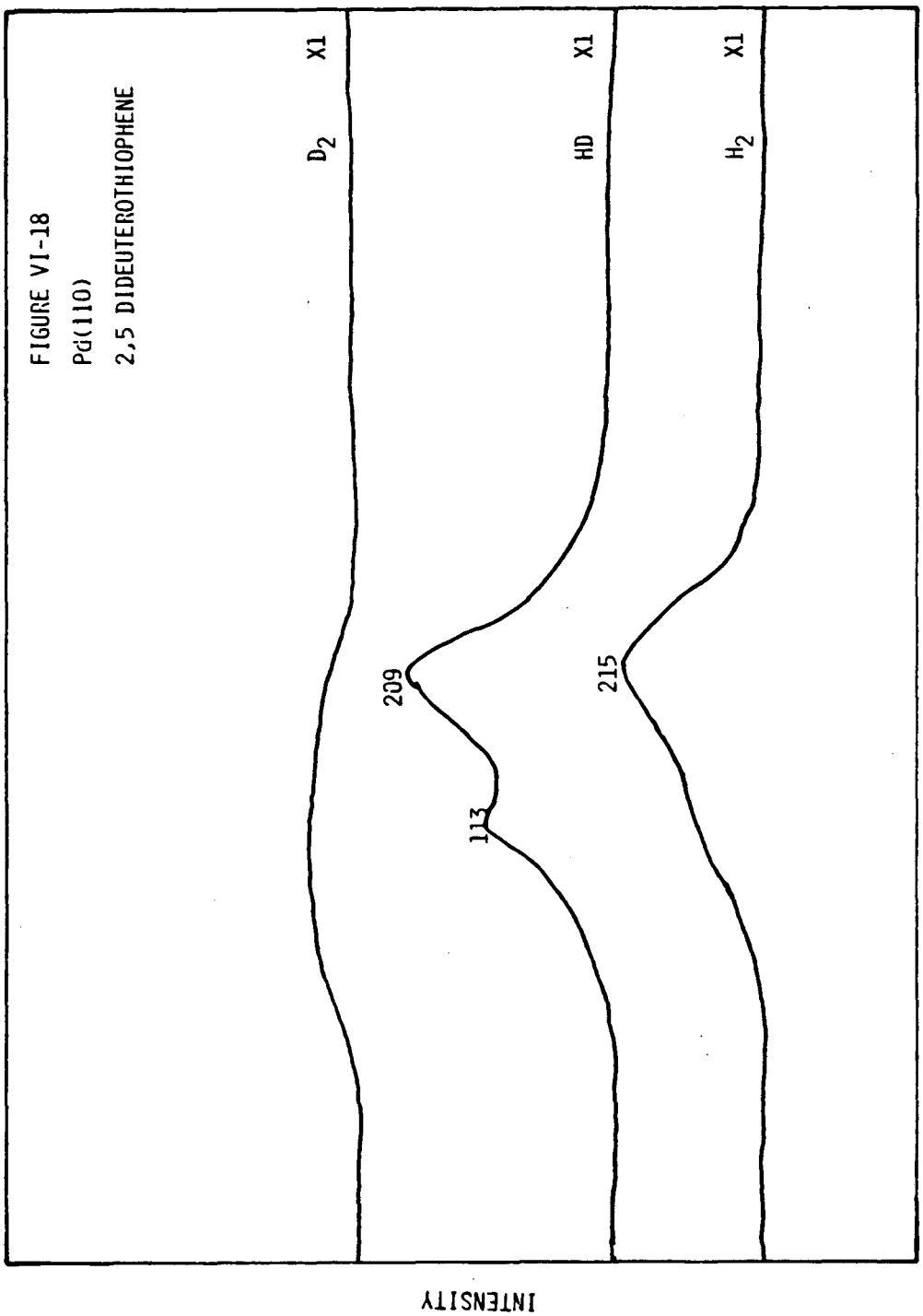
FIGURE VI-18
Pd(110)
2,5 DIDEUTEROTHIOPHENE
D_2 X1
HD X1
H_2 X1
209
113
215
INTENSITY
TEMPERATURE (°C)

XBL 846-2099

Figure VI-18. No regioselective carbon–hydrogen bond scission was observed in the thermal desorption of 1.0 L of 2,5-dideuterothiophene from Pd(110), as shown in this spectrum.

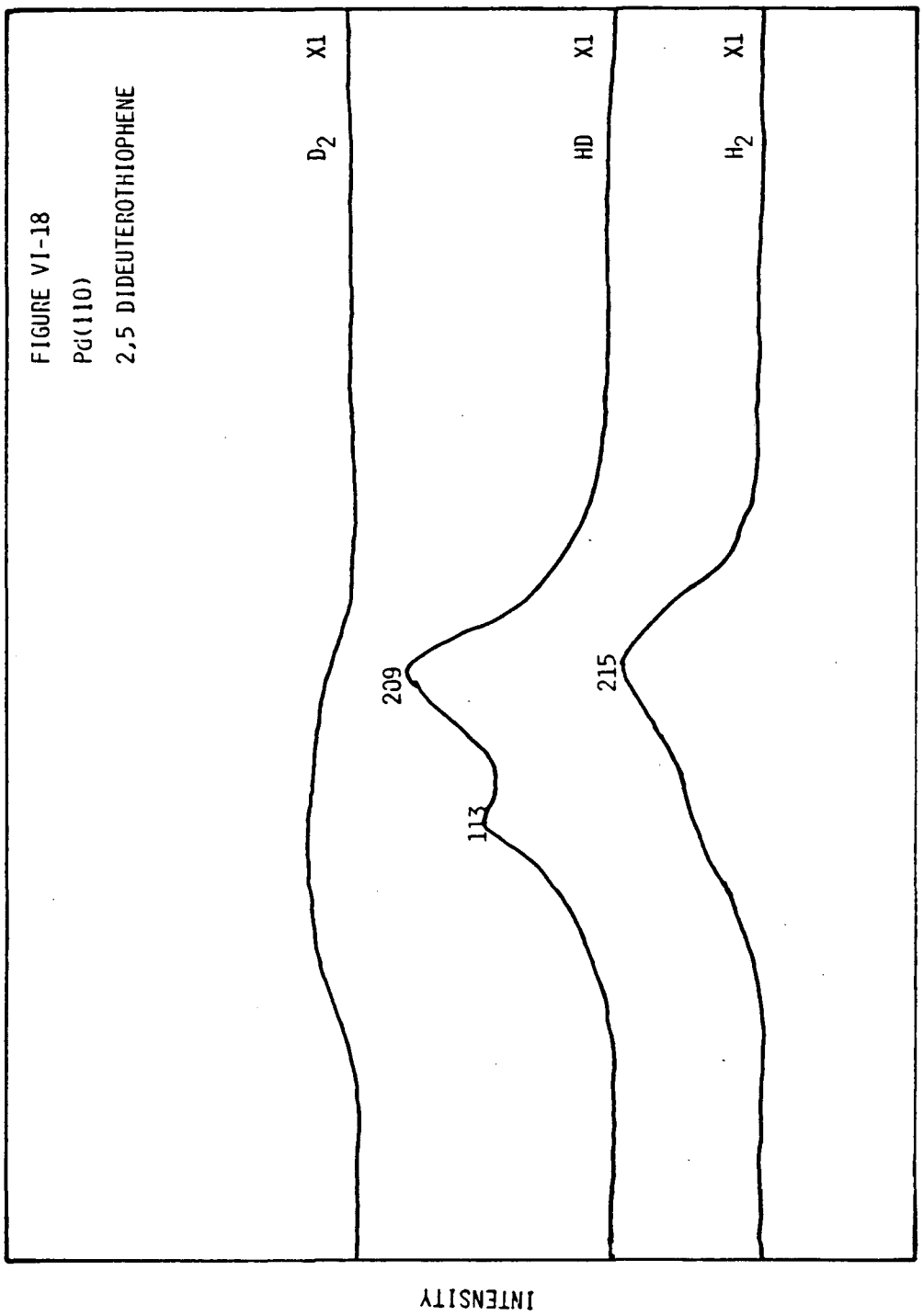
FIGURE VI-18
Pd(110)
2,5 DIDEUTEROTHIOPHENE
D_2 X1
HD X1
H_2 X1
209
113
215
INTENSITY
TEMPERATURE (°C)

XBL 846-2099

at -75°C, -35°C, and 50°C. A small butadiene maximum was observed at 150°C, and a hydrogen maximum was observed at 270°C (see Figure VI-17C).

J. Pd(110) - 2,5-dideuterothiophene

At low exposures (1.0 L) of 2,5-dideuterothiophene, all three species, H_2, HD, and D_2, were found to desorb from Pd(110). H_2 desorbed in a broad maximum at 215°C, with a long leading edge. HD desorbed in two maxima, at 115°C, and 205°C. D_2 was found to desorb in a broad maximum from 0°C to 200°C (see Figure VI-18). At increasing sulfur coverage, the yield of all three species decreased. At higher 2,5-dideuterothiophene exposures (3.0 L), two maxima, at 135°C, and 235°C, were observed for H_2, HD, and D_2 (see Figure VI-19A). On sulfur-covered Pd(110), θ_S = 0.23, a single maximum at 265°C was observed for H_2, HD, and D_2 (see Figure VI-19B).

K. Pd(110) - 3-methylthiophene

Both reversible and irreversible chemisorption were observed at low exposure (1.0 L) on Pd(110). A 3-methylthiophene thermal desorption maximum was observed at 25°C, and two hydrogen maxima were observed, at 50°C, and 220°C (see Figure VI-20A). After this experiment, the sulfur coverage was 0.20 monolayer. No hydrocarbons were observed to desorb from the surface. On sulfur-covered Pd(110), θ_S = 0.20, the fraction of 3-methylthiophene reversibly chemisorbed increased, with two thermal desorption maxima observed, at -80°C, and 40°C. Hydrogen

Figure VI-19. On both clean and sulfur-covered Pd(110), θ_S = 0.23, no regioselective carbon–hydrogen bond scission was observed in the thermal desorption of 3.0 L of 2,5-dideuterothiophene from Pd(110).

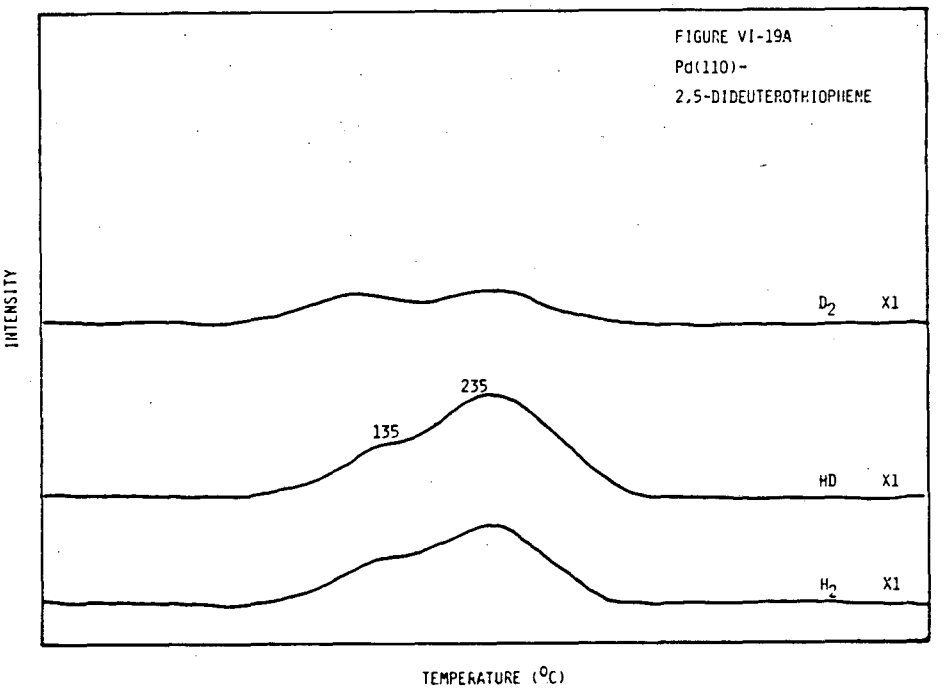
FIGURE VI-19A
Pd(110)-
2,5-DIDEUTEROTHIOPHEME
INTENSITY
D_2 X1
235
135
HD X1
H_2 X1
TEMPERATURE (°C)

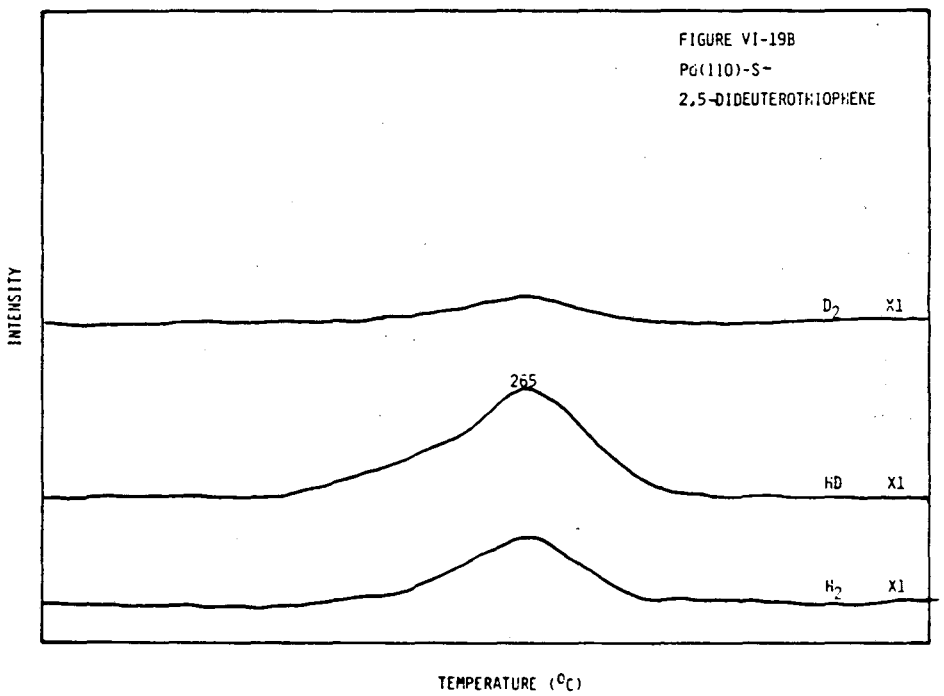
FIGURE VI-19B
Pd(110)-S-
2,5-DIDEUTEROTHIOPHENE
INTENSITY
D_2 X1
265
HD X1
H_2 X1
TEMPERATURE (°C)

XBL 846-2110

Figure VI-20. Chemisorption of 3-methylthiophene on Pd(110) at an exposure of 1.0 L exhibited both reversible and irreversible chemisorption in the subsequent thermal desorption experiment. Shown here are thermal desorption spectra of clean (A) and sulfur-covered surfaces, θ_S = 0.20 (B) and θ_S = 0.32 (C).

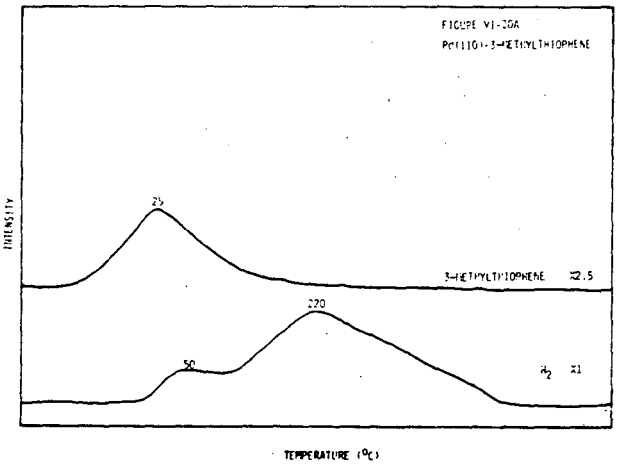
INTENSITY
25
3-METHYLTHIOPHENE X2.5
220
50
H2 X1
TEMPERATURE (°C)

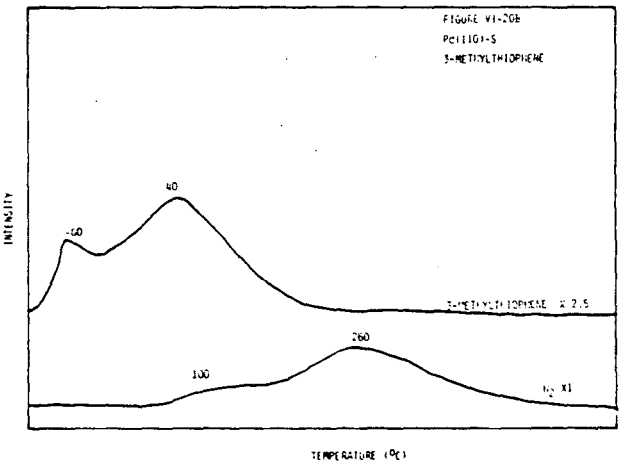
INTENSITY
40
-60
260
100
TEMPERATURE (°C)

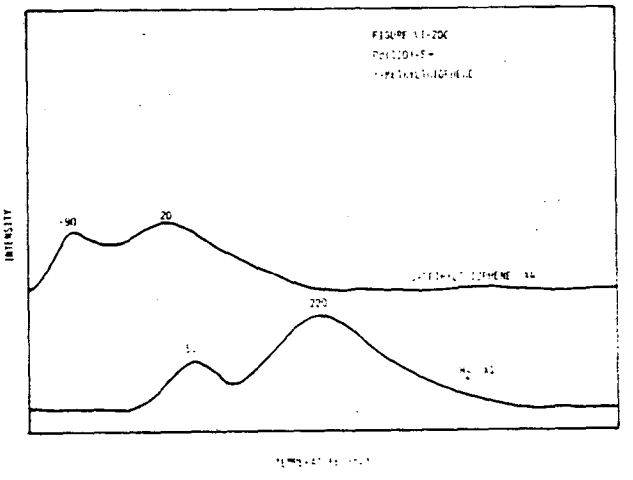
INTENSITY
-90
20
220

XBL 846-2105

Figure VI-21. At an exposure of 3.0 L, increased molecular desorption of 3-methylthiophene from both clean and sulfur-covered Pd(110) surfaces was observed. Spectra A, B, and C correspond to clean, θ_S = 0.26, and θ_S = 0.37, respectively.

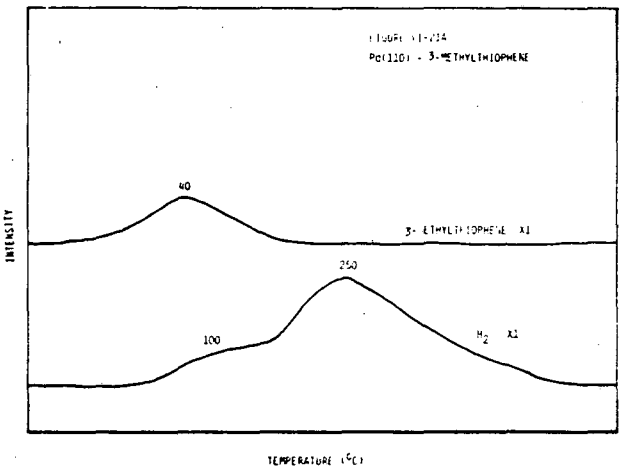
Pd(110) - 3-METHYLTHIOPHENE
40
3- ETHYLTHIOPHENE X1
250
100
H2 X1
INTENSITY
TEMPERATURE (°C)

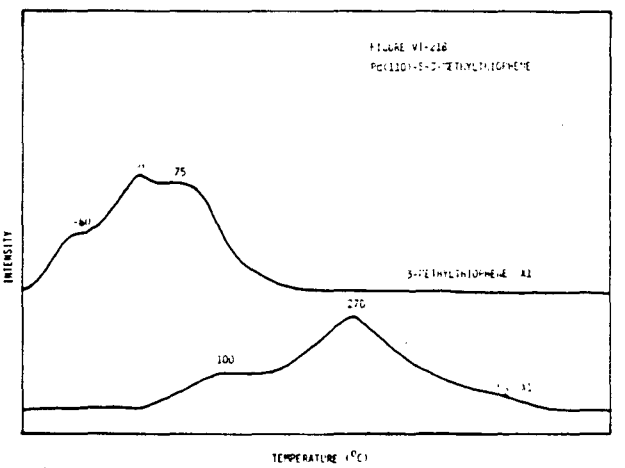
75
3-METHYLTHIOPHENE X1
270
100
INTENSITY
TEMPERATURE (°C)

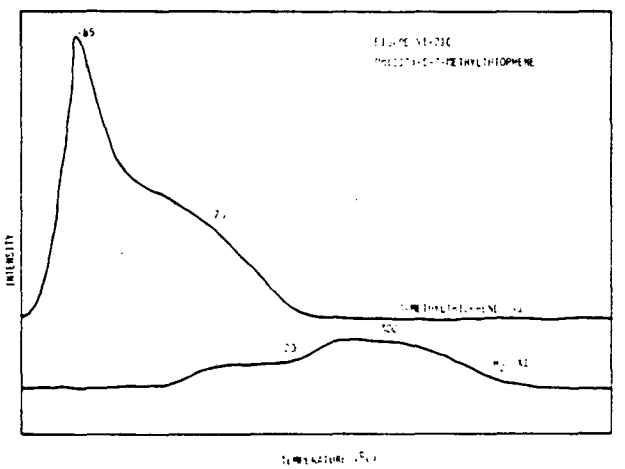
85
INTENSITY

XBL 846-2104

desorbed at maximal rates at 100°C, and 260°C (see Figure VI-20B). At higher exposures (3.0 L), an increase in the fraction of intact 3-methylthiophene desorbed from clean Pd(110), as compared to low exposures. A 3-methylthiophene maximum was observed at 40°C, and two hydrogen maxima were observed, at 100°C, and 250°C (see Figure VI-21A). On sulfur-covered Pd(110), θ_S = 0.20, three poorly resolved 3-methylthiophene maxima were observed, at -80°C, 0°C, and 75°C. Two hydrogen maxima were also observed, at 100°C, and 270°C (see Figure VI-21B). With increasing sulfur coverage, θ_S = 0.37, the chemisorption of 3-methylthiophene is largely reversible, with three poorly resolved maxima, at -85°C, -15°C, and 75°C. A plateau-like desorption from 100°C to 200°C, and a broad maximum at 300°C were observed (see Figure VI-21C).

L. Pd(110) - 2,5-dimethylthiophene

Benzene formation was observed in the thermal desorption spectrum of chemisorbed (1.0 L) 2,5-dimethylthiophene on clean Pd(110). A benzene thermal desorption maximum was observed at 170°C. Three hydrogen thermal desorption maxima were observed, at 0°C, 150°C, and 265°C; and a 2,5-dimethylthiophene maximum was observed at 30°C (see Figure VI-22A). On sulfur-covered Pd(110), θ_S = 0.20, the yield of benzene decreased (T_{max} = 150°C); an increase in molecular desorption, T_{max} = 35°C, was observed; and a corresponding decrease in the amount of hydrogen desorbing from the surface was observed (T_{max} = 100°C and 330°C) (see Figure VI-22B). At a sulfur coverage of 0.40

Figure VI-22. Benzene formation is shown from the thermal desorption of 2,5-dimethylthiophene chemisorbed on Pd(110). The presence of sulfur decreased of amount of benzene desorption. Shown here are thermal desorption spectra at 1.0 L exposure of 2,5-dimethylthiophene on clean (A) and sulfur-covered Pd(110) surfaces, θ_S = 0.20 (B) and θ_S = 0.22 (C).

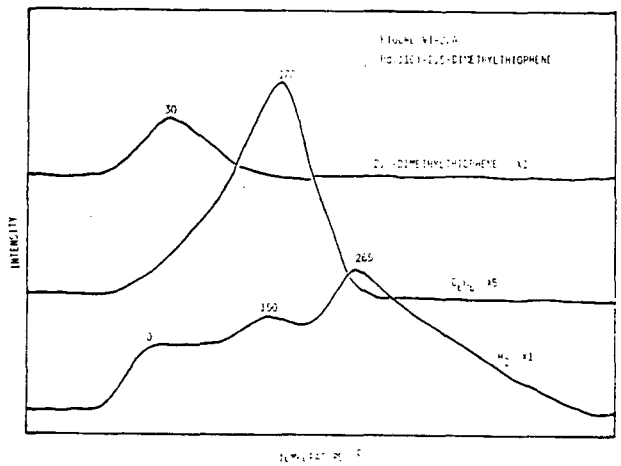

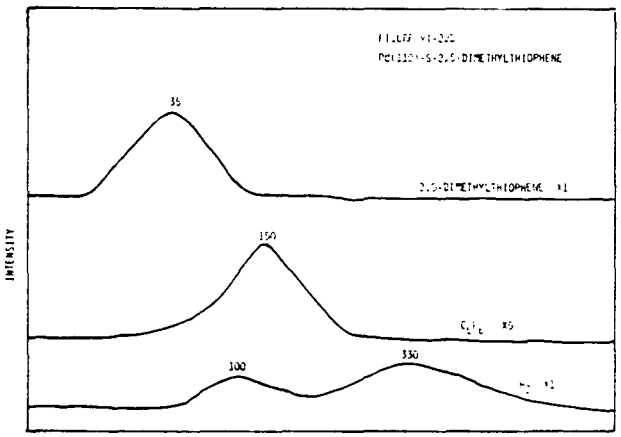

TEMPERATURE (°C)

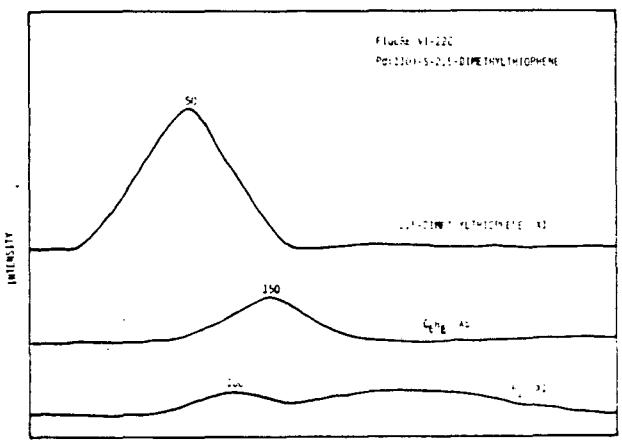

TEMPERATURE (°C)

XBL 846-2103

Figure VI-23. At 2,5-dimethylthiophene exposures of 3.0 L, benzene formation was observed in the thermal desorption spectra of both clean and sulfur-covered Pd(110). Shown here are the spectra for clean (A) and sulfur-covered Pd(110), θ_S = 0.24 (B).

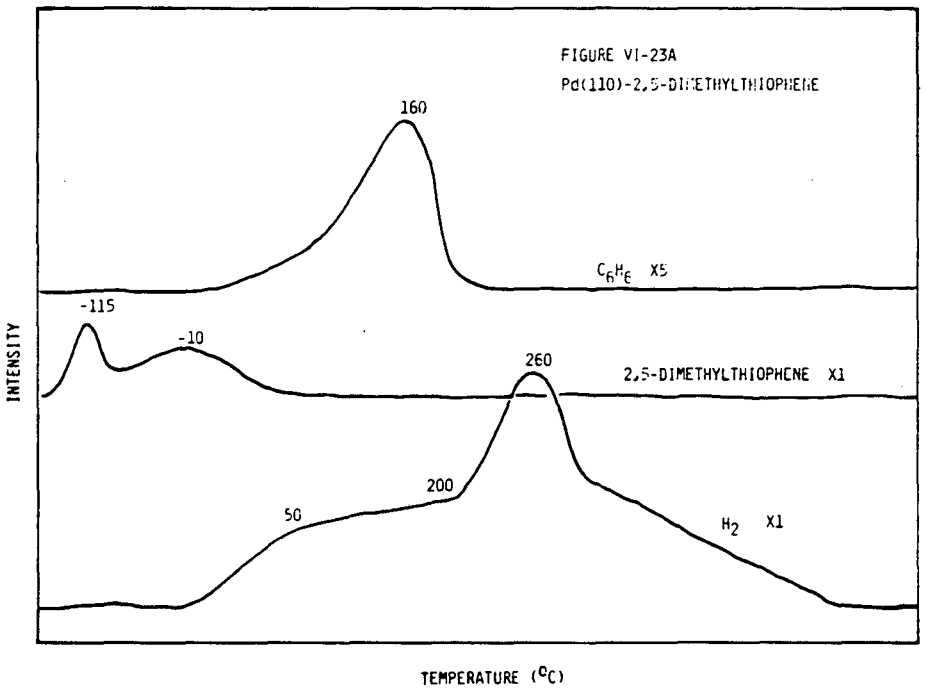
FIGURE VI-23A
Pd(110)-2,5-DIMETHYLTHIOPHENE
160
C_6H_6 X5
-115
-10
260
2,5-DIMETHYLTHIOPHENE X1
200
50
H_2 X1
INTENSITY
TEMPERATURE (°C)

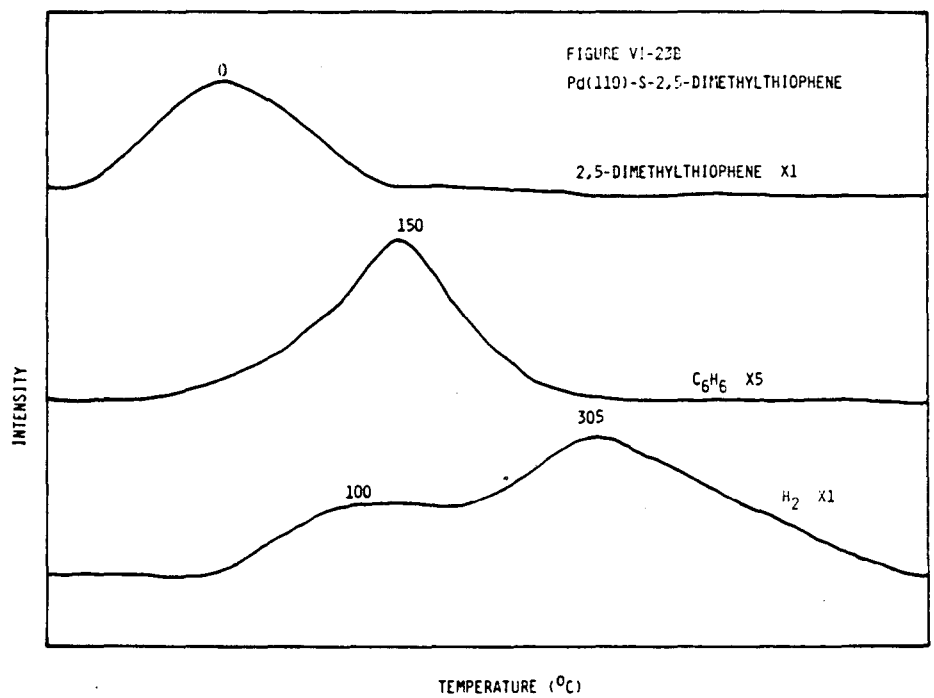
FIGURE VI-23B
Pd(110)-S-2,5-DIMETHYLTHIOPHENE
0
2,5-DIMETHYLTHIOPHENE X1
150
C_6H_6 X5
305
100
H_2 X1
INTENSITY
TEMPERATURE (°C)

XBL 846-2116

monolayer, a further decrease was observed in the benzene yield, T_{max} = 150°C. An increase in the 2,5-dimethylthiophene thermal desorption maximum at 50°C was observed, as well as a decrease in the hydrogen desorption (see Figure VI-22C). At a 2,5-dimethylthiophene exposure of 3.0 L, the yield of benzene decreased from clean Pd(110), as compared to a 1.0-L exposure. Two 2,5-dimethylthiophene maxima were observed, at -115°C, and -70°C. Hydrogen was observed in a broad plateau-like maximum from 50°C to 200°C, with another maximum at 260°C (see Figure VI-23A). On sulfur-covered Pd(110), θ_S = 0.24, the fraction of 2,5-dimethylthiophene desorbing intact increased, T_{max} = 0°C; the amount of irreversible desorption decreased (H_2 T_{max} = 100°C and 35°C); and the yield of benzene (T_{max} = 150°C) remained unchanged (see Figure VI-23B).

DISCUSSION

Chemisorbed thiophene and its methylsubstituted derivatives were found to exhibit complex chemistry on palladium single-crystal surfaces. Among these processes observed were molecular desorption, decomposition, and hydrocarbon formation. The chemistry of thiophene will be discussed first, followed by that of 3-methylthiophene and 2,5-dimethylthiophene.

All three palladium surfaces investigated, (111), (100), and (100), exhibited butadiene formation in the thermal desorption of thiophene. On the atomically flat surfaces, (111) and (100), a

greater yield of butadiene was observed compared to the superstepped (110) surface. At high sulfur coverages, butadiene formation was suppressed on all surfaces.

The hydrogen thermal desorption spectrum derived from chemisorbed thiophene was found to be a sensitive function of thiophene exposure. At low exposures, two H_2 thermal desorption maxima were observed on Pd(111), at 175°C and 370°C. Increasing the exposure resulted in a shift to a single hydrogen maximum at 415°C. These changes may be related to the orientation of the chemisorbed thiophene. At low exposures, thiophene may be bound in π fashion; that is, the plane of the thiophene ring containing the sulfur and four carbon atoms may be parallel or nearly parallel to the surface. In this orientation, the two C-H bonds adjacent to the surface may be cleaved first, followed by the other two C-H bonds. These studies do not define when the carbon-sulfur bond is broken, before or after C-H bond scission. At higher surface coverages of thiophene, an orientation change of thiophene may occur in which the plane of the thiophene ring makes an angle with the surface. In this configuration the C-H bonds would be far from the surface, and the high temperature hydrogen maximum may be expected. Similar behavior was exhibited from phenylacetylene chemisorbed on Pd(100).[7] Hydrogen did not desorb until very high temperatures were reached (T_{max} = 440°C). A species such as $C\text{-}CH_2C_6H_5$ similar to ethylidyne was postulated. If carbon-sulfur bond scission occurs before carbon-hydrogen bond scission, a surface metallocycle may occur. There is precedent in the organometallic

literature for sulfur extrusion from thiophene with metal complexes or metal atoms to form metallocycles.[8] Near-edge x-ray absorption fine-structure studies of chemisorbed thiophene on Pt(111) are also suggestive of sulfur extrusion and subsequent metallocycle formation on the surface.[9] Similar trends in the hydrogen thermal desorption derived from thiophene were also observed on both Pd(100) and Pd(110).

Butadiene formation may also go through this metallocycle intermediate. Butadiene chemisorption was found to be largely irreversible on palladium single-crystal surfaces. The temperature of desorption of butadiene (~120-150°C) derived from thiophene suggests that this reactively formed butadiene is not the same chemisorbed state as butadiene chemisorbed on palladium surfaces. It is tempting to speculate that the temperature of desorption of the reactively formed butadiene is nearly the same as the temperature where carbon-sulfur bond scission occurs.

Chemisorbed 3-methylthiophene on all three palladium surfaces exhibited no hydrocarbon formation at low 3-methylthiophene exposure. A low temperature hydrogen thermal desorption maximum, T_{max} = 75°C, was observed, along with two others, at 220°C, and 390°C, on Pd(111). The appearance of this low temperature H_2 maximum suggests that 3-methylthiophene is also in π-bonding orientation at low coverage. A shift to high temperature in the hydrogen thermal desorption was also observed, suggesting a change in orientation to a more perpendicular bonding for 3-methylthiophene. On the (100) and the (110) surfaces at low exposure, a marked increase in the intensity of the hydrogen

thermal desorption occurred at high temperatures (T_{max} = 250°C). A low temperature hydrogen maximum was also observed. These results suggest that at low exposure, a significant fraction of the 3-methylthiophene may have orientation nonparallel to the surface.

Benzene formation was observed from chemisorbed 2,5-dimethylthiophene on all three surfaces at high exposures. The (110) surface exhibited the highest yield of benzene, followed by the (111) and the (100) surfaces. Facile extrusion of sulfur into the troughs of the (110) surface may account for the increased activity of this surface for benzene formation. As with butadiene formation from thiophene, benzene formation was inhibited with increasing sulfur coverage. The mechanism of inhibition is no doubt related to the fact that, on sulfur-covered surfaces, sites of sulfur extrusion are already blocked. Also, as expected, an increase in the fraction of reversibly bound thiophene is also observed.

Sequential adsorption of D_2 and 2,5-dimethylthiophene on Pd(111) resulted in incorporation of at least four deuterium atoms in the reactively formed benzene. The H-D exchange in this process was much larger than for the sequential adsorption of D_2 and benzene. These results suggest that reversible carbon-hydrogen bond scission is occurring in a precursor to benzene formed from 2,5-dimethylthiophene. This exchange most probably is occurring on the methyl C-H bonds.

On all three surfaces, no regioselective carbon-hydrogen bond scission was observed in the thermal desorption of 2,5-dideuterothiophene. On Ni(100),[10] regioselective bond scission was evident,

whereas on Ni(111) it was not. On nickel surface no hydrogen formation was evident. The formation of butadiene on palladium surfaces may influence this process.

CONCLUSIONS

In this chapter, the desulfurization of thiophene and two methylsubstituted derivatives has been shown to be a sensitive function of both surface structure and composition. These results suggest that HDS activity of real catalysts may be correlated to the structure and composition of the catalyst. For example, the HDS of 2,5-dimethylthiophene should readily occur on a catalyst that has an orientation predominantly of (110), while HDS of thiophene may occur more readily on catalysts predominantly (111) or (100). Furthermore, the results of this chapter demonstrate the usefulness of ultrahigh-vacuum studies on palladium single crystals as models for chemistry that usually occurs at much higher pressures.

REFERENCES

1. (a) E. L. Muetterties, R. M. Wexler, T. M. Gentle, K. L. Shanahan, D. G. Klarup, K. B. Lewis, and T. B. Rucker, to be published. (b) A. J. Gellman, M. H. Farias, M. Salmeron, and G. A. Somorjai, Surf. Sci. 1984, 136, 217.
2. R. M. Wexler, M. C. Tsai, C. M. Friend, and E. L. Muetterties, J. Am. Chem. Soc. 1982, 104, 2034.
3. A. L. Johnson, E. L. Muetterties, and J. Stohr, J. Am. Chem. Soc. 1983, 105, 7183.
4. B. C. Gates, J. R. Katzer, and G. C. A. Schuit, Chemistry of Catalytic Processes, McGraw-Hill Book Co., New York, 1979, p. 393.
5. T. A. Pecoraro and R. R. Chianelli, J. Catal. 1981, 67, 430.
6. A. J. Gellman, M. H. Farias, and G. A. Somorjai, J. Catal., in press.
7. T. M. Gentle and E. L. Muetterties, J. Phys. Chem. 1983, 87, 2469.
8. (a). H. D. Kaesz, R. B. King, T. A. Manuel, L. D. Nichols, and F. O. A. Stone, J. Am. Chem. Soc. 1960, 82, 4749. (b) T. Chivers and P. L. Timms, J. Organomet. Chem. 1976 118, C37 (c) G. Dettalf and E. Weiss, J. Organomet. Chem. 1976, 108, 213.
9. A. L. Johnson, J. Stohr, and T. M. Gentle, private communication.
10. R. Wexler, Ph.D. Thesis, University of California Berkeley, 1983.

VII. CATALYTIC CHEMISTRY OF PALLADIUM SURFACES

INTRODUCTION

Reaction steps that may ensue after the chemisorption on a transition metal surface are thermodynamically a sensitive function of temperature and pressure. Low temperatures and high H_2 pressures, for example, favor C–H bond formation. The unusual conditions employed for some surface science, i.e., ultralow pressure and surface coverages of a monolayer or less, are not optimal for hydrogenation (C–H bond formation), addition, and oligomerization reactions. These involve bimolecular steps which are not favored by low surface coverages (particularly if the mobility of the surface species is low). Also, the probability of hydrogenation is low because the thermodynamic activity of chemisorbed hydrogen atoms is low at pressures of 10^{-10} to 10^{-11} torr. Hence, the typical ultrahigh-vacuum--low temperature course for chemisorbed hydrocarbons is dehydrogenation,[1-8] although there are well-established exceptions such as the hydrogenation of acetylene chemisorbed on Pt(111) from Pt(111)–CCH_3.[9-11] In the course of this thesis, it has been found that palladium surfaces under ultrahigh-vacuum conditions exhibit chemistry demonstrably different from those of nickel and platinum.[12] In this chapter the catalytic chemistry of single-crystal palladium surfaces under ultrahigh-vacuum conditions will be discussed. Some of this chemistry will be compared with reactions performed on polycrystalline films and supported

catalysts at much higher pressures. The high pressure studies were performed in collaboration with Mr. Richard Wilmer, Mr. Thomas Rucker, and Mr. Kenneth Lewis.

Dehydrogenation of cyclohexene and isomers of methylcyclohexene were studied on both single-crystal palladium surfaces under ultrahigh-vacuum conditions and polycrystalline films at much higher pressures. Similar chemistry was observed to occur in both pressure regimes.

RESULTS

Palladium surfaces under ultrahigh-vacuum conditions exhibit chemistry demonstrably different from those of nickel and platinum. Specifically, acetylene trimerizes to form benzene on the low Miller-index surfaces of palladium. The influence of structure, crystallography, and composition was discussed in Chapter III of this thesis. Other reactions compete with the trimerization, such as hydrogenation and decomposition, but benzene formation was found to be the major reaction, at least on Pd(111) surfaces near saturation coverage, provided that acetylene is initially adsorbed at low temperature, <-100°C, whereas benzene formation was a minor reaction at 25°C. The presence of adatoms was shown to influence the formation of benzene on all three surfaces studied, the (111), (100), and (110). For example, it was demonstrated that on a sulphided Pd(111) surface, benzene formation was the only process observed to occur; hydrogenation and decomposition reactions were both suppressed. Benzene formation

in these reactions is presumably acetylene trimerization, a reaction not commonly observed for metallic catalysts, but common to metal coordination catalysts.[13] The surface chemistry of other acetylenic compounds and mixtures of these compounds has been investigated on palladium single crystals.

The chemistry of acetylene observed on Pd(111) is markedly different from that observed on either Ni(111) or Pt(111).[14] Chemisorbed acetylene on Ni(111) yields no ethylene or benzene upon thermal desorption. Benzene could not be displaced by trimethylphosphene from a surface state formed by chemisorption of acetylene on Ni(111). Chemisorbed acetylene on Pt(111) yielded ethylene, but benzene was not observed.

Toluene could be generated as the major product by heating a mixture of propyne and acetylene on Pd(111). In these studies propyne and acetylene were sequentially adsorbed on Pd(111) at -120°C. The order of adsorption was found to influence the product distribution; benzene formation was also observed. If propyne at 2.0 L was adsorbed followed by acetylene at 2.0 L, toluene was found to be the predominant hydrocarbon product (see Figure VII-1). A toluene thermal desorption maximum was observed at 0°C; and two benzene thermal desorption maxima were observed, at -25°C and 220°C. Increasing the initial exposure of propyne to 3.0 L and decreasing the acetylene exposure to 1.0 L resulted in an increase in the yield of toluene and a decreased yield

Figure VII-1. Thermal desorption of the surface formed by sequential adsorption of propyne, 3.0 L, and acetylene, 2.0 L, on Pd(111) resulted in the formation of both toluene and benzene. Shown in this figure are the traces for hydrogen, benzene, and toluene.

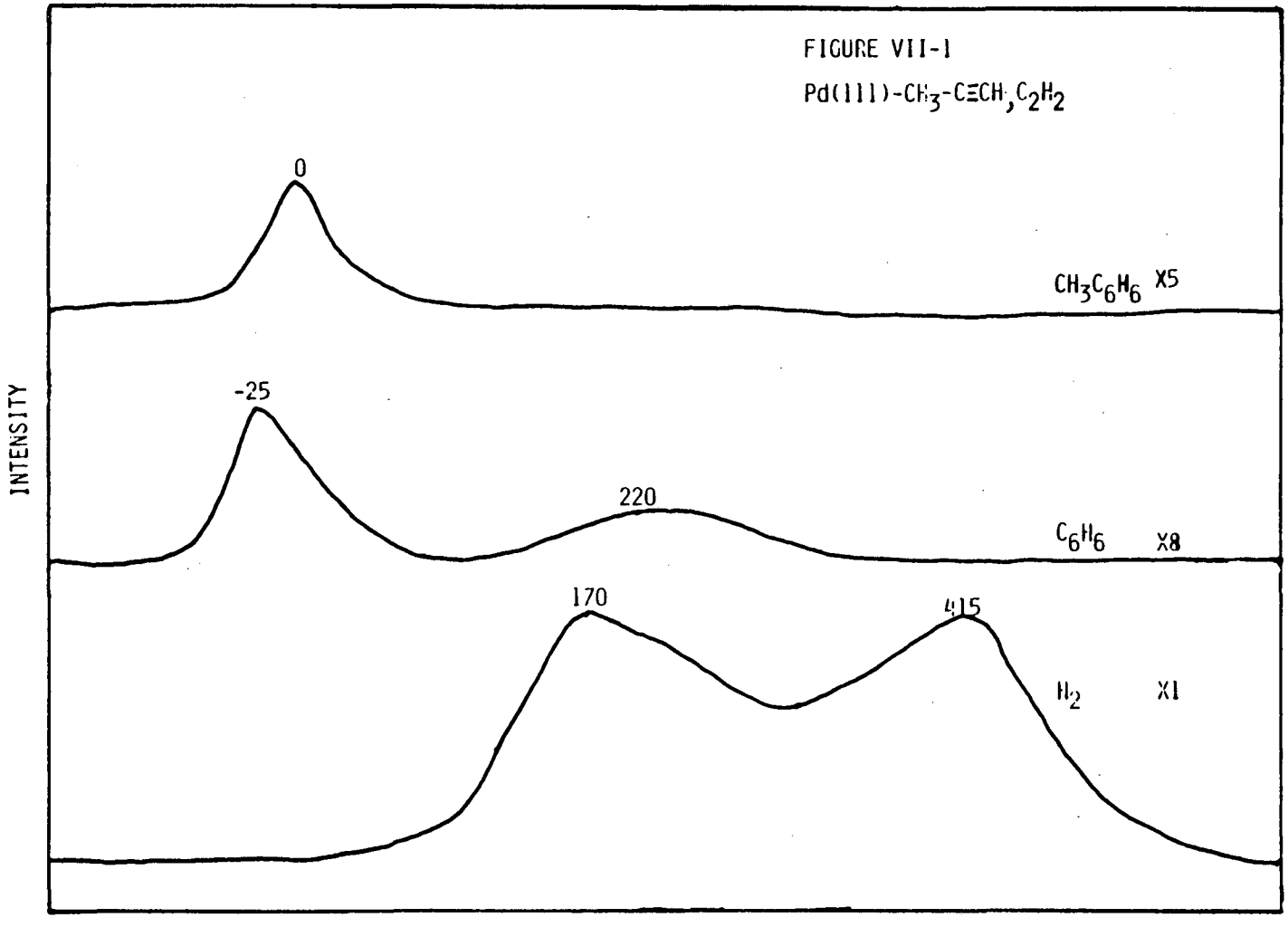
FIGURE VII-1
Pd(111)-CH3-C≡CH, C2H2
0
CH3C6H6 X5
-25
220
C6H6 X8
170
415
H2 X1
INTENSITY
TEMPERATURE (°C)

XBL 845-2068

Figure VII-2. The yield of benzene desorbing at low temperatures decreased in the thermal desorption of the surface state formed by sequential adsorption, 3.0 L of propyne and 1.0 L of acetylene. The H_2 desorption was similar to that in Figure VII-1.

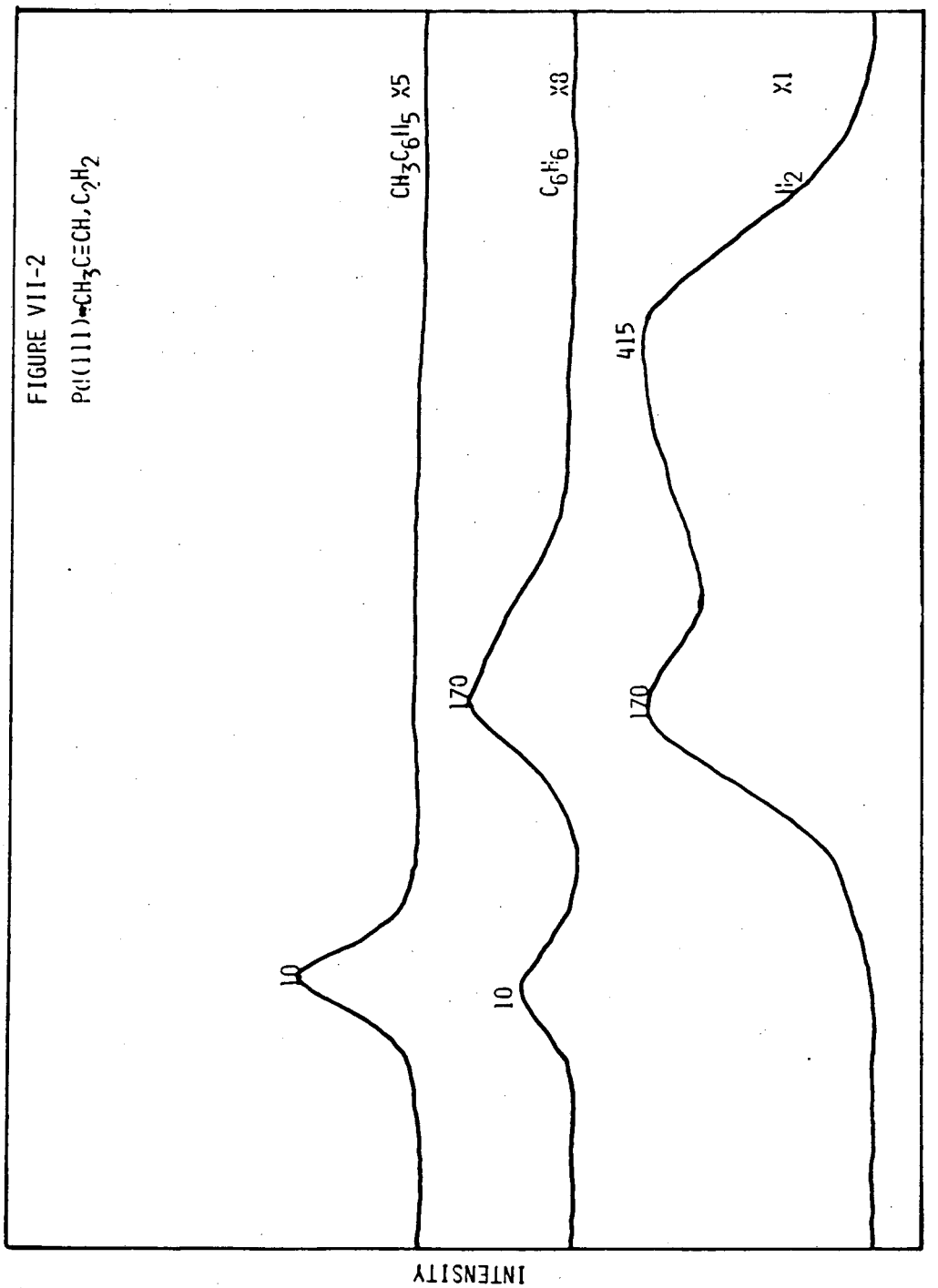
FIGURE VII-2
Pd(111)-CH3C≡CH, C2H2
CH3C6H5 x5
C6H6 x8
x1
415
170
170
10
10
INTENSITY
TEMPERATURE (°C)

XBL 845-2069

Figure VII-3. Adsorption of acetylene, 2.0 L, followed first by propyne, 2.0 L, on Pd(111) resulted in a decreased yield of toluene. The benzene thermal desorption spectrum was similar to that for chemisorbed acetylene on Pd(111).

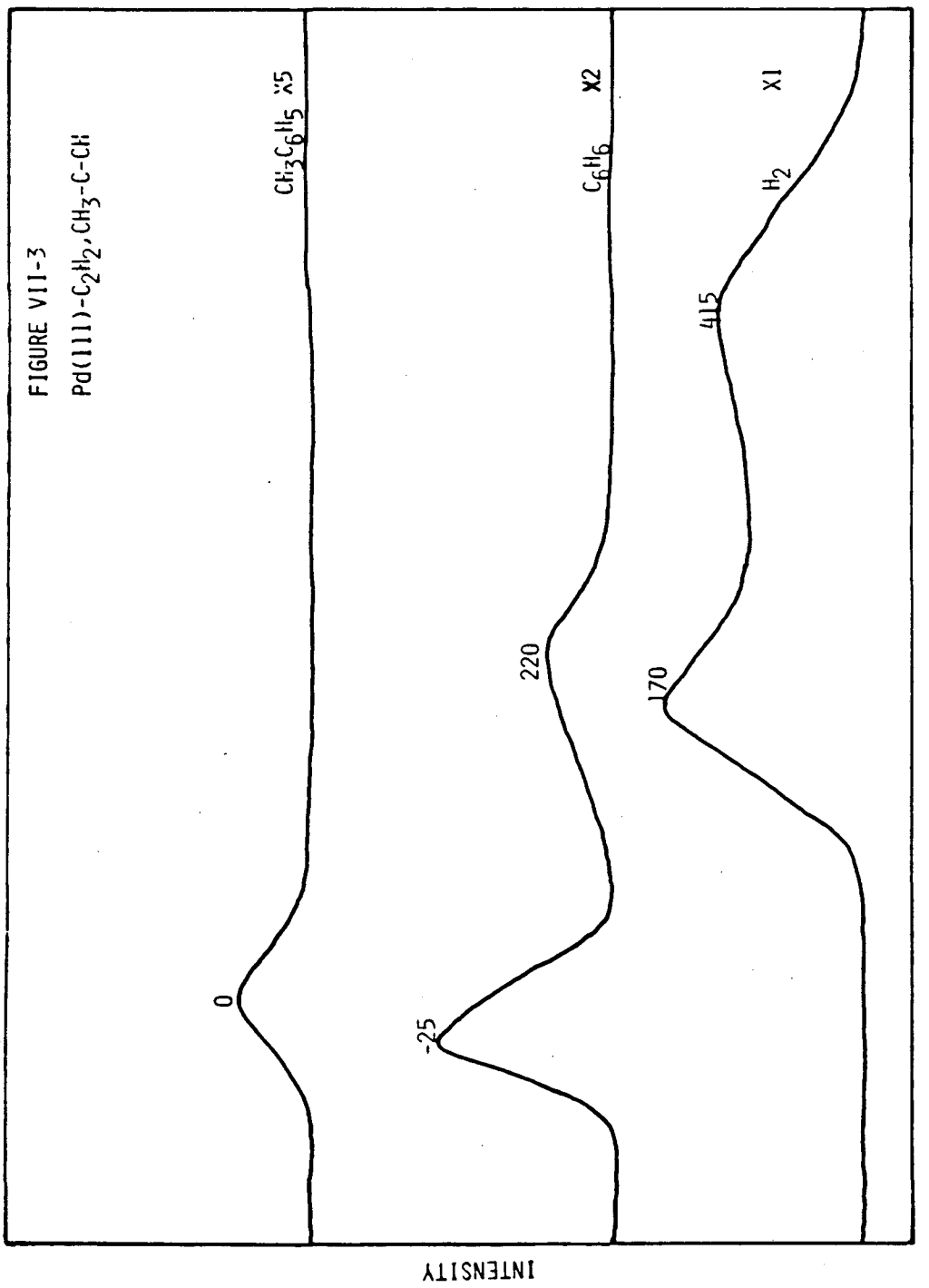
FIGURE VII-3
Pd(111)-C2H2,CH3-C-CH
CH2C6H5 X5
C6H6 X2
H2 X1
0
-25
220
170
415
INTENSITY
TEMPERATURE (°C)

XBL 845-2070

of benzene (see Figure VII-2). Inverting the order of adsorption (acetylene at 2.0 L followed by propyne at 2.0 L) resulted in a decreased yield of toluene and an increased yield of benzene (see Figure VII-3).

The presence of sulfur on Pd(111) was found to influence co-cyclotrimerization of acetylene and propyne. At a sulfur coverage of 0.33 monolayer on Pd(111), sequential adsorption of propyne (2.0 L) and acetylene (2.0 L) showed a decreased yield of toluene and benzene as compared to the clean surface (see Figure VII-4). Inverting the order of adsorption resulted in an increased yield of benzene, T_{max} = 0°C, and no change in the yield of toluene (see Figure VII-5). Adsorption of 3.0 L of propyne followed by 1.0 L of acetylene on sulfur-covered Pd(111), θ_S = 0.33, resulted in a decrease in the yield of both toluene and benzene as compared to the clean surface (see Figure VII-6). An increase in the yield of toluene was observed in the thermal desorption spectrum from the surface state formed by adsorption of 1.0 L of propyne followed by 3.0 L of acetylene on Pd(111)-S, θ_S = 0.33 (see Figure VII-7).

Propyne adsorbed on Pd(111) was also found to undergo both hydrogenation and cyclization reactions. Trimethylbenzene, T_{max} = 50°C, and benzene, T_{max} = 200°C, were observed in the thermal desorption spectrum (see Figure VII-8). Hydrogenation of propyne to propene, T_{max} = 25°C, was also found to occur. Propylene and trimethylbenzene were observed in the chemical displacement of chemisorbed propyne on Pd(111) with trimethylphospine (see Figure VII-9).

Figure VII-4. The presence of sulfur decreased the yield of both toluene and benzene from thermal desorption of propyne and acetylene coadsorption on Pd(111). In this experiment, the surface state was prepared by adsorption of 2.0 L of propyne followed by 2.0 L of acetylene. The sulfur coverage was 0.33 monolayer.

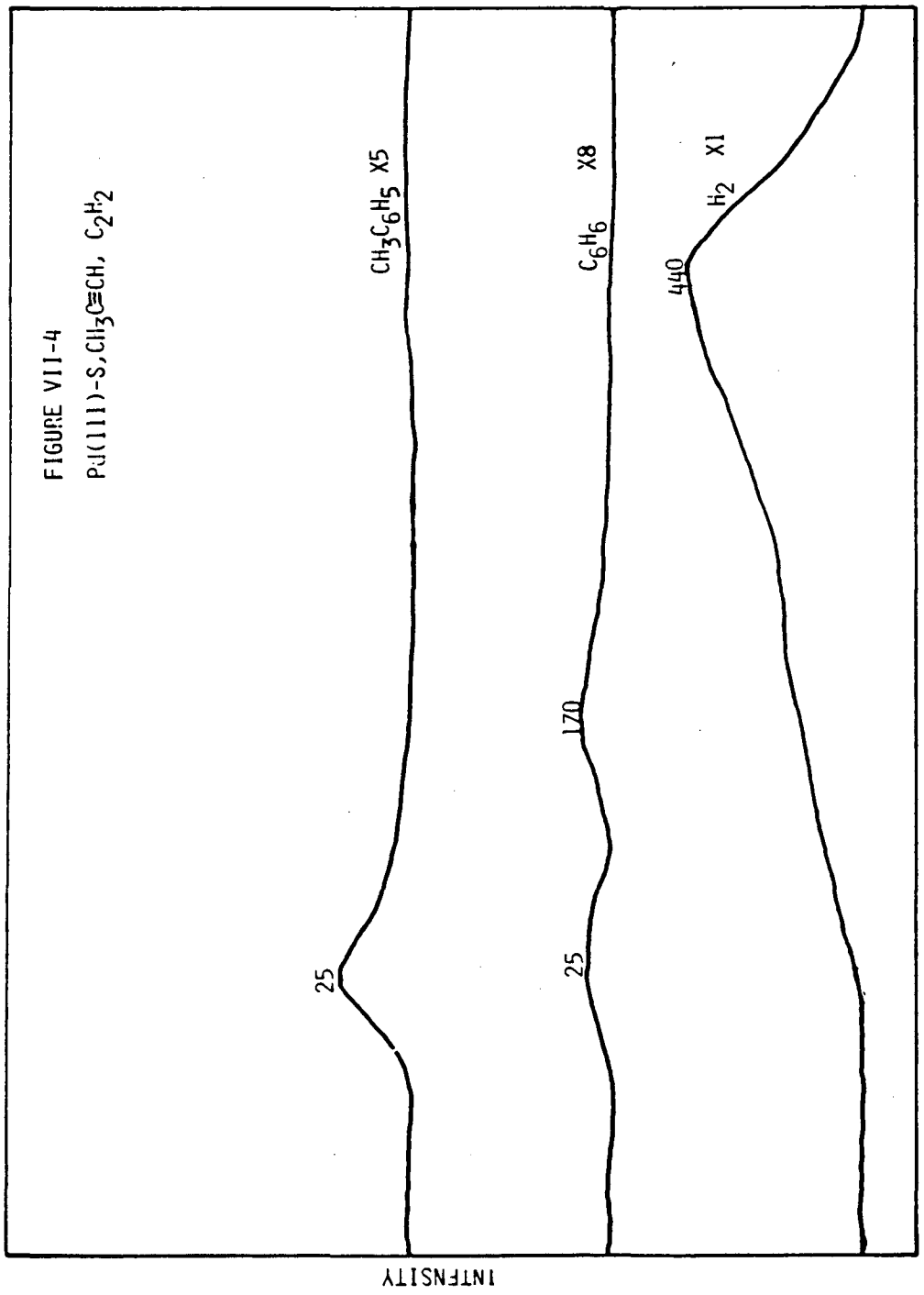

FIGURE VII-4
Pd(111)-S, $CH_3C{\equiv}CH$, C_2H_2

XBL 845-2071

Figure VII-5. The thermal desorption of the surface state formed by sequential adsorption of acetylene, 2.0 L, and propyne, 2.0 L, on sulfur-covered Pd(111), θ_S = 0.33, is illustrated. Note the increase in the desorption of benzene at low temperatures. Compare this benzene trace with the benzene trace in Figure VII-4.

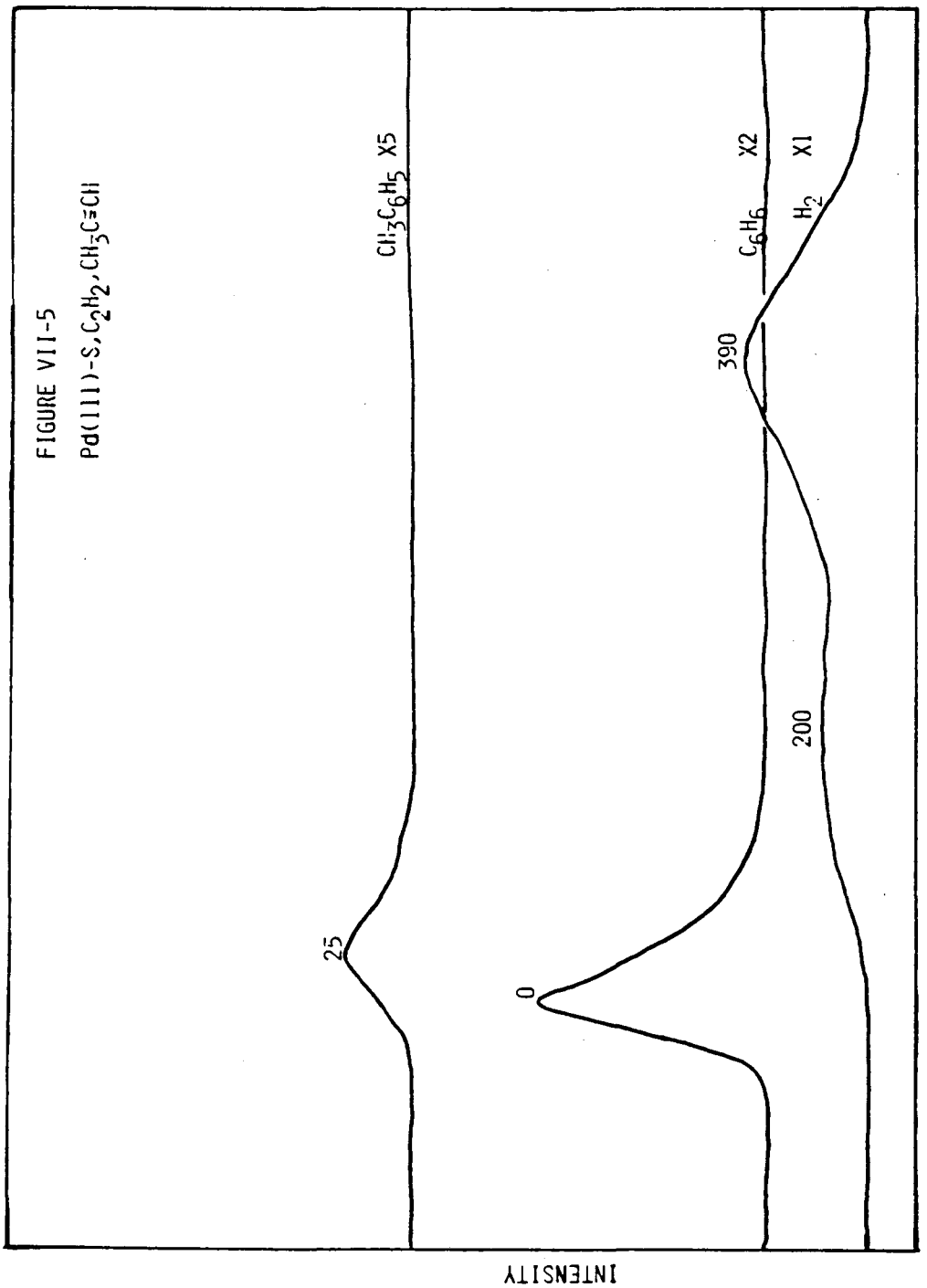
FIGURE VII-5
Pd(111)-S, C_2H_2, $CH_3C{\equiv}CH$
$CH_3C_6H_5$ X5
C_6H_6 X2
H_2 X1
25
0
390
200
INTENSITY
TEMPERATURE (°C)

XBL 845-2072

Figure VII-6. The yield of both benzene and toluene decreased in the thermal desorption of 3.0 L of propyne and 1.0 L of acetylene on sulfur-covered Pd(111), when compared to the clean surfaces. The sulfur coverage was 0.33 monolayer.

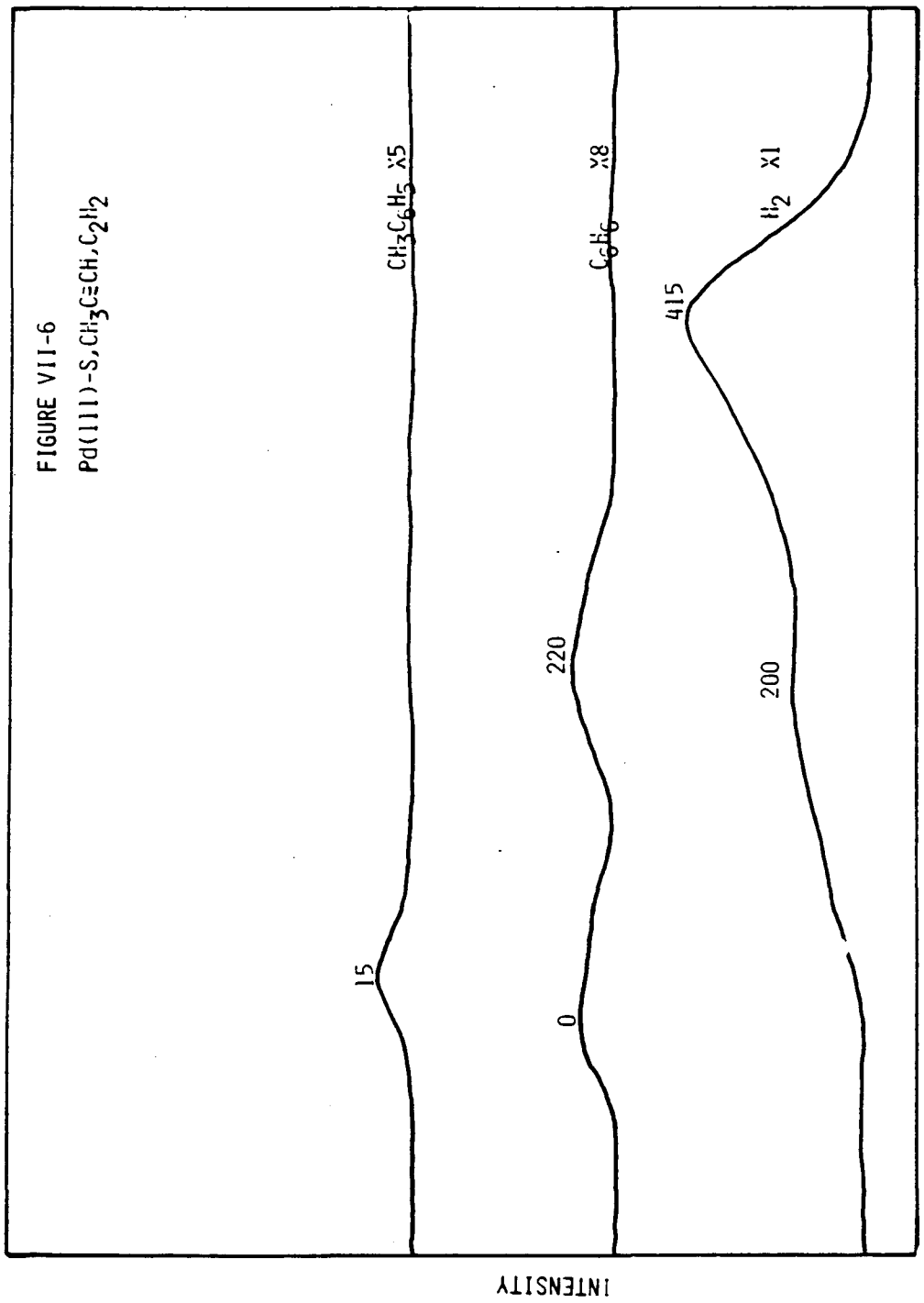
FIGURE VII-6
Pd(111)-S,CH3C≡CH,C2H2
CH2C6H5 X5
C6H6 X8
H2 X1
15
0
220
415
200
INTENSITY
TEMPERATURE (°C)

XBL 845-2073

Figure VII-7. Decreasing the exposure of propyne, 1.0 L, and increasing the exposure of acetylene, 3.0 L, on sulfur-covered Pd(111), θ_S = 0.33, resulted in an increased yield of toluene. Comparing the toluene thermal desorption spectrum shown in this figure with that in Figure VII-6 illustrates this point.

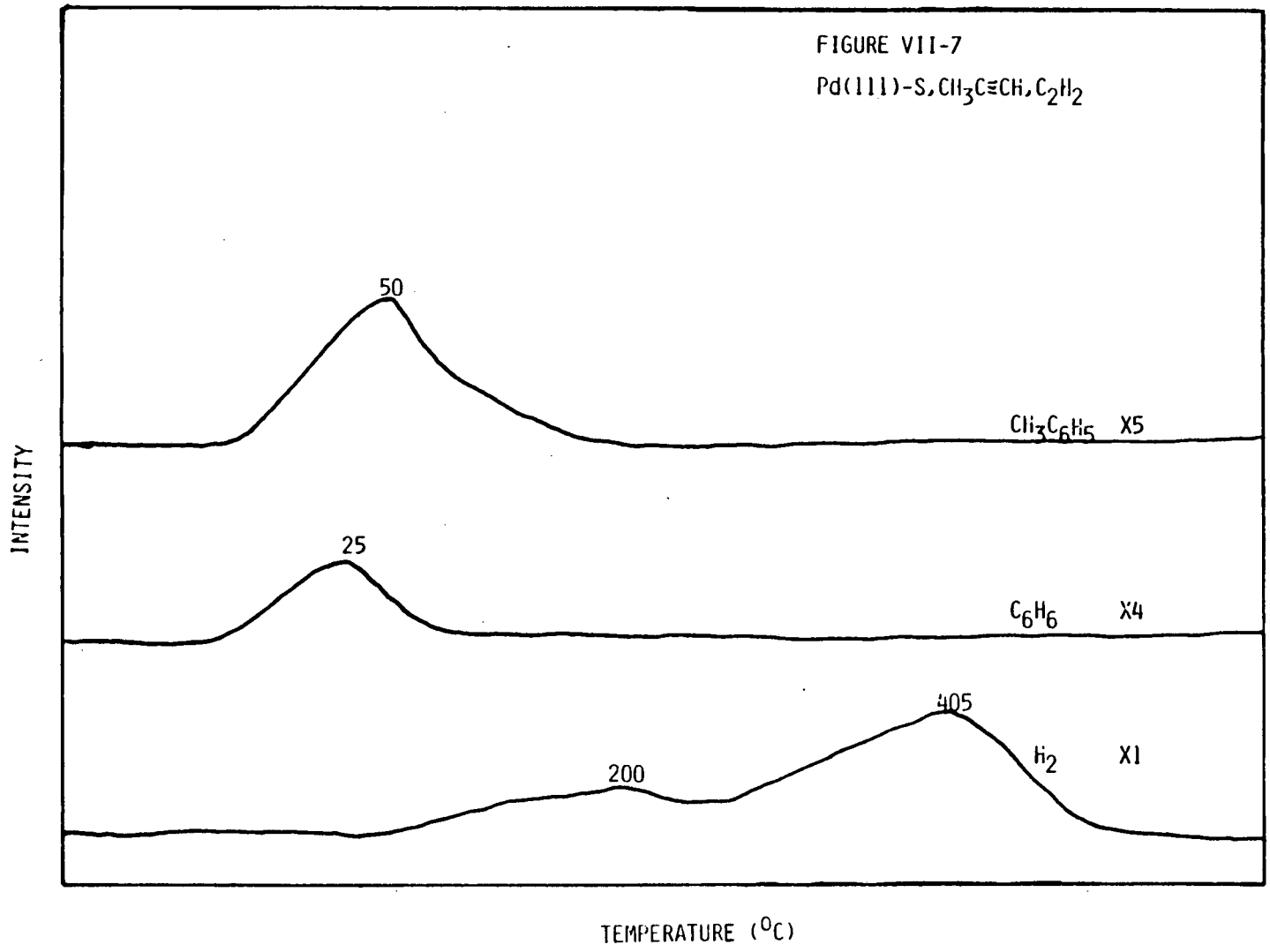
FIGURE VII-7
Pd(111)-S, $CH_3C{\equiv}CH$, C_2H_2
50
$CH_3C_6H_5$ X5
25
C_6H_6 X4
405
200
H_2 X1
INTENSITY
TEMPERATURE (^{0}C)

XBL 845-2074

Figure VII-8. Thermal desorption of propyne, 3.0 L, from Pd(111) exhibited a complex mixture of products. Propylene, the hydrogenation product, was observed. Trimerization of propyne was observed with the desorption of trimethylbenzene. Benzene formation was also observed. Along with these three molecules, molecular desorption of propyne was also observed.

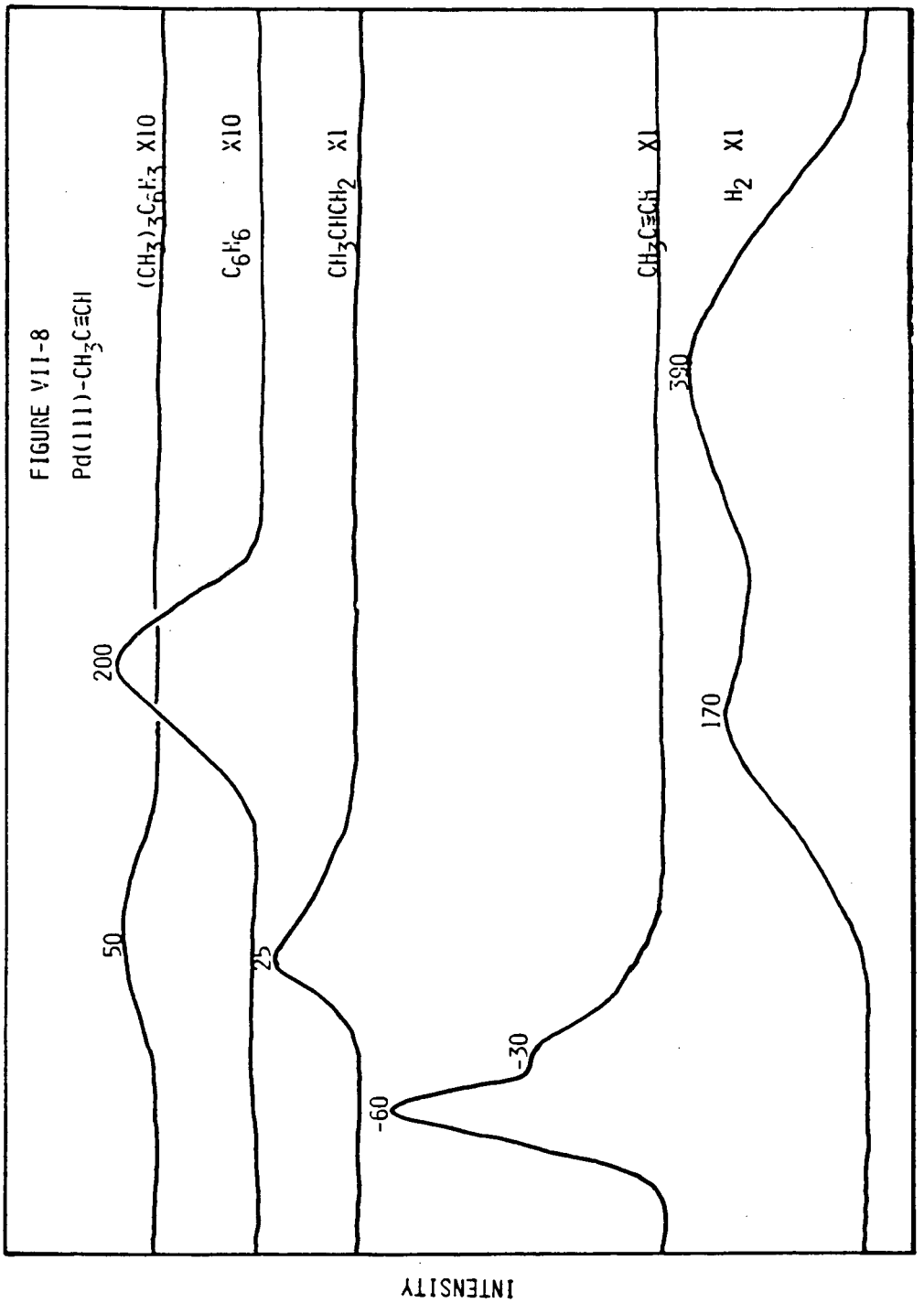
FIGURE VII-8
Pd(111)-CH3C≡CH
(CH3)3C6H3 X10
C6H6 X10
CH3CHCH2 X1
CH3C≡CH X1
H2 X1
200
50
25
-60
-30
390
170
INTENSITY
TEMPERATURE (°C)

XBL 845-2075

Figure VII-9. Propyne, propylene, and trimethylbenzene were displaced by trimethylphosphine from a surface state formed by chemisorption of propyne at 25°C. The results of this experiment are shown here. In this experiment benzene was not monitored.

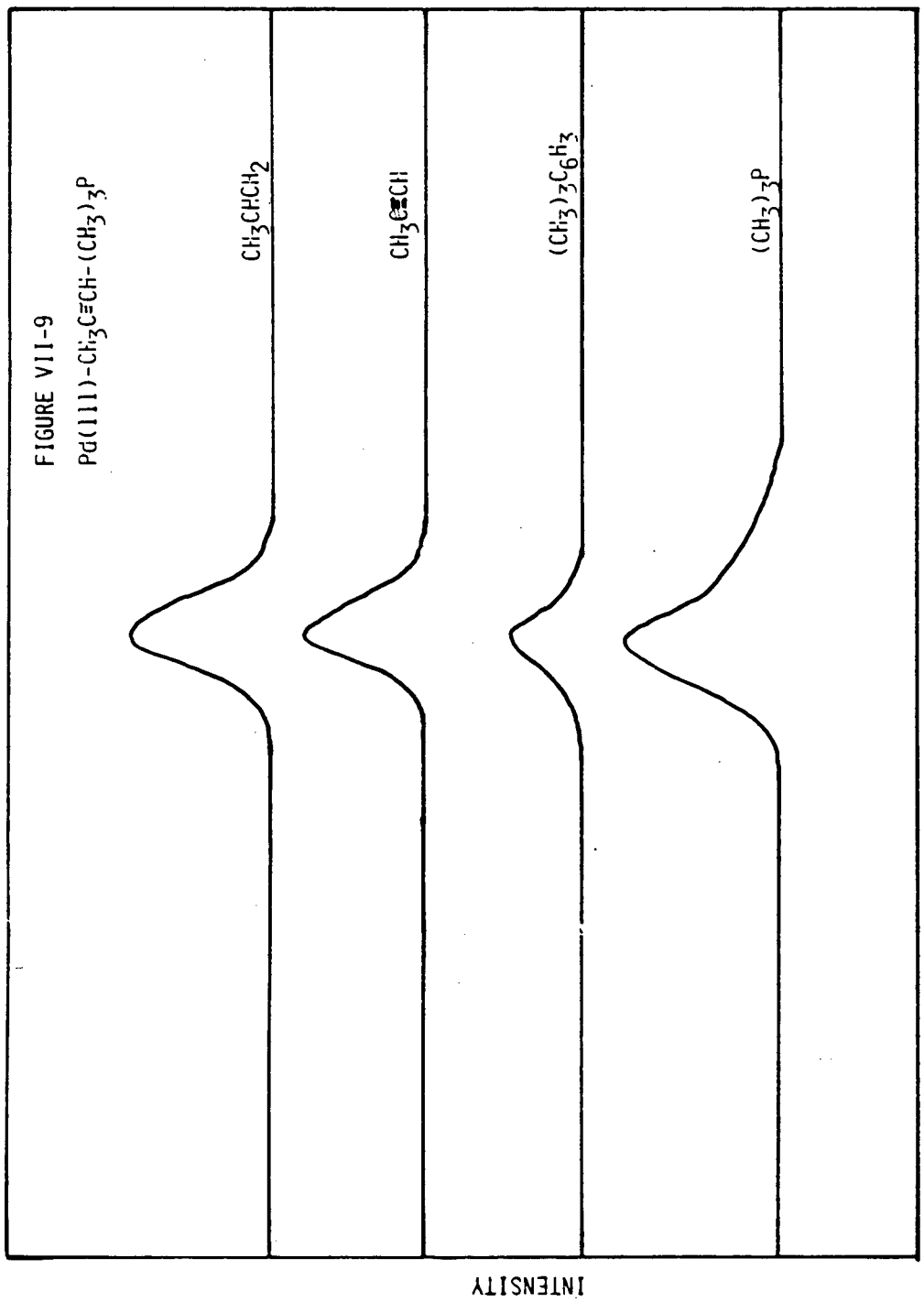
FIGURE VII-9
Pd(111)-CH3C≡CH-(CH3)3P
CH3CHCH2
CH3C≡CH
(CH3)3C6H3
(CH3)3P
INTENSITY
TIME

XBL 845-2076

Figure VII-10. Thermal desorption of trimethylsilylacetylene chemisorbed on Pd(111) resulted in the desorption of benzene. Along with benzene desorption, desorption of intact trimethylsilylacetylene and hydrogen was also observed. An exposure of 3.0 L of trimethylsilylacetylene was used in this thermal desorption experiment.

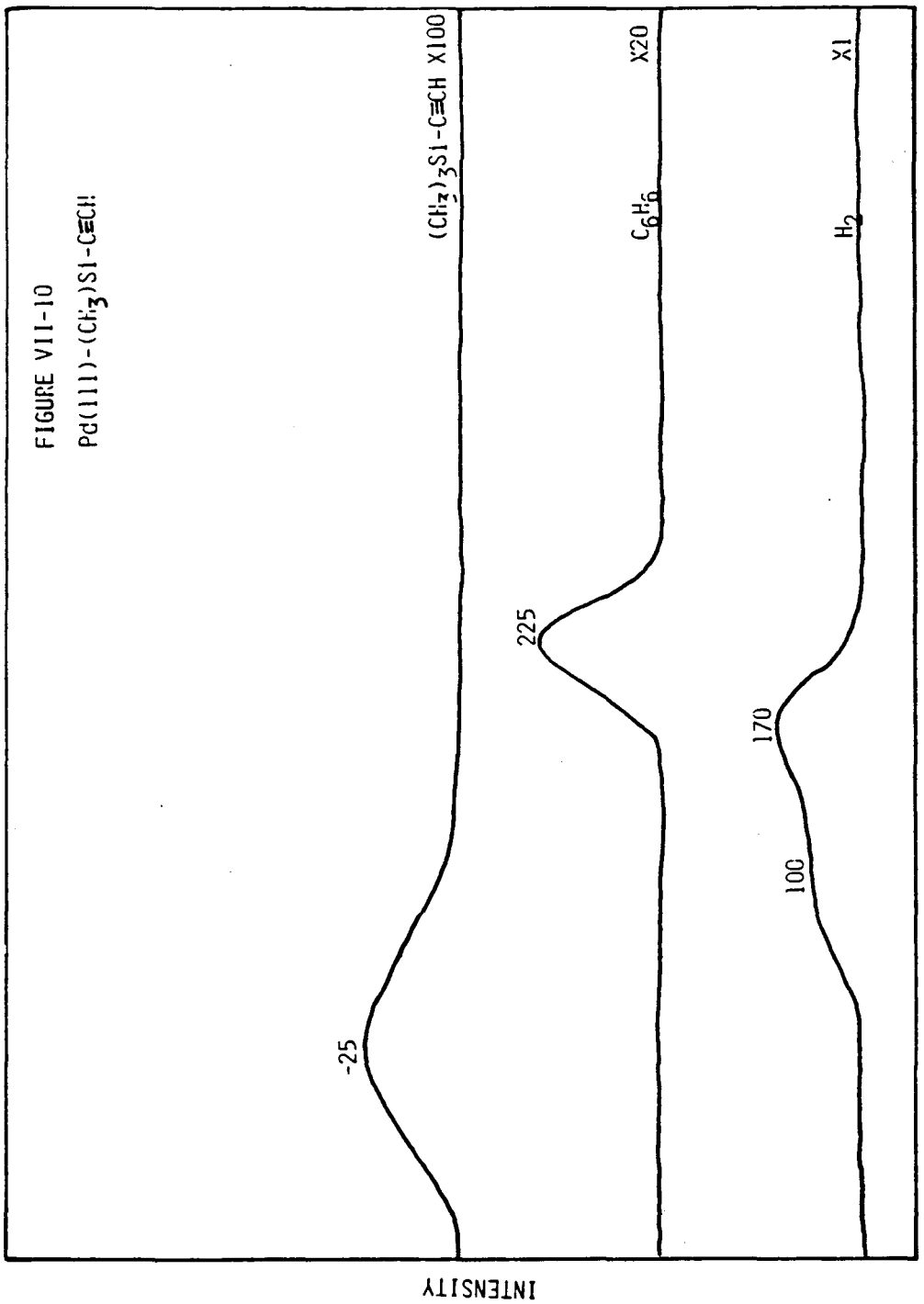
FIGURE VII-10
Pd(111)-(CH3)3Si-C≡CH
(CH3)3Si-C≡CH X100
X20
C6H6
X1
H2
-25
225
170
100
INTENSITY
TEMPERATURE (°C)
XBL 845-2077

Figure VII-11. The thermal desorption of 2-butyne from Pd(111) is shown. In contrast to acetylene and propyne, where trimerization reactions were observed, no trimerization products were observed. The trimerization product, hexamethylbenzene, could not be displaced by trimethylphosphine from 2-butyne on Pd(111). The absence of high temperature hydrogen thermal desorption maxima, which are characteristic of methylsubstituted benzene, also suggests that trimerization is not occurring.

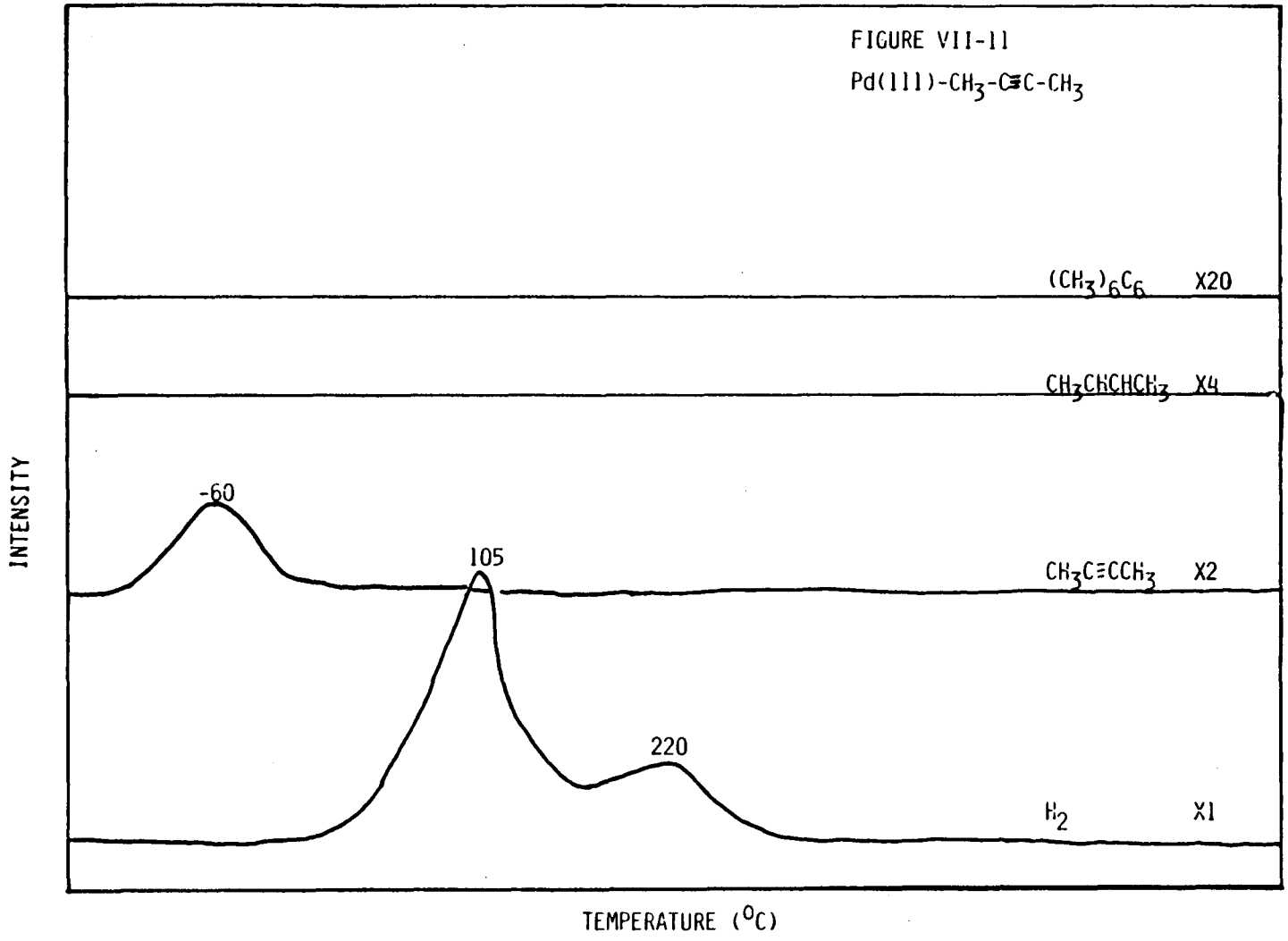
FIGURE VII-11
Pd(111)-CH3-C≡C-CH3
(CH3)6C6 X20
CH3CHCHCH3 X4
CH3C≡CCH3 X2
H2 X1
-60
105
220
INTENSITY
TEMPERATURE (°C)

XBL 846-2078

Trimethylsilylacetylene adsorbed on Pd(111) also yielded small amounts of benzene (T_{max} = 225°C) in the subsequent thermal desorption spectrum (see Figure VII-10). 2-butyne exhibited neither cyclization nor hydrogenation on Pd(111) (see Figure VII-11).

A series of experiments were performed to give insights into the mechanism of the cyclization reactions observed for acetylene, propyne, and trimethylsilylacetylene on Pd(111). In these experiments deuterium was preadsorbed on Pd(111), followed by adsorption of the desired acetylenic compound. Incorporation of deuterium into benzene during these reactions was probed by monitoring the following masses in subsequent thermal desorption experiments: 78 amu (C_6H_6), 79 amu (C_6H_5D), 80 amu ($C_6H_4D_2$), 81 amu ($C_6H_3D_3$), 82 amu ($C_6H_2D_4$), 83 amu (C_6HD_5), and 84 amu (C_6D_6). As discussed in Chapter III, the benzene yield decreases when hydrogen is preadsorbed on Pd(111). However, at low D_2 exposure benzene was still observed. A signal was observed in the 78 amu, 79 amu, and 80 amu channels, with 78 amu the most intense, followed by 79 amu and 80 amu (see Figure VII-12). Reversing the order of adsorption yielded only very small amounts of C_6H_5D (79 amu) and no higher masses (see Figure VII-13). Much more deuterium incorporation in the benzene formed from the Pd(111)-D_2-CH_3-C ≡ CH surface state. The most intense signal was 80 amu; however, a signal was observed at 82 amu, $C_6H_2D_4$. No signal above 82 amu was observed (see Figure VII-14). Almost equal intensities were observed in the 78 amu and 79 amu channels in the thermal desorption spectrum from the surface state

Figure VII-12. Thermal desorption of a surface state formed by sequential adsorption of deuterium, 0.25 L, and acetylene, 4.0 L, on Pd(111) exhibits limited deuterium incorporation in the benzene formed by trimerization of acetylene. Shown are traces for 78 amu, C_6H_6, 79 amu, C_6H_5D, and 80 amu, $C_6H_4D_2$. No masses greater than 80 amu were observed.

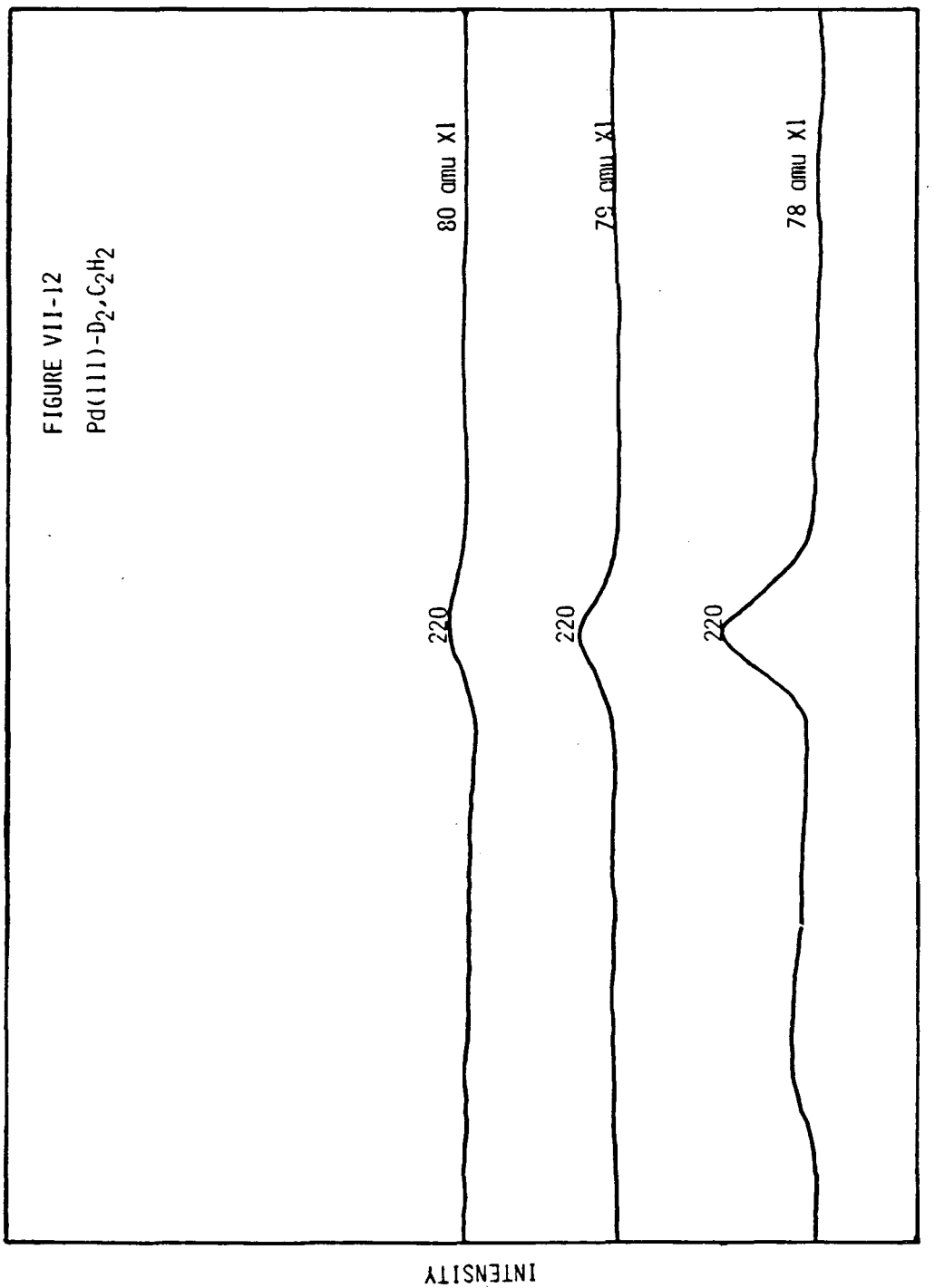

FIGURE VII-12
Pd(111)-D_2,C_2H_2

XBL 846-2079

Figure VII-13. Little H-D exchange was observed in the thermal desorption spectrum of a surface state formed by sequential adsorption of acetylene, 4.0 L, and deuterium, 2.0 L, on Pd(111). No masses greater than 79 amu were observed.

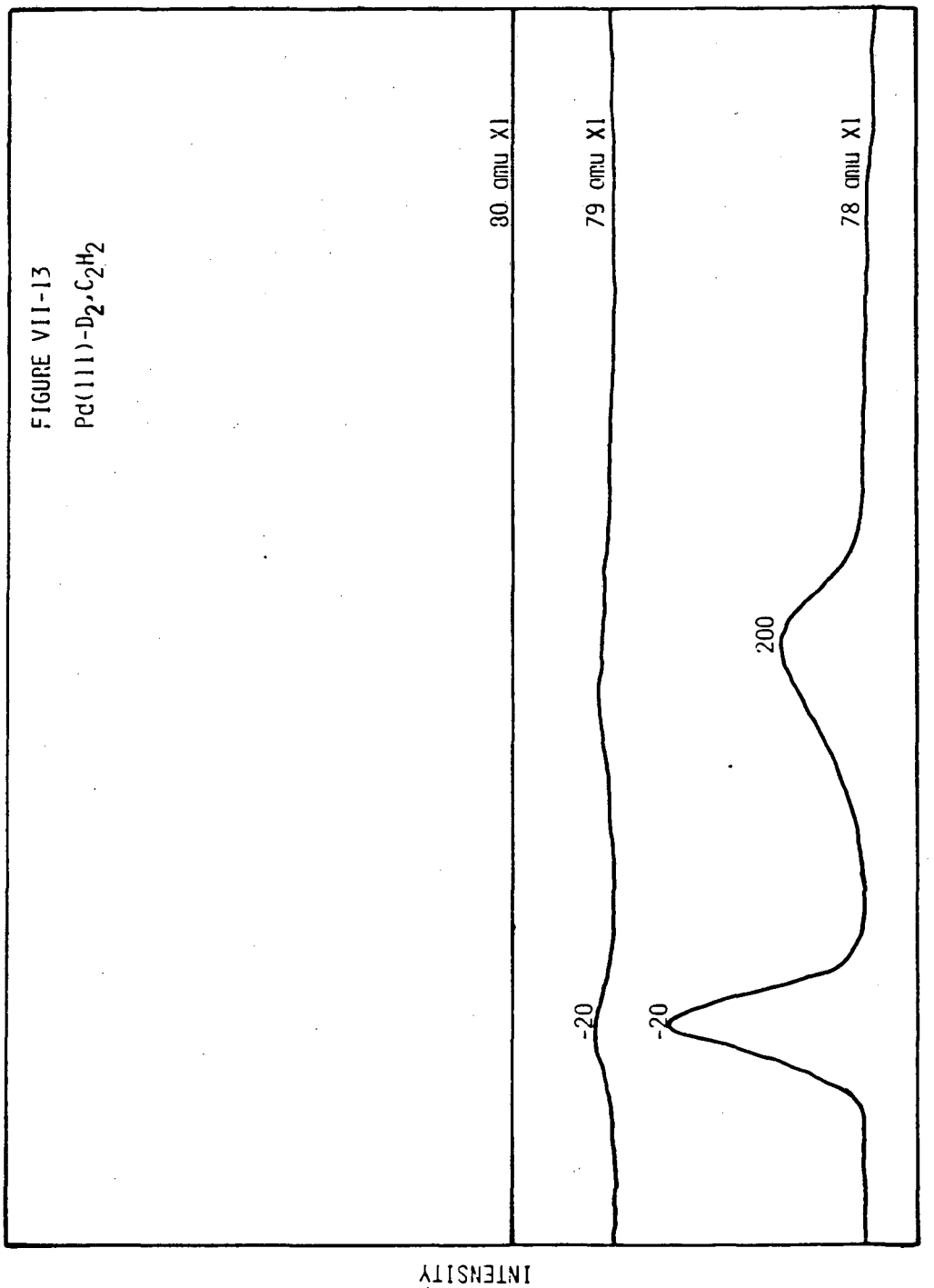
FIGURE VII-13
Pt(111)-D_2,C_2H_2
80 amu X1
79 amu X1
78 amu X1
-20
-20
200
INTENSITY
TEMPERATURE (^{o}C)
XBL 846-2080

Figure VII-14. The thermal desorption spectrum of the mixed chemisorption state, Pd(111)-D_2-CH_3-C≡CH, is shown here. This state was formed by sequential adsorption of D_2, 3.3 L, and propyne, 6.6 L. Substantial deuterium incorporation in the benzene desorbing from the surface is evident. Desorption of benzene containing up to four deuteriums, $C_6D_4H_2$, was observed.

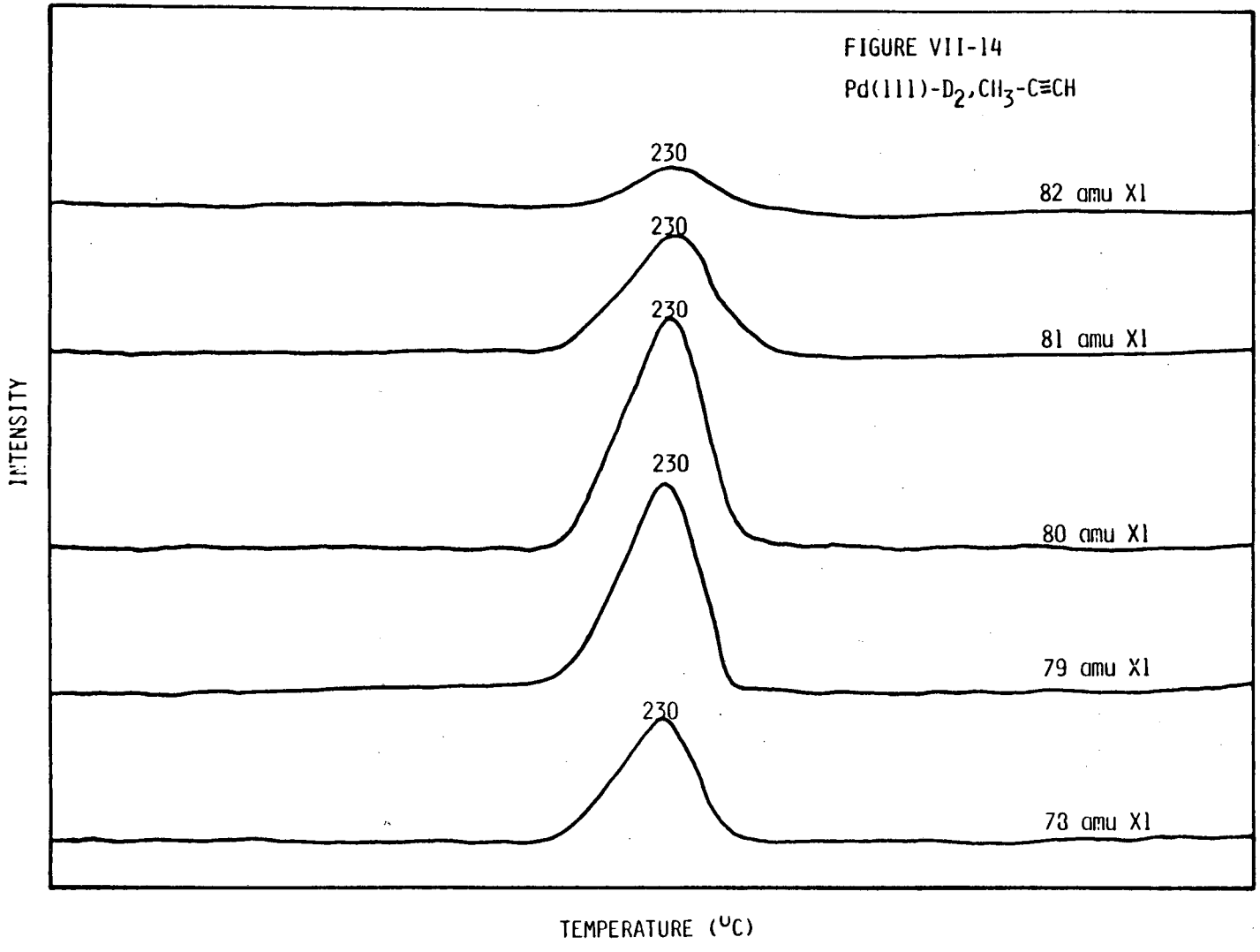
FIGURE VII-14
Pd(111)-D2,CH3-C≡CH
230
82 amu XI
230
81 amu XI
230
80 amu XI
230
79 amu XI
230
73 amu XI
INTENSITY
TEMPERATURE (°C)

XBL 846-2081

Figure VII-15. Incorporation of three deuterium atoms in the benzene formed was observed in the thermal desorption of deuterium and trimethylsilylacetylene from Pd(111). Deuterium, 3.3 L, and trimethylsilylacetylene, 6.6 L, were adsorbed sequentially.

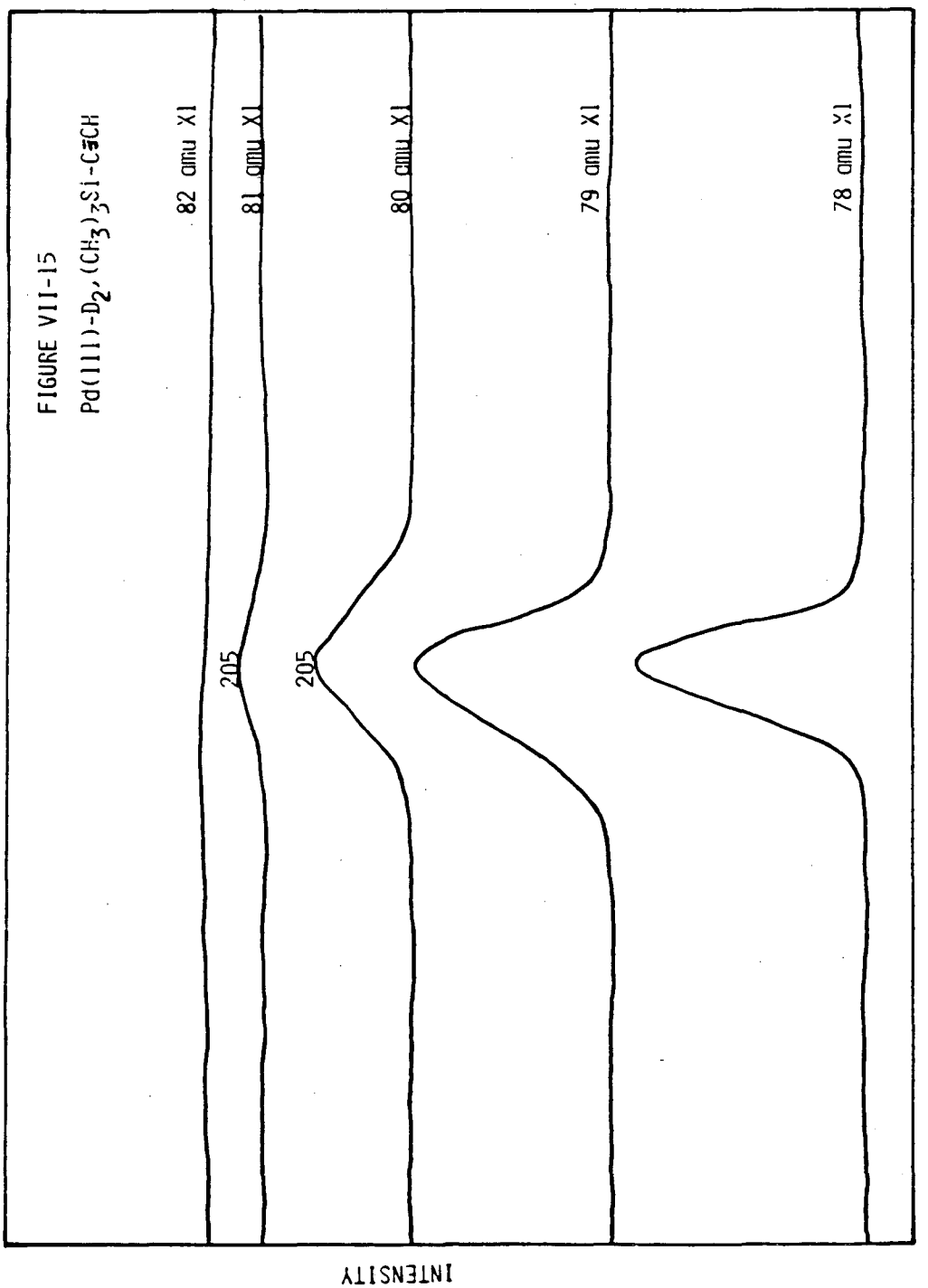
FIGURE VII-15
Pd(111)-D2, (CH3)3Si-C≡CH
82 amu X1
81 amu X1
80 amu X1
79 amu X1
78 amu X1
205
205
INTENSITY
TEMPERATURE (°C)

XBL 846-2082

formed by adsorption of D_2 and trimethylsilylacetylene on Pd(111) (see Figure VII-15).

Pyridine was formed from acetylene and hydrogen cyanide on Pd(111) in yields of approximately 10 percent. The acetylene and the hydrogen cyanide were coadsorbed at -110°C, and then the crystal was heated. Pyridine, NC_5H_5, desorbed at ~100°C, the characteristic desorption temperature for Pd(111)-NC_5H_5. Attempts to hydrogenate pyridine on this surface were unsuccessful.

On Pd(111) or Pd(100), the following hydrogenation reactions were observed: acetylene to ethylene, ethylene to ethane, benzene to cyclohexane, and norbornadiene to norbornane. The typical experimental protocol comprised (1) adsorption of hydrogen (or deuterium) followed by adsorption of the hydrocarbon at low temperature (<-130°C), and (2) thermal desorption with a heating rate of ~25°C. Appearance of the hydrogenated product was at ~0°C [C_2D_4 from C_2D_2 + D_2 on Pd(111)], 25°C [C_2D_6 from D_2+C_2D_4 on Pd(100)], 25°C [C-C_6D_{12} on Pd(110)], and 10°C [norbornane on Pd(111)]. These temperatures for the appearance of the alkanes are very similar and, in the case of ethane and cyclohexane, substantially exceed the characteristic desorption temperature of these alkanes on Pd(111). Hence the onset of rapid hydrogenation in these UHV systems is about 0°C-25°C for these palladium surfaces.

Hydrogenation of acetonitrile to ethylamine was also demonstrated. Cochemisorption of D_2 and CD_3CN at 25°C [Pd(100)],

Figure VII-16. The thermal desorption spectrum of the D_2-CD_3-CN-Pd(100) system shows the formation of the ethylamine by hydrogenation of CD_3CN. The order of adsorption of the reagents at 25°C on Pd(100) was deuterium followed by acetonitrile, CD_3CN.

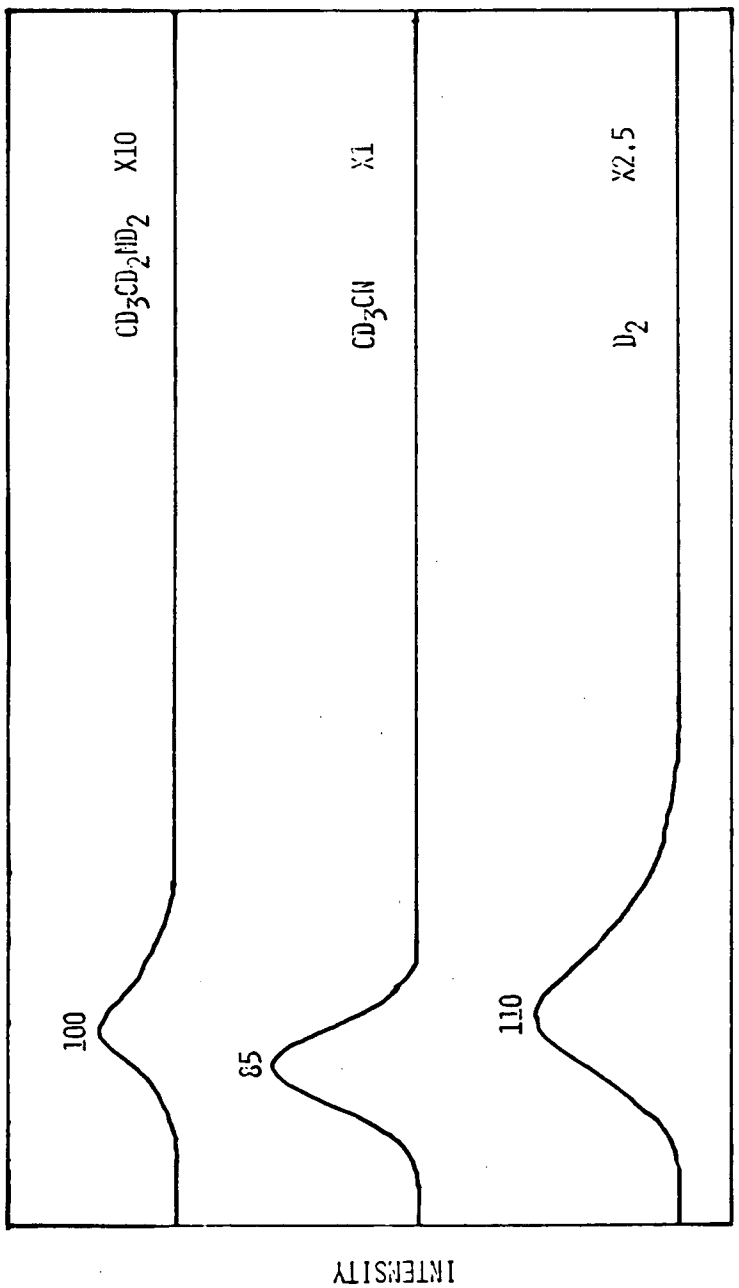
$CD_3CD_2ND_2$ X10
CD_3CN X1
D_2 X2.5
100
85
110
INTENSITY
TEMPERATURE(C)

XBL 837-6022

followed by the thermal desorption experiment, gave 5 percent conversion of CD_3CN to C_2D_5-ND_2, which desorbed at 80°C (see Figure VII-16).

Hydrogenation of alkynes are facile processes on palladium surfaces. When the hydrogenation of acetylene was performed with deuterium, the predominant ethylene formed was $C_2D_2H_2$ (see Figures VII-17 and VII-18). The hydrogenation of propyne and 2-pentyne produced the olefins with incorporation of two deuterium atoms; however, significant amounts of d^3 and d^4 olefins were observed (see Figures VII-19 and VII-20).

In Chapter VI, the chemistry of thiophene was discussed. One reaction which occurred on palladium surfaces was desulfurization to form butadiene. The surface chemistry of two other heterocycles, pyridine and furan, were investigated to determine if denitrogenation and deoxygenation reactions also occurred.

No hydrocarbon formation was observed in the thermal desorption spectrum of furan from Pd(111). Two hydrogen thermal desorption maxima were observed, at 110°C and 245°C; a carbon monoxide maximum was observed at 205°C; and a furan maximum was observed at 70°C (see Figure VII-21). Pyridine chemisorbed on Pd(111) yielded only hydrogen and molecular desorption in the thermal desorption spectrum. Two hydrogen maxima were observed, one at 200°C and a broad plateau-like maximum from 288°C to 370°C (see Figure VII-22). Another sulfur heterocycle which has been shown to undergo desulfurization is 2,5-dimethylthiophene. Benzene was found to form on the low

Figure VII-17. Sequential adsorption of deuterium and acetylene on Pd(111) at -130°C followed by rapid heating resulted in the formation of ethylene. The plots of mass spectral intensity versus temperature of the various deuterated ethylenes, $C_2H_xD_{4-x}$, are shown. The 30 amu signal ($C_2H_2D_2$) was the most intense. Small amounts (less than 3 percent) of C_2HD_3 (31 amu) were observed, but no C_2D_4 (32 amu) was detected. The majority of intensities in the 28 and 29 amu signals represent fragments of $C_2D_2H_2$. The mass spectrometric technique used in this experiment cannot be used to differentiate the various isomers of $C_2D_2H_2$.

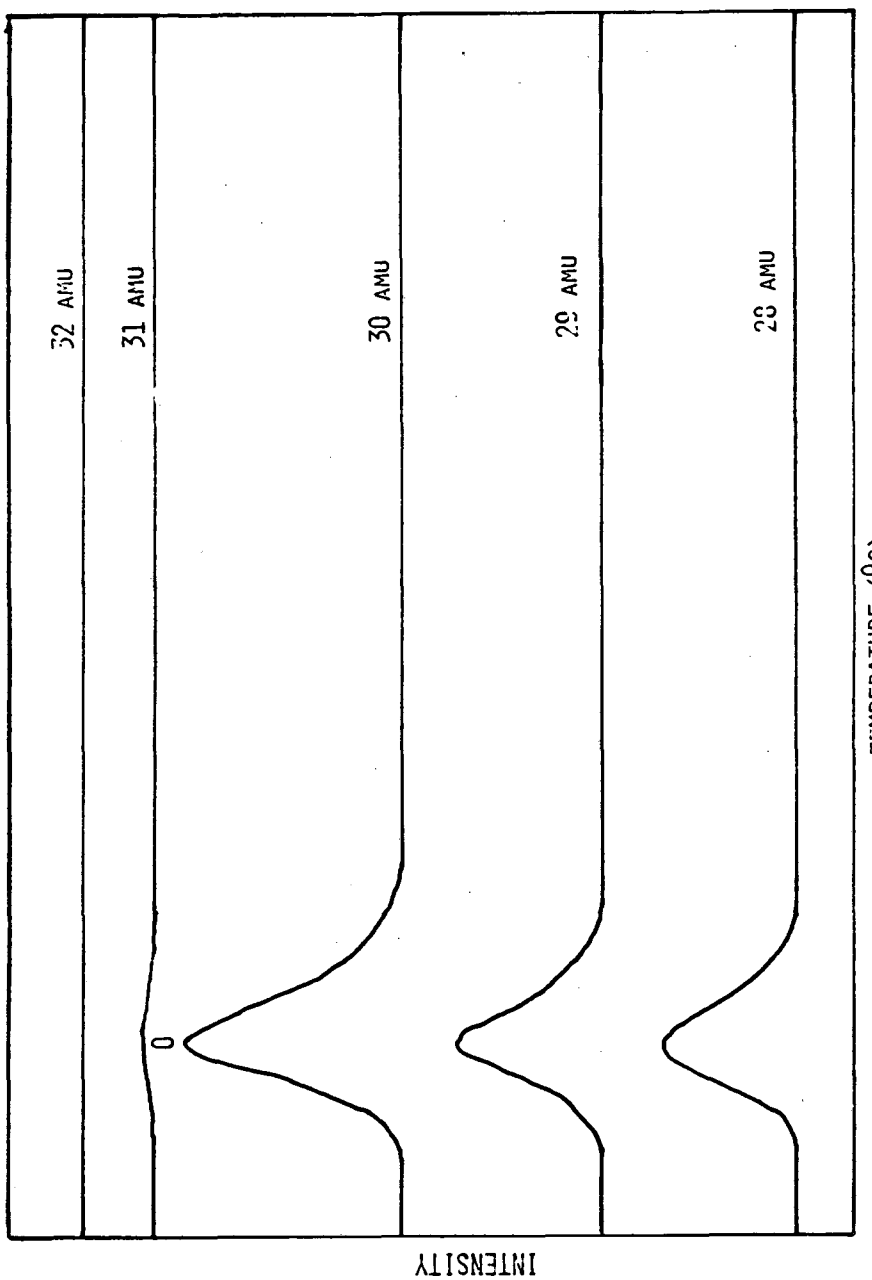

XBL 837-6019

Figure VII-18. The "corrected" thermal desorption spectra of the D_2-C_2H_2-Pd(111) are illustrated. The corrections are for the intensities of the 28 and 29 amu signals due to fragments of $C_2D_2H_2$. This corrected set of spectra clearly shows that $C_2D_2H_2$ is the major product (96 percent), and that C_2H_3D and C_2HD_3 are only minor products.

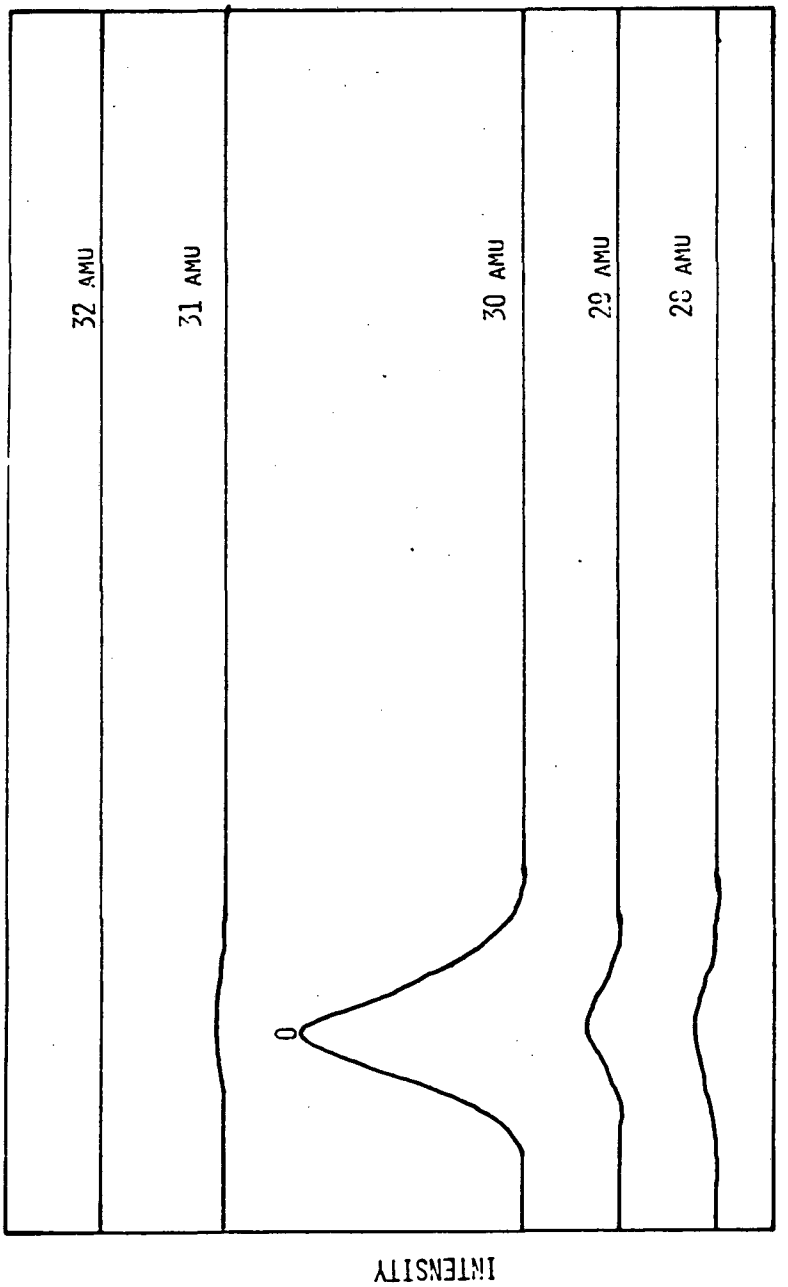

XBL 837-6021

Figure VII-19. The hydrogenation of propyne on Pd(111) was investigated with deuterium. The major propylene formed contained two deuteriums. These experiments do not define which isomer was formed. Substantial amounts of propylene containing three deuteriums were also formed, in contrast to the acetylene, where little C_2HD_3 was formed.

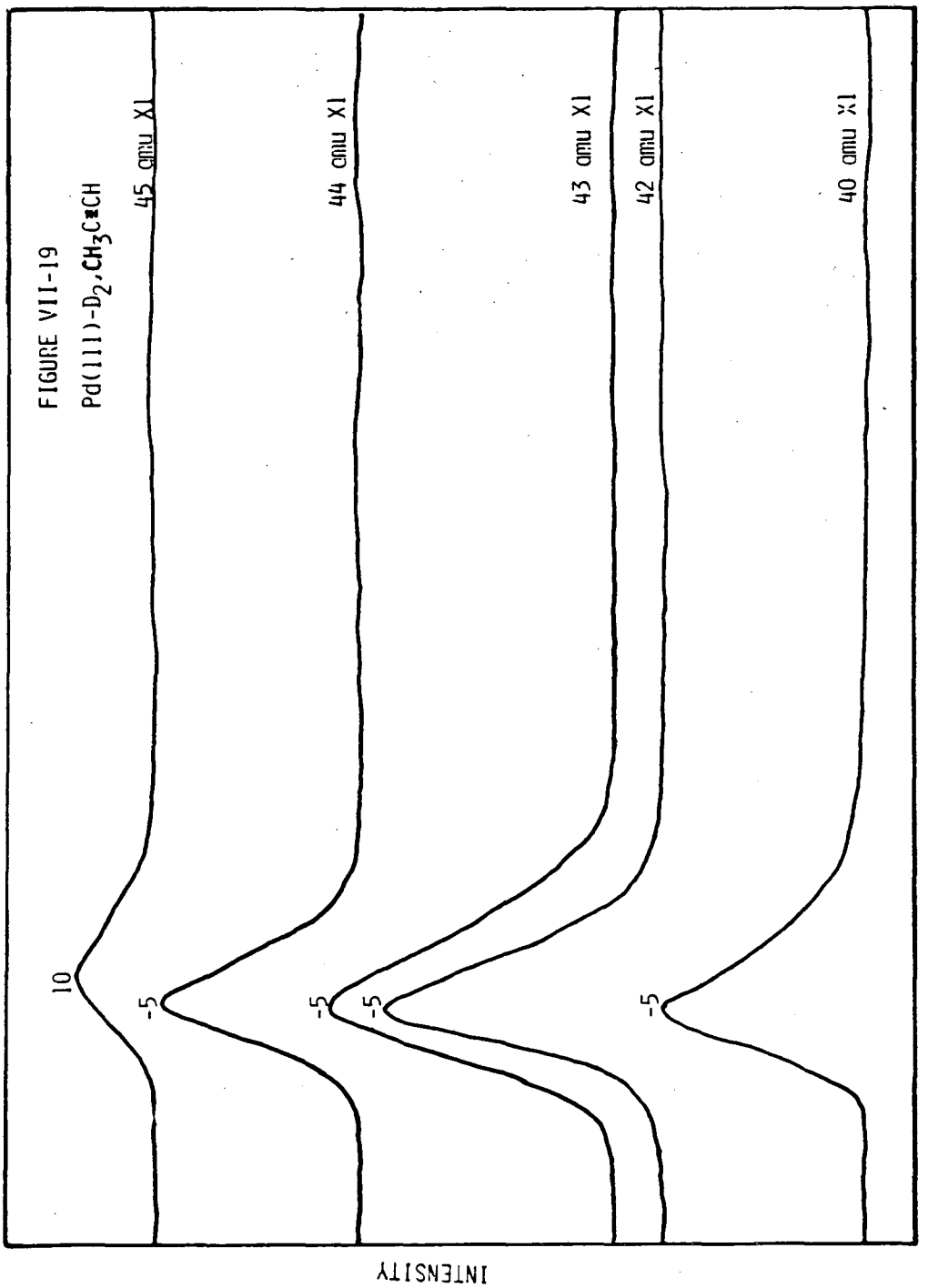
FIGURE VII-19
Pd(111)-D2,CH3C≡CH
45 amu X1
44 amu X1
43 amu X1
42 amu X1
40 amu X1
10
-5
-5
-5
-5
INTENSITY
TEMPERATURE (°C)
XBL 846-2083

Figure VII-20. Shown here is the thermal desorption spectrum of the surface state formed by sequential adsorption of deuterium and 2-pentyne on Pd(111). The major product is the olefin containing two deuteriums, 72 amu. The exposures used in this experiment were 3.0 L and 1.5 L for deuterium and 2-pentyne, respectively.

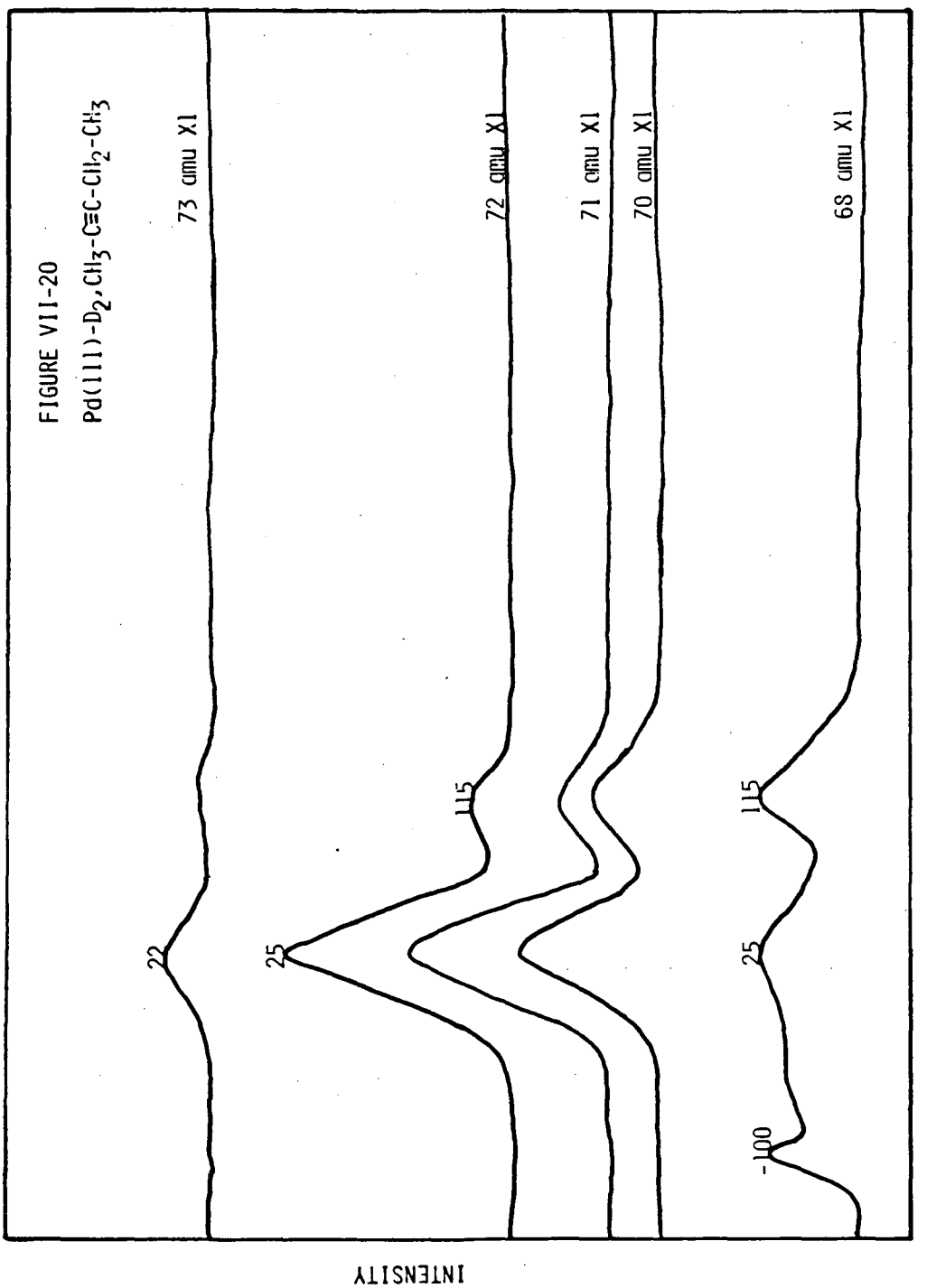
FIGURE VII-20
Pd(111)-D_2,CH_3-C≡C-CH_2-CH_3
73 amu X1
72 amu X1
71 amu X1
70 amu X1
68 amu X1
22
25
115
25
115
-100
INTENSITY
TEMPERATURE (°C)
XBL 846-2084

Figure VII-21. Carbon monoxide and hydrogen desorption were observed in the thermal desorption spectrum of furan from Pd(111). Molecular desorption was also evident. No desorption of C_4 hydrocarbons, the deoxygenation products, was observed. The furan exposure was 1.0 L in this experiment.

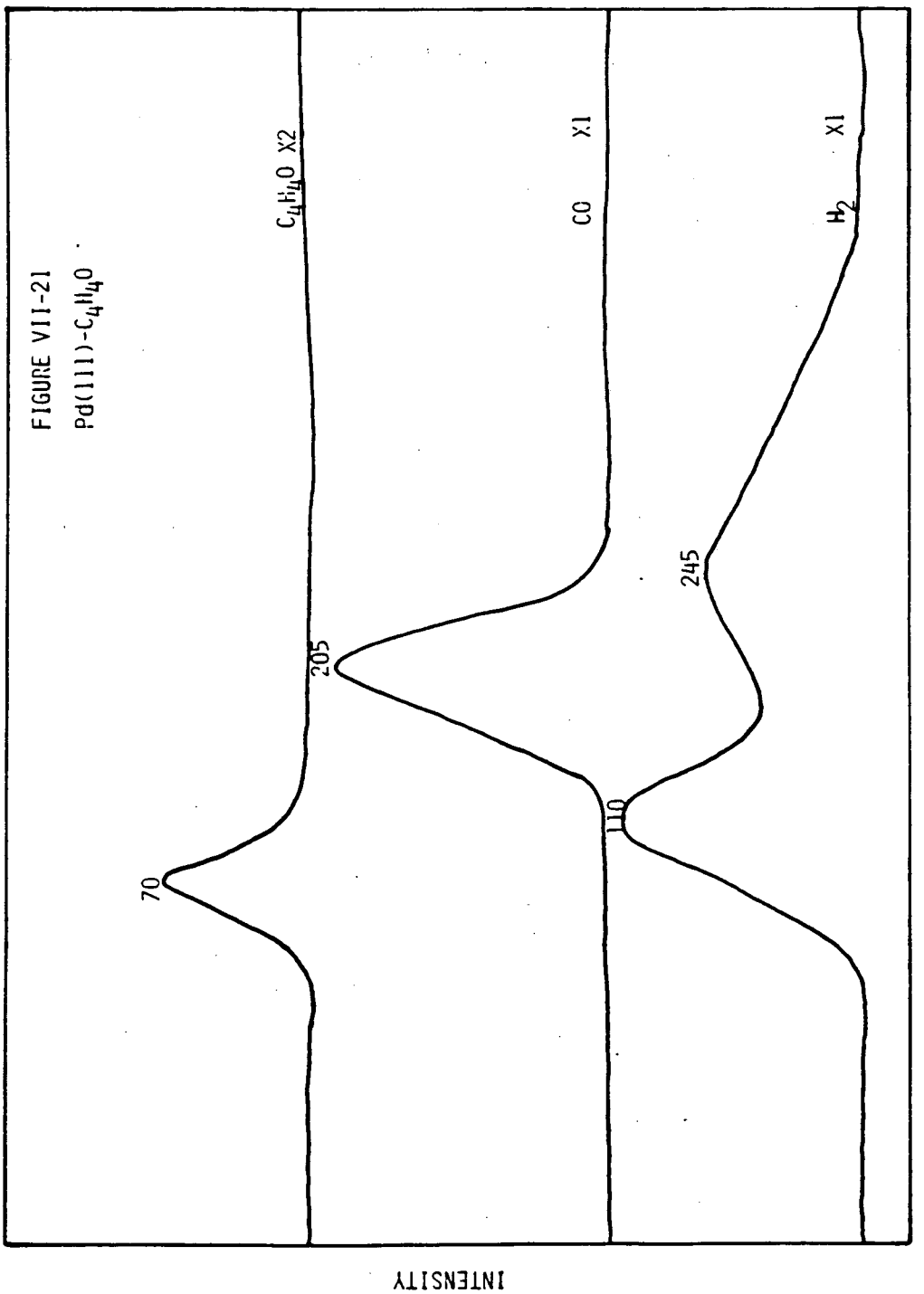
FIGURE VII-21
Pd(111)-C_4H_4O
C_4H_4O X2
CO X1
H_2 X1
70
205
110
245
INTENSITY
TEMPERATURE (°C)

XBL 846-2085

Figure VII-22. Both reversible and irreversible chemisorption were evident in the thermal desorption of pyridine from Pd(111). Only hydrogen and intact pyridene were observed to desorb from this surface. No hydrocarbon formation was observed.

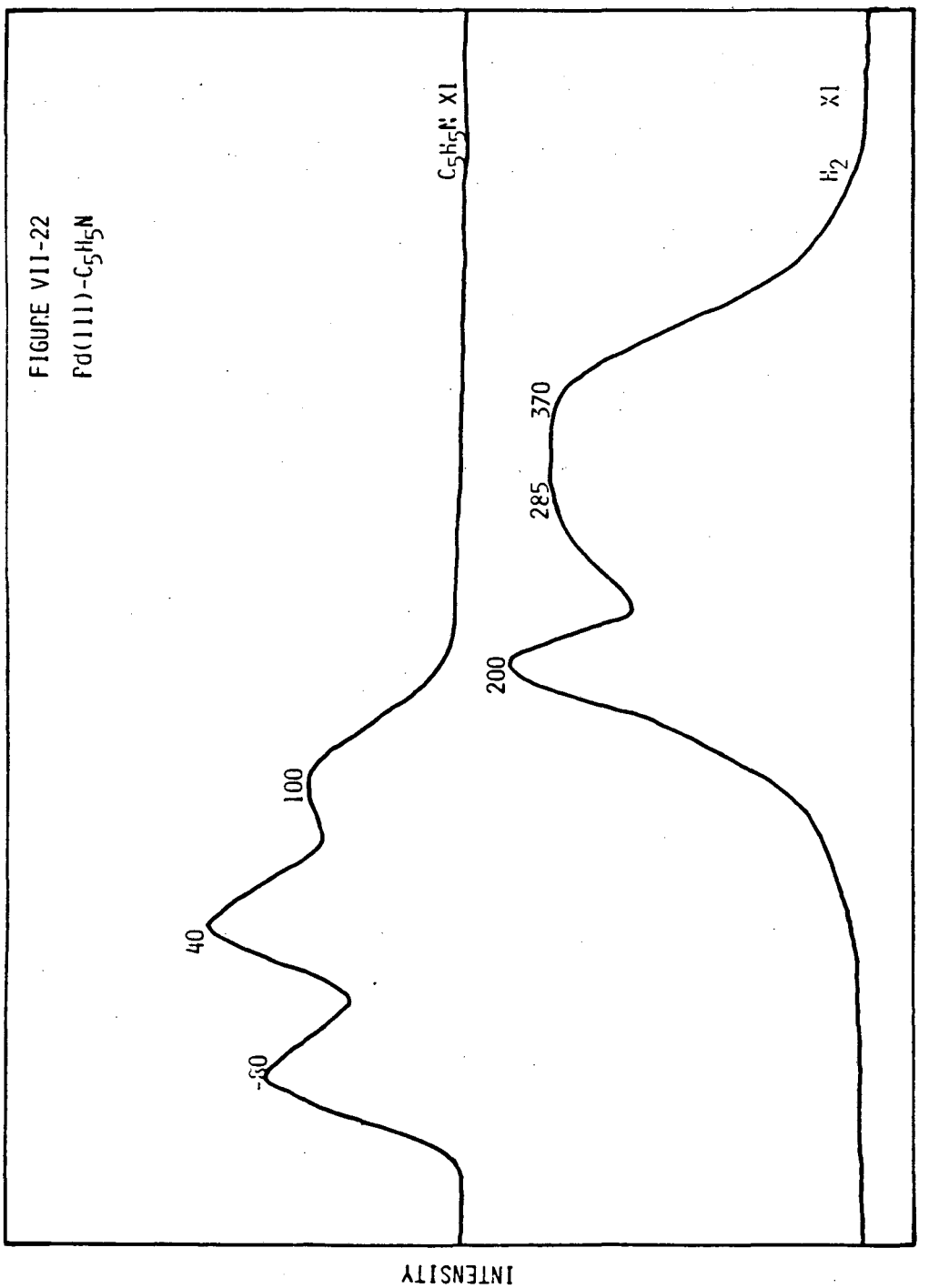
FIGURE VII-22
Pd(111)-C5H5N
C5H5N X1
H2 X1
-60
40
100
200
285
370
INTENSITY
TEMPERATURE (°C)
XBL 846-2086

Miller-index surfaces of palladium. The oxygen analog of this molecule, 2,5-dimethylfuran, does not exhibit this chemistry. Carbon monoxide formation has been observed from this molecule, but no other hydrocarbon was observed.[15]

Cyclicolefins have been found to dehydrogenate on transition metal surfaces. Cyclohexene, for example, has been found to form benzene on Ni[16] and Pt[17] surfaces. The chemistry of cyclohexene and four isomers of methylcyclohexene (1-methylcyclohexene, 3-methylcyclohexene, 4-methylcyclohexene, and methylenecyclohexene) on palladium single-crystal surfaces will be described. Following this, the chemistry of these molecules on polycrystalline films at much higher pressures will be described.

Chemisorbed cyclohexene was found to undergo three processes upon thermal desorption from Pd(111): (1) decomposition from carbon and hydrogen, (2) dehydrogenation to form benzene, and (3) molecular desorption. At an exposure of 4.0 L, two cyclohexene thermal desorption maxima were observed, at -100°C and -25°C. A broad benzene maximum was observed at 200°C, along with two hydrogen maxima, at 75°C and 275°C. The 275°C H_2 maximum had a plateau-like tail (see Figure VII-23). Phosphided Pd(111), θ_P = 0.40, resulted in an increase in the yield of benzene by a factor of two. A benzene thermal desorption maximum was observed at 170°C, a cyclohexene maximum was observed at -15°C, and two hydrogen maxima was observed, at 50°C and 270°C. The high temperature H_2 maximum had a plateau-like tail, and its intensity decreased as compared to the clean surface (see Figure VII-24).

Figure VII-23. Dehydrogenation to benzene was observed in the thermal desorption of cyclohexene from Pd(111). Along with benzene, hydrogen and intact cyclohexene were found to desorb from this surface. An exposure of 4.0 L of cyclohexene was used in this experiment.

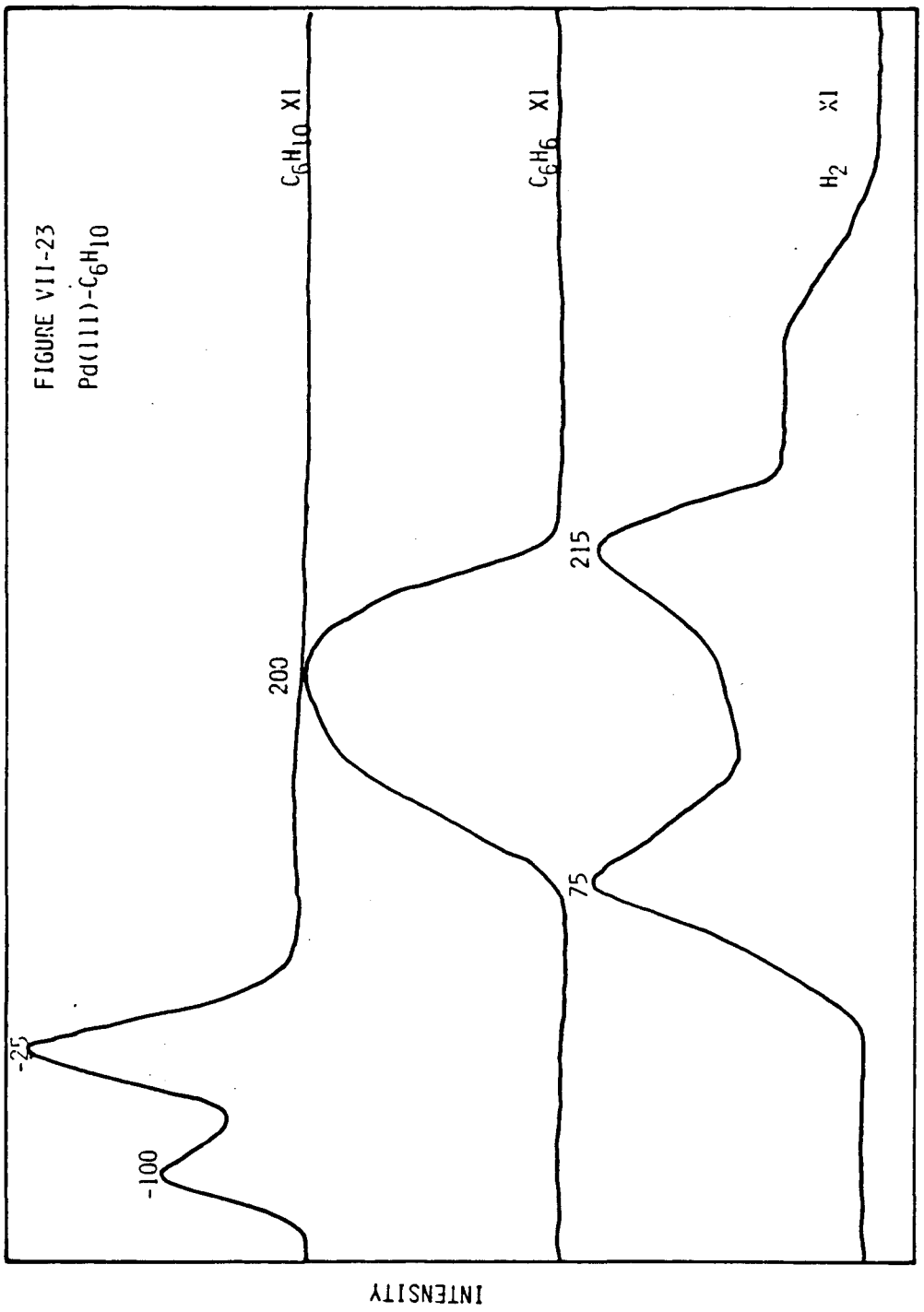
FIGURE VII-23
Pd(111)-C_6H_{10}
C_6H_{10} X1
C_6H_6 X1
H_2 X1
-25
-100
200
215
75
INTENSITY
TEMPERATURE (°C)

XBL 846-2087

Figure VII-24. Phosphiding Pd(111) resulted in an increased yield of benzene desorption in the thermal desorption spectrum of cyclohexene from Pd(111). A cyclohexene exposure of 4.0 L was used on this surface, with a phosphorus coverage of 0.41 monolayer.

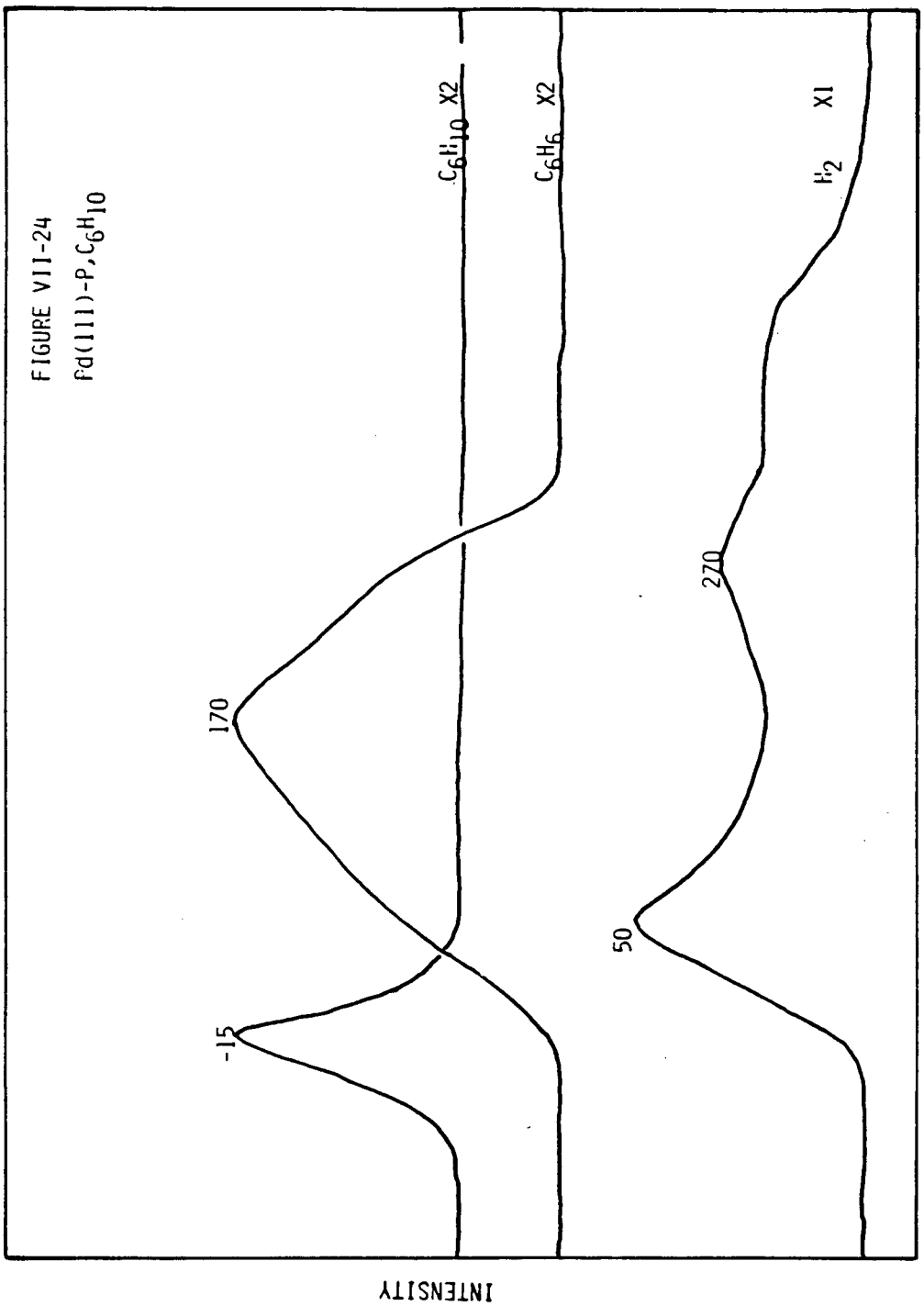
FIGURE VII-24
Pd(111)-P,C_6H_{10}
C_6H_{10} X2
C_6H_6 X2
H_2 X1
170
-15
270
50
INTENSITY
TEMPERATURE (°C)

XBL 846-2088

Figure VII-25. The presence of sulfur did not substantially increase the yield of benzene in the thermal desorption of cyclohexene from Pd(111). The benzene thermal desorption maximum did broaden at this sulfur coverage, $\theta_S = 0.27$. A 4.0 L exposure of cyclohexene was used in this experiment.

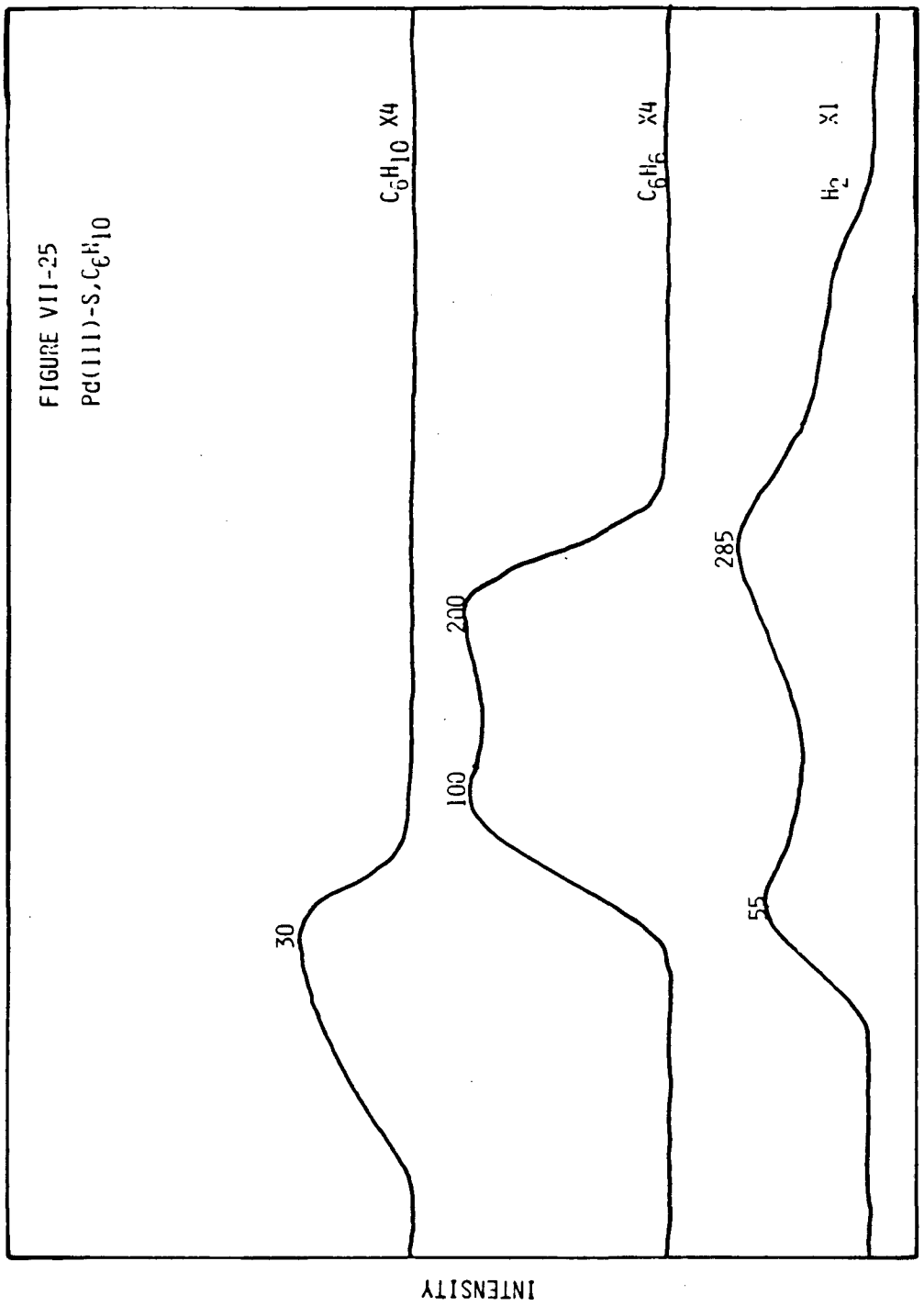
FIGURE VII-25
Pd(111)-S,C_6H_{10}
C_6H_{10} X4
C_6H_6 X4
H_2 X1
30
100
200
55
285
INTENSITY
TEMPERATURE (^oC)

XBL 846-2089

Sulfur was also found to influence the chemistry of cyclohexane on Pd(111). At a sulfur coverage of 0.30 monolayer, the yield of benzene was similar to that observed on the clean surface. Benzene desorbed in a broad plateau-like maximum from 100°C to 200°C. The yield of H_2 decreased as compared to the clean surface, T_{max} = 55°C and 285°C. A broad cyclohexane thermal desorption maximum was observed at 30°C (see Figure VII-25).

4-methylcyclohexane undergoes complex chemistry on Pd(111). The following processes were observed: (1) dehydrogenation to form toluene, (2) benzene formation, (3) molecular desorption, and (4) decomposition to carbon and hydrogen. A toluene thermal desorption maximum was observed at 75°C. Benzene was found to desorb, with two poorly resolved maxima, at 180°C and 225°C. Three hydrogen maxima were observed, at 75°C, 235°C, and 380°C. The ratio of benzene to toluene was ~80.0 (see Figure VII-26). The ratio of benzene to toluene was found to be influenced by the presence at sulfur or phosphorus on Pd(111). On sulfur-covered Pd(111) θ_S = 0.30, the yield of toluene increased, T_{max} = 105°C, while the yield of benzene decreased, T_{max} = 175°C. The yield of hydrogen was also found to decrease. The low temperature H_2 maximum exhibited a marked decrease, while a high temperature plateau was observed from 240°C to 390°C. The ratio of benzene to toluene was observed to be 1.0 (see Figure VII-27). Phosphided Pd(111), θ_P = 0.40, also increased the yield of toluene as compared to clean Pd(111). The ratio of benzene to toluene was observed to be 0.8 (see Figure VII-28). The following thermal

Figure VII-26. Both toluene and benzene were observed in the thermal desorption of 4-methylcyclohexene from Pd(111). At this 4-methylcyclohexene exposure, 4.0 L, benzene was observed in greater yields.

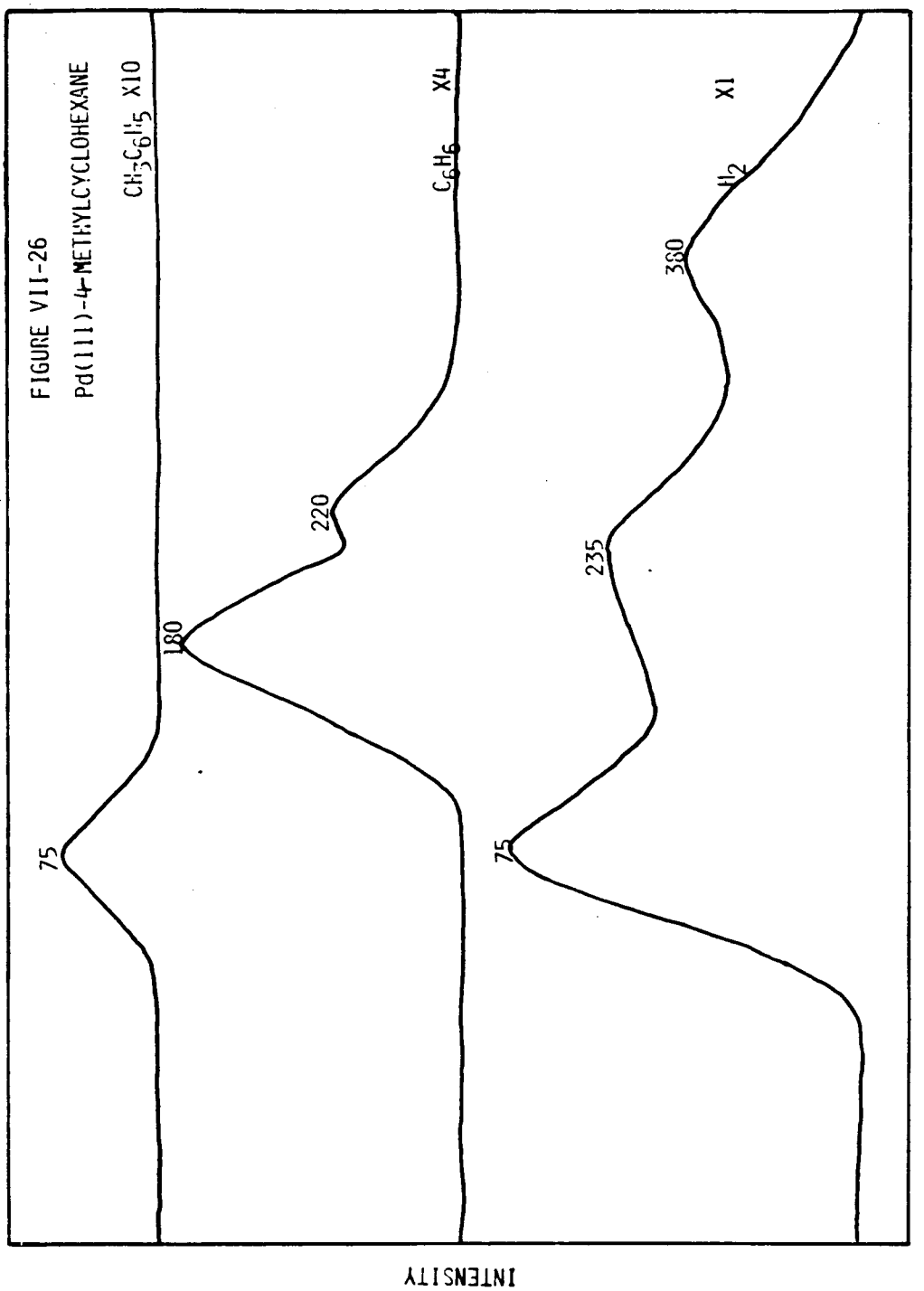
FIGURE VII-26
Pd(111)-4-METHYLCYCLOHEXANE
$CH_3C_6H_5$ X10
C_6H_6 X4
X1
H2
75
180
220
235
360
75
INTENSITY
TEMPERATURE (°C)

XBL 846-2090

Figure VII-27. The presence of sulfur on Pd(111), $\theta_S = 0.27$, increased the yield of toluene in the thermal desorption of 4-methylcyclohexene. Benzene desorption was found to decrease. The exposure of 4-methylcyclohexene was 4.0 L in this experiment.

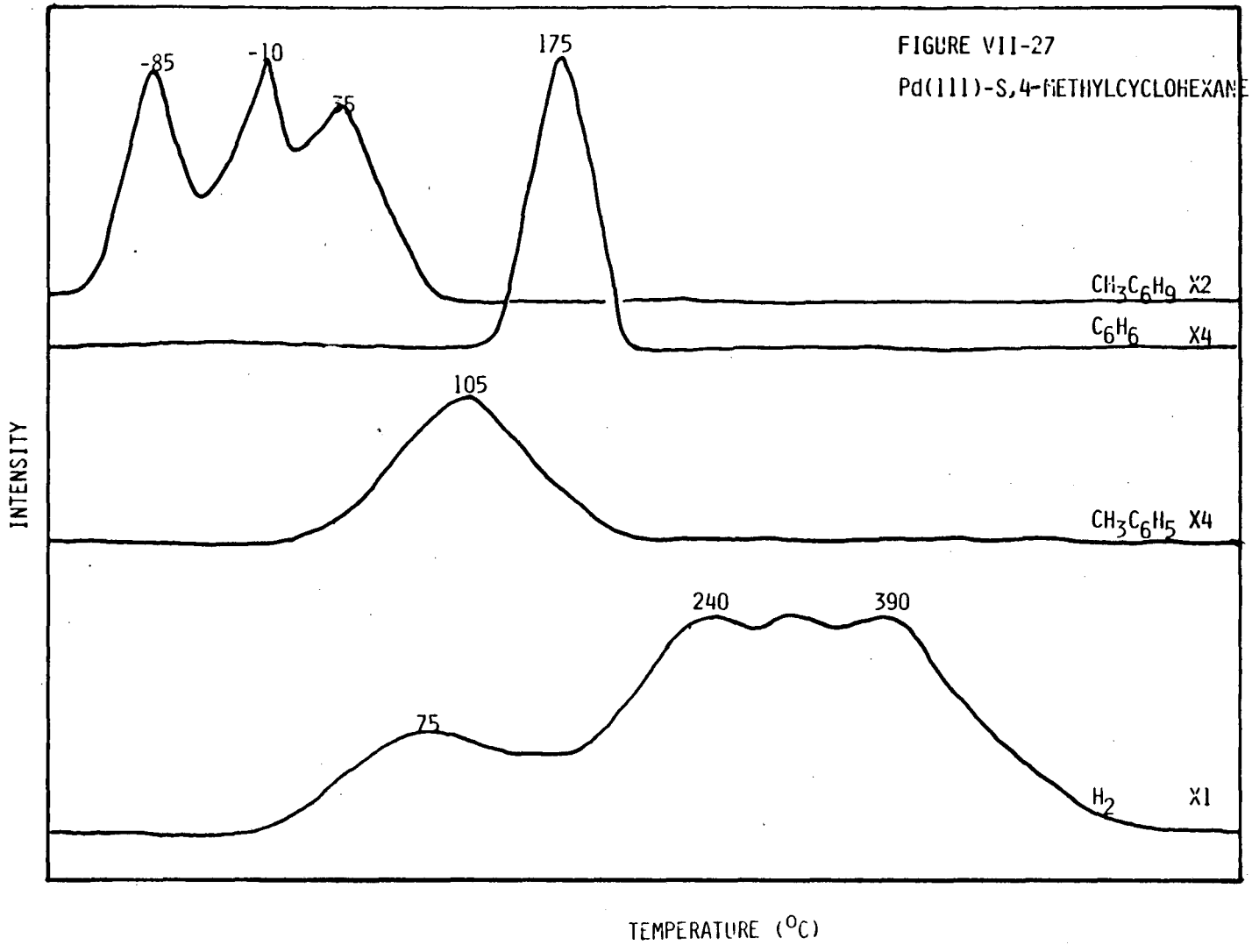
FIGURE VII-27
Pd(111)-S,4-METHYLCYCLOHEXANE
-85
-10
35
175
$CH_3C_6H_9$ X2
C_6H_6 X4
105
$CH_3C_6H_5$ X4
240
390
75
H_2 X1
INTENSITY
TEMPERATURE (°C)

XBL 846-2091

Figure VII-28. At a phosphorus coverage of 0.41 monolayer, toluene was the major hydrocarbon product observed in the thermal desorption spectrum of 4-methylclohexene from Pd(111). Significant quantities of benzene were also observed in this experiment. The exposure of 4-methylcyclohexene was 4.0 L.

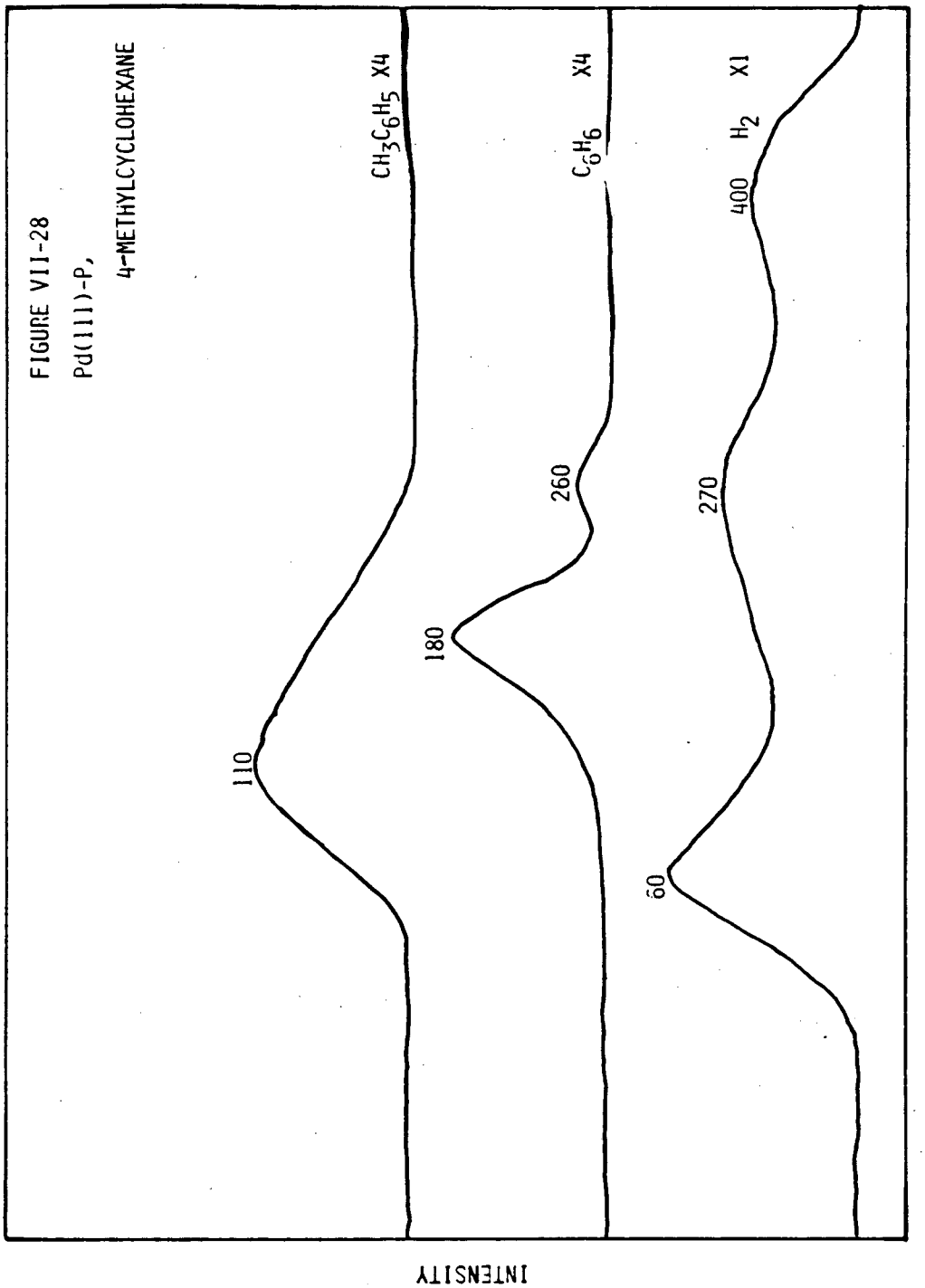
FIGURE VII-28
Pd(111)-P,
4-METHYLCYCLOHEXANE
$CH_3C_6H_5$ X4
C_6H_6 X4
H_2 X1
110
180
260
60
270
400
INTENSITY
TEMPERATURE (^oC)

XBL 846-2092

desorption maxima were observed from the Pd(111)-P-4-methylcyclohexene surface state: (a) a toluene maximum at 100°C, (b) two benzene maxima, at 180°C and 260°C, (c) a 4-methylcyclohexene maximum at -15°C, and (d) three hydrogen maxima, at 60°C, 270°C, and 400°C.

The yield of benzene observed in the thermal desorption of 3-methylcyclohexene from Pd(111) decreased by a factor of four as compared to 4-methylcyclohexene. The ratio of benzene, T_{max} = 185°C, to toluene, T_{max} = 125°C, was 2.4. Three hydrogen thermal desorption maxima were observed, two peaks at 235°C and 260°C and a broad maximum from 330°C to 420°C (see Figure VII-29).

No benzene formation was observed in the thermal desorption of chemisorbed 1-methylcyclohexene from Pd(111). A small toluene thermal desorption maximum was observed at 110°C. Three hydrogen thermal desorption maxima were observed, at 60°C, 225°C, and 285°C (see Figure VII-30). On sulfur-covered Pd(111), θ_S = 0.30, the yield of toluene increased, and benzene formation was also observed. Toluene desorbed with a single maximum at 120°C, and benzene desorbed with two maxima, at, 150°C and 270°C. Three hydrogen maxima were observed, at 50°C, 300°C, and 390°C (see Figure VII-31).

Phosphorus increased the amount of benzene desorbing from the surface. Two benzene maxima were observed, at 25°C and 260°C. Toluene desorbed with a maximum at 150°C, along with three hydrogen maxima at 50°C, 275°C, and 410°C (see Figure VII-32).

No benzene formation was observed in the thermal desorption of chemisorbed methylene cyclohexane from Pd(111). A small toluene

Figure VII-29. Reduced yields of toluene and benzene were observed in the thermal desorption spectrum of 3-methylcyclohexene from Pd(111), as compared to 4-methylcyclohexene (see Figure VII-26). The 3-methylcyclohexene exposure was 4.0 L in this thermal desorption experiment.

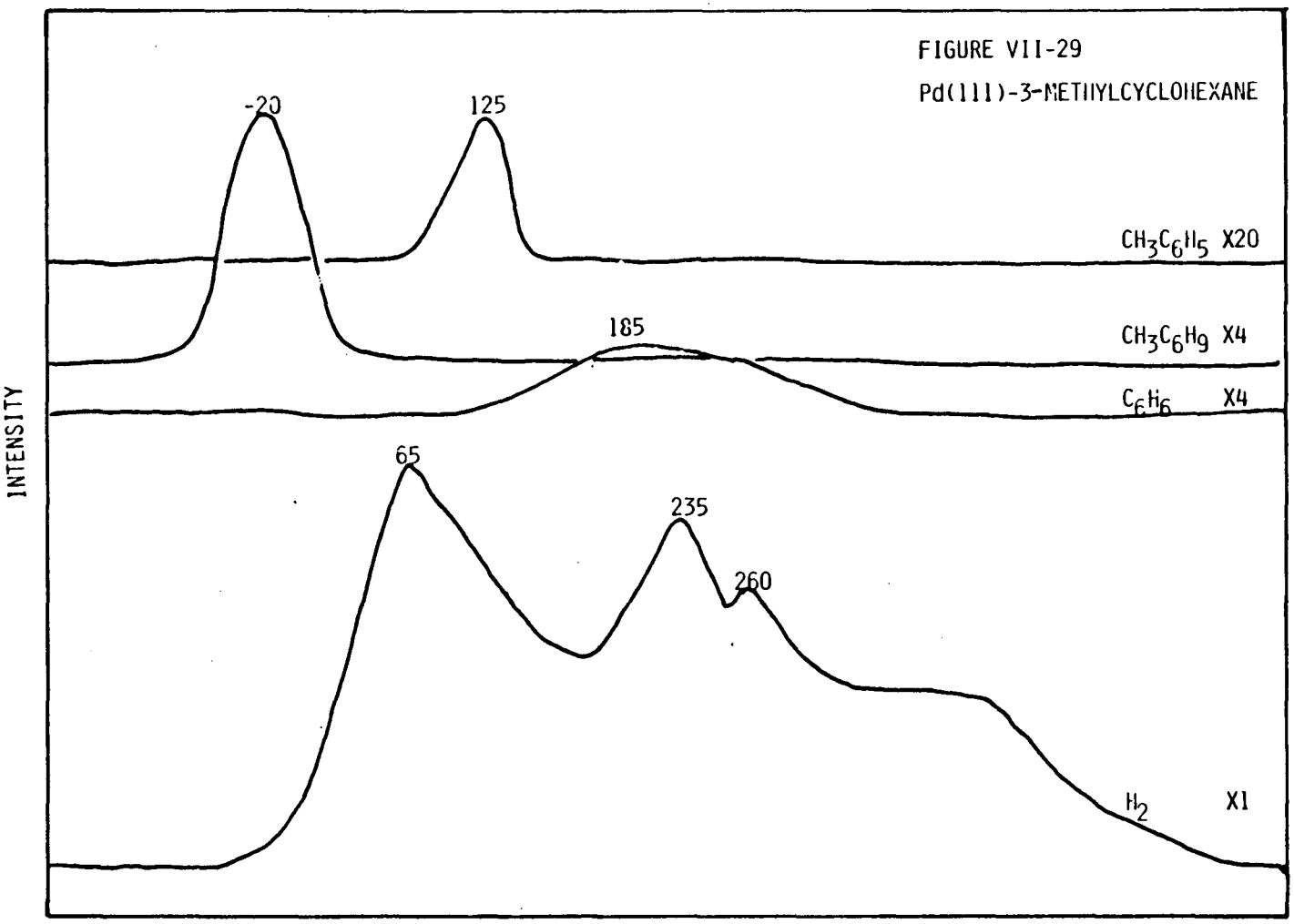
FIGURE VII-29
Pd(111)-3-METHYLCYCLOHEXANE
-20
125
$CH_3C_6H_5$ X20
185
$CH_3C_6H_9$ X4
C_6H_6 X4
65
235
260
H_2 X1
INTENSITY
TEMPERATURE (^{0}C)

XBL 846-2093

Figure VII-30. No benzene was observed in the thermal desorption of 1-methylcyclohexene from Pd(111). A small amount of toluene, however, was found to desorb. In this experiment an exposure of 4.0 L of 1-methylcyclohexene was used.

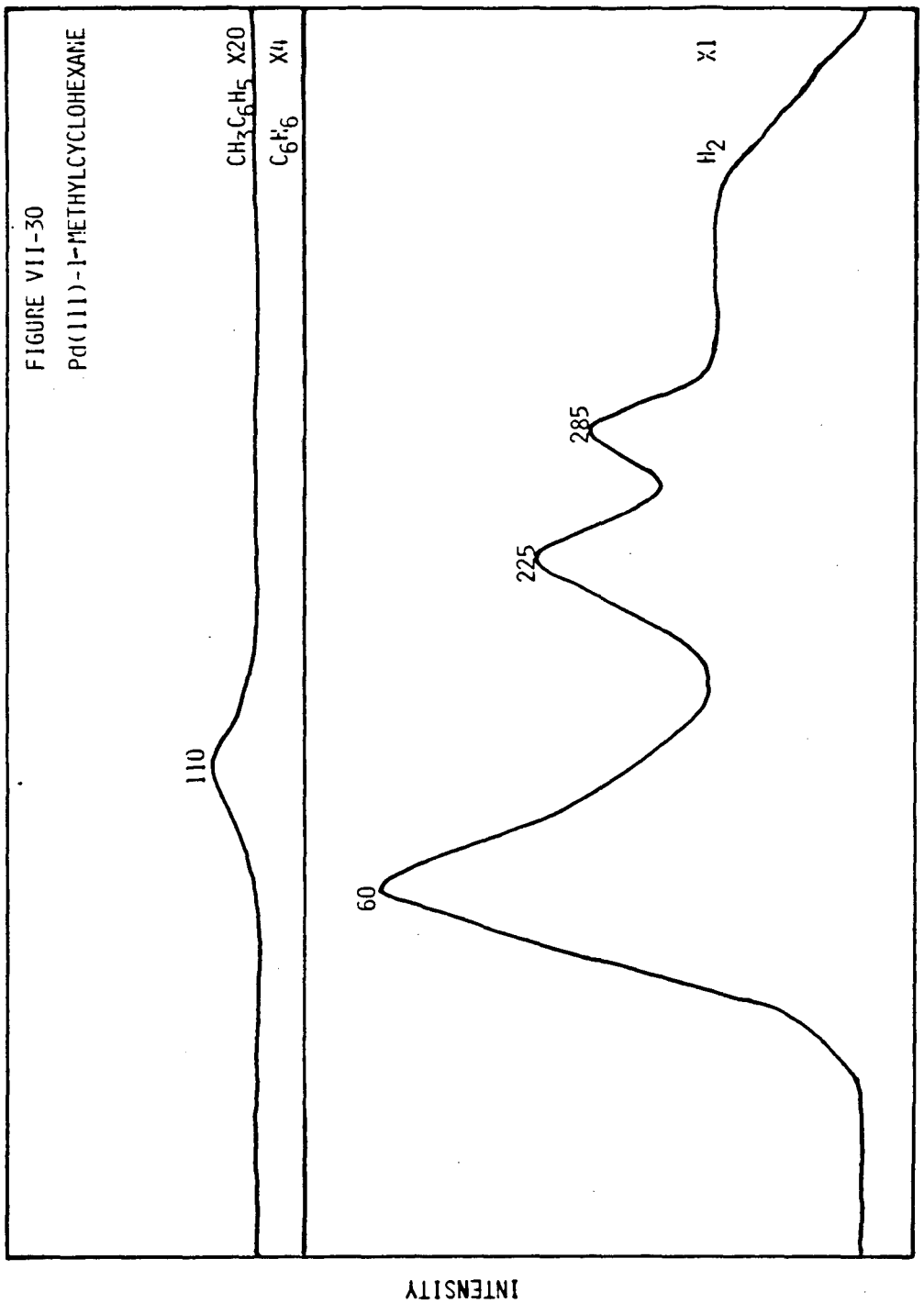
FIGURE VII-30
Pd(111)-1-METHYLCYCLOHEXANE
$CH_3C_6H_5$ X20
C_6H_6 X4
X1
H_2
110
60
225
285
INTENSITY
TEMPERATURE (°C)

XBL 846-2094

Figure VII-31. On sulfur-covered Pd(111), θ_S = 0.27, benzene desorption was observed in the thermal desorption spectrum of 1-methylcyclohexene from this surface. An increased yield of toluene was also observed. The exposure of 1-methylcyclohexene was 4.0 L in this experiment.

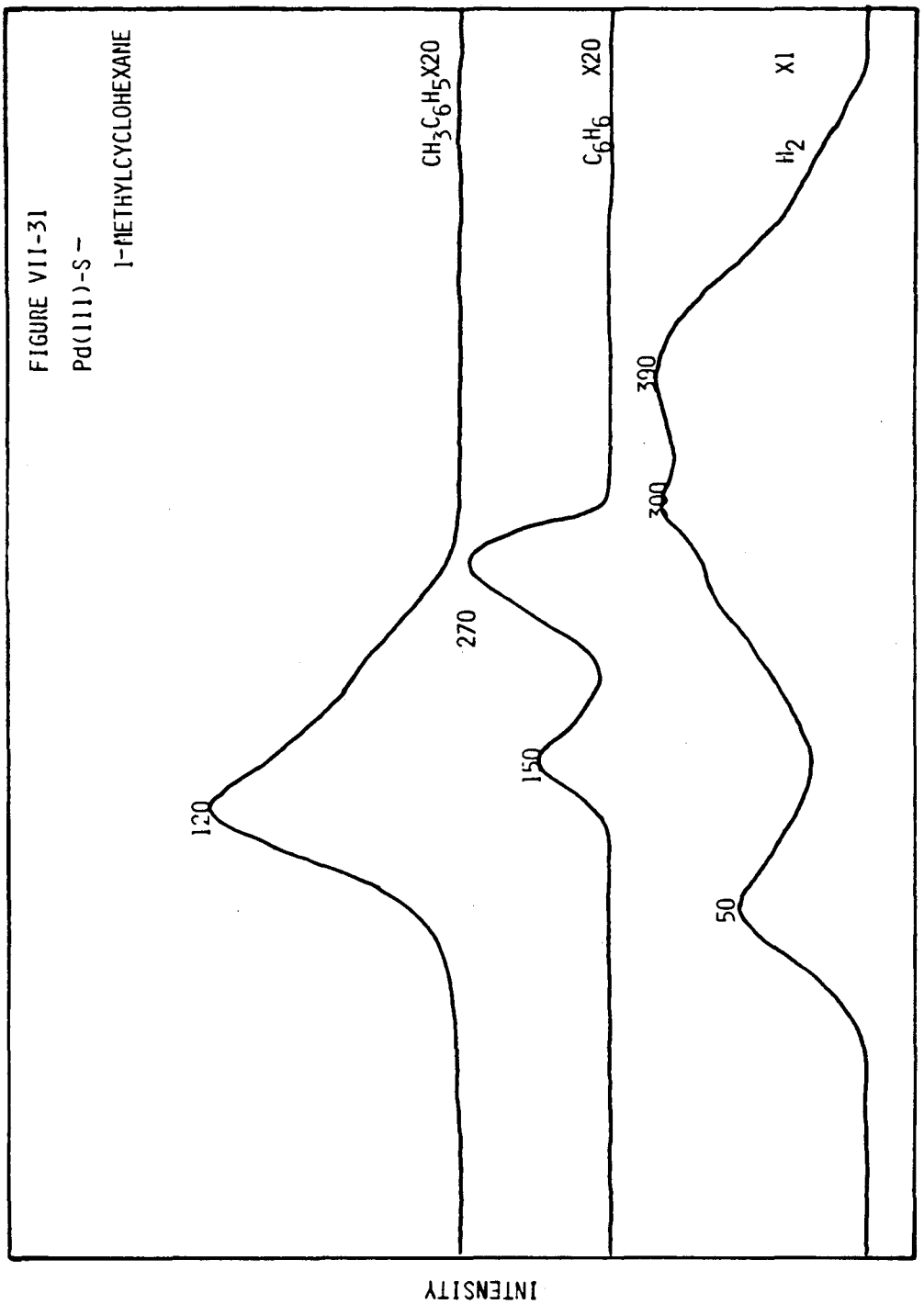
FIGURE VII-31
Pd(111)-S-
1-METHYLCYCLOHEXANE
$CH_3C_6H_5$X20
C_6H_6 X20
H_2 X1
120
270
150
390
300
50
INTENSITY
TEMPERATURE (°C)

XBL 846-2095

Figure VII-32. Both toluene and benzene desorption were observed in the thermal desorption spectrum of 1-methylcyclohexene from phosphorus-covered Pd(111), θ_P = 0.47. The yield of both molecules was greater on this surface than on clean Pd(111). A 4.0 L exposure of 1-methylcyclohexene was used in this experiment.

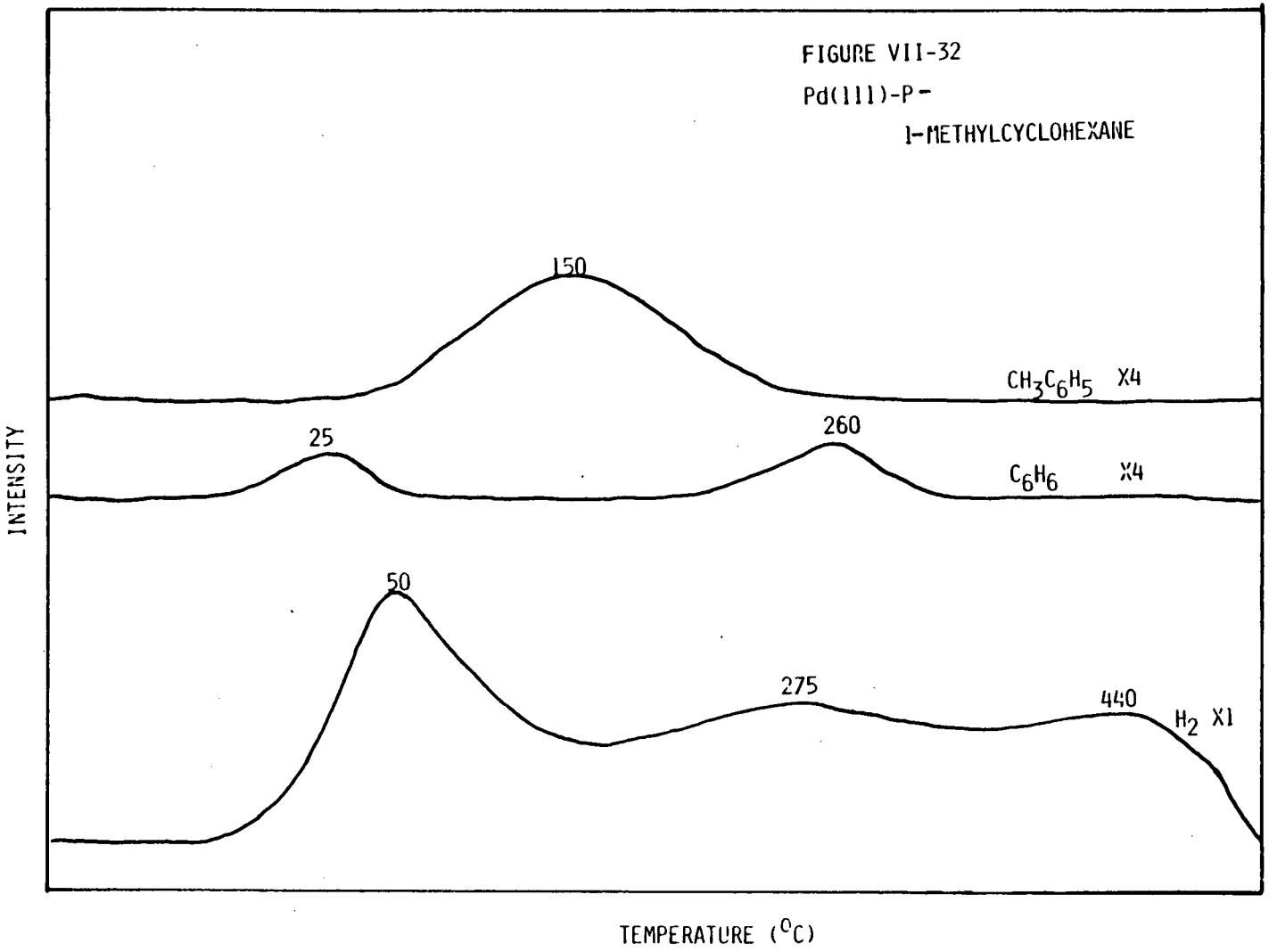
FIGURE VII-32
Pd(111)-P-
1-METHYLCYCLOHEXANE
150
$CH_3C_6H_5$ X4
25
260
C_6H_6 X4
50
275
440
H_2 X1
INTENSITY
TEMPERATURE (°C)

XBL 846-2096

Figure VII-33. Only a small amount of toluene was observed in the thermal desorption spectrum of methylenecyclohexene from Pd(111). No benzene was observed at the exposure used in this experiment, 4.0 L.

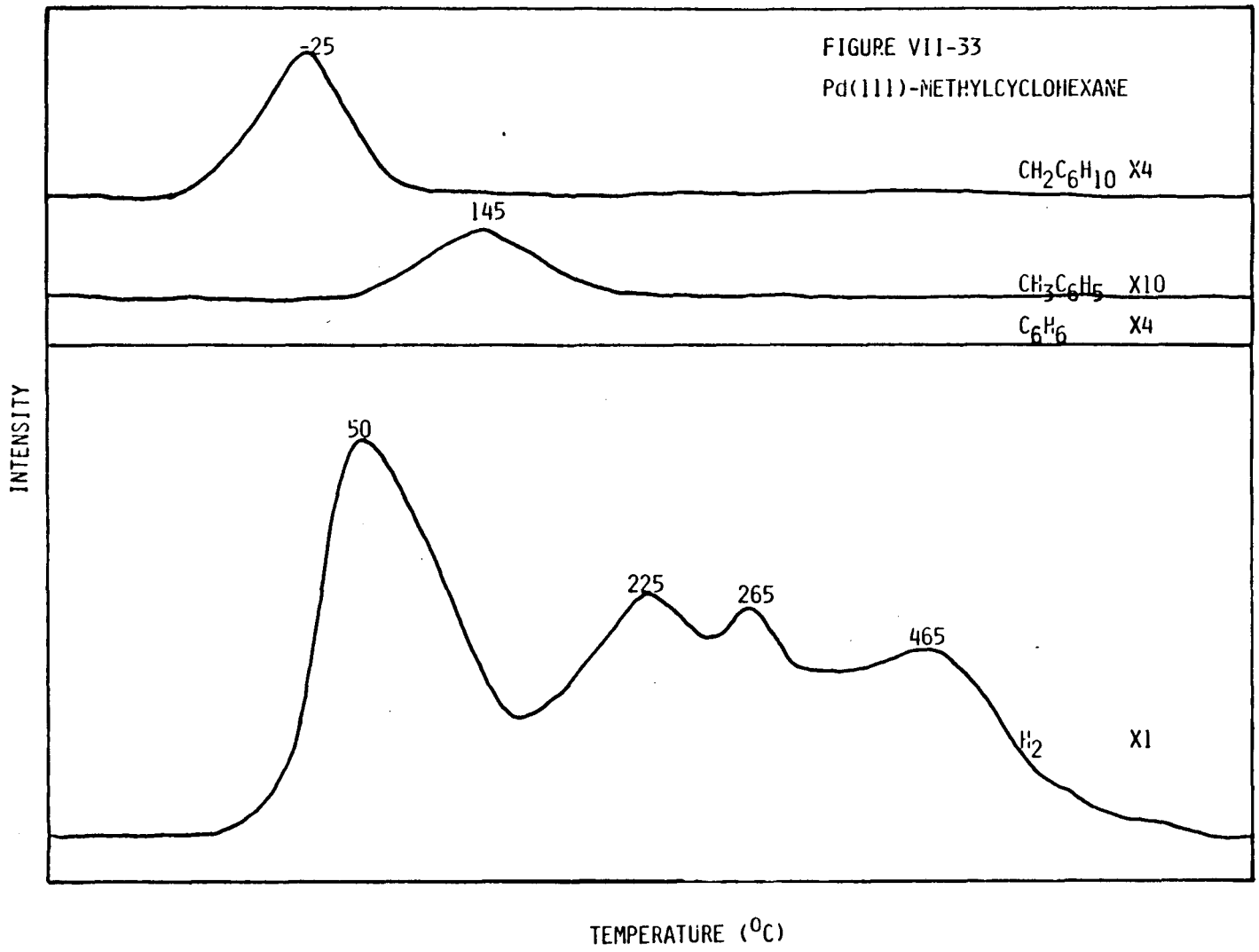
FIGURE VII-33
Pd(111)-METHYLCYCLOHEXANE
-25
$CH_2C_6H_{10}$ X4
145
$CH_3C_6H_5$ X10
C_6H_6 X4
INTENSITY
50
225
265
465
H_2
X1
TEMPERATURE (^{0}C)

XBL 846-2097

thermal desorption maximum was observed at 145°C. Hydrogen desorbed in four maxima, at 50°C, 225°C, 285°C, and 405°C (see Figure VII-33).

Polycrystalline films of palladium were evaporated on the inside of a Pyrex bell jar. The bell jar was pumped with a diffusion pump, and the typical base pressure was $<1 \times 10^{-6}$ torr. The reactor was equipped with a manifold for introduction and removal of samples. All reactions were performed at room temperature on freshly deposited palladium films. The reactions of cyclohexene, 4-methylcyclohexene, 3-methylcyclohexene, 2-methylcyclohexene, and methylenecyclohexene were investigated. The typical initial pressure was in the range of 50-400 millitorr.

Benzene was the major hydrogen product from the reaction of cyclohexene on polycrystalline palladium. Small amounts of cyclohexane were also observed. Complete conversion of cyclohexene was observed for a reaction time of 100 hours with an initial cyclohexene pressure of 400 millitorr. Both benzene and toluene were observed from the reaction of 4-methylcyclohexene on polycrystalline palladium. Nearly complete conversion of 4-methylcyclohexene was observed after 100 hours. Benzene and toluene were also observed from 3-methylcyclohexene, but the conversion was significantly less than 50 percent. Little or no reaction of both 1-methylcyclohexene and methylcyclohexane was observed on polycrystalline palladium.

The reaction of acetylene was investigated at higher pressures on both polycrystalline films and supported catalysts. To review, acetylene chemisorbed on Pd(111) yielded both ethylene and benzene in

subsequent thermal desorption. Preadsorption of hydrogen on Pd(111) was found to inhibit the trimerization of acetylene to benzene and increase the yield of ethylene. Ethylene chemisorbed on Pd(111) did not form benzene during thermal desorption; only decomposition and molecular desorption were observed. The reaction of 400 millitorr of ethylene yielded very little benzene (<1 percent conversion) at room temperature. In sharp contrast, acetylene (400 millitorr) on freshly deposited polycrystalline palladium film yielded both ethylene and benzene. Complete conversion of acetylene was observed in ~4 hours. Preadsorption of hydrogen on thin palladium films also inhibited the trimerization of acetylene to benzene; only ethylene and small amounts of ethane were observed.

The reaction of acetylene on supported palladium catalysts (5 percent Pd on Al_2O_3) at a pressure of ~15 psi resulted in formation of both ethylene and benzene. Consistent with the results obtained under ultrahigh-vacuum conditions and at 10^{-3} torr, ethylene did not trimerize to form benzene on this supported catalyst.

The hydrosilation of acetylene with trimethylsilane on both clean and adatom-covered surfaces was discussed in Chapter III. The yield of the hydrosilation product, vinyltrimethylsilane, was found to be a function of surface structure and composition. The hydrosilation of acetylene on Pd(111) is not limited to trialkylsilanes under ultrahigh-vacuum conditions. The hydrosilation of acetylene on Pd(111) was also affected by chlorodimethylsilane to form chlorodimethylvinylsilane (see Figure VII-34).

Figure VII-34. On Pd(111), the hydrosilation of acetylene with chlorodimethylsilane was observed. In the above thermal desorption experiment, acetylene, 2.0 L, and chlorodimethylsilane, 2.0 L, were sequentially adsorbed on Pd(111). The hydrosilation product, chlorodimethylvinylsilane, desorbed at a maximum rate at 50°C.

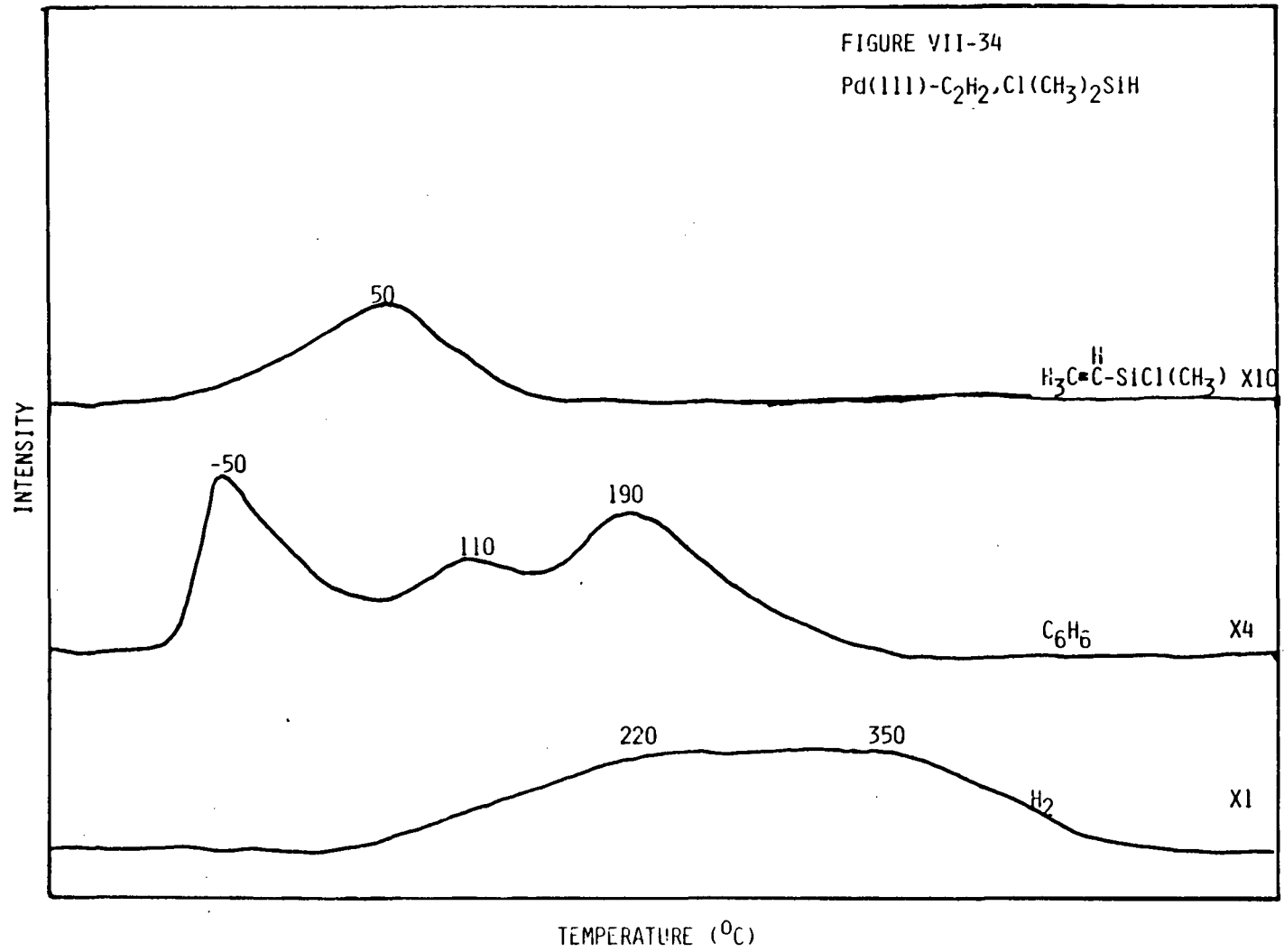
FIGURE VII-34
Pd(111)-C_2H_2,$Cl(CH_3)_2SiH$
50
$H_3C-\overset{H}{C}-SiCl(CH_3)$ X10
-50
110
190
C_6H_6
X4
220
350
H_2
X1
INTENSITY
TEMPERATURE (^oC)

XBL 846-2098

A variety of molecules were coadsorbed to determine if catalytic reactions occurred on Pd(111). In the following coadsorption experiments no reactions were adsorbed: (1) acetylene and ammonia, (b) hydrogen and t-BuNC, (c) hydrogen and furan, (d)) hydrogen and thiophene, (e) hydrogen and pyridine, (f) acetylene and water, and (g) ethylene and water.

DISCUSSION

In this chapter, palladium single-crystal surfaces have been shown to catalyze a variety of reactions that usually occur at much higher pressures. Furthermore, ultrahigh-vacuum studies have been found to be good models for these reactions on both polycrystalline films and supported catalysts. Ultrahigh-vacuum studies allow the influence of structure and composition to be well-defined on catalytically active surfaces. In this discussion the results of the ultrahigh-vacuum studies will be discussed in terms of their implication concerning mechanisms of these reactions. Finally, the ultrahigh-vacuum studies will be compared with the high pressure studies.

Oligomerization was demonstrated to occur for chemisorbed alkynes and mixtures of alkynes [alkynes coadsorbed on Pd(111)]. The formation of benzene from propyne may proceed through two possible routes: (a) dimerization of a three-carbon species on the surface, or (b) trimerization of a two-carbon species, presumably acetylene. At first glance, the second route does not seem probable until the

results of the chemisorption of trimethylsilylacetylene are considered. Benzene formation was observed in the thermal desorption of trimethylsilylacetylene chemisorbed on Pd(111). In this system, after adsorption of trimethylsilylacetylene, carbon-silicon bond scission must occur, leading to a surface - C ≡ CH species. Hydrogen addition to form acetylene and subseuquent trimerization would yield benzene. To further probe the mechanism of these oligomerizations, deuterium incorporation into reactively formed benzene observed in the thermal desorption of coadsorbed deuterium and the desired acetylene compound was investigated.

Only small amounts of deuterium incorporation were observed for coadsorbed deuterium and acetylene. This exchange was comparable to that observed between coadsorbed deuterium and benzene on Pd(111). Much more deuterium incorporation was observed in the coadsorption of deuterium and propyne. The fact that increased deuterium incorporation was observed is consistent with the formation of -C ≡ CH on the surface, followed by reaction with D to form DC ≡ CH. However, H-D exchange between D_2 and propyne followed by dimerization could yield similar results. Increased deuterium incorporation was observed in the benzene formed from chemisorbed trimethylsilylacetylene. Ostensibly, trimerization of DC ≡ CH leads to benzene in this situation. The question of whether benzene formation is the result of a dimerization of a three-carbon species or a trimerization of acetylene derived from decomposition of propyne has not been answered

unambiguously. The results, however, suggest trimerization of acetylene as the mechanism of formation.

The Pd(111) surface chemistry of the four isomers of methylcyclohexene (4-methylcyclohexene, 3-methylcyclohexene, 1-methylcyclohexene, and methylenecyclohexane) was found to be a function of the position of the methyl group on the six-membered ring. Chemisorbed 4-methylcyclohexene on Pd(111) was found to have the highest yield of both benzene and toluene. In this isomer, the methyl group is the greatest distance from the carbon-carbon double bond. If the first step in the mechanism of the reaction leading to the observed products, benzene and toluene, is the coordination to the surface through the double bond, then the least hindered isomer would be expected to be the most reactive. The isomers with the methyl group closer to the double bond should be less reactive. The results of the chemisorption of these isomers on Pd(111) yield the following order of reactivity: 4-methylcyclohexene > 3-methylcyclohexene > 1-methylcyclohexene > methylenecyclohexane. This order is consistent with the above mechanism.

The reaction of the four isomers of methylcyclohexene on polycrystalline palladium at much higher pressures, 10^{-2} torr, yield similar results. The correspondence between high pressure studies and under high-vacuum studies here is quite remarkable. Palladium single crystals are in this case a very good model for these reactions occurring at much higher pressures.

Examination of the thermal desorption spectrum of cyclohexene chemisorbed on Pd(111) yields insights into the dehydrogenation process. Comparing this spectrum with the spectrum obtained from benzene chemisorbed on Pd(111) also adds further enlightenment. The hydrogen thermal desorption spectrum from chemisorbed cyclohexene exhibits two maxima, at 75°C and 275°C. The second maximum is similar in both position and shape to that obtained from chemisorbed benzene. This result suggests that some of the benzene formed from dehydrogenation of cyclohexene is irreversibly bound. The genesis of the first hydrogen maximum may be the hydrogen produced in the dehydrogenation of cyclohexene. Combining this result with the observation that no low temperature benzene desorption is observed in the dehydrogenation of cyclohexene, an estimate of temperature where dehydrogenation and carbon-hydrogen bond scission occurs can be made. Two benzene thermal desorption maxima were observed, at -40°C and 220°C, from benzene chemisorbed on Pd(111). The lack of the low temperature benzene maximum in the cyclohexene spectrum suggests that dehydrogenation occurs in the range from -40°C to 75°C. Phosphorus on Pd(111) was found to increase the amount of benzene desorbing in the thermal desorption spectrum of chemisorbed cyclohexene. A significant decrease was not observed in the low temperature hydrogen maximum; however, a decrease in the high temperature maximum was observed. The results indicate that phosphorus does not inhibit the carbon-hydrogen bond scission occurring in the dehydrogenation process but it does inhibit carbon-hydrogen bond scission in the decomposition of

benzene. Furthermore, this result suggests that these processes may be occurring at different sites on the surface.

The hydrogen thermal desorption spectrum obtained from chemisorbed cyclohexene on sulfur-covered Pd(111) suggests that both processes, dehydrogenation of cyclohexene and decomposition of benzene, are inhibited by the presence of sulfur. Both phosphorus and sulfur were found to exhibit carbon-carbon bond scission occurring in the thermal desorption spectrum of chemisorbed 4-methylcyclohexene on Pd(111). Both toluene and benzene were observed on clean Pd(111). On both sulfur and phosphorus, the yield of toluene increased, as expected if carbon-carbon bond scission is inhibited, along with a corresponding decrease in the yield of benzene.

Trimerization of acetylene was also investigated over a wide pressure range. Acetylene in trimerization is commonly catalyzed by transition metal complexes, however, not for metallic catalysts. The observations of acetylene trimerization under ultrahigh-vacuum conditions leads to studies on polycrystalline films at 10^{-3} torr and on supported catalysts at pressures near one atmosphere. Here again the correspondence between ultrahigh-vacuum studies and high pressure studies is outstanding. It has been demonstrated that chemisorption studies on palladium single-crystal surfaces are useful models for catalytic reactions occurring at pressures 12 orders of magnitude greater.

In summary, in this chapter the occurrence of catalytic reactions of unsaturated hydrocarbons that usually occur at much higher pressure has been demonstrated under ultrahigh-vacuum conditions. A remarkable correspondence between the chemistry of unsaturated under high-vacuum conditions and at much higher pressure on polycrystalline films and supported catalysts has also been demonstrated.

REFERENCES

1. J. L. Gland, K. Baron, and G. A. Somorjai, J. Catal. 1975, 36, 305.
2. D. W. Blakely, and G. A. Somorjai, J. Catal. 1976, 42, 181.
3. S. Lehwald, and H. Ibach, Surf. Sci. 1979, 89, 425.
4. C. M. Friend, J. Stein, and E. L. Muetterties, J. Am. Chem. Soc. 1981, 103, 767.
5. C. M. Friend, and E. L. Muetterties, J. Am. Chem. Soc. 1981, 103, 773.
6. M.-C. Tsai, C. M. Friend, and E. L. Muetterties, J. Am. Chem. Soc. 1982, 104, 2539.
7. M. C. Tsai and E. L. Muetterties, J. Phys. Chem. 1982, 86, 5067.
8. M.-C. Tsai, J. Stein, C. M. Friend, and E. L. Muetterties, J. Am. Chem. Soc. 1982, 104, 3533.
9. L. L. Kesmodel, L. H. DuBois, and G. A. Somorjai, Chem. Phys. Lett. 1978, 56, 267.
10. M. Salmeron, and G. A. Somorjai, J. Phys. Chem. 1982, 86, 341.
11. E. L. Muetteries, M.-C. Tsai, and S. R. Kelemen, Proc. Nat. Acad. Sci. USA 1981, 78, 6571.
12. (a) T. M. Gentle and E. L. Muetterties, J. Am. Chem. Soc. 1983, 105, 304 (b) T. M. Gentle and E. L. Muetterties, J. Phys. Chem. 1983, 87, 2469.
13. G. W. Parshall, Homogeneous Catalysis, Wiley, New York, 1980, p. 165.
14. T. M. Gentle, V. H. Grassian, D. G. Klarup, and E. L. Mutterties, J. Am. Chem. Soc. 1983, 105, 6766.

15. T. G. Rucker, private communication.

16. C. M. Friend, Ph.D. Thesis, University of California, Berkeley, 1981.

17. M.-C. Tsai, Ph.D. Thesis, University of California, Berkeley, 1982.

This report was done with support from the Department of Energy. Any conclusions or opinions expressed in this report represent solely those of the author(s) and not necessarily those of The Regents of the University of California, the Lawrence Berkeley Laboratory or the Department of Energy.

Reference to a company or product name does not imply approval or recommendation of the product by the University of California or the U.S. Department of Energy to the exclusion of others that may be suitable.

TECHNICAL INFORMATION DEPARTMENT
LAWRENCE BERKELEY LABORATORY
UNIVERSITY OF CALIFORNIA
BERKELEY, CALIFORNIA 94720